INVESTIGATING THE BIOSYNTHETIC AND METABOLIC PATHWAYS OF 3-IODOTHYRONAMINE

By

Sarah Ann Hackenmueller

A DISSERTATION

Presented to the Department of Physiology & Pharmacology
and
the Oregon Health & Science University School of Medicine
In partial fulfillment of the requirements for the degree of

Doctor of Philosophy

May 2012

School of Medicine

Oregon Health & Science University

_____

CERTIFICATE OF APPROVAL

This is to certify that the Ph.D. dissertation of
Sarah Ann Hackenmueller
has been approved

_____
Thomas S. Scanlan, Ph.D.   Dissertation advisor

_____
Dennis Koop, Ph.D.   Committee Chair

_____
Michael Cohen, Ph.D.   Committee Member

_____
Peter Rotwein, M.D.   Committee Member

_____
Xiangshu Xiao, Ph.D.   Committee Member

Table of Contents

List of Figures

List of Tables

List of Schemes

Acknowledgements

The following dissertation would not have been possible without the help and support of numerous people. First and foremost, I would like to thank my mentor Thomas Scanlan. Thank you for the opportunity to work on this project and the freedom to explore it in different directions. Thank you for your guidance and insight as I navigated through this project, and your perpetual optimism that things would work out helped keep me motivated to continue. I want to thank several former members of the Scanlan lab: Aaron Nilsen for helping orient me to the lab and start off in the right direction; Travis Geraci for doing much of the background work on training me on the extraction of T_1AM; and Barbara Hettinger for training me to work with mice and general support and guidance.

To the members of the Bioanalytical Share Resource/Pharmacokinetics Core, Dennis Koop, Andrea DeBarber, Jenny Luo, Lisa Bleyle, and Anuradha Pappu, thank you for your continued support, assistance and patience throughout this project. To Dr. Koop, thank you for giving me the opportunity to learn about mass spectrometry to the extent that I did and taking the time to work with me. Thank you to Andrea and Jenny for training me and assisting with my numerous questions. Thank you to Lisa for sharing your space with me, and for many thought provoking discussions.

I would like to thank my family for their constant support. To my parents, Joe and Shirley, thank you for pushing me to believe in myself, set goals, and work hard to achieve them. To my siblings, Paul and Ellen, thank you for encouraging me to stay motivated, and also for providing much needed distractions at times. Finally, I would like to thank my husband, Bill McCarthy, for his support through every step of this process. I could not have done this without you.

x

Abstract

3-Iodothyronamine (T_1AM) is an endogenous derivative of thyroid hormone with a unique pharmacological profile. T_1AM acutely induces hypothermia in rodents, decreases cardiac function, and alters fuel utilization. These actions are opposite those typically associated with thyroid hormone and suggest that T_1AM may play a role in regulating thyroid hormone action. Structural similarities between T_1AM and thyroid hormone include a core biaryl ether carbon structure and the presence of iodine, but thyroid hormone contains an amino acid side chain while T_1AM has an ethylamine side chain. *In vitro*, T_1AM is a substrate for metabolism by similar pathways to those that metabolize thyroid hormone, including glucuronidation and sulfation. Oxidative deamination of T_1AM and higher iodothyronamines also produce thyroacetic acids, known metabolites of thyroid hormone, *in vitro* and *in vivo*.

The similarities in structure and metabolism between T_1AM and thyroid hormone have led to the hypothesis that T_1AM is a decarboxylated and deiodinated metabolite of thyroid hormone. This hypothesis was tested *in vivo* using a stable isotope labeled thyroid hormone and a hypothyroid mouse model. Analysis by liquid chromatography-tandem mass spectrometry allows for distinction between endogenous compounds and those arising from metabolism of the labeled thyroid hormone. The results indicate that T_1AM biosynthesis is dependent on thyroid gland function, but it is not produced through extrathyroidal metabolism of thyroid hormone.

The *in vivo* metabolism of T_1AM was characterized following a single IP injection in mice. Using information dependent acquisition methods and liquid chromatography-tandem mass spectrometry, serum metabolites of T_1AM were identified and quantified. Two novel compounds, N-acetyl-T_1AM and T_1AM-glucuronide, were identified in mouse serum. T_1AM is also sulfated and oxidatively deaminated in mouse serum. This panel of metabolites was quantified in serum and several metabolites were present at greater concentrations than unmodified T_1AM. This indicates that metabolism of T_1AM is extensive, similar to the metabolism observed for thyroid hormones, and likely plays an important role in regulating the distribution and action of endogenous T_1AM.

Chapter 1: Introduction to thyroid hormone metabolism

1.1 Overview

Thyroid hormones (THs) are endocrine signaling molecules that regulate a variety of physiological effects. The importance of THs is clearly illustrated when examining cases of thyroid dysfunction. Hypothyroidism, a state of low TH levels, is characterized by increases in body weight and cholesterol levels, decreases in cardiac output and body temperature, as well as bradycardia and depression (1, 2). Thyrotoxicosis, a state of increased TH levels, is characterized by increases in bone turnover (osteoporosis) and body temperature, decreases in body weight and cholesterol levels, as well as tachycardia and hypertension (1, 3). TH is synthesized in the thyroid gland primarily as 3,5,3',5'-tetraiodothyronine (thyroxine, T_4). The structure of T_4 (Figure 1-1) includes a biaryl ether carbon skeleton with a hydroxyl group on the outer ring and an amino acid side chain on the inner ring. T_4 contains four iodine atoms, two on the outer ring in the 5' and 3' positions, and two on the inner ring in the 3 and 5 positions. T_4 is generally considered a pro-hormone that undergoes extrathyroidal enzymatic deiodination to 3,5,3'-triiodothyronine (T_3, Figure 1-1), the active form of TH, indicating that metabolism of TH is critical to regulating activity and a central feature in TH action.

1.2 Historical perspective of thyroid hormone metabolism

Since the late 1800's, it was understood that treatment with a thyroid gland was able to correct cretinism associated with hypothyroidism, and that the active component within the gland contained iodine (4-6). In the early 1900's, the active component was isolated from the thyroid gland and identified as thyroxine (T_4) (7-9). It wasn't until the 1950's

that an additional iodothyronine was detected in plasma and determined to be T_3 (10, 11), introducing the idea that multiple TH derivatives may be present endogenously. The observation of *in vivo* conversion of T_4 to T_3 (12, 13) was the beginning of research into TH metabolism. Much progress has been made in understanding the extensive metabolism of THs since the 1950's and multiple pathways of TH metabolism have been identified and characterized (Figure 1-1). This chapter reviews the current understanding of TH metabolism and outlines the remaining unanswered questions in the field.

Figure 1-1: Pathways of TH metabolism.
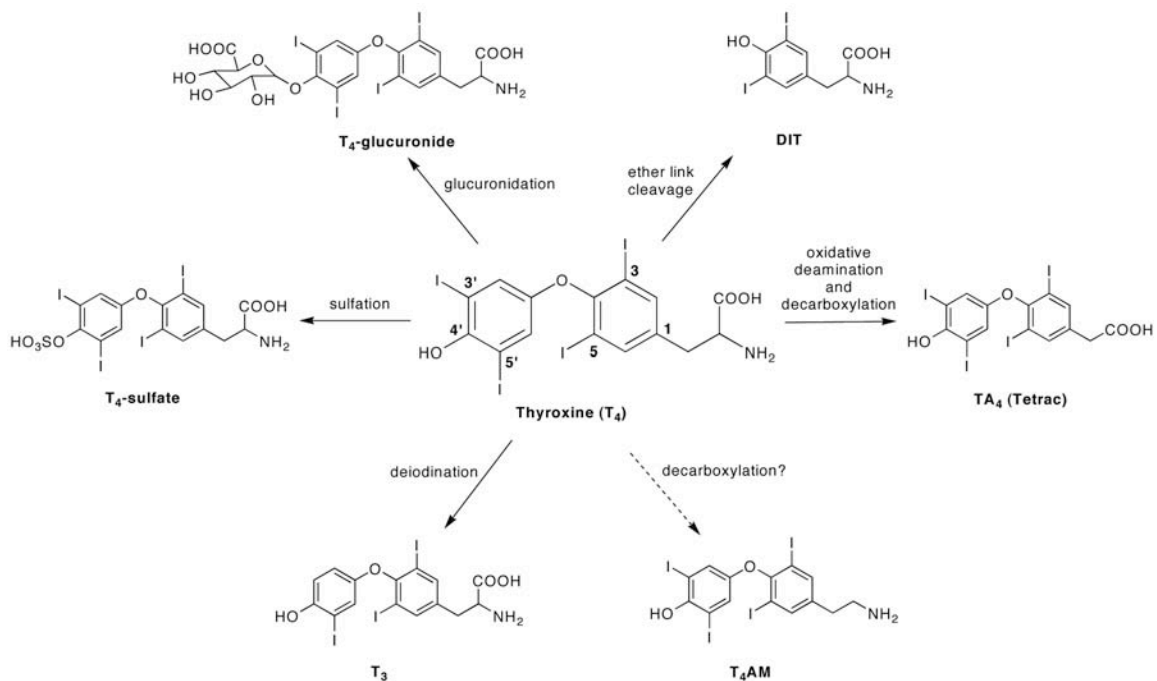
Known pathways of TH metabolism (solid arrows) and proposed pathways of metabolism (dashed arrow); DIT, diiodotyrosine.

1.3 Biosynthesis of thyroid hormone

The biosynthesis of TH occurs within the thyroid gland. The substrate for thyroid hormone production is the protein thyroglobulin, which is related to the esterase family of proteins but lacks esterase activity (14). Thyroglobulin has a molecular weight of 670 kDa and contains approximately 134 tyrosine residues (14), which represent the biosynthetic precursors to TH. Since iodine is a key structural component of TH, it must be present and available for incorporation into TH within the thyroid gland. The sodium-iodide symporter (NIS) is responsible for concentrating inorganic iodide into the thyroid gland in a sodium-dependent manner (15). The NIS transport of iodide results in a 30-fold concentration of iodide within the thyroid gland (16). Inorganic iodide is inactive, and must be activated prior to use in TH synthesis. Thyroperoxidase (TPO) within the thyroid gland oxidizes iodide to an active form of iodine that is used for iodination of tyrosine residues in thyroglobulin (15). TPO catalyzed iodination results in monoiodination and diiodination of ~18-22% of tyrosines within thyroglobulin (14, 17). TPO also catalyzes the coupling of distal iodotyrosines within thyroglobulin to form covalently bound iodothyronines and dehydroalanine at the site of the distally coupled iodotyrosine (15). Iodothyronines are stored in the thyroid gland covalently bound within thyroglobulin until proteolytic cleavage and secretion occur in response to thyroid-stimulating hormone (TSH) (15).

Only a small percentage of iodine in thyroglobulin is incorporated into T_4 molecules. Both monoiodotyrosine (MIT) and diiodotyrosine (DIT) are present in greater concentrations than T_4, and together account for ~70% of thyroidal iodine (14, 15). In addition to T_4, MIT and DIT, the thyroid gland also produces small amounts of T_3, 3,3',5'-

triiodothyronine (reverse-T_3, rT_3), 3,3'-diiodothyronine (3,3'-T_2), 3',5'-T_2, and 3,5-T_2

(Figure 1-2) (14, 18). While T_4 is the main product secreted from the thyroid gland, small

amounts of T_3, rT_3 and DIT are also released into circulation (14).

Figure 1-2: Thyroid gland iodo-compounds.
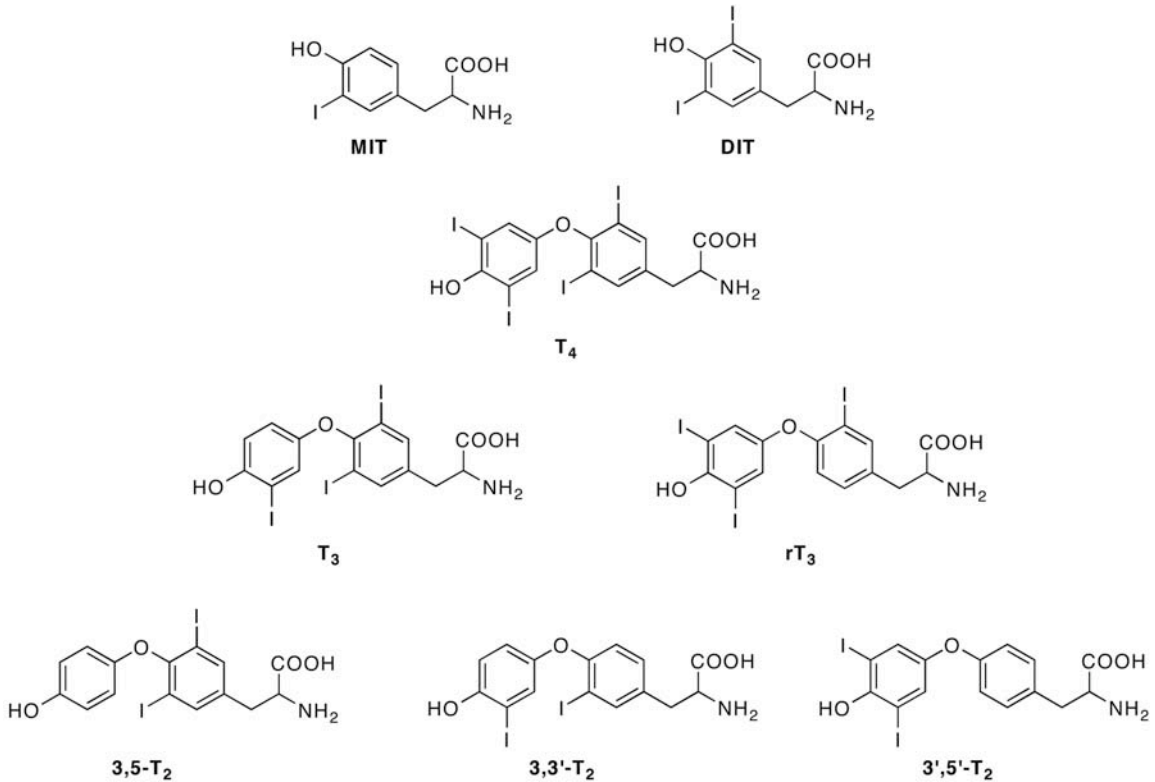
Iodotyrosines and iodothyronines in the thyroid gland; MIT, monoiodotyrosine; DIT, diiodotyrosine.

Synthesis of TH in the thyroid gland is regulated through a negative feedback loop

through the hypothalamic-pituitary-thyroid (HPT) axis. In response to low circulating

levels of TH, thyrotropin-releasing hormone (TRH) is secreted from the hypothalamus,

which stimulates secretion of thyroid-stimulating hormone (TSH) from the pituitary (14).

TSH stimulation of the thyroid gland increases hormone synthesis, degradation of

5

thyroglobulin, and secretion of TH into circulation (14). Increased circulating levels of TH

act negatively on the hypothalamus to inhibit further release of TRH.

1.4 Thyroid Hormone Deiodination

T_4, the main secretory product of the thyroid gland, is largely considered a pro-hormone

that undergoes extrathyroidal enzymatic activation. T_4 is deiodinated on the outer

phenolic ring to T_3 (Figure 1-1), which binds to TH nuclear receptors (TRs) (1). Binding

of T_3 to TRs results in regulation of downstream TH responsive genes (1), and is

considered the main pathway of TH action. Transcriptional activity is dependent upon

conversion of T_4 to T_3, which is tightly regulated by the action of iodothyronine

deiodinase enzymes. Three deiodinase isoforms exist, including type 1, type 2 and type

3 (D1, D2 and D3) deiodinases. All three deiodinases are selenoenzymes with a

selenocysteine residue in the catalytic site (19). The deiodinase enzymes are all

membrane bound and localize intracellularly to either the endoplasmic reticulum or

plasma membranes (20).

The three deiodinase enzymes differ in their sites of iodothyronine deiodination and

tissue distribution. D1 primarily deiodinates the outer phenolic ring at the 5' position and

deiodinates T_4 to produce T_3, and also 3,3',5'-triiodothyronine (rT_3) to produce 3,3'-

diiodothyronine (3,3'-T_2) (Figure 1-3) (21). D1 is also able to deiodinate the inner tyrosyl

ring at the 5 position (21). D1 is primarily located in the liver, kidney and thyroid (19, 21)

and is thought to contribute to circulating levels of T_3. D2 deiodinates exclusively on the

outer phenolic ring and also contributes to T_3 formation through deiodination of T_4 (21).

D2 is located in the pituitary, brown adipose tissue (BAT), brain, heart and skeletal

6

muscle, and is thought to contribute to local production of T_3 (19, 21, 22). D3

deiodinates exclusively on the inner tyrosyl ring, converting T_4 to rT_3 and T_3 to 3,3'-T_2,

and is generally considered to be the inactivating deiodinase (21). D3 is widely

distributed and is present in the central nervous system, placenta, skin and BAT, but is

not present in liver, kidney or thyroid (19, 23, 24).

The deiodinase enzymes differ in their regulation of activity as well as susceptibility to

inhibitors. The D1 promoter, for instance, contains a TRE and shows upregulation of

gene transcript levels in response to T_3 (24). D2 enzymatic activity is inhibited by both

T_4 and rT_3 (20). D1 and D3 activity are increased in hyperthyroidism and decreased in

hypothyroidism, while D2 activity is decreased in hyperthyroidism and increased in

hypothyroidism (24) suggesting acute regulation of deiodinase activity is dependent

upon the local concentration of THs. All three deiodinase enzymes are inhibited by

iopanoic acid, but 6-propylthiouracil (PTU) only inhibits D1 activity (20).

The tissue distribution and sites of deiodination outlined above generate a large number

of iodonidated thyronines. All nine thyronines (T_4, T_3, rT_3, 3,5-T_2, 3,3'-T_2, 3',5'-T_2, 3-T_1,

T_1 and T_0) are endogenous compounds (25-30). *In vivo* and *in vitro* studies have shown

that iodothyronines are deiodinated on both the inner and/or outer ring, depending upon

sites of iodination, to generate a lesser iodinated compound (12, 13, 27, 28, 31-35), with

the exception of outer ring deiodination of T_3 to 3,5-T_2 (Figure 1-3). Despite a single

report of normal 3,5-T_2 serum levels in hypothyroid patients on T_4 replacement (36), a

second study found no correlation between 3,5-T_2 levels and thyroid status (37) and

there is no direct evidence for outer ring deiodination of T_3 to 3,5-T_2 (25, 31, 34, 38).

Since 3,5-T_2 is present in thyroid, it is unclear at this point if 3,5-T_2 in serum is solely the

result of direct gland secretion or if it is generated through extrathyroidal metabolism (18, 39). The biosynthetic origin of 3,5-T2 is one unanswered question in TH metabolism.

Figure 1-3: Pathways of iodothyronine deiodination.
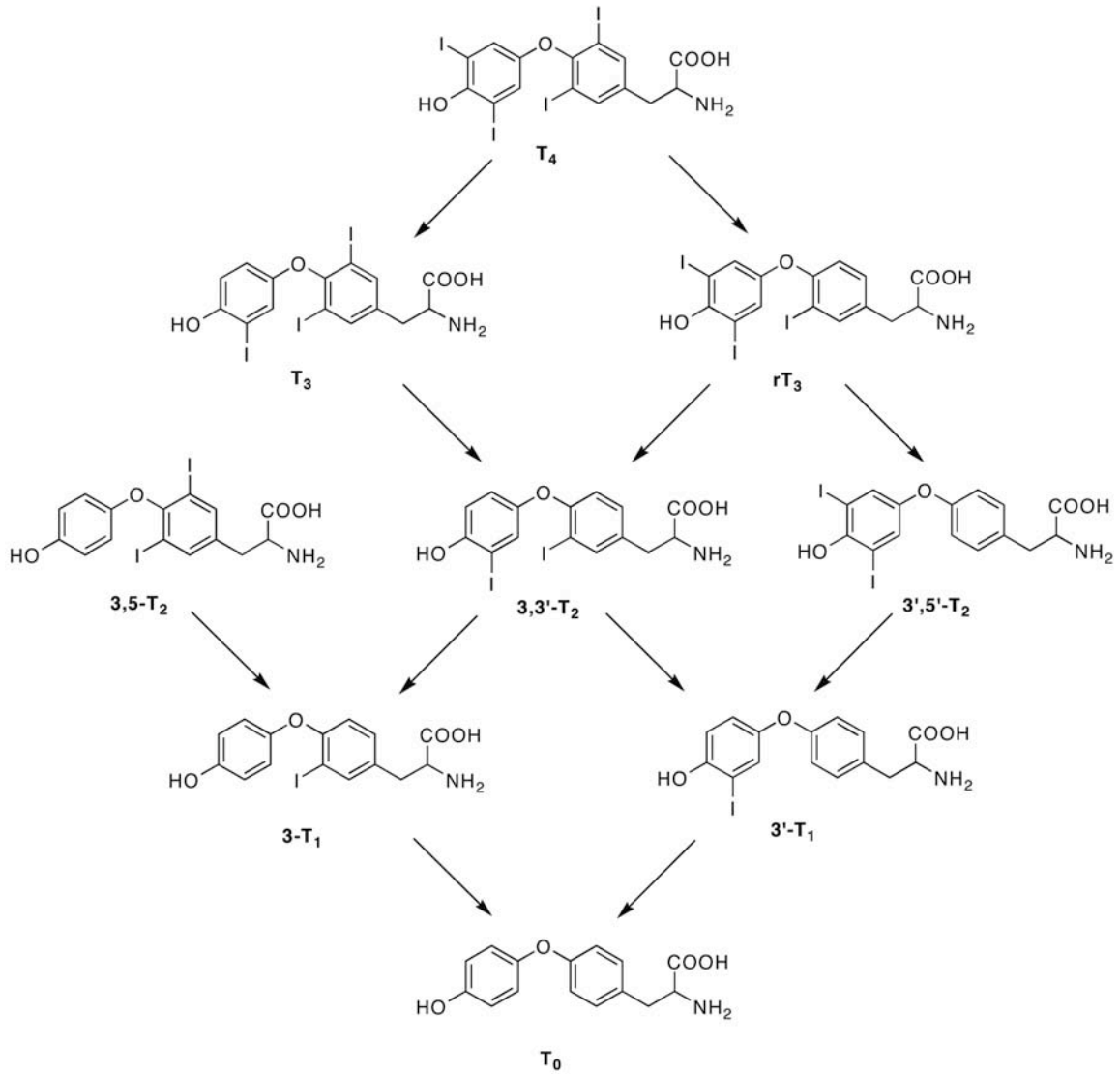
Known pathways of iodothyronine deiodination by D1, D2 and D3 enzymes.

1.5 Glucuronidation and Sulfation of Thyroid Hormones

THs are substrates for phase II metabolism, including glucuronidation and sulfation of the outer ring hydroxyl. Glucuronidation involves conjugation of glucuronic acid, from uridine diphosphate (UDP)-glucuronic acid with THs, including T_4, T_3 and 3,3'-T_2. This reaction is mediated by the UDP-glucuronosyltransferase (UGT) enzyme family. In human liver or kidney microsomes, T_4 is glucuronidated by the UGT1A1, UGT1A3, UGT1A8 and UGT1A10 isoforms (40). Injection of T_4 into rats results in detection T_4-glucuronide and rT_3-glucuronide in bile (41), while injection of T_3 results in T_3-glucuronide as the primary compound detected in bile (42). This suggests glucuronidation is a robust metabolic pathway in liver. In some cases, glucuronidation alters deiodination. In rat hepatocytes, T_3-glucuronide is not deiodinated, and the detectable 3,3'-T_2-glucuronide arises from direct glucuronidation of 3,3'-T_2 and not through deiodination of T_3-glucuronide (43). However, T_4-glucuronide is deiodinated to T_3-glucuronide, but the rate of this deiodination is slower than the rate of T_4 to T_3 deiodination (44).

In euthyroid humans, T_4-glucuronide, T_3-glucuronide, rT_3-glucuronide, 3,3'-T_2-glucuronide, and 3',5'-T_2-glucuronide are all detected in urine (45), suggesting that at least some of the glucuronidated conjugates are targeted for elimination. However, glucuronidation does not occur exclusively in the liver or kidneys (38, 46) and is a reversible modification (47), which suggests that glucuronidation may not exclusively target elimination pathways. Rat cardiofibroblasts are capable of conjugating and secreting T_4 and T_3 glucuronides, and T_4 and T_3 glucuronides are taken up by cultured H9c2(2-1) myoblasts at a faster rate than unconjugated hormones and also stimulate

differentiation to myotubes to the same extent as unconjugated T_4 and T_3 (38, 48). The presence of β-glucuronidase activity in H9c2(2-1) myotubes, rat cardiofibroblasts and rat heart homogenates (38, 46, 48) as well as UGT activity in rat heart homogenates (46) suggest glucuronidation may be important for tissue specific action of TH.

THs are substrates for sulfation on the outer ring hydroxyl group. Isoforms of the sulfotransferase (SULT) enzyme family catalyze sulfation of TH, including human SULT1A1 and SULT1A3, and rat SULT1B1 and SULT1C1 (49, 50). Sulfation of THs, including T_4, T_3, rT_3, and $3,3'$-T_2, also occurs in human and rat liver, kidney and brain cytosols (49, 50). T_3-sulfate (T_3S) is present in rat liver and hypothalamus, and $3,3'$-T_2S is present in brain, but undetectable in liver or pituitary (25). While the concentration of T_3S is lower than unconjugated T_3 (164 fmol/g and 2106 fmol/g in liver, respectively) (25), the differing tissue distributions of sulfated hormones suggest that sulfation is a tissue and hormone specific modification that may play a role in regulating hormone action and distribution.

$3,3'$-T_2S is present in euthyroid human serum (0.86 nM), and increases in cases of hyperthyroidism and pregnancy (51). In a developing fetal sheep, serum concentrations of both T_3S and $3,3'$-T_2S (50 ng/dL and 68 ng/dL, respectively) are greater than the serum concentration of T_3 (18 ng/dL) (52). Sulfated THs are able to transfer from the fetus to the mother, as indicated by increased maternal serum and urine T_3S and $3,3'$-T_2S following an injection of T_3 into the fetus (53). Sulfated iodothyronines are thought to function as a regulatory mechanism for the availability of T_3, since T_3S is more rapidly deiodinated than T_3 in rat liver microsomes (54, 55). Since sulfation is reversible, it is

possible that, similar to glucuronidation, sulfation may contribute to tissue specific TH actions (55).

1.6 Iodothyroacetic acids

THs undergo alanine side chain oxidative deamination to form iodothyroacetic acids (TA_x, Figure 1-1). TA_4 and TA_3 were first identified as endogenous compounds in mouse liver and kidney (56). Later, it was determined that T_4 and T_3 are both converted into the corresponding acetic acids, TA_4 and TA_3 *in vitro* in rat kidney, liver, and heart (57-59), and *in vivo* in rats and humans (13, 60, 61).

Iodothyroacetic acids are metabolized by similar pathways as iodothyronines. In rat liver TA_3 is glucuronidated and sulfated, and also sequentially deiodinated on the inner ring to $3,3'-TA_2$ and $3'-TA_1$ (62). Both $3'-TA_1$ and $3,3'-TA_2$ are glucuronidated in rat liver, and $3,3'-TA_2$ is sulfated as well (62). These conjugation and deiodination pathways are similar to what is observed for T_3 and other iodothyronines, suggesting parallel metabolic pathways regulate endogenous TH derivatives.

1.7 Ether link cleavage

A proposed pathway of TH metabolism that involves modification of the carbon skeleton is cleavage of the ether linkage to produce DIT. Ether link cleavage has been shown to occur *in vitro* in rat liver microsomes and extracts (63, 64). However, no evidence of ether link cleavage *in vivo* has been found using radiolabeled THs (29, 65, 66). In fact, T_0 and TA_0, the fully deiodinated thyronine and thyroacetic acid, respectively, each with

intact ether linkages, have been detected in human urine (29, 30). Additionally,

circulating levels of DIT in human were found to correlate with thyroid status, and levels

of DIT in athyreotic (lacking a functional thyroid gland) patients on T_4 replacement were

lower than DIT levels in hypothyroid patients (10-25 pM vs 101 ± 71 pM, respectively)

(67). This suggests that ether link cleavage is not a major component of TH metabolism

in the euthyroid state, and circulating DIT is likely due to direct gland secretion.

1.8 Non-T_3 mediated action of thyroid hormones

While most effects of TH are thought to result from T_3 binding to TR, additional TH

metabolites display some biological activity. A cell surface receptor, the αVβ3 integrin

receptor, binds T_4 and is thought to be responsible for some non-genomic effects of TH,

including activation of mitogen-activated protein kinase (MAPK) (68). Both T_4 and rT_3

stimulate actin polymerization in astrocytes, and 3,5-T_2 affects mitochondrial respiration

(39).   The thyroacetic acids also display some biological activity. TA_3 binds to the TR

with greater affinity than T_3 (39) and TA_4 inhibits T_4 mediated activation of MAPK (69).

The physiological significance of non-genomic action of TH metabolites is an ongoing

area of research.

1.9 Iodothyronamines

A proposed metabolic pathway of THs is decarboxylation of the alanine side chain to

form iodothyronamines (T_xAM) (Figure 1-1). The earliest reported syntheses and

studies of thyronamines date to the 1920's (70, 71). Later studies from the 1950's and

1960's showed deamination of non-iodothyronamine (T_0AM) to the corresponding

thyroacetic acid, suggesting thryonamines may be biosynthetic intermediates in the

metabolism of thyronines to thyroacetic acids (72). In a functional assay, T_3AM was

more effective than T_3 or T_4 in stimulating tadpole metamorphosis (73). This led to the

hypothesis that thyronamines were decarboxylated metabolites of TH, despite the lack of

detection of an endogenous iodothyronamine (72, 74).

In the last 10 years, 3-iodothyronamine (T_1AM) and T_0AM have been identified as

endogenous compounds in mouse and guinea pig (Figure 1-4) (75). T_1AM is present

endogenously in hamsters, rat and human (76-81), and has a unique set of

pharmacological effects. A single dose of T_1AM acutely induces hypothermia (with a

nadir at two hours post injection) and a torpor-like state, and decreases cardiac output,

heart rate and systolic pressure (75). Similar cardiac effects were also observed in *ex

vivo* perfused heart systems in the presence of T_1AM (80). *In vivo*, T_1AM induces

ketonuria, and also a shift in the respiratory quotient (RQ) from ~0.9 to 0.7 indicating a

shift in fuel utilization from predominately carbohydrates to predominately lipids (75, 76).

T_1AM has also been shown to induced hyperglycemia and hypoinsulinemia, which peak

two hours after injection of T_1AM (82).

Interestingly, the physiological effects of T_1AM are similar to effects typically associated

with T_3, although opposite in magnitude and occurring on a much more rapid time scale.

While the endogenous target of T_1AM remains unknown, several *in vitro* targets have

been identified. First, T_1AM does not bind to the TRs and is not transported by the

thyroid hormone transporter MCT8 (75, 83), suggesting there are distinct molecular

targets for iodothyronines and iodothyronamines. T_1AM has also been shown to bind the

α2A-adrenergic receptor (82) but does not activate the β2-adrenergic receptor (75).

T_1AM binds and activates rat and mouse trace amine associated receptor 1 (TAAR1), a G protein-coupled receptor, *in vitro* (75), but this receptor does not mediate the *in vivo* hypothermic action of T_1AM (84), indicating that TAAR1 is likely not the endogenous target of T_1AM. T_1AM inhibits the dopamine, norepinephrine and vesicular monoamine transporters in rat brain synaptosome preparations (85) and alters tyrosine phosphorylation patterns in rat heart homogenates (80). While several potential targets have thus far been identified, more work is needed to clarify the *in vivo* targets of T_1AM.

Despite differences in pharmacological properties, T_1AM and other iodothyronamines share some similarities with THs, particularly metabolic modifications (Figure 1-4). *In vitro*, iodothyronamines are substrates for the deiodinase enzymes (86), and the human SULT enzymes (87). T_0AM, T_1AM and T_3AM are all substrates for SULT1A3 (87), which also catalyzes the sulfation of 3,3'-T_2, rT_3, T_3 and T_4 (49), suggesting that thyronamines and thyronines are metabolized by overlapping pathways. To date, there is no *in vivo* evidence for thyronamine deiodination or sulfation. The only evidence of *in vivo* thyronamine metabolism involves oxidative deamination of T_1AM in rats to 3-iodothyroacetic acid (TA_1) (88). However, the deamination of T_1AM and T_3AM has been observed *in vitro* in HepG2 cells (88) which is consistent to previously reported deamination of T_0AM in rat kidney mitochondria (72).

Figure 1-4: Metabolic pathways of T$_1$AM.
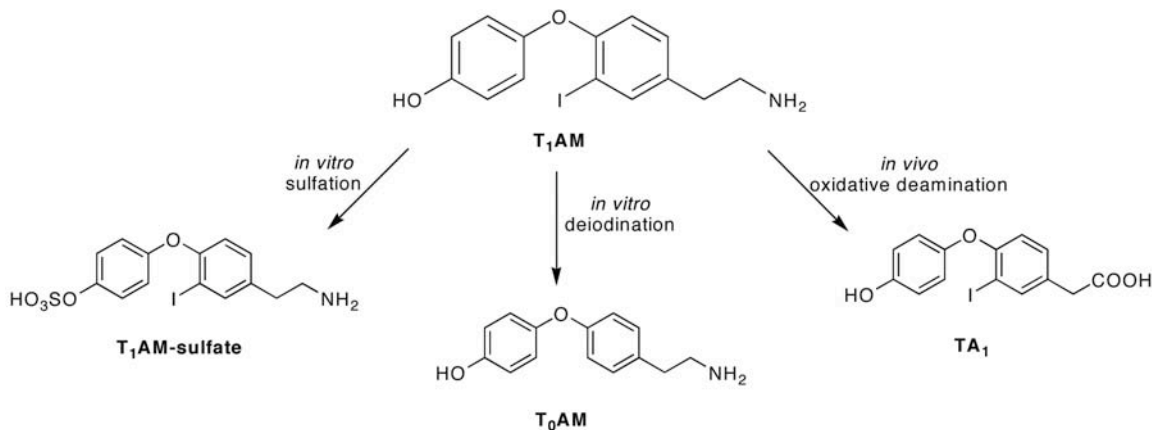
T$_1$AM is metabolized by sulfation and deiodination *in vitro* and oxidative deamination *in vivo*.

1.10 Methods of Analysis

Many of the early studies of TH metabolism utilized radiolabeled hormones that could be distinguished from endogenous compounds. The radiolabel employed was typically ^{131}I, and the readout was either column or paper chromatography in which the location of radioactivity was correlated to the location of known standards (10-13, 58). While this approach can be valuable, it also has many drawbacks. First, chromatographic conditions that are unable to clearly separate compounds make it difficult to definitively identify radioactively labeled spots (56). Second, the use of radiolabels can provide relative distributions of compounds by counting the total radioactivity, but does not provide quantitative values (11, 13, 56, 58). Finally, the use of radiolabels is useful for monitoring the fate of the radiolabel, but provides little information on additional pathways of metabolism. For example, the use of radioiodine in investigating the

15

hypothetical metabolism of T_4 to T_1AM may not provide definitive answers. T_4 contains four iodines while T_1AM contains just one. Most studies have used commercially available, outer-ring labeled T_4 or T_3, and this outer-ring radioiodine would be removed during the putative conversion to T_1AM. Additionally, the hypothetical metabolism of T_4 to T_1AM would require decarboxylation of the alanine side chain. Alterations to the carbon structure are not directly monitored with the use of radioiodine.

The use of radiolabeled THs was later applied to quantitation of endogenous hormone levels. Radioimmunoassays (RIAs), using radiolabeled standards, have been extensively used to quantify various THs (25-27, 36, 37). RIAs are useful in providing quantitative information but are not ideal for studying hormone metabolism. A few drawbacks to RIAs are that antisera must be generated separately for each compound to be studied (26) and each assay provides information on only one compound. Cross-reactivity with other compounds can also interfere with results. One RIA for 3,3'-T_2S displays 5.3% cross reactivity with T_1S (51) and an RIA for T_0 displays 160% cross-reactivity with TA_0 (30). Another drawback is that cross-reactivity must be assessed individually for each potentially interfering compound and does not account for compounds not directly assessed or unknown compounds.

More recently, liquid chromatography-tandem mass spectrometry (LC-MS/MS) methods have been developed and implemented for studying THs (89-92). LC-MS/MS methods couple an HPLC, providing chromatographic separation of a mixture of compounds, with a tandem MS, which provides improved structural information for the compounds of interest. LC-MS/MS methods have many advantages over RIAs for quantifying endogenous compounds. For instance, LC-MS/MS methods can quantify multiple

16

hormones from a single sample and a single injection (18, 34, 89). Another advantage of LC-MS/MS methods over RIAs is improved sensitivity. RIAs for T_4 report the lower limit of quantitation (LLOQ) at 1.2 μg/dL (93), while lower limits of detection (LLOD) for T_4 by LC-MS/MS are reported at 0.5 ng/dL or lower (89, 94). LC-MS/MS has thus far been the method of choice to analyze T_1AM (75, 77, 79-81). LC-MS/MS methods for T_1AM have LLODs and LLOQs ranging from 100 pM to 300 pM (34, 77), which are ~100 fold lower than the LLOQ of the single immunoassay for T_1AM, which is 10 nM (78). LC-MS/MS methods can distinguish isotopically labeled compounds (77, 80, 81), making it a suitable technique for metabolism studies utilizing isotopically labeled precursors. LC-MS/MS is the ideal technique to address questions of T_1AM metabolism.

1.11 Summary

The relationship between iodothyronines and iodothyronamines is a major question in TH metabolism that remains unanswered. Iodothyronines and T_1AM share structural similarities including a biaryl ether carbon skeleton and the presence of iodine. Iodothyronamines are metabolized by pathways similar to iodothyronines and are oxidatively deaminated *in vitro* to produce a known T_3 metabolite (88). These similarities between iodothyronamines and iodothyronines generated the hypothesis that the endogenous compound T_1AM is an extrathyroidal metabolite of T_4. The following dissertation investigates the metabolic relationship between THs and T_1AM.

Chapter 2: The synthesis of $^{13}C_9$-^{15}N-labeled 3,5-diiodothyronine and thyroxine

This work is in press as "The synthesis of $^{13}C_9$-^{15}N-labeled 3,5-diiodothyronine and thyroxine" by Hackenmueller SA and Scanlan TS, *Synthetic Communications* (production tracking number: LSYC 639005), and is reprinted by permission of Taylor & Francis Group (http://www.tandfonline.com). HRMS and MS/MS spectra for ^{13}C-labeled compounds were obtained from the Mass Spectrometry Laboratory at the University of Illinois at Urbana-Champaign. David Peyton and Cheryl Hodson at Portland State University assisted with obtaining and interpreting ^{13}C-decoupled ^{1}H, ^{13}C, HSQC and HMBC NMR spectra.

2.1 Introduction

Thyroid hormones (THs) are important endocrine signaling molecules that regulate a variety of physiological functions, including body temperature, cardiac function, metabolism and mood. THs are synthesized and secreted by the thyroid gland predominantly as 3,5,3',5'-tetraiodothyronine (T_4, thyroxine), which undergoes extrathyroidal deiodination to 3,5,3'-triiodothyronine (T_3). T_3 is largely considered to be the active form of the hormone and exerts its effects by binding to TH nuclear receptors and regulating transcription of TH responsive genes. In addition to the commonly known transcriptional actions of TH, there are rapid, non-transcriptionally mediated effects of TH that remain less well understood, suggesting the existence of additional biologically active TH metabolites (1, 68).

T_1AM is an endogenous compound present in serum and various tissues of rat, hamster and human (75-78). Acute administration of T_1AM *in vivo* results in induction of a torpor-like state characterized by hypothermia, bradycardia, a shift in respiratory quotient from carbohydrate to lipid utilization, hyperglycemia and hypoinsulinemia (75, 76, 82). In an *ex vivo* perfused rat heart, T_1AM decreases cardiac output (75, 80). These effects tend to oppose those normally attributed to T_3, and suggest that T_1AM may also play a role in TH signaling by modulating the effects of T_3.

Figure 2-1: Structures of T_4, 3,5-T_2 and T_1AM.
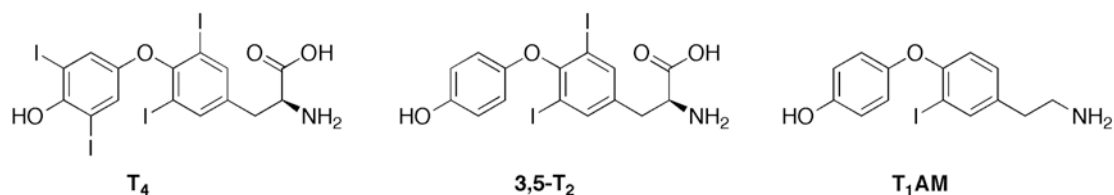
Structural similarities between T_4 and T_1AM (Figure 2-1) have led to speculation that

T_1AM is a deiodinated and decarboxylated derivative of TH, but this relationship has not

been directly investigated. In order to test this metabolic question, it is necessary to

definitively trace the fate of a suspected precursor, which can be accomplished through

incorporation of a label in T_4. Several methods for analyzing T_1AM by liquid

chromatography coupled with tandem mass spectrometry (LC-MS/MS) have been

reported (34, 77, 81). This technique is ideal for analysis of isotopically labeled

compounds, since any metabolites arising from a labeled precursor would contain a

mass signature distinct from endogenous compounds. T_4, as the predominant form of

TH produced endogenously, is the first candidate to test as a suspected precursor to

T_1AM. Based on *in vitro* data showing that T_3 is not a substrate for outer ring

deiodination, it remains unclear if 3,5-diiodothyroinine (3,5-T_2), another endogenous TH,

arises from extrathyroidal metabolism of T_4 or some alternate biosynthetic pathway (34).

This indicates a second potential candidate for a biosynthetic precursor to T_1AM. Herein

we describe the novel syntheses of $^{13}C_9$-^{15}N-3,5-T_2 and $^{13}C_9$-^{15}N-L-thyroxine ($^{13}C_9$-^{15}N-T_4)

that can be used to study TH metabolism by LC-MS/MS.

2.2 Results and Discussion

2.2.1 Determination of Synthetic Route

As T_4 is an endogenous compound used for therapeutic purposes, the synthesis has been previously reported. For this synthesis of isotope labeled $3,5-T_2$ and T_4, the synthetic route used by Glaxo for commercial scale T_4 was initially attempted (95). Unlabeled material was used to investigate and optimize all synthetic routes prior to use of labeled material. Following the commercial scale synthesis of T_4 for a labeling strategy was unsuccessful since reaction products were unable to be purified by crystallization due to the smaller scale of this synthesis.

In the absence of a suitable existing synthetic route to T_4, a novel synthesis with acceptable yields needed to be developed and optimized. A retrosynthetic analysis of T_4 (Figure 2-2) indicates tyrosine as the likely starting material. The first key intermediate in the synthesis would be protected diiodo-tyrosine. The first step in optimizing the synthesis of T_4 was to determine the optimal order of reactions; iodination followed by protection of the amine and carboxylic acid, or protection of the amine and carboxylic acid followed by iodination. Bis-iodination of tyrosine with HCl and ICl in water, followed by O-methyl ester and N-Boc protections (96-98) produced the desired product, Boc-3,5-diiodo-L-tyrosine-OMe, but yields were 16% or less over 3 steps. These yields were lower than desired for the initial steps of the synthesis.

Figure 2-2. Retrosynthetic analysis of T₄.
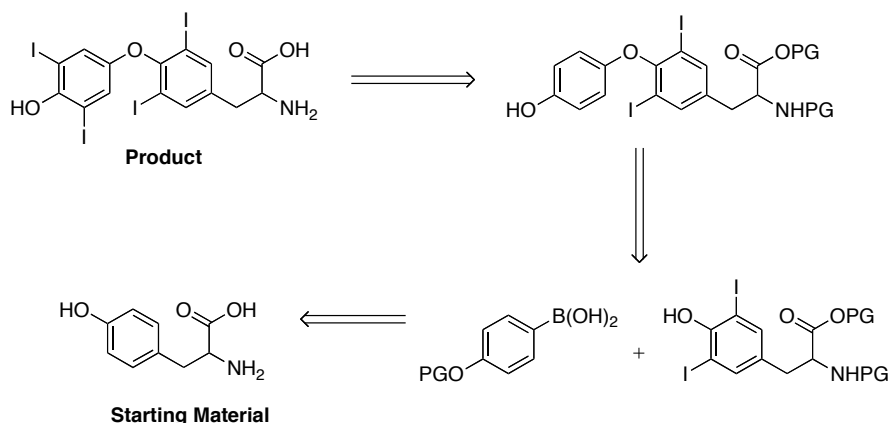
In order to increase the yields for the first steps of the reaction, the carboxylic acid and amine of tyrosine were protected prior to iodination. O-methyl ester formation followed by N-Boc protection produced **2** (Scheme 2-1) in 79% yield or greater and was used for all future syntheses (97, 98). The next step was to optimize conditions for bis-iodination of N-Boc-L-tyrosine-OMe. Iodination methods involving I_2 and KI in 40% $MeNH_2$ (A. Nilsen, unpublished results), ICl in AcOH, or IPy_2BF_4 in DCM were not successful (99, 100). The method of Bovonsombat *et al.* using N-iodosuccinimide (NIS) in acetonitrile produced the desired product in 32% yield (101). This method was used as the basis for optimization of bis-iodination of Boc-L-tyrosine-OMe. Conditions are given in Table 2-1. NIS in DCM at 0 °C for 30 minutes resulted in a 64% yield and was used for all future bis-iodinations of Boc-L-tyrosine-OMe.

Table 2-1: Optimization of Bis-iodination of Boc-L-tyrosine-OMe.

Reagent/Solvent	Temperature, Time	Yield (%)
NIS, CH$_3$CN	RT, 6 hours	32.1
NIS, CH$_3$CN	RT, 24 hours	15.4
NIS, CH$_3$CN	RT, 90 minutes	34.5
NIS, DCM	RT, 2.5 hours	45.8
NIS, CH$_3$CN	0 °C, 30 minutes	38.4
NIS, DCM	0 °C, 30 minutes	64.2

2.2.2 Synthesis of $^{13}C_9$-^{15}N-3,5-T$_2$

Scheme 2-1: Synthesis of $^{13}C_9$-^{15}N-3,5-T$_2$.
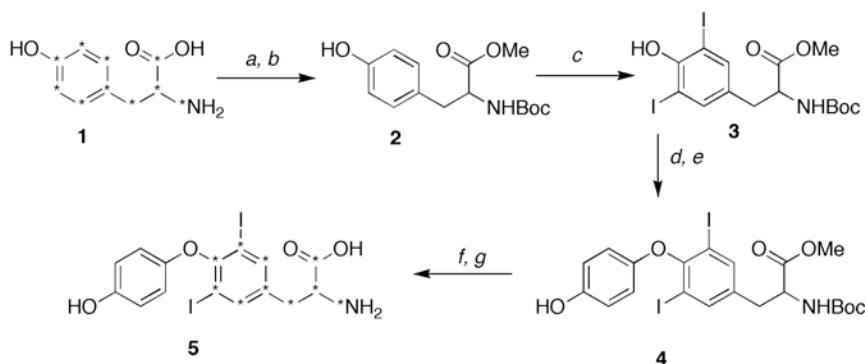
Reagents and conditions: *a*, HCl, 2,2-dimethoxypropane; *b*, BOC$_2$O, NaHCO$_3$, THF/H$_2$O; *c*, NIS, DCM; *d*, 4-(Triisopropyl)silyloxyphenyl boronic acid, Cu(OAc)$_2$, DIPEA, pyridine, DCM; *e*, TBAF, THF; *f*, LiOH, MeOH/H$_2$O; *g*, HCl, dioxane; * indicates ^{13}C or ^{15}N.

The synthesis of $^{13}C_9$-^{15}N-L-T$_2$ was carried out in parallel with unlabeled T$_2$ according to the route shown in Scheme 2-1. Commercially available $^{13}C_9$-^{15}N-L-tyrosine **1** was N-Boc and O-methyl ester protected and bis-iodinated with N-iodosuccinimide in DCM, a modification of the method of Bovonsombat *et al.*, to give Boc-$^{13}C_9$-^{15}N-3,5-diiodo-L-tyrosine-OMe **3** in 59% yield over the 3 steps (97, 101). 4-(Triisopropyl)silyloxyphenyl boronic acid was synthesized as previously described and coupled to **3** via a copper (II) mediated biaryl ether formation (98, 102). Deprotection with TBAF gave Boc-3,5-diiodo-$^{13}C_9$-^{15}N-L-thyronine-OMe **4** in 30% yield over two steps. Sequential deprotection with lithium hydroxide to cleave the methyl ester and hydrochloric acid to cleave the t-Boc

23

gave $^{13}C_9$-^{15}N-3,5-T_2 **5**, in 28% yield as the TFA salt after purification by preparative

HPLC (103). Due to difficulty in interpreting ^1H NMR spectra as a result of ^{13}C coupling

effects, labeled intermediates and $^{13}C_9$-^{15}N-3,5-T_2 were characterized by HRMS and

chromatographic comparison to unlabeled standards, which were synthesized in parallel

to $^{13}C_9$-^{15}N-labeled compounds. MS/MS fragmentation spectra of $^{13}C_9$-^{15}N-3,5-T_2 and

unlabeled T_2 are shown in Figure 2-3. As expected, the labeled T_2 is 10 amu heavier

than unlabeled T_2.

Figure 2-3: MS/MS of T_2.
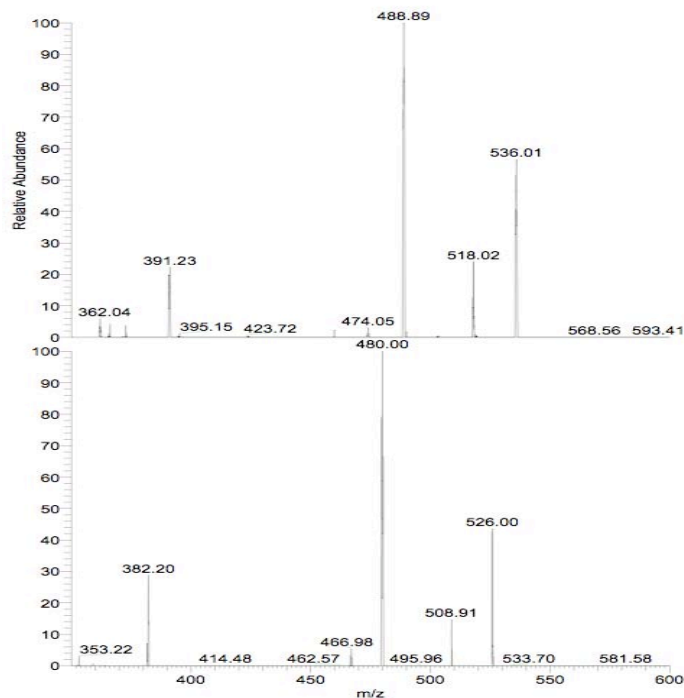
MS/MS fragmentation spectra of $^{13}C_9$-^{15}N-3,5-T_2 (top) and T_2 (bottom).

24

2.2.3 Synthesis of $^{13}C_9$-^{15}N-L-T$_4$

Scheme 2-2: Synthesis of $^{13}C_9$-^{15}N-T$_4$.
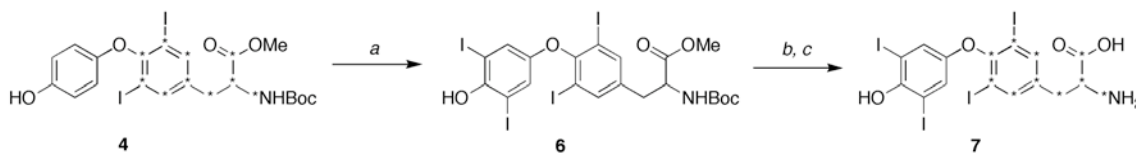
Reagents and conditions: *a*, ICl, BuNH$_2$, 4:1 DCM/DMF; *b*, LiOH, MeOH/H$_2$O; *c*, HCl, dioxane; * indicates ^{13}C or ^{15}N.

The synthesis of $^{13}C_9$-^{15}N-L-T$_4$ was carried out in parallel with unlabeled T$_4$ according to the route shown in Scheme 2-2. Biaryl ether **4** was bis-iodinated on the outer ring with iodine monochloride and butylamine to give N-Boc-$^{13}C_9$-^{15}N-T$_4$-OMe **6** in 37% yield (98). Sequential deprotection of **6** as described above produced $^{13}C_9$-^{15}N-T$_4$ **7**, which was purified by preparative HPLC as the TFA salt in 23% yield from **6**. As described for $^{13}C_9$-^{15}N-3,5-T$_2$, synthetic intermediates and $^{13}C_9$-^{15}N-L-T$_4$ were characterized by HRMS and chromatographic comparison to unlabeled standards, which were synthesized in parallel. MS/MS fragmentation spectra and HPLC chromatograms of $^{13}C_9$-^{15}N-L-T$_4$ and unlabeled T$_4$ are shown in Figure 2-4, again confirming the correct *m/z* shift for the labeled T$_4$.

Figure 2-4: MS/MS of T$_4$.
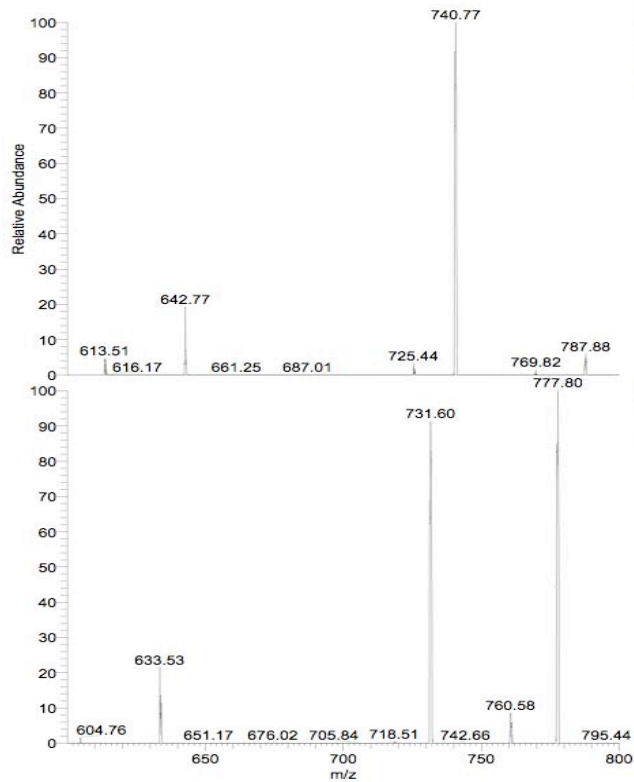
MS/MS fragmentation spectra of $^{13}C_9$-^{15}N-L-T$_4$ (top) and T$_4$ (bottom).

^{125}I, ^{131}I, and ^{14}C labeled THs have been used to study TH metabolism and pharmacokinetics but the use of radiolabels in metabolism studies is limited to tracing the fate of the radioactivity and does not provide information on metabolic pathways that do not involve radiolabeled portions of the hormones (13, 61, 104-111). In addition, the use of outer ring labeled [^{125}I]-T$_4$, the most commonly employed labeled form of T$_4$, could not be used to follow T$_4$ metabolites that are deiodinated in the outer ring, such as 3,5-T$_2$ and T$_1$AM. The incorporation of non-radioactive isotopes such as ^{13}C or ^{15}N into T$_4$ and other THs, allow for complete metabolite coverage of alternate pathways of TH metabolism by LC-MS/MS. The syntheses of unlabeled and of ^{13}C-labeled T$_4$ and T$_3$

26

have been reported, but here we report an alternate synthetic route to produce a novel labeled T_4 containing ^{15}N and ^{13}C (95, 102, 112-114). While the synthesis of ^{125}I-3,5-T_2 has been reported, to our knowledge this is the first reported synthesis of a stable isotope labeled T_2 (115).

2.3 **Experimental**

2.3.1 *General*

All chemicals used for synthesis were purchased from Aldrich, Sigma-Aldrich, Fluka, Acros or TCI. Anhydrous solvents were obtained from an in-house solvent distillation system. Intermediates were purified by flash chromatography (HPFC) on a Biotage SP1 purification system with a fixed wavelength UV detector (Biotage, Charlotte NC). Syntheses of unlabeled and ^{13}C-^{15}N labeled compounds were carried out in parallel. The synthetic scheme was prospected using unlabeled material, which also served as standards to match ^{13}C-^{15}N-labeled compounds by TLC. NMR spectra for ^{13}C-labeled compounds were difficult to interpret due to ^{13}C J-couplings. For this reason, ^{13}C labeled compounds were characterized by high-resolution mass spectrometry (HRMS). ^{1}H NMR were taken for unlabeled compounds. ^{13}C-decoupled ^{1}H, ^{13}C, HSQC and HMBC NMR spectra were obtained for compound **4**. NMR spectra were taken on a Bruker 400 (400 MHz) and spectra were processed using ACD/NMR Processor Academic Edition or Bruker TopSpin software. NMR spectra are available in Supplementary material. HRMS and MS/MS fragmentation using electrospray ionization (ESI) in positive polarity was performed at the Mass Spectrometry Laboratory at the University of Illinois at Urbana-Champaign (UIUC). MS/MS fragmentation using ESI in

positive polarity was performed at the Mass Spectrometry Laboratory at UIUC or on a TSQ Quantum Discovery triple-quadrupole (Thermo, San Jose CA) at OHSU. HRMS are reported for all novel compounds. ^{1}H NMR for all unlabeled intermediates as well as MS/MS fragmentation spectra for labeled intermediates are in Appendix A.

2.3.2 Boc-L-Tyrosine-OMe

Concentrated hydrochloric acid (2.7 ml) was added drop-wise to a stirring solution of L-tyrosine (0.500 g, 2.76 mmol) in 2,2-dimethyoxypropane (33 ml). The reaction was stirred at room temperature for 24 hours and the crude reaction mixture was used in the next step.

NaHCO$_3$ (7.5 ml, 1.1 M in water) was added to crude L-Tyrosine-OMe and Boc$_2$O (0.620 g, 2.85 mmol) in THF (12 ml). The reaction was stirred at room temperature for 24 hours. The reaction was diluted with ether (20 ml) and the aqueous layer was extracted twice with ether. The combined organic layers were washed with 0.5 M HCl and brine, and dried over MgSO$_4$. The crude material was purified by HPFC (10-80% ethyl acetate/hexanes over 10 column volumes) to give Boc-OMe-L-Tyrosine (0.787 g, 2.66 mmol, 96.5% yield). ^{1}H NMR (400 MHz, CHLOROFORM-d)δ ppm 1.42 (s, 9 H) 2.98 - 3.04 (m, 2 H) 3.71 (s, 3 H) 4.54 (d, J=7.33 Hz, 1 H) 4.98 (d, J=7.58 Hz, 1 H) 5.10 (br. s., 1 H) 6.74 (d, J=7.83, 2 H) 6.98 (d, J=8.34, 2 H). Previously reported ^{1}H NMR (200 MHz, CHLOROFORM-d) δ ppm 1.4 (s, 9H) 3.0 (m, 2 H) 3.7 (s, 3 H) 4.55 (m, 1 H) 5.1 (d, J=8.3, 1 H) 6.75 (d, J=8.4, 2 H) 6.95 (d, J=8.4, 2 H) (97).

Boc-$^{13}C_9$-^{15}N-L-tyrosine-OMe **2** was synthesized using the same procedure with $^{13}C_9$-^{15}N-l-tyrosine (0.500 g, 2.62 mmol) as starting material, in 87.2% yield (0.702 g, 2.30 mmol). HRMS (ESI+) for $C_6^{13}C_9H_{22}^{15}NO_5$ [M+H] calculated 306.1770, found 306.1776.

2.3.3   Boc-3,5-diiodo-L-Tyrosine-OMe

N-iodosuccinimide (1.2 g, 5.32 mmol) was added to a stirring solution of Boc-L-Tyrosine-OMe (0.787 g, 2.66 mmol) in DCM (17.7 ml) at 0 °C. The reaction was monitored by TLC (40% ethyl acetate/hexanes) for consumption of starting material, which occurred in ~40 minutes. A solution of 10% $Na_2S_2O_3$ was added drop-wise, and the reaction mixture was diluted with water and extracted three times with ethyl acetate. The ethyl acetate layers were combined and dried over $MgSO_4$. The crude material was purified by HPFC (10-80% ethyl acetate/hexanes over 10 column volumes) to give Boc-3,5-diiodo-L-Tyrosine-OMe as a white solid (0.908 g, 1.66 mmol, 67.5% yield). ^{1}H NMR (400 MHz, CHLOROFORM-d) δ ppm 1.45 (s, 9 H) 2.86-3.05 (m, 2 H) 3.74 (s, 3 H) 4.48 (br. s., 1 H) 5.02 (br. s., 1 H) 5.70 (s, 1 H) 7.44 (s, 2 H). ^{1}H NMR spectrum is available in supplemental figure S3. Previously reported ^{1}H NMR (400 MHz, CHLOROFORM-d) δ 1.45 (s, 9 H) 2.91 (dd, J=8.0 Hz, J=14.0 Hz, 1 H) 3.00 (dd, J=4.0 Hz, J=14.0 Hz, 1 H) 3.74 (s, 3 H) 4.49 (dd, J=4.0 Hz, J=8.0 Hz, 1 H) 5.01 (s, 1 H) 7.44 (s, 1 H) (116).

Boc-3,5-diiodo-$^{13}C_9$-^{15}N-L-Tyrosine-OMe **3** was synthesized following the same procedure from Boc-$^{13}C_9$-^{15}N-L-tyrosine-OMe (0.702 g, 2.30 mmol) starting material, in 67.5% yield (0.864 g, 1.55 mmol). HRMS (ESI+) for $C_6^{13}C_9H_{19}I_2^{15}NNaO_5$ [M+Na] calculated 579.9523, found 579.9528.

2.3.4 Boc-3,5-diiodo-L-Thyronine-OMe

4Å molecular sieves were added to a round bottom flask that was then flame dried and flushed with dry air. 4-(Triisopropyl)silyloxyphenyl boronic acid (0.612 g, 2.08 mmol), DCM (6.3 ml), diisopropylethylamine (4.15 mmol) and pyridine (4.15 mmol) were added under argon. Dry copper(II) acetate (0.151 g, 0.83 mmol) was added and the reaction mixture was stirred under argon for 10 minutes. Boc-3,5-diiodo-L-tyrosine-OMe (0.452 g, 0.83 mmol) was added in DCM (2 ml) over 5 minutes. The reaction was stirred at room temperature under dry air for 48 hours. The reaction was diluted with ether, filtered through silica/celite, and sequentially washed with HCl, H_2O and brine, and dried over $MgSO_4$. The crude reaction material was taken into the next reaction.

Crude biaryl ether was dissolved in THF and cooled to 0 °C. Tetra-N-butylammonium fluoride (3.15 mmol) was added drop-wise over 5 minutes. The reaction was stirred at room temperature for 15 minutes. The reaction was diluted with ethyl acetate and washed with HCl. The aqueous layer was washed with ethyl acetate, and the combined organic layers were washed sequentially with H_2O and brine, and dried over $MgSO_4$. The crude product was purified by HPFC (10-80% ethyl acetate/hexanes over 10 column volumes) to yield Boc-3,5-diiodo-L-thyronine-OMe as a solid (0.196 g, 0.31 mmol, 37.0% yield over two steps). ^{1}H NMR (400 MHz, CHLOROFORM-d)δ ppm 1.45 (s, 9 H) 2.81 - 3.16 (m, 2 H) 3.76 (s, 3 H) 4.54 (br. s., 1 H) 4.68 (br. s., 1 H) 5.11 (d, J=8.84, 1 H) 6.67 - 6.83 (m, 4 H) 7.63 (s, 2 H); HRMS (ESI+) for $C_{21}H_{23}I_2NNaO_6$ [M+Na] calculated 661.9512, found 661.9512.

Boc-3,5-diiodo-[13]C$_9$-^{15}N-L-Thyronine-OMe **4** was synthesized following the same procedure from Boc-3,5-diiodo-[13]C$_9$-^{15}N-L-tyrosine-OMe (0.547 g, 0.98 mmol) starting

material, in 29.9% yield (0.190 g, 0.29 mmol). HRMS (ESI+) for $C_{12}{}^{13}C_9H_{24}I_2{}^{15}NO_6$ [M+H] calculated 649.9965, found 649.9966. Additional characterization of this final common intermediate included ^1H, ^{13}C-decoupled ^1H, ^{13}C, HSQC and HMBC NMR spectra, which are in Appendix A.

2.3.5   3,5-Diiodo-$^{13}C_9$-^{15}N-L-Thyronine ($^{13}C_9$-^{15}N-T$_2$) **5**

To cleave the methyl ester, lithium hydroxide (0.39 mmol, 100 µl of 3.9 M in H_2O) was added to a stirred solution of Boc-3,5-diiodo-$^{13}C_9$-^{15}N-L-thyronine-OMe (0.051 g, 0.078 mmol) in methanol (300 µl) at 4 °C. The reaction was stirred at 4 °C for 90 minutes. Solvent was removed under argon and the crude reaction product was dried in a modified Abderhalden drying apparatus for use in the next step.

The dried crude reaction product from the methyl ester deprotection was dissolved in 4 M HCl in dioxane (300 µl). The reaction was stirred under argon at room temperature overnight. The reaction mixture was diluted with 500 µl of 1:1 water:acetonitrile and purified by preparatory HPLC using a Rainin HPXL Solvent Delivery system and a Prostar PDA detector (Varian Inc., Paolo Alto CA). Reaction product was injected onto a Varian Dynamax Microsorb C18 21.4x250 mm column and monitored at wavelength 254 nm. Mobile phases were A (water + 0.1% TFA) and B (acetonitrile + 0.1% TFA) with gradient conditions as follows: 5% B 0-5 minutes, 5-95% B 5-50 minutes, 95% B 50-65 minutes, 95-5% B 65-75 minutes, 5% B 75-90 minutes. Commercially available 3,5-T$_2$ was used to determine the retention time of the product, 31.5 minutes. Purity of final compound and comparison to commercial material was determined by analytical HPLC using a Poroshell 120 EC-C18 4.6 x 100 mm 2.7 µm column (Agilent Technologies,

Santa Clara CA), with mobile phases as described above and the following gradient conditions: 5% B 0-2 minutes, 5-95% B 2-10 minutes, 95% B 10-12 minutes, 95-5% B 12-13 minutes, 5% B 13-15 minutes. HRMS (ESI+) for $C_6{}^{13}C_9H_{14}I_2{}^{15}NO_4$ [M+H] calculated 535.9284, found 535.9291. HPLC chromatographs of synthetic $^{13}C_9$-^{15}N-T_2 and commercially available 3,5-T_2 are shown in Figure 2-5.

Figure 2-5. HPLC of T$_2$.
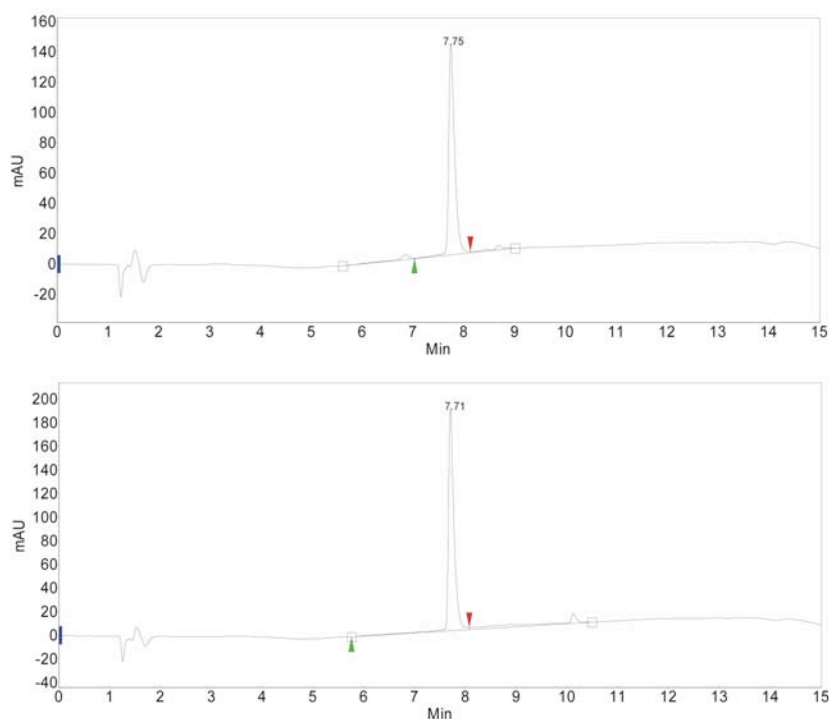
HPLC chromatographs of $^{13}C_9$-^{15}N-3,5-T_2 (top) and T_2 (bottom).

2.3.6   *Boc-3,3',5,5'-tetraiodo-L-thyronine-OMe*

Iodine monochloride in DCM (0.26 mmol, 260 µl) was added drop wise to a stirring solution of Boc-3,5-diiodo-L-thyronine-OMe (0.072 g, 0.11 mmol) and butylamine (0.64 mmol, 64 µl) in 4:1 DCM:DMF (3.7 ml) at 0 °C. The reaction was stirred at 0 °C for 20

minutes. The reaction was diluted with ethyl acetate and washed sequentially with HCl, 10% sodium thiosulfate, H_2O and brine, and dried over $MgSO_4$. The crude product was purified by HPFC (10-80% ethyl acetate/hexanes over 10 column volumes) to yield 3,3',5,5'-tetraiodo-N-Boc-OMe-L-thyronine as a brown solid (0.022 g, 0.025 mmol, 22.9% yield). ^1H NMR (400 MHz, CHLOROFORM-d)δ ppm 1.45 (s, 9 H) 2.91-3.18 (m, 2 H) 3.76 (s, 3 H) 4.54 (br. s, 1 H) 5.13 (br. s., 1 H) 5.48 (br. s., 1 H) 7.10 (s, 2 H) 7.64 (s, 2 H); HRMS (ESI+) for $C_{21}H_{21}I_4NNaO_6$ [M+Na] calculated 913.7445, found 913.7437.

Boc-3,3'-5,5'-tetraiodo-$^{13}C_9$-^{15}N-L-thyronine-OMe **6** was synthesized following the same procedure using Boc-3,5-diiodo-$^{13}C_9$-^{15}N-L-thyronine-OMe (0.150 g, 0.23 mmol) as starting material, in 36.9% yield (0.076 g, 0.085 mmol). HRMS (ESI+) for $C_{12}{}^{13}C_9H_{21}I_4{}^{15}NNaO_6$ [M+Na] calculated 923.7718, found 923.7715.

2.3.7   3,3',5,5'-Tetraiodo-$^{13}C_9$-^{15}N-L-Thyronine ($^{13}C_9$-^{15}N-T_4) **7**

To cleave the methyl ester, lithium hydroxide (0.43 mmol, 110 µl of 3.9 M in H_2O) was added to a stirred solution of Boc-3,3',5,5'-tetraiodo-$^{13}C_9$-^{15}N-L-thyronine-OMe (0.076 g, 0.085 mmol) in methanol (330 µl) at 4 °C. The reaction was stirred at 4 °C for 90 minutes. Solvent was removed under argon and the crude reaction product was dried in a modified Abderhalden drying apparatus for use in the next step.

The dried crude reaction product from the methyl ester deprotection was dissolved in 4 M HCl in dioxane (320 µl). The reaction was stirred under argon at room temperature overnight. To the reaction mixture, 500 µl of 1:1 water:acetonitrile was added, and the solution filtered through a 0.22 µm filter prior to purification by preparatory HPLC as

described previously. Commercially available T_4 was used to determine the retention time of the product, 37.7 minutes. Final product purity was determined by analytical HPLC using conditions described previously. HRMS (ESI+) for $C_6{}^{13}C_9H_{11}I_4{}^{15}NO_4$ [M+H] calculated 787.7217, found 787.7218. MS/MS fragmentation spectrum is available in supplemental figure S15. HPLC chromatographs of synthetic $^{13}C_9$-^{15}N-T_4 and commercially available T_4 are shown in Figure 2-6.

Figure 2-6: HPLC of T_4.
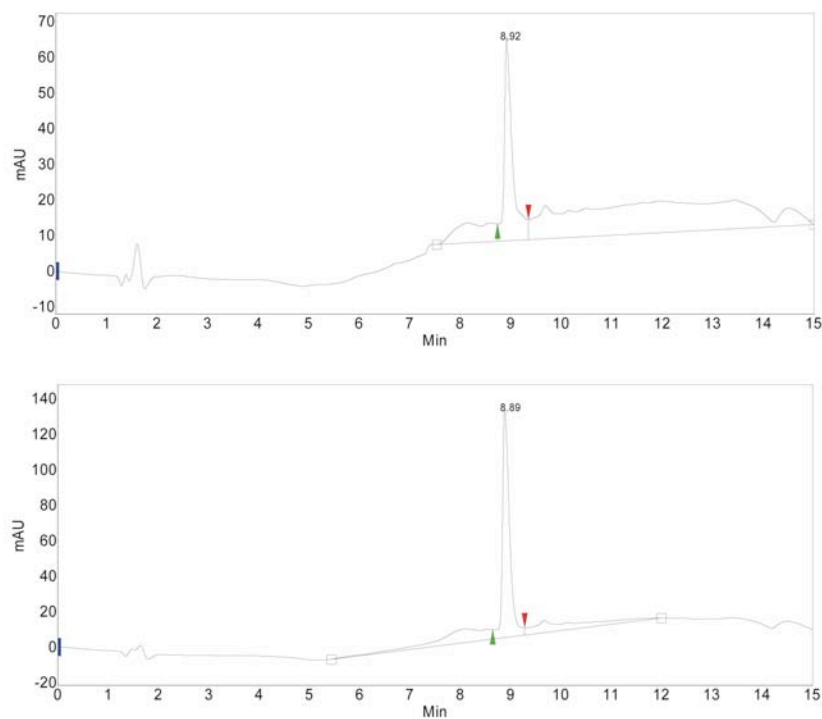
HPLC chromatographs of $^{13}C_9$-^{15}N-T_4 (top) and T_4 (bottom).

Chapter 3: The biosynthesis of 3-iodothyronamine is dependent on the thyroid gland and not on extrathyroidal thyroxine metabolism

This work is in submission as: Hackenmueller SA, Marchini M, Saba A, Zucchi R and Scanlan TS. Biosynthesis of 3-iodothyronamine (T_1AM) is dependent on the sodium-iodide symporter and thyroperoxidase but does not involve extrathyroidal metabolism of thyroxine. All animal experiments were conducted at Oregon Health & Science University in Portland, OR. Mouse tissues were shipped to the University of Pisa, where extraction of T_1AM and analysis by LC-MS/MS was done in collaboration with Riccardo Zucchi, Maja Marchini and Alessandro Saba.

3.1 Introduction

Thyroid hormone (TH) is synthesized in the thyroid gland predominantly as 3,5,3',5'-tetraiodothyronine (thyroxine, T_4). The first step in the biosynthesis of T_4 involves concentration of dietary iodide in the thyroid gland by the sodium-iodide symporter, which is followed by thyroperoxidase (TPO)-catalyzed iodination of tyrosine residues within the thyroglobulin protein. T_4 is a pro-hormone that is secreted from the thyroid gland and undergoes enzymatic outer ring deiodination to form 3,5,3'-triiodothyronine (T_3). T_3 is the active form of TH and it binds to the TH nuclear receptors to regulate transcription of TH responsive genes (117). TH mediated gene transcription affects a variety of physiological processes, including cardiac function, metabolism, bone turnover, body temperature, and cholesterol levels (1). While most effects of TH are transcriptionally mediated, there are some rapid effects that are thought to be transcriptionally independent (118, 119).

In addition to outer ring deiodination, T_4 is deiodinated on the inner ring to form 3,3',5'-triiodothyronine (reverse-T_3, rT_3), a metabolite with unknown physiological significance. Inner ring deiodination of either T_4 or T_3 is thought to be a mechanism for deactivating TH (19), yet deiodination pathways sequentially produce diiodo- and monoiodothyronines (27, 120). Additional metabolic pathways of TH include conjugation with either a sulfate or a glucuronic acid (55). T_4 and T_3 can undergo oxidative deamination of the alanine side chain to form the thyroacetic acid derivatives, Tetrac and Triac, both of which have biological activity. Triac has thermogenic effects (121) while

36

Tetrac inhibits T_4 actions initiated at the plasma membrane (69). This extensive

metabolism of TH beyond direct activation and deactivation of T_3 indicates that TH

metabolism is critical for regulating hormone action.

3-Iodothyronamine (T_1AM) is an endogenous derivative of TH present in rat, mouse,

hamster and human, with acute pharmacological effects (75, 76, 78, 79, 81). A single

pharmacological dose of T_1AM results in hypothermia, bradycardia, a shift in the

respiratory quotient, hyperglycemia and hypoinsulinemia within minutes to a few hours

(75, 76, 82). Structural similarities between T_4 and T_1AM, including the presence of

iodine and the biaryl ether carbon skeletons (Figure 3-1), suggest that T_1AM is a

metabolite of T_4. T_1AM is sulfated and deiodinated *in vitro,* and oxidatively deaminated

in vivo (86-88), indicating it is a substrate for the same metabolic pathways that act on

TH. A hypothesized biosynthetic pathway for T_1AM involves deiodination and

decarboxylation of TH. If decarboxylation of TH occurs, this would represent a

previously uncharacterized branch of TH metabolism and signaling.

Figure 3-1: Structures of T_4 and T_1AM
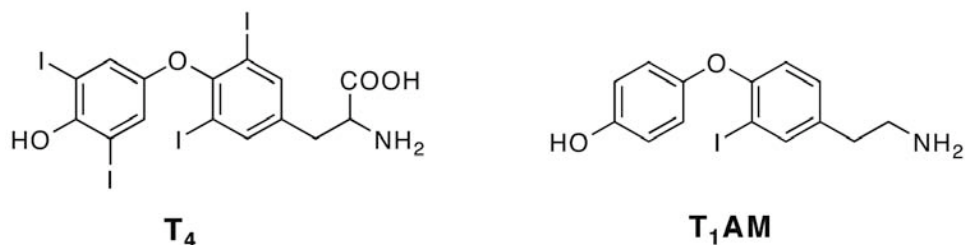
Several analytical methods have been developed to measure T_1AM levels, including an immunoassay and liquid chromatography-tandem mass spectrometry (LC-MS/MS) assays (34, 77, 78, 81). The advantage of LC-MS/MS over an immunoassay is that additional structural information is obtained. We have recently synthesized an isotope labeled T_4, $^{13}C_9$-^{15}N-T_4 (Hackenmueller & Scanlan. The synthesis of $^{13}C_9$-^{15}N-labeled 3,5-diiodothyronine and thyroxine. Synthetic Commun. Forthcoming 2012). $^{13}C_9$-^{15}N-T_4 ("heavy-T_4", H-T_4) is 10 amu heavier than unlabeled T_4, creating a unique mass signature that is detectable by mass spectrometry. This mass signature allows for H-T_4 and any metabolite arising from H-T_4 to be distinguishable from unlabeled T_4 and metabolites. In this study we use the labeled H-T_4 to test the hypothesis that T_1AM is a metabolite of T_4.

3.2 Materials and Methods

3.2.1 Animals

Male C57Bl/6J mice, 8-10 weeks old, were housed 4-5 per cage in a climate controlled room with a 12 hour light-dark cycle. All animals had *ad libitum* access to food and water. Experimental protocols were in compliance with the National Institutes of Health Guide for the Care and Use of Laboratory Animals and approved by the Oregon Health & Science University Institutional Animal Care & Use Committee.

3.2.2 Chemicals

For use with animals, potassium perchlorate ($KClO_4$) was purchased from MP Biomedicals (Solon OH). Methimazole (MMI) was purchased from Acros Organics

(Pittsburg PA). T_4 was purchased from Sigma (St. Louis MO) and H-T_4 was synthesized as previously described (Hackenmueller SA and Scanlan TS. The synthesis of $^{13}C_9$-^{15}N-labeled 3,5-diiodothyronine and thyroxine. Synthetic Commun. Forthcoming 2012). Human sera deficient in T_4 and T_3 was purchased from Sigma.

3.2.3 Hormone Manipulations

To determine the length of treatment necessary to induce hypothyroidism, mice were treated with 0.1% MMI and 0.2% $KClO_4$ in drinking water for 2, 4 or 6 weeks (122). Blood was collected and allowed to clot on ice for at least 30 minutes prior to centrifugation at 6000 x g. Sera was removed and stored at -80 °C until further use. Total serum T_4 was measured using a Coat-A-Count Total T_4 radioimmunoassay (RIA) kit (Siemens Healthcare Diagnostics, Deerfield IL).

For T_4 replacement studies, mice were pre-treated for 2 weeks and subsequently maintained on MMI and $KClO_4$ in drinking water for the duration of hormone replacement. T_4 or H-T_4 was dissolved in 0.01 N NaOH in sterile saline (0.9% NaCl, Hospira, Lake Forest IL) and administered as once daily subcutaneous injections (123). T_4 was administered once daily for 2, 3, 4 and 5 weeks to determine the time necessary to establish steady-state serum hormone levels. H-T_4 was injected once daily for 3 weeks to reestablish euthyroid hormone levels. At 24 hours following the final injection, serum was collected as described above, and tissues, including liver, heart, brain and kidney, were frozen immediately on dry ice and stored at -80 °C until used for hormone extraction. Total serum T_4 levels following hormone replacement were determined using the RIA kit described above.

3.2.4 T_1AM, T_3 and T_4 Extraction from Liver

T_1AM, T_3 and T_4 were extracted from mouse livers following a similar protocol to what has been previously described (77). Frozen livers were thawed, weighed, and homogenized in cold homogenization buffer (1 mL per 1 g of tissue, 154 mM NaCl, 10 mM NaH_2PO_4, pH 7.4) with 30 passes in a Potter-Elvehjem tissue homogenizer attached to a Glas-Col motor drive. Homogenates were centrifuged at 4000 x g for 15 min. Supernatants were collected and transferred to clean 15 mL polypropylene tubes, and 2.5 pmol d_4-T_1AM, and 25 pmol each of $^{13}C_6$-T_3 and $^{13}C_6$-T_4 were added as internal standards.   An additional 60 mg of NaCl was added per 1 mL of supernatant and the samples were incubated at rt for 1 h. Acetone was added to each sample to precipitate proteins at a ratio of 2:1 acetone:supernatant volume, and samples were vortexed and left on ice for 30 min. Samples were centrifuged at 2000 x g for 15 min and supernatants were evaporated in an Eppendorf Concentrator Plus 5301 evaporator (Eppendorf, Hamburg Germany) to remove acetone. Potassium acetate buffer (1 mL of 0.1 M, pH 4.0) was added to each sample prior to solid phase extraction (SPE).

 Bond-Elut Certify SPE cartridges (130 mg, 3 mL, Varian Inc, Middleburg The Netherlands) were pre-conditioned by gravity with 2 mL of methylene chloride/isopropanol (75:25 by volume), followed by 2 mL of methanol and 2 mL of potassium acetate buffer.   Samples in potassium acetate buffer were added to the SPE cartridges, and the cartridges were washed sequentially with 3.5 mL water, 1.6 mL 0.1 M HCl, 7 mL methanol and 3.5 mL methylene chloride/isopropanol (75:25). T_1AM was eluted with 2 mL methylene chloride/isopropanol/ammonium hydroxide (70:26.5:3.5 by

volume) in clean borosilicate glass tubes. Eluates were transferred to Eppendorf tubes

and evaporated to dryness in the Eppendorf evaporator described previously. Dried

residues were redissolved in 100 μL of 1:1 methanol:0.1 M HCl prior to injection for LC-

MS/MS analysis.

3.2.5 LC-MS/MS Analysis

Samples were analyzed by LC-MS/MS using previously established selected reaction

monitoring (SRM) method (77). A 200 series HPLC system (Perkin Elmer, Boston MA),

constituted by a binary micro-pump system, a column oven, and an autosampler, was

coupled to an API 4000 triple quadrupole mass spectrometer (Applied Biosystems-MDS

Sciex, Concord Ontario Canada) with a Turbo-V IonSpray source operated in the

positive mode. Samples were injected onto a Gemini C18 2x50 mm, 3-μm particle size

column (Phenomenex, Torrance CA). Buffer A (0.1% formic acid in water) and Buffer B

(0.1% formic acid in methanol/acetonitrile (1:4)) were used in the following gradient: 5-

100% A from 0 to 5 min; 100% A from 5 to 6 min; equilibrate 6 to 9 min. IonSpray

voltage (IS) was 5.25 kV, gas source 1 was 70, gas source 2 was 55, turbo temperature

was 650 °C, and collision-activated dissociation gas pressure (CAD) was 5.7 mPa.

Declustering potential (DP), collision energy (CE) and collision exit potential (CXP)

parameters for each SRM monitored are listed in Table 3-1.

Table 3-1: MS/MS instrument parameters

Analyte	ID	Retention Time (min)	Q1 (*m/z*)	Q3 (*m/z*)	CE	DP	CXP
T_1AM	Known analyte	2.4	356	339	18	53	10
				212	28	53	18
				195	36	53	17
d_4-T_1AM	Internal standard	2.4	360	343	18	53	10
				216	28	53	18
				199	36	53	17
H-T_1AM	Predicted metabolite	2.4	365	347	18	53	10
				220	28	53	18
				203	36	53	17
T_3	Known analyte	3.4	652	606	29	103	17
				508	29	103	15
				479	47	103	14
$^{13}C_6$-T_3	Internal standard	3.4	658	612	29	103	17
				514	29	103	15
				485	47	103	14
H-T_3	Predicted metabolite	3.4	662	615	29	103	17
				517	29	103	15
				488	47	103	14
T_4	Known analyte	3.6	778	732	33	106	20
				634	34	106	18
				605	51	106	16
$^{13}C_6$-T_4	Internal standard	3.6	784	738	33	106	20
				640	34	106	18
				611	51	106	16
H-T_4	Predicted metabolite	3.6	788	741	33	106	20
				643	34	106	18
				614	51	106	16

3.2.6 Statistics

Data are presented as mean ± SEM. Data were analyzed by one-way ANOVA to determine statistical significance.

3.3 Results

3.3.1 Hypothyroid and Hormone Replacement Mouse Model

Multiple reports in the literature utilize a combination of MMI and ClO_4^- to induce

hypothyroidism over the course of 4-14 weeks (122, 124, 125). Since the half-life of T_4

in mice is 13-18 hours, we hypothesized that a period of treatment shorter than 4 weeks

may be sufficient to induce hypothyroidism (126). To test this, we conducted a time

course experiment with MMI and $KClO_4$ administered in drinking water and monitored

biweekly thyroid status as indicated by total serum T_4.   Wild type euthyroid mice had

serum T_4 levels of 2.52 ± 0.32 µg/dL prior to inducing hypothyroidism with MMI and

$KClO_4$. After two weeks of treatment with MMI and $KClO_4$ total serum T_4 levels were

below the assay limit of detection (0.82 µg/dL). From these experiments we concluded

that two weeks of MMI and $KClO_4$ treatment was sufficient to induce hypothyroidism.

For future experiments involving hormone replacement, mice were pre-treated with MMI

and $KClO_4$ for two weeks and maintained on MMI and $KClO_4$ in drinking water

throughout the duration of the experiments to inhibit endogenous TH synthesis.

Next a time course experiment was conducted to determine the length of time necessary

to reestablish steady-state serum T_4 in a hypothyroid mouse. Previous studies in the

literature involving TH replacement in Pax8 knockout or Pax8/MCT8 double knockout

mice use a dose of 20 ng/g daily, and thus we used this as our initial replacement dose

of T_4 (123, 127). At 2, 3, 4 and 5 weeks of T_4 replacement, total serum T_4 levels were

significantly decreased with respect to euthyroid mice (Figure 3-2A), but were not

significantly different from each other. Based on these data, T_4 serum levels reach

steady-state within two weeks but the replacement dose of 20 ng/g was insufficient to

reestablish euthyroid serum T_4 levels. A previous report in the literature found that three weeks of hormone replacement were necessary for the thyroid axis to reach steady-state, as measured by thyroid-stimulating hormone (TSH) (128), prompting us to use a three week hormone replacement duration (127). Since a 20 ng/g T_4 replacement dose did not reestablish complete euthyroid serum T_4 levels, a dose response study was conducted. Hypothyroid mice were hormone replaced for three weeks with T_4 ranging in doses from 0-500 ng/g (Figure 3-2B), which resulted in dose-dependent restoration of serum T_4. We selected 100 ng/g T_4 as a replacement dose for future studies since this dose resulted in serum T_4 levels closest to those of the euthyroid control.

Figure 3-2: Establishment of a hypothyroid and TH replacement mouse model.
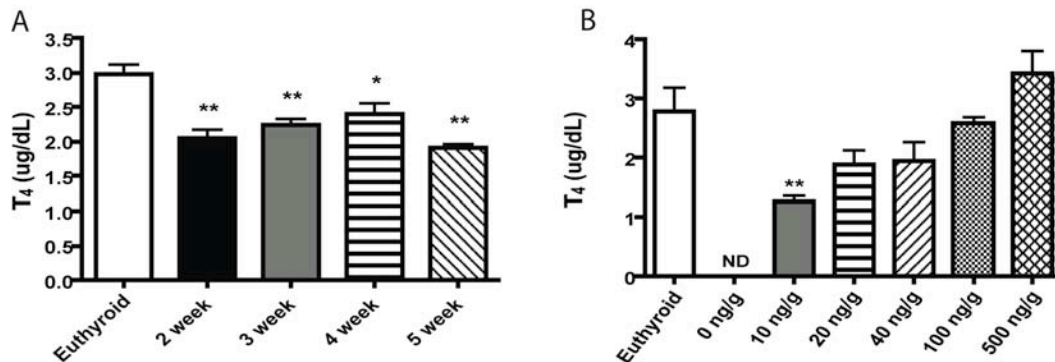
Serum T_4 levels were measured by RIA following treatment with 0.1% MMI and 0.2% $KClO_4$ and replacement with 20 ng/g T_4 for 2-5 weeks (A) or replacement with 0-500 ng/g T_4 for 3 weeks (B); n = 3-5 per group; * $P < 0.05$, ** $P < 0.01$ vs euthyroid; ND, not detectable.

3.3.2   H-T_4 Replacement

In hypothyroid mice, replacement with 100 ng/g H-T_4 did not restore serum T_4 to euthyroid levels, however 200 ng/g H-T_4 resulted in euthyroid serum T_4 levels (2.79 ± 0.54 ng/dL) (Figure 3-3A). Replacement with either 100 ng/g T_4 or 200 ng/g H-T_4 also

normalized body weight following hypothyroid induced weight loss (Fig 3-3B). One

interpretation of our results is that the T_4 antibody in the RIA kit binds less efficiently to

isotope labeled H-T_4 than to T_4 resulting in artificially lower T_4 serum concentrations in H-

T_4 replaced mice. To determine if the difference in replacement doses between T_4 and

H-T_4 were due to isotope effects on antibody binding, the response of T_4 and H-T_4 in the

RIA kit was investigated. T_4 and H-T_4 were spiked into T_4/T_3 deficient human serum and

analyzed by RIA. There was no difference in detection of H-T_4 from T_4 by the T_4

antibody from 0-12.5 µg/dL (Figure 3-3C). This suggests the difference in doses is not

due to the presence of ^{13}C isotopes but is likely due to a lack of bioequivalence between

the T_4 and H-T_4 formulations, an issue that has been documented for different T_4

preparations (129).

Figure 3-3: Euthyroid replacement with T_4 and H-T_4.
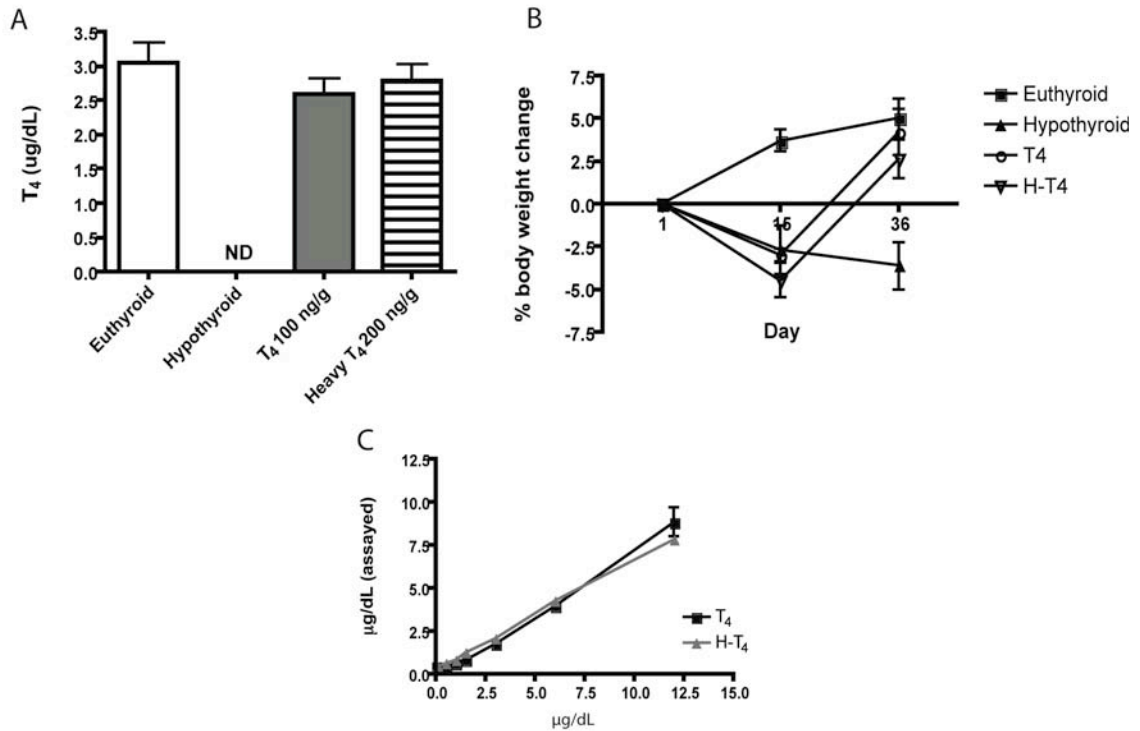
H-T_4 replacement in a hypothyroid mouse model. A) Total serum T_4 levels as measured by RIA following 2 weeks of treatment with 0.1% MMI and 0.2% $KClO_4$ and replacement with T_4 or H-T_4; n = 4-5 per group. B) Body weights of euthyroid, hypothyroid, T_4, and H-T_4 replaced mice. Hypothyroid, T_4 and H-T_4 replaced mice were treated with 0.1% MMI and 0.2% $KClO_4$ starting on day 1 and continuing through day 36. At day 15, replaced mice began receiving daily injections of either T_4 or H-T_4; n = 4-8 per group; ND, not detectable. C) Comparison of T_4 and H-T_4 measured by RIA; n = 2.

3.3.3 Endogenous T_1AM Levels in Mouse Liver

To test if T_1AM biosynthetic origins are related to thyroid status, we measured

endogenous T_1AM following induction of hypothyroidism. T_1AM was analyzed in liver

due to the low concentration of T_1AM in serum and high concentration in liver previously

observed in rodents (77). T_4 and T_3 were monitored as experimental controls, since T_4

and T_3 levels are known to decrease in hypothyroidism. Endogenous T_1AM from liver

homogenates was analyzed by LC-MS/MS, and the chromatographic trace

corresponding to the *m/z* transition of 356.2 to 339.1 shows a decrease in T_1AM peak intensity following induction of hypothyroidism for two weeks (Figure 3-4). As expected, T_4 and T_3 also decrease by over 90% upon induction of hypothyroidism.

Figure 3-4: T_1AM, T_3 and T_4 from euthyroid and hypothyroid mouse livers.
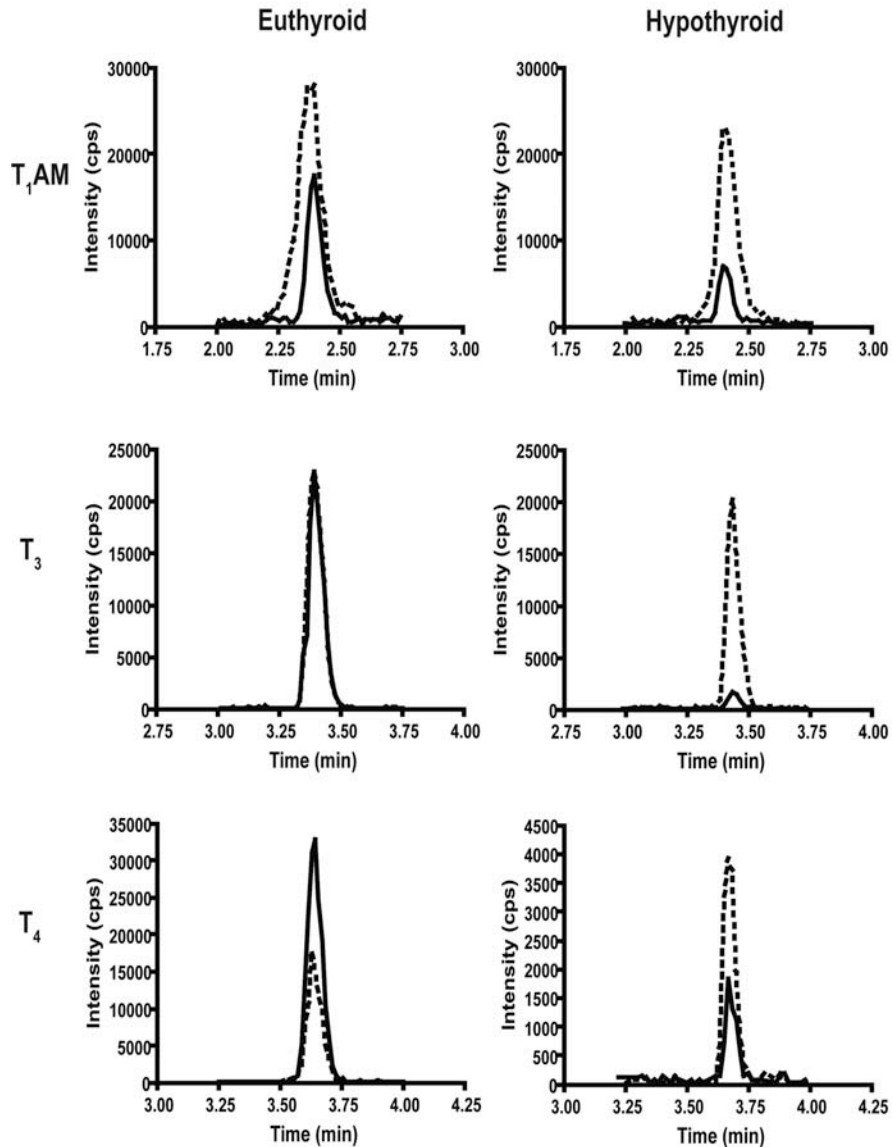
Representative extracted ion chromatograms (XIC) for T_1AM, T_3 and T_4 in euthyroid and 2-week hypothyroid mouse livers. The *m/z* transitions represented are: T_1AM, 356 to 339; d_4-T_1AM, 360 to 343; T_3, 652 to 606; $^{13}C_6$-T_3, 658 to 612; T_4, 778 to 732; $^{13}C_6$-T_4, 784 to 738. Solid black line, endogenous analyte; dashed line, internal standard.

Due to sample dependent variations in ionization efficiencies, to quantify T_4, T_3 and

T_1AM, peak areas were integrated with respect to the corresponding internal standard

(d_4-T_1AM, $^{13}C_6$-T_3, or $^{13}C_6$-T_4). We integrated the peak areas of T_1AM and d_4-T_1AM to

determine the concentration of endogenous T_1AM and found that liver T_1AM

concentration decreases time dependently with induction of hypothyroidism (Figure 3-5).

Figure 3-5: Liver T$_1$AM concentration.
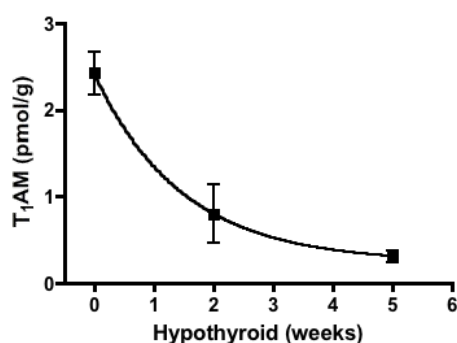
T_1AM levels decrease in mouse liver as a function of time of 0.1% MMI and 0.2% $KClO_4$
treatment, as measured by LC-MS/MS; n = 3-5 per time point.

3.3.4   Metabolism of Exogenous T_4 and H-T_4

We next investigated if T_1AM is an extrathyroidal metabolite of T_4 by measuring T_1AM in

hypothyroid mice that were hormone replaced with either T_4 or H-T_4. Homogenized

livers were analyzed by LC-MS/MS for the presence of unlabeled and labeled (H-T_1AM)

forms of T_1AM. T_4, T_3, and the corresponding heavy labeled forms, H-T_4 and H-T_3,

served as positive controls since T_3 is a known metabolite of T_4. Representative

chromatographic traces for T_4 and H-T_4 replaced mouse livers are shown in Figure 7.

The retention times of internal standards are used to additionally verify analytes, since

the internal standards and corresponding unlabeled or heavy analytes co-elute. In

hypothyroid mice, replacement with T_4 results in increased peak intensities for T_4 and T_3

relative to hypothyroid levels, but no increase in T_1AM peak intensity (Figure 3-6).

Replacement with $H-T_4$ results in the detection of chromatographic peaks corresponding

to $H-T_4$ and $H-T_3$, but no detectable chromatographic peak corresponding to $H-T_1AM$.

Figure 3-6: T_1AM, T_3 and T_4 from T_4 and $H-T_4$ replaced mouse livers.
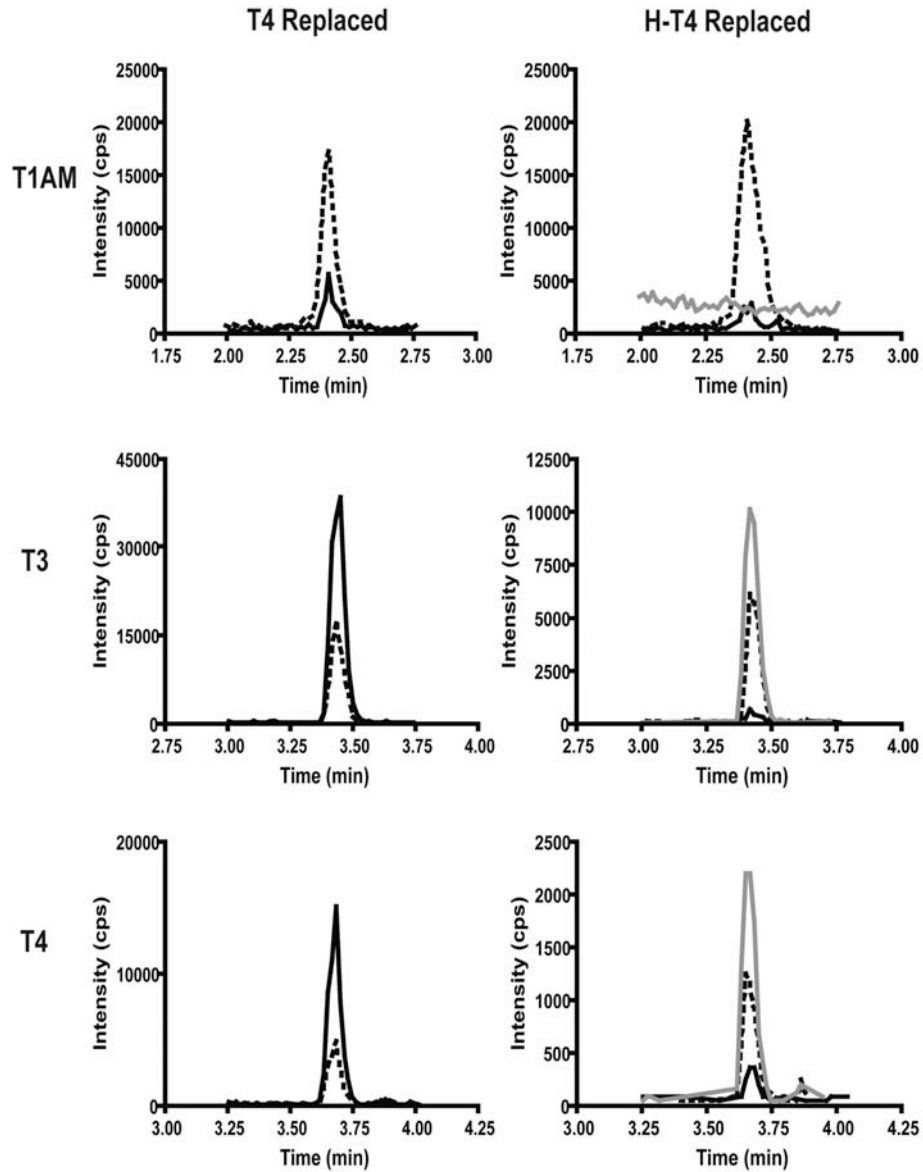
Representative XIC for T_1AM, T_3 and T_4 in T_4 and $H-T_4$ replaced mouse livers. The *m/z* transitions represented are: T_1AM, 356 to 339; d_4-T_1AM, 360 to 343; $H-T_1AM$, 365 to 347; T_3, 652 to 606; $^{13}C_6-T_3$, 658 to 612; $H-T_3$, 662 to 615; T_4, 778 to 732; $^{13}C_6-T_4$, 784 to 738; $H-T_4$, 788 to 741. Solid black line, endogenous analyte; dashed line, internal standard; grey line, heavy metabolite.

49

To quantify liver concentrations of unlabeled and labeled T_4, T_3 and T_1AM, we integrated peak areas with respect to the corresponding internal standard in euthyroid, 2-week hypothyroid, T_4 replaced and H-T_4 replaced mice (Figure 3-7). Inducing hypothyroidism decreases endogenous T_4 and T_3 by 92% and 93.6%, respectively (52.0 ± 16.0 pmol/g to 4.1 ± 3.5 pmol/g for T_4 and 25.0 ± 5.5 pmol/g to 1.6 ± 0.7 pmol/g for T_3). Replacement with T_4 increases liver T_4 to 91% and liver T_3 to 161.6% of euthyroid liver concentrations. Replacement with H-T_4 results in liver H-T_4 and H-T_3 levels 46% (24.0 ± 8.2 pmol/g) and 114.4% (28.6 ± 6.8 pmol/g) of euthyroid levels, respectively, while endogenous, unlabeled T_4 and T_3 remain decreased, at 4.2 ± 2.3 pmol/g and 1.6 ± 0.3 pmol/g. Endogenous, unlabeled liver T_1AM concentration decreases with hypothyroidism, from 2.4 ± 0.4 pmol/g to 0.8 ± 0.6 pmol/g and remains decreased upon replacement with either T_4 (0.4 ± 0.1 pmol/g) or H-T_4 (0.2 ± 0.1 pmol/g). No H-T_1AM was detected from any mouse liver replaced with H-T_4.

Figure 3-7: Liver T_4, T_3, T_1AM and H-T_4, H-T_3 and H-T_1AM levels in euthyroid, hypothyroid and hypothyroid mice with T_4 or H-T_4 replacement.
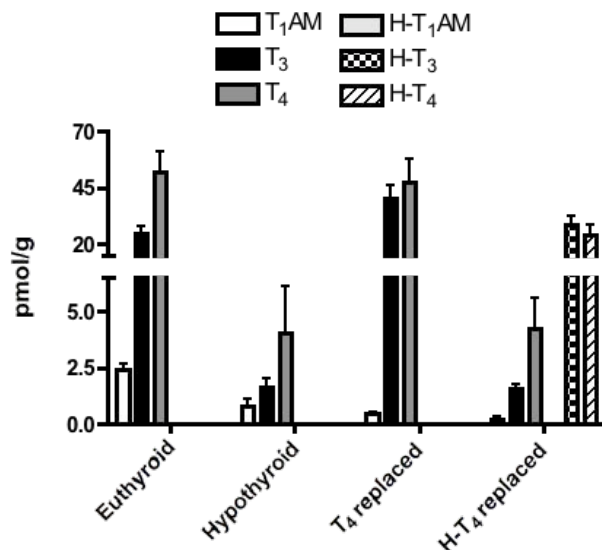
Inducing hypothyroidism for 2 weeks decreases endogenous T_4, T_3 and T_1AM. Replacement with T_4 results in normal T_4 and increased T_3 with respect to euthyroid, but no increase in T_1AM with respect to hypothyroid. Replacement with H-T_4 results in measurable H-T_4 and H-T_3, no increase in endogenous T_4, T_3 or T_1AM, and no detectable H-T_1AM. H-T_4 and H-T_3 were only detected in mice replaced with H-T_4; n = 3 for euthyroid, hypothyroid and H-T_4 replaced; n = 2 for T_4 replaced.

3.4 Discussion

T_1AM is a recently discovered endogenous compound that contains the unique chemical signature of a thyroid hormone, namely a biaryl ether core structure containing an iodine substituent. Like the thyroid hormones T_4 and T_3, T_1AM is found in various of tissues and in circulation (77), and circulating T_1AM is largely bound to lipoprotein particles (130). Recent advances in the quantitative analysis of T_1AM using methods based on LC-MS/MS and T_1AM-specific immunoassay have established that endogenous T_1AM is present in tissues and circulation at levels that are comparable with those of total T_4, whereas other established T_4 metabolites are significantly lower levels (77, 78).

Since its discovery, it has been proposed—if not assumed—that T_1AM is produced as a metabolite of T_4 by deiodination and decarboxylation, the hypothetical enzymatic steps required for conversion of T_4 to T_1AM. In support of this notion, plausible iodothyronamine deiodination pathways have been demonstrated *in vitro* (86). However, iodothyronine decarboxylation to iodothyronamines has not been demonstrated, and the well studied aromatic amino acid decarboxylase (AACD), a somewhat non-specific enzyme with respect to aromatic amino acid substrates, was recently shown to be unable to catalyze iodothyronine decarboxylation (131), suggesting that the enzymatic conversion of an iodothyronine to an iodothyronamine is not as straightforward as was originally thought. We have attempted here to address this question directly with a labeling experiment using a stable isotope labeled form of T_4 (heavy, H-T_4) designed to afford a correspondingly labeled T_1AM if T_1AM were to arise from enzymatic processing of extrathyroidal T_4. Detecting the H-T_4 and its metabolites is done using LC-MS/MS thus avoiding the use of radioactivity. Moreover, the labeled atoms of H-T_4 reside in the thyronine skeleton and are not lost upon deiodination, as would be the case with commercially available outer-ring [^{125}I]-T_4. Of note, a study designed similarly to ours was recently attempted and failed because the investigators were unable to extract and detect endogenous T_1AM by LC-MS/MS (132).

Our results show that endogenous liver T_1AM concentration decreases significantly in hypothyroid versus euthyroid mice, indicating a role for a functioning thyroid gland in the biosynthesis of T_1AM. However, hypothyroid mice treated with H-T_4 did not generate detectable levels of H-T_1AM, whereas H-T_3 was unequivocally detected. Taken together, these results indicate that T_1AM biosynthesis can be inhibited by the anti-thyroid drugs MMI and $KClO_4$ that target thyroid gland function by inhibiting

52

thyroperoxidase and the sodium-iodide symporter, respectively (133, 134), yet does not appear to involve extrathyroidal deiodination and decarboxylation of T_4, the previously favored and often hypothesized route of production of T_1AM. The site of action of these anti-thyroid drugs restricts T_1AM synthesis to the thyroid gland and eliminates the possibility that T_1AM biosynthesis is originating through a *de novo* pathway involving extrathyroidal iodination and cross-coupling of tyrosine. These unexpected results lead to the conclusion that like T_4, T_1AM is a direct product of the thyroid gland, or a metabolite of another thyroid gland product that does not arise from extrathyroidal metabolism of T_4.

At least three hypothetical thyroid gland-dependent pathways for T_1AM biosynthesis can be considered, all of which are dependent upon thyroglobulin, the substrate for T_4 biosynthesis. The first of these three involves extrathyroidal coupling of a phenol to monoiodotyrosine, a known by-product of thyroglobulin proteolysis that occurs in the T_4 secretion process (135). The outer ring phenol could theoretically derive from tyrosine, however, the chemistry required for this putative coupling reaction is not presently known. The second possibility is that T_1AM is secreted directly from the thyroid gland as a direct cleavage product of thyroglobulin. This putative pathway would begin with a thyroglobulin-bound 3-iodothyronine residue arising from TPO-mediated cross-coupling of monoiodotyrosine and tyrosine residues within thyroglobulin. Release of T_1AM would then require an unknown proteolytic decarboxylation reaction, or proteolysis followed by specific 3-iodothyronine decarboxylation occurring within the thyrocyte. The final possibility is that T_1AM is a metabolite of a non-T_4 thyroid gland product, or a metabolite of T_4 that is specifically generated within the thyroid gland. One potential candidate for such a T_1AM precursor could be 3,5-diiodothyronine (3,5-T_2) (39). To date, there is no

reported direct evidence for outer ring deiodination of T_3 *in vivo* to produce $3,5-T_2$ (25, 34), leaving open the possibility that like T_1AM, $3,5-T_2$ is not an extrathyroidal metabolite of T_4. If $3,5-T_2$ is not a simple deiodination product of circulating T_4, then it most likely is produced from thyroglobulin bound $3,5-T_2$ arising from TPO catalyzed cross coupling of 3,5-diiodotyrosine and tyrosine residues of thyroglobulin, respectively. Alternatively, if free T_4 within the thyroid gland were converted to some other derivative via a reversible thyroid gland specific biochemical process (e.g. N-methylation or acetylation), and this putative derivative was the direct biosynthetic precursor of T_1AM, then a lack of labeled T_1AM arising from labeled extrathyroidal T_4 might also be expected to occur.

Future studies are needed to distinguish between these possible routes or to discover alternative pathways from those proposed above. This work also points to a compelling need to reassess the unique chemistry that occurs within the thyroid gland. The powerful bioanalytical tools available today may reveal new chemical insights into the function of this important endocrine organ.

Chapter 4: Metabolism of 3-Iodothyronamine

This work is in submission as: Hackenmueller SA and Scanlan TS. Identification and quantification of 3-iodothyronamine metabolites in mouse serum using information dependent acquisition and liquid chromatography-tandem mass spectrometry. This work used instrumentation maintained by the Bioanalytical Shared Resource/Pharmacokinetics Core at Oregon Health & Science University in Portland, OR. O-sulfonate-T_1AM was synthesized by Warren Wood and Federico Espinosa, d_4-T_1AM, d_4-T_0AM, TA_1, TA_0, d_4-TA_1 and d_4-TA_0, T_1AM, and T_0AM were synthesized by Aaron Nilsen and Warren Wood.

4.1 Introduction

3-Iodothyronamine (T_1AM) is an endogenous derivative of thyroxine (T_4), the main thyroid hormone produced by the thyroid gland. T_1AM is found in circulation and in tissues of rat, mice, guinea pig, hamster and human (75, 76, 78-80). T_1AM is a decarboxylated and deiodinated derivative of T_4 (Figure 4-1) and has a unique pharmacological profile (75). In rodents, T_1AM acutely induces hypothermia, decreases cardiac function and shifts the respiratory quotient (RQ) from predominantly carbohydrate to predominantly lipid utilization (75, 76, 80), suggesting a role for T_1AM in regulating metabolic homeostasis.

Figure 4-1: Structures of T_4, T_1AM, and T_1AM metabolites TA_1, T_0AM, S-T_1AM, TA_0, Ac-T_1AM and T_1AM-glucuronide.
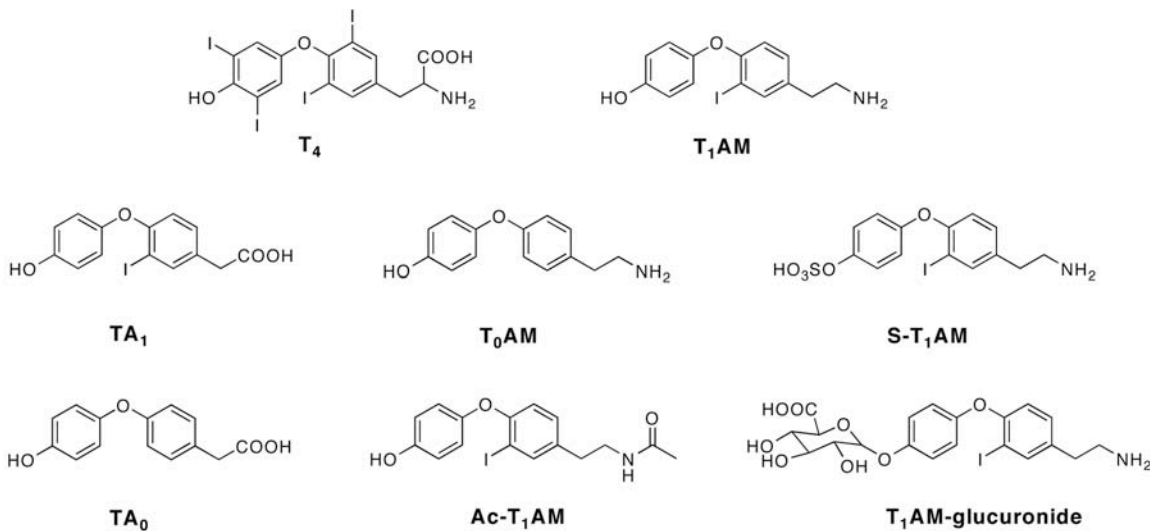
Due to the unique pharmacological effects of T_1AM, there has been much interest in measuring endogenous levels of T_1AM. Multiple analytical assays have been developed to quantify endogenous T_1AM in circulation and in tissues of multiple species. Liquid

56

chromatography-tandem mass spectrometry (LC-MS/MS) methods have been validated

using multiple reaction monitoring (MRM) to increase selectivity for T_1AM by monitoring

multiple *m/z* transitions (34, 77, 81). In addition, an immunoassay has also been

developed to quantify T_1AM in human serum (78), and unexpectedly shows serum T_1AM

to be 100 fold higher than when measured by LC-MS/MS (77, 78). This discrepancy led

us to hypothesize that endogenous T_1AM is covalently modified *in vivo*, resulting in pools

of endogenous modified T_1AM recognizable by the T_1AM antibody but not by an MRM

LC-MS/MS method. To date, the only *in vivo* study on the metabolism of T_1AM shows

oxidative deamination in rat to form 3-iodothyroacetic acid (TA_1) (Figure 4-1), another

thyroid hormone derivative (88). *In vitro* data show T_1AM is a substrate for the type 3

inner ring deiodinase enzyme and human liver sulfotransferases, resulting in the non-

iodinated thyronamine, T_0AM (86) and O-sulfonate-T_1AM (S-T_1AM) (87), respectively

(Figure 4-1). To date, there are no data on covalent modifications of T_1AM occurring *in*

vivo.

LC-MS/MS methods are valuable analytical tools due to the selectivity and sensitivity

that can be routinely achieved. In the current situation, however, the selectivity of

existing LC-MS/MS methods may be limiting studies of endogenous T_1AM since the

MRM methods monitor only for unmodified T_1AM (34, 77, 81) and are unable to monitor

for potential covalent modifications. Unknown modifications of T_1AM can be studied

using LC-MS/MS when information dependent acquisition (IDA) methods are used. IDA

methods utilize unbiased survey scans to identify possible compounds that are

structurally related to the parent compound, T_1AM, and generate MS/MS fragmentation

spectra that provide additional structural information. In this study we 1) use IDA

methods to identify *in vivo* metabolites of T_1AM, 2) develop and validate an MRM LC-

MS/MS method to quantify metabolites of T_1AM in mouse serum following a single injection of T_1AM, and 3) provide a relative assessment for the tissue distribution of T_1AM metabolites.

4.2 Materials and Methods

4.2.1 Chemicals and Reagents

T_1AM, d_4-T_1AM, TA_1 and d_4-TA_1 were synthesized as described previously (88, 98, 136), and T_0AM, d_4-T_0AM, TA_0 and d_4-TA_0 were synthesized using similar methods differing only in the lack of iodination. O-sulfonate-T_1AM (S-T_1AM) was synthesized in one step from Boc-protected T_1AM using thionyl chloride, followed by hydrolysis of the Boc-protecting group. Mouse serum was purchased from Invitrogen (Carlsbad, CA) and mouse liver microsomes were purchased from BD Biosciences (San Jose, CA). β-glucuronidase from bovine liver was purchased from Sigma-Aldrich (St. Louis, MO). HPLC grade solvents were purchased from Burdick and Jackson (Muskegon, MI) or Fisher (Pittsburg, PA).

4.2.2 Animal Studies

Experimental protocols were in compliance with the National Institutes of Health Guide for the Care and Use of Laboratory Animals and approved by the Oregon Health & Science University Institutional Animal Care & Use Committee. Wild type male C57Bl/6 mice, aged 8-10 weeks, were housed in a climate controlled room with a 12 hour light-dark cycle with *ad libitum* access to food and water. T_1AM was dissolved in 1:1 DMSO:saline (0.9% NaCl). Mice were injected intraperitoneally (IP) with 25 mg/kg

T$_1$AM. Following euthanasia at 10, 20, 45 and 90 minutes, 3 and 6 hours, blood was

removed and allowed to clot on ice for a minimum of 30 minutes prior to centrifugation at

7500 x g. Sera was removed and stored at -80 °C until further use. Tissues were frozen

immediately on dry ice and stored at -80 °C until further use. Samples were used within

one month of collection.

4.2.3 N-Acetyl-T$_1$AM

Triethylamine (75 µL, 0.53 mmol) was added to T$_1$AM hydrochloride (0.187 g, 0.48

mmol) in tetrahydrofuran (3 mL). Acetic anhydride (50 µL, 0.53 mmol) was added

dropwise and the reaction was stirred at room temperature over night. The reaction was

diluted with ethyl acetate and washed with 0.5 M HCl, water and brine, and dried over

MgSO$_4$. The crude material was purified by flash chromatography (HPFC) on a Biotage

SP1 purification system with a fixed wavelength UV detector (Biotage, Charlotte NC)

with a gradient of 2-20% methanol/methylene chloride over 10 column volumes, to give

N-acetyl-T$_1$AM (0.135 g, 0.34 mmol, 70.7% yield). A ^{1}H NMR spectrum was taken on a

Bruker 400 (400 MHz) and processed using ACD/NMR Processor Academic Edition

software. The ^{1}H NMR spectrum is in Appendix A.

4.2.4 T$_1$AM-glucuronide

T$_1$AM-glucuronide was synthesized enzymatically using a modified protocol for T$_4$

glucuronidation (137). Briefly, 150 µl reaction buffer (75 mM Tris-HCl pH 7.8, 7.5 mM

MgCl$_2$, 30 mM UDP-glucuronic acid, 1 µM T$_1$AM, 0.1 µM iopanoic acid, 0.1 µM

iproniazid) was incubated with 50 µL of a mouse liver microsome dilution (4 µg/µL in

reaction buffer) for 60 minutes at 37 °C. The reaction was stopped by adding 200 µL ice

cold methanol and samples were left on ice for 20 minutes. Samples were centrifuged at 12,000 x g for 45 minutes at 5 °C and supernatants were filtered with 0.22 µm centrifugal filters prior to injection for LC-MS/MS analysis.

4.2.5 Sample preparation

Serum standards

Commercial mouse serum was used to prepare samples for use in standard curves and as calibrants. A mix of standards (T_1AM, T_0AM, S-T_1AM, Ac-T_1AM, TA_1 and TA_0) was added to mouse serum to produce the following final concentration of standards: 0.05, 0.1, 0.25, 0.5, 1, 2.5, 5, 10 and 40 µM. Samples were stored at -80 °C until analysis. Each sample was prepared by adding 10 µL of internal standard mix (10 µM each of d_4-T_1AM, d_4-T_0AM, d_4-TA_1 and d_4-TA_0) to 40 µL of serum standard. Samples were vortexed and 100 µL of sodium acetate (100 mM, pH 5.0) was added. To each sample, 50 µL of β-glucuronidase (1 mg/100 µL 0.2% NaCl) was added and standards were incubated for 60 minutes at 37 °C. Reactions were stopped with the addition of ice-cold methanol (200 µL) and samples were left on ice for 20 minutes. Samples were centrifuged at 12000 x g for 10 minutes at 5 °C and supernatants were filtered with 0.22 µm centrifugal filters prior to injection for LC-MS/MS analysis. Standard curves were analyzed with a 1/x weighted regression analysis. To determine intra-assay precision (RSD) and accuracy, six samples were analyzed at the lower limit of quantitation (LLOQ) and upper limit of quantitation. To determine inter-assay precision and accuracy, calibrants at the LLOQ and upper limit of quantitation were processed and analyzed on at least four separate days over the course of one month.

Serum sample preparation

Each mouse serum sample was processed in the presence and absence of β-glucuronidase. For each sample, 10 µL of internal standard mix was added to 40 µL of serum. Samples were vortexed, and 100 µl of sodium acetate (100 mM, pH 5.0) was added. To each sample, 50 µL β-glucuronidase (0.1 mg/mL in 0.2% NaCl) or 0.2% NaCl was added and samples were incubated for 60 minutes at 37 °C. Reactions were stopped with the addition of ice-cold methanol (200 µL). Samples were vortexed and left on ice for 20 minutes. Samples were centrifuged at 12000 x g for 10 minutes at 5 °C and supernatants were filtered with 0.22 µm centrifugal filters prior to injection for LC-MS/MS analysis.

Tissue sample preparation

Tissues, including liver, kidney, heart, brain brown adipose tissue (BAT) and white adipose tissue (WAT) were weighed and sodium acetate (100 mM, pH 5.0) was added in a ratio of 1 mL per 1 gram of tissue, except for BAT samples, which each received 150 µL. Tissues were homogenized using 20 passes in a motorized dounce homogenizer. Samples were centrifuged at 12000 x g for 10 minutes, and the volume of supernatant was recorded. For each sample, 10 µL of internal standard mix was added to 50 µL of homogenized tissue supernatant. Samples were vortexed and 50 µL ice-cold methanol was added. Samples were vortexed again and incubated on ice for 20 minutes to allow for complete protein precipitation. Samples were centrifuged at 12000 x g for 10 minutes and supernatants were filtered with 0.22 µm centrifugal filters prior to injection for LC-MS/MS analysis.

4.2.6   LC-MS/MS

General

Instrumentation was housed in the Bioanalytical Shared Resource/Pharmacokinetics Core at Oregon Health & Science University. A Shimadzu Prominence HPLC (CANBY OR) was coupled to a 4000 QTRAP mass spectrometer (AB Sciex, Foster City, CA) using electrospray ionization (ESI). For all samples, 10 µL was injected onto a Poroshell120 2.1 x 100 mm C_{18} column (Agilent Technologies, Santa Clara, CA). Solvent A was water with 0.05% acetic acid and Solvent B was acetonitrile with 0.05% acetic acid. The flow rate was 0.3 mL/min and the gradient conditions were as follows: 10% B to 45% B from 0 to 14 min; 45% B to 95% B from 14 to 15 min; 95% B from 15 to 18 min; 95% B to 10% B from 18 to 19 min; 10% B from 19 to 22 min. The autosampler was kept at 4 °C and the oven temperature was 30 °C.

IDA Methods

Four IDA methods were used to screen for potential T_1AM metabolites. All methods were generated using AB Sciex LightSight software. The four methods used were a T_1AM precursor 212 survey scan, a T_1AM MRM survey scan, a TA_1 precursor 127 survey scan, and a TA_1 MRM survey scan. For the T_1AM and TA_1 MRM survey scans, Q1/Q3 ion pairs were generated by LightSight based on commonly occurring biotransformations. For all methods, the IDA experiment was an enhanced product ionization (EPI) scan, which was triggered when the intensity exceeded 500 cps for the MRM survey scans or 1000 cps for the precursor survey scans. For all EPI scans, the scan rate was 4000 Da/s over the mass ranges 80-179.2 and 174- 609.2 (precursor 127), 174-596 (precursor 212), 174-692 (T_1AM MRM) or 174-681.2 (TA_1 MRM). The following parameters were used for all IDA methods: curtain gas (CUR), 20; collision gas

(CAD), high; temperature, 550 °C; ion source gas 1, 50; ion source gas 2, 50. For the precursor 212 and T_1AM MRM methods, the ionspray voltage (IS) was 5200 V and for the precursor 127 and TA_1 MRM methods the IS was -4500 V. The precursor 212 and precursor 127 methods used the following parameters, respectively: declustering potential (DP), 40 V and -5 V; collision energy (CE), 27 V and -12 V; and collision exit potential (CXP), 14 V and -17 V.

MRM Methods

Two separate MRM methods were validated to quantify T_1AM metabolites in serum. Method 1 was operated in the positive mode with the following parameters: CUR, 30; CAD, medium; IS, 4500 V; temperature, 500 °C; ion source gas 1, 50; ion source gas 2, 40. Method 2 was operated in the negative mode with the following parameters: CUR, 50; CAD, medium; IS, -4000; temperature, 500 °C; ion source gas 1, 30; ion source gas 2, 40. DP, CE and CXP values for all MRM transitions are given in Table 1. The scan rate was 15 msec for Method 1 and 75 msec for Method 2.

Table 4-1: MRM Method 1 and Method 2 instrument parameters.

Analyte	Q1 (m/z)	Q3 (m/z)	DP (V)	CE (V)	CXP (V)
T_1AM	356	339	81	10	17
		212	81	10	27
d_4-T_1AM	360	343	96	17	10
		216	96	27	22
T_0AM	230	213	66	27	14
		109	66	35	20
d_4-T_0AM	234	217	71	17	16
		113	76	43	6
T_1AM-glucuronide	532	515	81	10	11
		356	81	10	11
		339	81	10	11
		212	81	10	11
S-T_1AM	436	419	81	10	12
		339	81	10	10
		212	81	10	14
Ac-T_1AM	398	356	66	27	14
		339	66	27	14
		271	66	27	14
		212	66	27	14
TA_1	369	325	-5	-8	-13
		127	-5	-12	-17
d_4-TA_1	373	329	-50	-6	-9
		127	-50	-26	-11
TA_0	243	199	-5	-14	-39
		106	-5	-26	-19
d_4-TA_0	247	203	-30	-14	-17
		106	-30	-26	-15
		97	-30	-31	-12

4.3 Results

4.3.1 IDA Screen

IDA methods were used to screen for potential metabolites of T_1AM. Mice received a single IP injection of T_1AM (25 mg/kg) to increase the concentration of potential metabolites. Four IDA methods were created using the LightSight software and used for metabolite screening. IDA methods included a precursor survey scan method using the m/z 212 fragment of T_1AM and an MRM method using Q1/Q3 ion pairs generated in

LightSight based on predicted biotransformations of T_1AM. Since T_1AM is oxidatively

deaminated to TA_1 in rat (88), additional IDA methods were generated using TA_1 as the

parent compound to look for potential covalent modifications. The TA_1 based IDA

methods included a precursor survey scan method using the *m/z* 127 fragment and an

MRM method using Q1/Q3 ion pairs generated in LightSight based on predicted

biotransformation of TA_1. T_1AM based IDA methods were operated in positive ion mode

while TA_1 IDA methods were operated in negative ion mode. Data were analyzed

manually and LightSight was used to identify possible metabolites of T_1AM.

An initial screen with IDA methods using serum collected 10 minutes post-T_1AM injection

identified potential metabolites corresponding to *m/z* shifts of +176, +80, +42 and -112

using the positive ion mode methods, and a metabolite corresponding to unmodified TA_1

using the negative ion mode methods. Mass shifts of +176, +80 and +42 correspond to

the addition of glucuronide, sulfonate and acetyl groups, respectively, while the mass

shift of -112 would correspond to the predicted transformation of both deiodination and

oxidative deamination to the thyroacetic acid, TA_0.

TA_1, TA_0, and S-T_1AM have all been previously synthesized and were used as authentic

standards. To confirm the identity of metabolites corresponding to *m/z* shifts of +42 and

+176, N-acetyl-T_1AM (Ac-T_1AM) was synthesized chemically and T_1AM-glucuronide was

synthesized enzymatically using mouse liver microsomes (Figure 4-1). MS/MS

fragmentation spectra were compared to the EPI spectra generated in the IDA methods

for the +42 and +176 compounds. As shown in Figure 4-2, spectra for synthetic Ac-

T_1AM and the +42 compound both show ions with an *m/z* of 398, 356, 339, 217 and 212

(Figure 4-2A), and spectra for T_1AM-glucuronide and the +176 compound both show

ions with an *m/z* of 532, 515, 356, 339 and 212 (Figure 4-2B).

Figure 4-2: MS/MS of Ac-T_1AM and T_1AM-glucuronide.
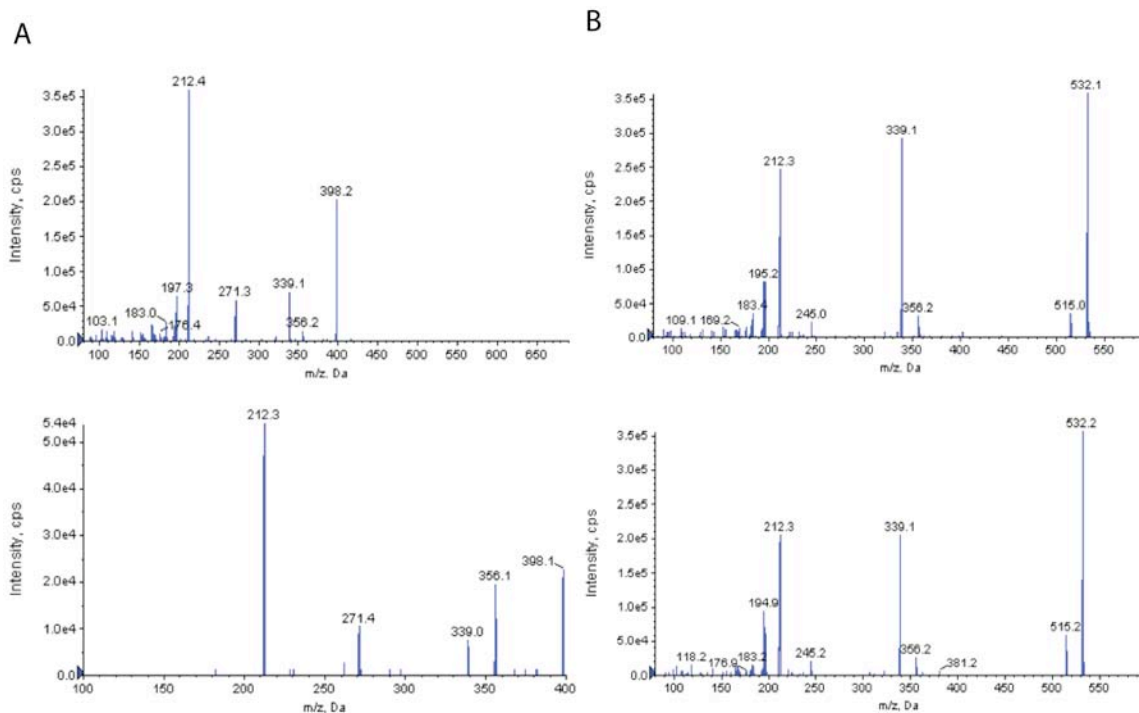
Identification of Ac-T_1AM and T_1AM-glucuronide in mouse serum 10 minutes post-T_1AM injection. A) The EPI spectrum of the +42 metabolite identified in serum (top panel) and the MS/MS spectrum of synthetic N-acetyl-T_1AM (bottom panel). B) The EPI spectrum of the +176 metabolite identified in serum (top panel) and the EPI spectrum generated for enzymatically synthesized T_1AM-glucuronide (bottom panel).

Since Ac-T_1AM was synthesized chemically, it was used in the MRM method to generate

a standard to curve to quantify serum Ac-T_1AM; enzymatically generated T_1AM-

glucuronide was not produced in a great enough quantity to purify and generate a

standard curve for quantification. Cleavage of T_1AM-glucuronide resulted in

undetectable T_1AM-glucuronide and an increase in unmodified T_1AM (Figure 4-3),

allowing for indirect quantification of serum T_1AM-glucuronide. In the MRM method,

T_1AM-glucuronide was monitored using Q1/Q3 ion pairs based on fragments identified in the MS/MS spectra (Figure 4-2B).

Figure 4-3: T_1AM and T_1AM-glucuronide chromatographic traces.
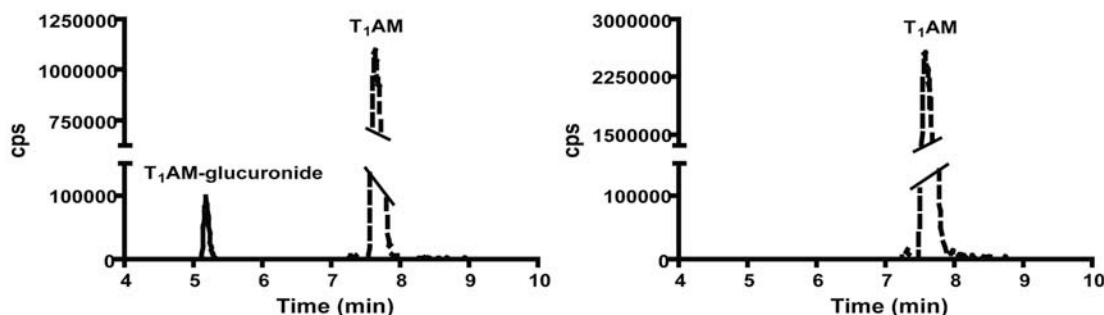
Extracted ion chromatograms (XIC) for T_1AM-glucuronide (RT = 5.2 min) and T_1AM (RT = 7.6 min) from a serum sample 20 minutes post-T_1AM injection, in the absence (left) or presence (right) of β-glucuronidase. Dashed line corresponds to T_1AM-glucuronide and solid line corresponds to T_1AM. There is no detectable peak corresponding to T_1AM-glucuronide following treatment with β-glucuronidase.

4.3.2   LC-MS/MS MRM Method Validation

Two separate LC-MS/MS MRM methods were developed and validated to quantify T_1AM metabolites in mouse serum. Method 1 was operated in the positive mode to quantify T_1AM, T_0AM, Ac-T_1AM, S-T_1AM and T_1AM-glucuronide. D_4-T_0AM was used as the internal standard for T_0AM, and d_4-T_1AM was used as the internal standard for T_1AM, S-T_1AM and Ac-T_1AM (Table 4-1). Method 2 was operated in the negative mode to quantify TA_1 and TA_0 using d_4-TA_1 and d_4-TA_0, respectively, as internal standards (Table 4-1). Although T_0AM was not identified in any IDA methods, it was included in the MRM method since T_1AM was previously shown to be an *in vitro* substrate for deiodination (86). Calibration samples were analyzed on at least four separate days over the course

of one month. The lower limit of quantitation (LLOQ) was 0.1 µM for T_1AM, T_0AM and

$Ac-T_1AM$, and 0.25 µM for $S-T_1AM$, TA_1 and TA_0, and the upper limit of quantitation was

40 µM for all compounds. Intra- and inter-assay precision (RSD) and accuracy (bias, %)

were within 20% for all compounds at the LLOQ and within 15% for all compounds at the

upper limit of quantitation (Tables 4-2 and 4-3), which is consistent with published

guidelines for method validation (138). Typical slopes for linear regression of standard

curves are given in Table 4-4.

Table 4-2: Intraassay precision and accuracy for Method 1 and Method 2.

	LLOQ				40 µM			
	Avg (µM)	Bias (%)	RSD (%)	n	Avg (µM)	Bias (%)	RSD (%)	n
T_1AM^a	0.11	8.7	13.0	6	40.6	1.6	3.4	6
T_0AM^a	0.10	-2.3	12.7	6	39.3	-1.9	2.2	6
$Ac-T_1AM^a$	0.10	-2.8	15.3	6	44.3	10.8	6.2	6
$S-T_1AM^b$	0.22	-12.3	6.6	6	41.7	4.3	3.3	6
TA_1^b	0.24	-3.8	12.7	6	38.4	-3.9	3.0	6
TA_0^b	0.24	-2.4	12.7	6	40.2	0.5	4.3	6

a, LLOQ = 0.1 µM; *b*, LLOQ = 0.25 µM.

Table 4-3: Interassay precision and accuracy for Method 1 and Method 2.

	LLOQ				40 µM			
	Avg (µM)	Bias (%)	RSD (%)	n	Avg (µM)	Bias (%)	RSD (%)	n
T_1AM^a	0.10	2.4	19.3	7	40.8	2.0	11.0	7
T_0AM^a	0.11	8.8	17.1	7	41.3	3.3	14.8	7
$Ac-T_1AM^a$	0.12	5.3	12.0	6	42.5	6.2	6.7	6
$S-T_1AM^b$	0.22	-11.5	16.1	5	38.9	-2.6	5.8	7
TA_1^b	0.26	4.4	10.1	4	39.9	-0.2	5.0	7
TA_0^b	0.26	2.8	10.9	4	42.1	5.3	10.8	7

a, LLOQ = 0.1 µM; *b*, LLOQ = 0.25 µM.

Table 4-4: Typical regression equations for standard curves.

Analyte	Slope	Intercept	r^2
T_1AM	0.310	0.006	0.998
T_0AM	0.496	-0.004	0.998
$S\text{-}T_1AM$	0.0204	0.0003	0.989
$Ac\text{-}T_1AM$	0.305	-0.019	0.964
TA_1	0.407	0.016	0.994
TA_0	0.351	0.001	0.999

4.3.3 T_1AM Metabolites in Serum

The validated LC-MS/MS MRM method was used to quantify T_1AM metabolites in serum following a single IP injection of T_1AM. Sera were analyzed between 0 (vehicle injected) and 6 hours post T_1AM injection. Serum samples were processed in the presence or absence of β-glucuronidase in order to quantify T_1AM-glucuronide. At 10 minutes post T_1AM injection, all metabolites are detectable (Figure 4-4).

Figure 4-4: Chromatographic traces for T_1AM and T_1AM metabolites.
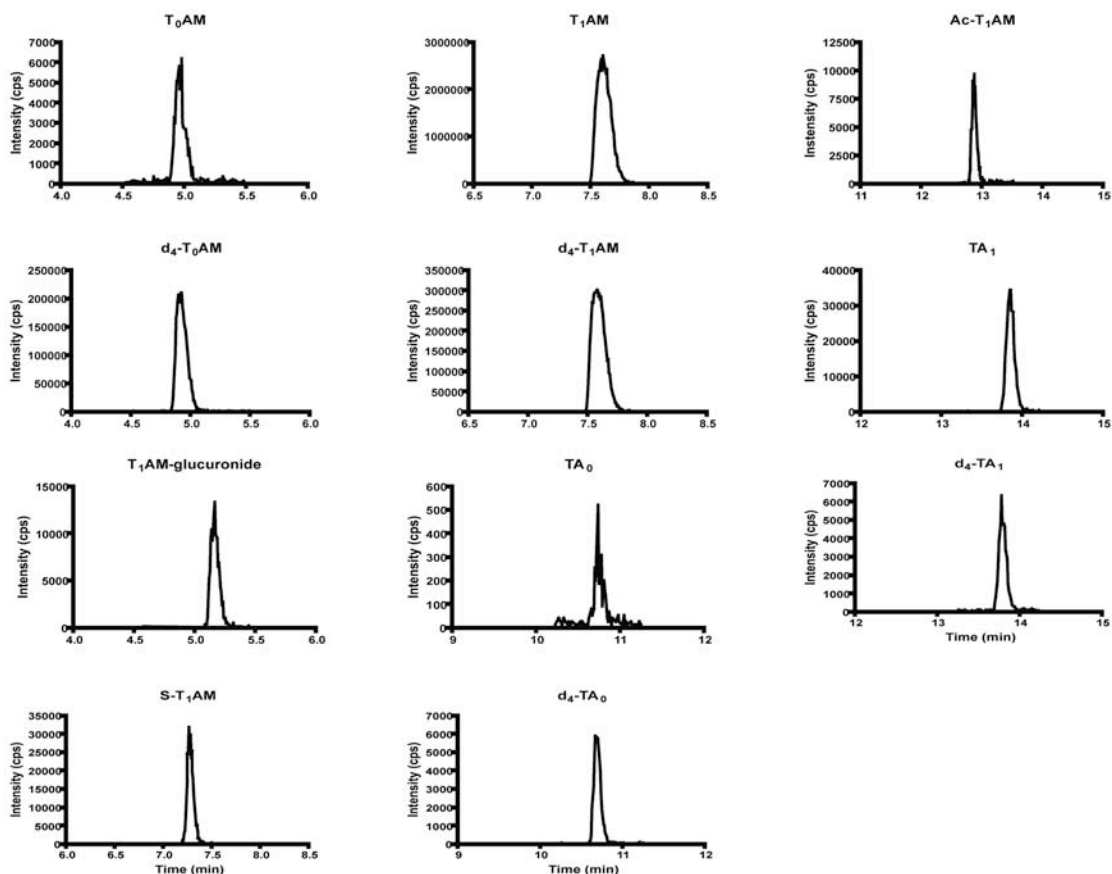
Representative XIC's for T_1AM metabolites from mouse serum at 10 minutes post-T_1AM injection. Traces correspond to the following *m/z* transitions: T_0AM, 230-213; d_4-T_0AM, 234-217; T_1AM-glucuronide, 532-515; S-T_1AM, 436-418; T_1AM, 356-339; d_4-T_1AM, 360-343; TA_0, 243-106; d_4-TA_0, 247-106; Ac-T_1AM, 398-212; TA_1, 369-127; d_4-TA_1, 373-127.

Each metabolite was quantified at all time points collected to determine the metabolite profile of T_1AM in serum (Figure 4-5A). At 10 minutes post-injection, the serum concentration of TA_1 is 17.7 ± 4.6 µM, which is equal to the concentration of unmodified T_1AM, 16.6 ± 8.5 µM. At 20 minutes post-injection, the concentrations of TA_1 and T_1AM are 23.5 ± 13.2 µM and 5.6 ± 3.1 µM, respectively, suggesting oxidative deamination is a major and rapid pathway of T_1AM metabolism. Between 20 minutes and 6 hours, the

70

concentrations of TA_1, $S-T_1AM$ and T_1AM-glucuronide are all greater than or equal to the

concentrations of unmodified T_1AM. The maximum serum concentrations for TA_1, $S-T_1AM$ and T_1AM-glucuronide all occur at 20 minutes post T_1AM injection, and are 23.5 ±

13.2 µM, 10.2 ± 3.3 µM and 6.74 ± 3.01 µM, respectively. $Ac-T_1AM$ is quantifiable in at

least 3 out of 4 samples between 0 and 90 minutes, reaching a maximum serum

concentration of 0.30 ± 0.11 µM at 20 minutes, and decreases to remain measurable at

the LLOQ in only one sample at 3 hours.

Figure 4-5: Serum T_1AM metabolites.
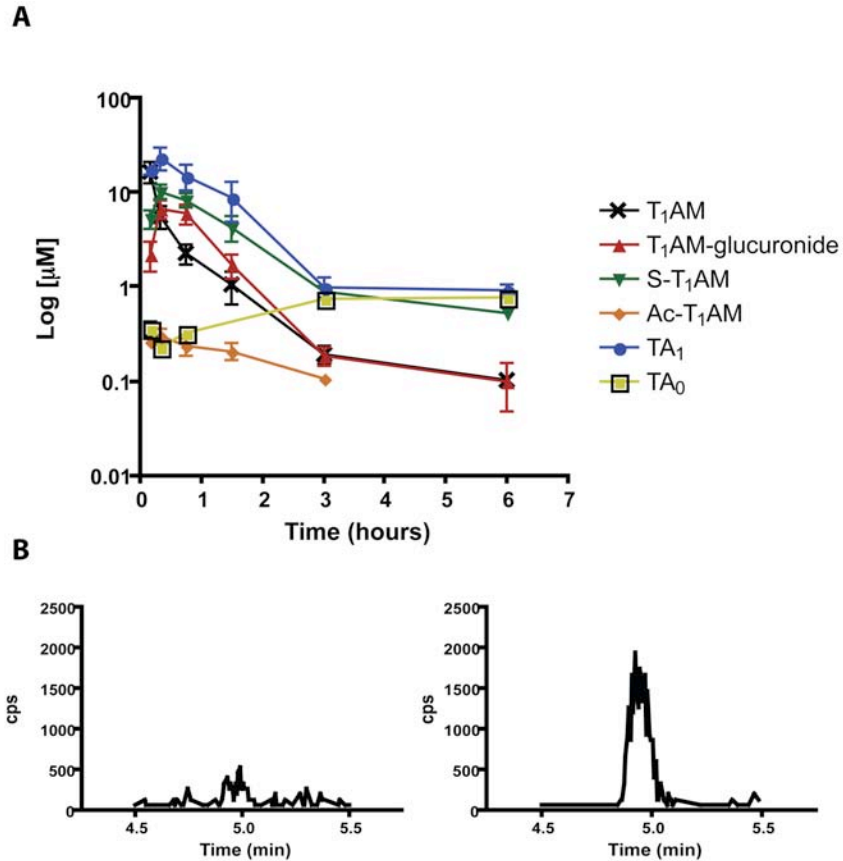
T_1AM metabolites in mouse serum. A) Concentrations of T_1AM, T_1AM-glucuronide, $S-T_1AM$, $Ac-T_1AM$, TA_1 and TA_0 between 10 minutes and 6 hours after a single IP injection of T_1AM; n = 3-4 per point, except for the following: T_1AM and T_1AM-glucuronide, 6 hours, n = 2; $Ac-T_1AM$, 3 hours, n = 1; TA_0, 10 and 45 minutes, n = 2; TA_0, 20 minutes and 3 hours, n = 1. B) XIC of T_0AM in serum at 20 minutes post-T_1AM injection in the absence (left) or presence (right) of β-glucuronidase.

71

TA$_0$ and T$_0$AM, the deiodinated thyroacetic acid and thyronamine, respectively, were not

observed in high quantities in serum. TA$_0$ is quantifiable in two out of four samples at 10

and 45 minutes, and one out of four samples at 20 minutes and 3 hours. The greatest

concentration of TA$_0$ occurs is at 6 hours post-injection (0.77 ± 0.16 µM). T$_0$AM is

occasionally detectable, but always below the LLOQ. Interestingly, the T$_0$AM peak

intensity increases at some time points following incubation with β-glucuronidase (Figure

4-5B), which suggests T$_0$AM-glucuronide may be a minor metabolite. T$_0$AM remains

below the LLOQ even after incubation with β-glucuronidase. Measured concentrations

in serum for all metabolites at all time points are reported in Table 4-5.

Table 4-5: Serum T$_1$AM and T$_1$AM metabolite concentrations.

Metabolite	10 min	20 min	45 min	90 min	3 hours	6 hours
T$_1$AM	16.6 ± 8.5[a]	5.57 ± 3.10[a]	2.27 ± 1.08[a]	1.05 ± 0.81[a]	0.19 ± 0.08[a]	0.10 ± 0.02[c]
T$_1$AM-glucuronide	2.22 ± 1.60[a]	6.74 ± 3.01[a]	5.93 ± 2.67[a]	1.69 ± 0.95[a]	0.19 ± 0.08[a]	0.10 ± 0.08[c]
S-T$_1$AM	5.27 ± 2.40[a]	10.2 ± 3.3[a]	8.23 ± 2.89[a]	4.28 ± 2.54[a]	0.88 ± 0.27[a]	0.52 ± 0.08[a]
Ac-T$_1$AM	0.26 ± 0.03[a]	0.30 ± 0.11[a]	0.23 ± 0.10[a]	0.21 ± 0.07[b]	0.11[d]	-
TA$_1$	17.7 ± 4.6[a]	23.5 ± 13.2[a]	15.0 ± 9.1[a]	8.85 ± 7.96[a]	1.0 ± 0.5[a]	0.91 ± 0.30[a]
TA$_0$	0.36 ± 0.09[c]	0.23[d]	0.32 ± 0.04[c]	-	0.75[d]	0.77 ± 0.16[b]

Calculated concentration (µM) of T1AM metabolites in serum between 0 and 6 hours post-T1AM injection.
No compound was quantifiable at t=0 (vehicle injected), and T0AM was always below the LLOQ; a, n = 4; b,
n = 3; c, n = 2; d, n = 1.

4.3.4 Tissue Distribution of T$_1$AM Metabolites

The method reported here is validated to quantify metabolites from mouse serum. Due

to matrix effects, we were unable to use this method to quantify metabolites in tissues.

In order to determine the relative tissue distribution of metabolites, the area ratio (peak

area of metabolite to deuterated internal standard) for each metabolite was normalized

to the mass of tissue analyzed. Figure 4-6 illustrates the relative tissue distributions of

metabolites following T$_1$AM injection. Tissues analyzed include liver, kidney, heart,

brain, BAT and WAT. T_1AM is distributed in all six tissues at 6 hours, the final time point analyzed. T_0AM is detectable at 6 hours in liver and kidney, but only intermittently at earlier time points in brain, heart and WAT, and not detectable in BAT at any time point. T_1AM-glucuronide remains detectable in both liver and kidney at 6 hours, suggesting these tissues may be sites of T_1AM-glucuronide accumulation. $S\text{-}T_1AM$ is transiently present in BAT (at 90 minutes), but remains in liver, kidney, heart and WAT at 6 hours, while brain is not a major site of distribution. $Ac\text{-}T_1AM$ is distributed to all tissues analyzed, and remains in kidney, heart and brain at 90 minutes, and in liver, BAT and WAT at 6 hours. TA_1 is also distributed to all tissues analyzed, but only minimally to brain (to 90 minutes) while remaining present in liver, kidney, heart, BAT and WAT at 6 hours. TA_0 was detectable in liver and kidney between 0 and 6 hours, but was only detectable in heart at 6 hours and was not detectable at any time point in brain, BAT or WAT.

Figure 4-6: Relative tissue distribution of T_1AM metabolites.
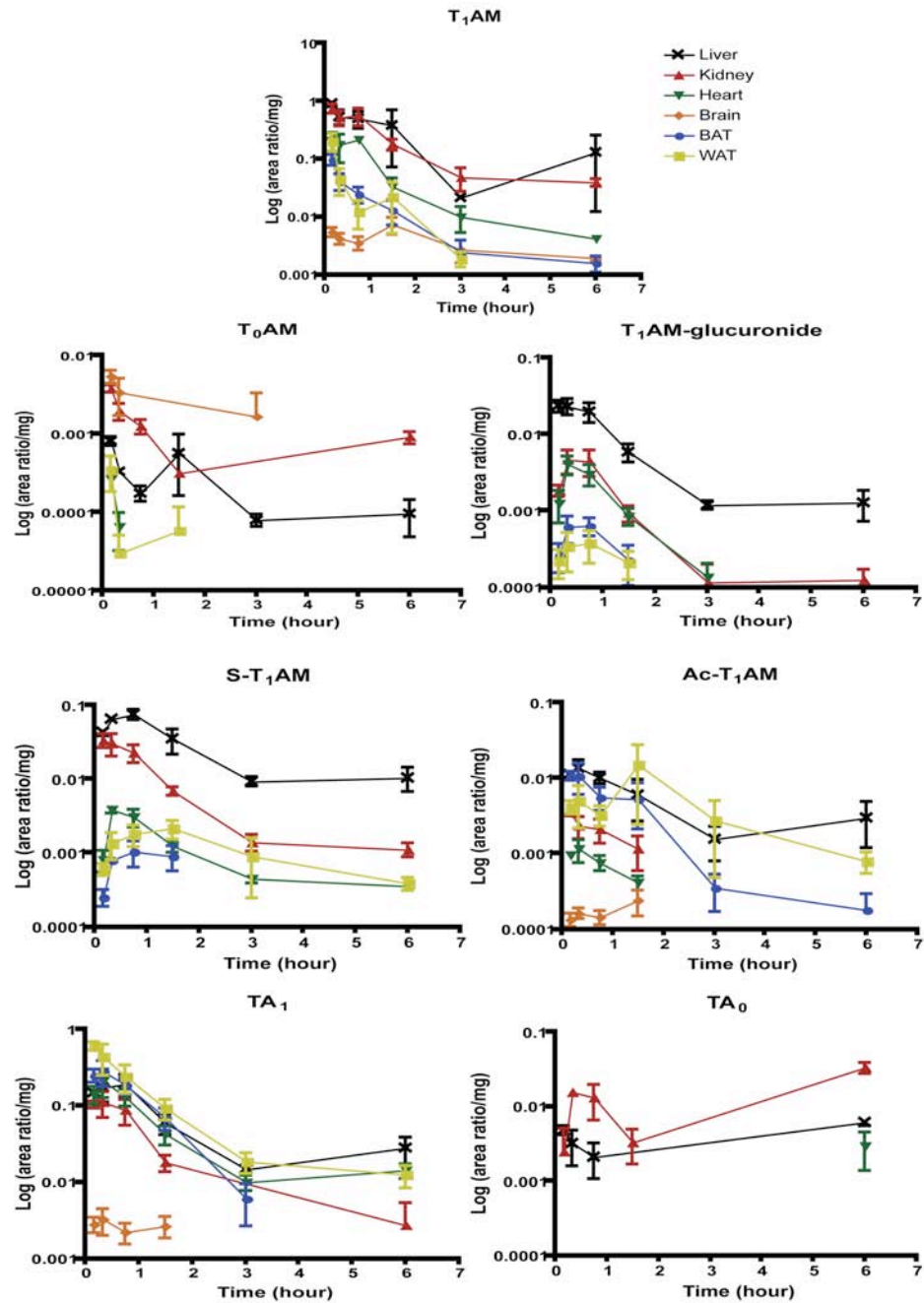
Relative tissue distribution of T_1AM metabolites to liver, kidney, heart, brain, BAT and WAT. Peak areas were integrated with respect to the deuterated internal standard (d_4-T_1AM used for T_1AM-glucuronide, S-T_1AM and Ac-T_1AM) and the area ratio was normalized to the amount of tissue analyzed; n = 1-3 per point. T_0AM was not detectable in BAT. TA_0 was not detected in brain, BAT or WAT, and was only detected in heart at 6 hours (n = 2).

74

4.4 Discussion

IDA methods offer a means to perform an unbiased screen for unknown metabolites of small molecules by LC-MS/MS. Here we report the use of IDA methods to identify novel *in vivo* metabolites of T_1AM. This study provides the first report of thyronamine metabolites in mouse, including TA_1, which was previously shown to be a metabolite in rat (88), and the first report of $S-T_1AM$ occurring *in vivo*, which was previously suggested as a metabolite in an *in vitro* enzymatic assay (87). The use of IDA methods also identified two novel compounds that occur as T_1AM metabolites, $Ac-T_1AM$ and T_1AM-glucuronide.

Since little was known about T_1AM metabolites in serum prior to this study, the compounds identified using IDA methods were used to develop a validated MRM method to quantify this panel of metabolites in mouse serum. In order to determine which compounds may represent major pathways of metabolism, mouse serum was analyzed following a single IP injection of T_1AM. At 20 minutes post-injection, three metabolites, TA_1, $S-T_1AM$ and T_1AM-glucuronide, are present in serum at greater concentrations than unmodified T_1AM. This suggests that oxidative deamination, sulfation and glucuronidation represent the major pathways of T_1AM metabolism in mice. $Ac-T_1AM$ and TA_0 were also quantified in serum, although in lesser concentrations than the other metabolites, indicating these may be minor metabolic pathways. Since T_1AM is known to be a substrate for deiodination to form T_0AM (86), it was interesting that T_0AM was never present above the LLOQ for the method, suggesting this is a minor pathway *in vivo*. Although it remained below the LLOQ, the increased peak intensity for T_0AM following treatment with β-glucuronidase suggests that T_0AM-glucuronide may be

also be a minor T_1AM metabolite. Another reason for low T_0AM levels could be that deiodination to T_0AM results in rapid elimination of the compound, preventing an accumulation of this metabolite to measurable quantities.

While absolute values were not quantified, we also investigated the relative tissue distribution of T_1AM metabolites. Similar to the serum results, T_0AM and TA_0 appear to be minor metabolites and minimally distributed to tissues. TA_0 does appear to accumulate in liver and kidney, and was detectable in brain at 6 hours post-injection. This is a similar pattern of accumulation that was seen in serum, in which the highest concentration of TA_0 (0.77 ± 0.16 µM) was observed at 6 hours post-injection. T_0AM also appears to accumulate in liver and kidney at 6 hours post-injection, which contrasts with serum, where T_0AM was not quantifiable. Since it appears that T_0AM-glucuronide is present to some extent in serum (Figure 4-5B), tissue distribution of T_0AM-glucuronide may be interesting to investigate in the future.

TA_1 and S-T_1AM are extensively distributed and remain in most tissues at 6 hours post-injection. This is similar to the elevated levels of TA_1 and S-T_1AM measured in serum. TA_1 is distributed to all tissues analyzed, although is not detectable in brain longer than 90 minutes post-T_1AM injection. S-T_1AM does not appear to be distributed to brain, and is not detectable in BAT longer than 90 minutes post-injection. This suggests that tissue specific distribution of these metabolites may be important for regulating their action. Ac-T_1AM is measurable in liver, kidney and WAT at 6 hours (Figure 4-6), whereas it is not quantifiable in serum 3 hours post-injection (Figure 4-5A). This apparent accumulation of Ac-T_1AM in liver and WAT likely reflects specific tissue binding of this metabolite since fat is more poorly perfused than liver. Likewise, T_1AM-glucuronide

appears to accumulate in liver and kidney, which is evidenced by detection of this metabolite in these tissues at 6 hours; unlike Ac-T_1AM, T_1AM-glucuronide is still detectable in serum 6 hours post-injection. This accumulation of T_1AM-glucuronide in liver and kidney is similar to a recent report of T_4-glucuronide present in liver and kidney (139), suggesting these tissues may serve as storage for glucuronide-conjugates.

We have reported the occurrence of novel *in vivo* metabolites of T_1AM, relative tissue distribution of metabolites and a validated LC-MS/MS MRM method to quantify these metabolites from mouse serum. The number of T_1AM metabolites (Figure 4-1) is similar to the extensive metabolism observed for T_4 (55) and rich, diverse metabolism such as this is not generally seen with synthetic drugs or xenobiotics. This suggests that covalent modifications may be critical for regulating endogenous T_1AM exposure and biological activity. As interest in measuring T_1AM remains high and new analytical methods continue to be developed (77, 78), this method represents a valuable analytical tool to study endogenous T_1AM metabolites. Since several metabolites, notably S-T_1AM, Ac-T_1AM and T_1AM-glucuronide remain detectable in tissues at 6 hours, investigating endogenous tissue distribution of these metabolites is essential for improving our understanding of T_1AM action and regulation.

Chapter 5: Development of a protocol to extract 3-iodothyronamine

The existing extraction protocol in the Scanlan Lab that was the starting point for this work was developed largely by Travis Geraci, a former member of the Scanlan Lab. Iodothyronamines (T_4AM, T_3AM, rT_3AM, $3,5\text{-}T_2AM$, $3,3'\text{-}T_2AM$, T_1AM and T_0AM) were synthesized by former members of the Scanlan Lab. Deuterated iodothyronamines ($d_4\text{-}T_0AM$, $d_4\text{-}T_1AM$, $d_4\text{-}rT_3AM$ and $d_4\text{-}T_4AM$) were synthesized by Aaron Nilsen. $[^{125}I]\text{-}T_1AM$ was synthesized by Gouriprasanna Roy.

5.1 Introduction

The discovery of endogenous T_1AM in a variety of species (75, 76, 80) has led to interest in developing analytical methods to quantify endogenous T_1AM levels. Liquid chromatography-tandem mass spectrometry (LC-MS/MS) has been the method of detection used in most reported cases of endogenous T_1AM (75, 76, 80) and seems an ideal method of detection continuing forward due to the levels of sensitivity and selectivity that can be achieved. Prior to analysis by LC-MS/MS, however, some form of sample preparation, either protein precipitation or enrichment of the compound of interest (T_1AM), or both, is necessary to facilitate detection. The ideal sample preparation method would result in consistently reproducible extraction of endogenous T_1AM from serum and/or tissue. Several versions of extraction protocols have existed in the Scanlan Lab over the years, and one version of a Scanlan Lab extraction method was the starting point for this work. The following chapter discusses various aspects of the work done to establish a method to reliably extract endogenous T_1AM from biological samples. While this work was not successful in establishing a reliable protocol, the information presented here may be useful in guiding future work on T_1AM extraction methods.

5.2 Methods

5.2.1 General

Rat (normal, pooled) and mouse (C57Bl6) sera were purchased from Innovative Research (Novi, MI) and normal mouse serum was purchased from Invitrogen

(Carlsbad, CA). T_4/T_3 deficient human serum was purchased from Sigma-Aldrich (St. Louis, MO), and normal human serum was purchased from Innovative Research or provided as patient samples from Samuel Refetoff at The University of Chicago Medical Center. Human tissue samples were provided by Drs. Kathryn Schuff and Mary Samuels at OHSU. Control mouse livers were obtained as extra tissue from C57Bl6 mice used for other experiments (see Chapters 3 and 4). Amicon Ultrafree-MC 0.22 µm or Amicon Microcon YM-30 filters were purchased from Millipore (Billerica MA). Bond-Elut Certify (3 mL, 130 mg) SPE cation exchange cartridges were from Varian (Lake Forest, CA). Radioactive samples were counted in a Beckman gamma counter. Lipoprotein lipase was purchased from MP Biomedicals (Salon, OH) and Proteinase K from *Tritrachium album* (≥30 U/mg) from Fisher Scientific (Pittsburg, PA).

Iodothyronines (T_0, T_1, 3,5-T_2, 3,3'-T_2, T_3, rT_3 and T_4) were purchased from either Sigma-Aldrich or Toronto Research Chemicals (Canada), and iodothyronamines (T_0AM, T_1AM, 3,5-T_2AM, 3,3'-T_2AM, T_3AM, rT_3AM, T_4AM), deuterated iodothyronamines (d_4-T_0AM, d_4-T_1AM, d_4-rT_3AM, d_4-T_4AM) and ^{125}I-T_1AM were synthesized as described previously (98, 136). HPLC grade solvents were purchased from Burdick and Jackson (Muskegon, MI) or Fisher Scientific. Unless otherwise specified, buffers were prepared using Milli-Q purified water, and remaining supplies and reagents were purchased from Fisher or Sigma-Aldrich.

5.2.2 Solid Phase Extractions

The existing protocol in the Scanlan lab used solid phase extraction (SPE) to enrich the final sample for T_1AM. For serum samples, 10 pmol of d_4-T_1AM was added to 100 µL of serum and samples were vortexed. Urea (8 M) was added in a ratio of 3:1 and samples were incubated at 80 °C for 30 minutes. Samples were quenched with the addition of

2:1 acidic acetone (pH 4-5, by pH meter). Samples were vortexed and centrifuged at 20800 x g for 5 minutes. Supernatants were then transferred to 13 x 100 borosilicate test tubes. For tissue samples, tissues were weighed and then added to a clean 15-ml falcon tube with 3 mL of chilled 100 mM phosphate buffer. To each sample, 10 pmol of d_4-T_1AM was added and tissues were homogenized using a PowerGen 125 homogenizer (Fisher). Proteins were precipitated from the tissue homogenate with the addition of 2:1 chilled acidic acetone and samples were left on ice for 10 minutes. Samples were centrifuged at 2340 x g for 5 minutes, and supernatants were transferred to clean 13 x 100 borosilicate test tubes. For both serum and tissues, supernatants were evaporated to dryness in a Savant speedvac with refrigerated vapor trap. SPE cartridges were preconditioned by gravity flow with 2 mL MeOH, 2 mL deionized water and 1.4 mL phosphate buffer (pH 6). Dried sample residues were redissolved in 2 mL phosphate buffer (0.1 M) and applied to the SPE cartridges. SPE cartridges were washed with 2 mL deiodized water and dried under positive pressure argon for 10 minutes. Samples were eluted with 2 mL MeOH:NH_4OH (98:2) followed by an additional 2 x 0.5 mL MeOH:NH_4OH (98:2). Eluates were evaporated to dryness in a speedvac, and the residues were redissolved in 80 µL 1:1 MeOH:0.1 M HCl with shaking for 2 hours. Samples were centrifuged at 20800 x g for 5 minutes, filtered through 0.22 µm filters, and stored at -80 °C until analysis by LC-MS/MS.

In the course of method development, two major modifications were made to the SPE protocol. First, Proteinase K was used to remove protein from the sample, which had been previously used in an earlier version of the protocol in the Scanlan Lab. Second, the solvents used with SPE were modified based on what has previously been used to extract thyronines by SPE (140). Additional minor changes to the protocol included the

addition of iproniazid and iopanoic acid to inhibit potential oxidative deamination (88) and deiodination (23), respectively, and sodium dodecyl sulfate (SDS) to denature proteins and stimulate protein degradation by Proteinase K (141).

For Sample Set I-A, d_4-T_1AM (10 pmol) was added to 2 mL human serum. Iproniazid and iopanoic acid were added to final concentrations of 100 μM and 10 μM, respectively, and SDS was added to a final concentration of 1%. Proteinase K was added at a concentration of 4 μg protein/μL serum and incubated at 55 °C for 5 hours. For tissue samples (thyroid or fat from human), tissues were weighed and added to a clean 15-mL conical tube with 3 mL potassium phosphate (100 mM, pH 6) and 10 pmol d_4-T_1AM. Iproniazid and iopanoic acid were added to final concentrations of 100 μM and 10 μM, respectively. Tissues were homogenized and centrifuged at 3200 x g for 5 minutes. Supernatants were transferred to clean 15-mL conical tubes and SDS was added to a final concentration of 1%. Proteinase K was added to each sample at a concentration of 5.2 – 6.9 μg Proteinase K/mg tissue, and samples were incubated at 55 °C for 5 hours. For both serum and tissue samples, proteins were precipitated with the addition of 2:1 ice-cold acidic acetone (0.03% HCl in acetone) and samples were centrifuged at 3200 x g for 5 minutes. Supernatants were transferred to 13 x 100 borosilicate tubes and evaporated to dryness under nitrogen.

SPE cartridges were pre-conditioned with 2 mL DCM:iPOH (75:25), 2 mL MeOH and 2 mL 0.1 M potassium phosphate (pH 6). Sample residues were redissolved in 2 mL potassium phostphates (0.1 M, pH 6), applied to SPE cartridges and washed sequentially with 3.3 mL water, 1.7 mL 0.1 M HCl, 6.7 mL MeOH and 3.3 mL DCM:iPOH (75:25). T_1AM was eluted with 2 mL DCM:iPOH:NH$_4$OH (70:26.5:3.5). Eluates were

evaporated to dryness under nitrogen and redissolved in 80 μL 1:1 MeOH:0.1 M HCl.

Samples were centrifuged at 20800 x g for 5 minutes, filtered through 0.22 μm filters and

stored at -80 °C until analysis by LC-MS/MS.

5.2.3 [^{125}I]-T$_1$AM Extractions

Since analyzing samples by LC-MS/MS is expensive in terms of both time and money, a

crude [^{125}I]-T$_1$AM based assay was developed to quickly determine the effectiveness of

various treatments on the extraction T$_1$AM from serum. Specific experimental details are

provided below, but briefly, [^{125}I]-T1$_1$AM was incubated with serum to equilibrate with

serum binding proteins before being treated with different extraction conditions to disrupt

protein binding interactions. Radioactivity was counted to determine the percent of ^{125}I-

T$_1$AM extracted relative to the total amount of [^{125}I]-T$_1$AM added to the sample. In the

following experiments, the concentration of [^{125}I]-T$_1$AM varied in order to maintain

radioactive counts in the experiments as [^{125}I] decayed (t$_{1/2}$ = 60 days).

Sample Set II-A treatment conditions are given in Table 5-1. For all samples, 5 μl of

~1.25 mM [^{125}I]-T$_1$AM was incubated with 500 μl human serum at 37 °C overnight, prior

to sample treatment. The supernatant from each sample treatment was counted to

determine the presence of [^{125}I]-T$_1$AM.

Table 5-1: Sample Set II-A treatment conditions.

Sample	Treatment	Reference
A1	125 µl Buffer 1 (1.5 ml of 10 M KOH + 8.5 ml saturated NaHCO$_3$); 1250 µl toluene; vortex and centrifuge.	(142)
A2	125 µl Buffer 1 (1.5 ml of 10 M KOH + 8.5 ml saturated NaHCO$_3$); 1250 µl DCM; vortex and centrifuge.	(142)
A3	125 µl Buffer 1 (1.5 ml of 10 M KOH + 8.5 ml saturated NaHCO$_3$); 1250 µl EtOAc; vortex and centrifuge.	(142)
A4	50 µl 5 M KOH; 0.3 g anhydrous sodium sulfate; centrifuge.	(143)
A5	100 µl 0.1 M NaOH; extract with 1200 µl DCM.	(144)
A6	100 µl 1 M HCl; vortex and leave on ice for 15 minutes; 500 µl CHES buffer (pH 9.0); adjust to pH 10-11 with 40% KOH; 1500 µl EtOAc; remove top (organic) layer.	Previous Scanlan Lab tissue extraction protocol.
A7	500 µl CHES buffer (pH 9.0); adjust to pH 10-11 with 40% KOH; 1500 µl EtOAc; remove top (organic) layer.	Previous Scanlan Lab tissue extraction protocol.
A8	1000 µl acidic acetone (0.03% HCl in acetone).	Scanlan Lab serum extraction.
A9	125 µl water and 1250 µl EtOAc; centrifuge.	Control (protein precipitation but not acid/base treatment of serum).
A10	100 µl Proteinase K; 37 °C for 90 minutes; 1200 µl acidic acetone (0.037% HCl in acetone); vortex and leave on ice for 10 minutes; centrifuge.	Scanlan Lab Proteinase K serum extraction protocol.

For Sample Set II-B, 5 µl of ~1.25 mM [^{125}I]-T$_1$AM was incubated with 500 µl human serum at 37 °C overnight prior to treatment. Each sample was vortexed with 1000 µl ice-cold acetone or acetonitrile, with 0-3.72% HCl. Protein precipitates were pelleted with centrifugation and supernatants were removed for counting.

For Sample Set II-C, 5 µl of ~1.25 mM $[^{125}I]$-T_1AM was incubated with 500 µl human or rat serum at 37 °C for 24 or 72 hours prior to treatment. Each sample was vortexed with 1000 µl ice-cold acetone or acetonitrile with 0-3.72% HCl. Additionally, rat serum only was brought to a final concentration of 2 N NaOH or 2 N HCl to precipitate proteins. All protein precipitates were pelleted with centrifugation and supernatants were removed for counting.

Sample Set II-D treatment conditions are given in Table 5-2. For all samples, 5 µl of ~2.5 mM $[^{125}I]$-T_1AM was incubated with 500 µl of rat serum at 37 °C for 24 hours. Following treatment, each fraction (organic, aqueous, supernatant and/or pellet) was counted in order to account for 100% of the added radioactivity.

Table 5-2: Sample Set II-D treatment conditions.

Sample	Treatment	Fractions Counted for Radioactivity	Reference
D1	5 1-hour extractions at room temperature with 500 µl EtOAc:Ether (3:1).	Organic extractions and aqueous layer.	(145)
D2	5 1-hour extractions at room temperature with 500 µl EtOAc:Ether (3:1); acetone precipitation of aqueous layer.	Organic extractions, acetone supernatant and protein pellet.	(145)
D3	1000 µl isopropanol; shake overnight; centrifuge.	Organic supernatant and protein pellet.	(146)
D4	1000 µl isopropanol; vortex for 1 minutes and centrifuge.	Organic supernatant and protein pellet.	(146)
D5	10 µl concentrated HCl; 1000 µl $CHCl_3$; vortex; remove acid layer (top); adjust aqueous to pH 8-10 with 40% NaOH; 1000 µl $CHCl_3$; remove organic layer (bottom).	First chloroform layer, aqueous layer, second chloroform wash, "pellet" between aqueous and organic layers.	

Sample Set II-E treatment conditions are given in Table 5-3. For all samples, 4 µl of

~2.5 mM $[^{125}I]$-T_1AM was incubated with 400 µl of rat serum at 37 °C for 24 hours.

Following treatment, both organic and aqueous fractions were counted in order to

determine 100% recovery of added radioactivity. In the case of the TRIZOL extractions

(Samples E5 and E6), the aqueous RNA fraction, DNA pellet, protein pellet and

remaining supernatant were counted for radioactivity.

Table 5-3: Sample Set II-E treatment conditions.

Sample	Treatment
E1	50 µl of 10% Triton X-100; incubate at 37 °C for 1 hour; 40% NaOH to pH 12-13; 800 µl CHCl$_3$.
E2	50 µl of 10% CHAPS; incubate at 37 °C for 1 hour; 40% NaOH to pH 12-13; 800 µl CHCl$_3$.
E3	50 µl of 10% Tween 20 (TBSt); incubate at 37 °C for 1 hour; 40% NaOH to pH 12-13; 800 µl CHCl$_3$.
E4	Incubate at 37 °C for 1 hour; 40% NaOH to pH 12-13; 800 µl CHCl$_3$.
E5	TRIZOL extraction: 4000 µl TRIZOL reagent; 800 µl CHCl$_3$; separate top aqueous layer (containing RNA) and the phenol-chloroform interphase; 1200 µl EtOH to phenol-chloroform; separate pellet (containing DNA) and phenol-EtOH; add 6000 µl iPOH to phenol-EtOH layer; separate pellet (containing precipitated protein) and supernatant.
E6	40% NaOH to pH 12-13; TRIZOL extraction: 4000 µl TRIZOL reagent; 800 µl CHCl$_3$; separate top aqueous layer (containing RNA) and the phenol-chloroform interphase; 1200 µl EtOH to phenol-chloroform; separate pellet (containing DNA) and phenol-EtOH; add 6000 µl iPOH to phenol-EtOH layer; separate pellet (containing precipitated protein) and supernatant.

Sample Set II-F treatment conditions are given in Table 5-4. For all samples, 4 µl of

~2.5 mM $[^{125}I]$-T_1AM was incubated with 400 µl of rat serum at 37 °C for 24 hours.

Table 5-4: Sample Set II-F treatment conditions.

Sample	Treatment	Fractions Counted for Radioactivity
F1	Adjust to pH 2 with concentrated HCl; 37 °C for 2 hours, with rotating; 800 µl CHCl$_3$, vortex, remove organic; 800 µl CHCl$_3$ to remaining aqueous.	First CHCl$_3$ wash; second CHCl$_3$ wash; aqueous; intermediate precipitate (between aqueous and organic).
F2	Adjust to pH 2 with concentrated HCl; 100 µl 10% Triton X-100; 37 °C for 2 hours, with rotating; 800 µl CHCl$_3$, vortex, remove organic; 800 µl CHCl$_3$ to remaining aqueous.	First CHCl$_3$ wash; second CHCl$_3$ wash; aqueous; intermediate precipitate (between aqueous and organic).
F3	Adjust to pH 2 with concentrated HCl; 100 µl 10% CHAPS; 37 °C for 2 hours, with rotating; 800 µl CHCl$_3$, vortex, remove organic; 800 µl CHCl$_3$ to remaining aqueous.	First CHCl$_3$ wash; second CHCl$_3$ wash; aqueous; intermediate precipitate (between aqueous and organic).
F4	Adjust to pH 2 with concentrated HCl; 100 µl 10% Tween 20 (TBSt); 37 °C for 2 hours, with rotating; 800 µl CHCl$_3$, vortex, remove organic; 800 µl CHCl$_3$ to remaining aqueous.	First CHCl$_3$ wash; second CHCl$_3$ wash; aqueous; intermediate precipitate (between aqueous and organic).
F5	Adjust to pH 2 with concentrated HCl; 50 µl 10% Triton X-100 and 50 µl 10% CHAPS; 37 °C for 2 hours, with rotating; 800 µl CHCl$_3$, vortex, remove organic; 800 µl CHCl$_3$ to remaining aqueous.	First CHCl$_3$ wash; second CHCl$_3$ wash; aqueous; intermediate precipitate (between aqueous and organic).
F6	50 µl 10% Triton X-100 and 50 µl 10% CHAPS; adjust to pH 2 with concentrated HCl; 37 °C for 2 hours, with rotating; 800 µl CHCl$_3$, vortex, remove organic; 800 µl CHCl$_3$ to remaining aqueous; separate CHCl$_3$ and aqueous; 800 µl acetone to aqueous; vortex, centrifuge, remove supernatant.	First CHCl$_3$ wash; second CHCl$_3$ wash; intermediate precipitate (between aqueous and organic); acetone supernatant; pellet from acetone precipitation.

Filtering through 0.22 µm filters was used to determine the ratios of protein bound and

unbound [^{125}I]-T$_1$AM following incubation with serum. [^{125}I]-T$_1$AM (4 µl of ~2.5 mM) was

added to 400 µl of rat serum or Milli-Q filtered water. Samples were vortexed for 30

seconds, applied to the filters and centrifuged at 14K rpm for 5 minutes. Both the flow through fractions and membranes were counted for radioactivity, with the flow through corresponding to unbound $[^{125}I]$-T_1AM and radioactivity remaining on the filter corresponding to protein bound $[^{125}I]$-T_1AM. Water was used as a control for non-specific binding to the filters since it lacks serum-binding proteins.

5.2.4 Charcoal Based Extraction

The approach to extracting T_1AM was shifted to a non-specific pull-down of small molecules that could then be re-extracted from the solid support. This approach is based generally on the protocol from Sigma-Aldrich to prepare T_4/T_3 deficient human serum. Briefly, serum is incubated with dextran-coated charcoal in a ratio of 1 g per 100 mL serum (147) for 48 hours at 4 °C while shaking. The supernatant is then incubated with silica in a ratio of 10 g per liter for 24 hours at 4 °C. Both the charcoal and silica are extracted with organic solvents. Organic extracts were evaporated to dryness under a stream of nitrogen and redissolved in 60 µL water/methanol/acetic acid (90:10:1) (34).

For Sample Set III-A, 400 µl of serum was incubated with 10 pmol d_4-T_1AM. Samples were run in duplicate, either with or without the addition of 30 pmol standard mix (5 pmol/µL each T_4, T_4AM, T_3, T_3AM, rT_3, rT_3AM, 3,5-T_2, 3,5-T_2AM, 3,3'-T_2, 3,3'-T_2AM, T_1, T_1AM, T_0 and T_0AM). Serum was adjusted to ~pH 11 with the addition of 1 drop (Pasteur pipette) of 4.4 M NaOH or left without a pH adjustment. Charcoal pellets were extracted with 1 mL + 2 x 0.5 mL 1:1 EtOAc:DCM or Ether:DCM. Silica pellets were extracted with 1 mL + 2 x 0.5 mL 1:1 MeOH:DCM.

For Sample Set III-B, 400 µL of serum was incubated with 30 pmol d_4-T_1AM. Samples were run in duplicate, either with or without the addition of 30 pmol standard mix. Charcoal pellets were incubated for 1 hour at 60 °C with 1 mL of EtOAc:DCM (1:1), MeOH:DCM (1:1), EtOAc:DCM (1:1) with 1% HCl, or MeOH:DCM (1:1) with 1% HCl, followed by two additional extractions of 0.5 mL. Silica pellets were extracted with 1 mL + 2 x 0.5 mL MeOH:DCM:NH_4OH (50:50:1) at RT. One sample contained 120 pmol of standards in 1:1 MeOH:DCM with 1% HCl, and was incubated at 60 °C for 1 hr to determine the stability of the standards to the extraction conditions.

For Sample Set III-C, serum samples were treated to disrupt protein binding prior to charcoal and silica extraction. To each 400 µL serum sample, 30 pmol of d_4-T_1AM was added. Serum was then incubated with Proteinase K (800 µg), lipoprotein lipase (1 unit), 2:1 urea (10 M), acidified to pH 1 (200 µl of 30% HCl), treated with urea and Proteinase K, Proteinase K and lipoprotein lipase, or urea, proteinase K and lipoprotein lipase. One sample contained 30 pmol of standards and was incubated with urea, proteinase K and lipoprotein lipase to determine the stability of the standards to extraction conditions. Samples containing enzymes or urea were incubated for 1 hr at 37 °C, and samples treated with both urea and enzymes were first incubated with urea for 1 hr at 37 °C followed by the addition of enzymes and a second incubation for 1 hr at 37 °C. Charcoal pellets were extracted with 1 mL 1:1 DCM:MeOH with 1% HCl for 1 hr at 60 °C, followed by two additional extractions of 0.5 mL 1:1 DCM:MeOH with 1% HCl. Silica pellets were extracted with 1 mL + 2 x 0.5 mL 50:50:1 MeOH:DCM:NH_4OH.

For Sample Set III-D, 30 pmol d_4-T_1AM was added to 400 µL mouse serum. Serum was treated with 2:1 urea (10 M) for 1 hr at 37 °C; Protection Solution (100 µL of 25 mg/mL

each of ascorbic acid, citric acid and DTT) followed by 2:1 acetone precipitation and incubation at RT for 30 min (92); NaCl (82 µL of 5 M) for 1 hr at RT followed by acetone precipitation (77); or 2:1 guanidinium-HCl (8 M) for 1 hr at 37 °C. For urea and guanidinium-HCl treatments, pH of the sample was either unaltered or adjusted to pH 4-5 prior to incubation with charcoal. Charcoal pellets were extracted with 1 mL 1:1 DCM:MeOH + 1% HCl for 1 hr at 60 °C, followed by 2 x 0.5 mL 1:1 DCM:MeOH + 1% HCl. Samples were not incubated with silica following charcoal incubations.

For Sample Set III-E, 30 pmol d_4-T_1AM was added to 400 µL mouse serum. Serum was treated with 2:1 urea (10 M) for 1 hr at 37 °C; Protection Solution (100 µL of 25 mg/mL each of ascorbic acid, citric acid and DTT) followed by acetone precipitation and incubation at RT for 30 min (92); Protection Solution (100 µl) followed by 2:1 urea (10 M) for 1 hr at 37 °C; or Protection Solution (100 µL of 25 mg/mL each of ascorbic acid, citric acid and DTT) with acetone precipitation and incubation at RT for 30 min, followed by evaporation of acetone under nitrogen and incubation with 2:1 urea (10 M) for 1 hr at 37 °C.

5.2.5 Zucchi Lab Protocol

Much effort was made to successfully reproduce the published T_1AM extraction protocol from Riccardo Zucchi's lab at the University of Pisa in Italy (77). In this work, the Zucchi protocol was used to analyze mouse livers only, since this protocol detected the greatest concentration of T_1AM in rat liver (77). Livers were homogenized in potassium acetate buffer (0.1 M, pH 4) at a ratio of 1 mL per 1 g of tissue with 30 passes in a motorized dounce homogenizer with a PTFE coated plunger. Potassium acetate buffer was

prepared with HPLC grade water (Fisher). Supernatants were centrifuged for 10

minutes at 1430 x g and the volume of supernatant was recorded. Internal standards

were added (20 pmol each of d_4-T_1AM, d_4-T_0AM, d_4-rT_3AM and d_4-T_4AM) followed by

NaCl (60 mg/mL of supernatant). Samples were vortexed and incubated at room

temperature for 1 hour. Ice-cold acetone was added (2:1 volume), samples were

vortexed, and incubated on ice for 30 minutes. Samples were centrifuged and

supernatants were transferred to clean tubes (13 x 100 borosilicate test tubes) and

evaporated to dryness in a speedvac. SPE cartridges were pre-conditioned with 2 mL

DCM:iPOH (75:25), 2 mL MeOH and 2 mL 0.1 M potassium acetate buffer (pH 4). Dried

sample residues were redissolved in 1 mL potassium acetate buffer (0.1 M, pH 4) and

applied to SPE cartridges by gravity. SPE cartridges were washed with 3.5 mL water,

1.6 mL 0.1 M HCl, 7 mL MeOH and 3.5 mL DCM:iPOH (75:25). T_1AM was eluted with 2

mL DCM:iPOH:NH_4OH (70:26.5:3.5) and evaporated to dryness in the speedvac.

Samples were redissolved in 100 µL H_2O:MeOH:acetic acid (90:10:1) (86) and filtered

through 0.22 µm filters prior to analysis.

5.2.6 LC-MS/MS Methods

Three LC-MS/MS methods were used at various points in the method development

process. Method 1 was previously published (81) and used a Thermo Surveyor auto-

sampler and HPLC pump with a Thermo TSQ Quantum Discovery triple quadrupole

mass spectrometer (San Jose, CA). Samples were injected (20 µL) onto a

ThermoHypersil Hypurity C_{18}, 200 x 2.1 mm, 5 µm column with a guard column

(Waltham, MA). Samples were eluted with an isocratic mobile phase consisting of 5 µM

ammonium formate in methanol and water (45:55) with 0.01% TFA. The flow rate was

0.3 mL/min, and the column temperature was 30 °C. Samples were ionized using electrospray ionization (ESI) in the positive mode. Remaining instrument settings were as follows: spray voltage, 3.0 kV; sheath nitrogen gas flow rate, 45; aux nitrogen gas flow rate, 20; tube lens voltage, 150 V; capillary voltage, 35 V; and capillary temperature, 325 °C. All m/z transitions had collision energy of 18 V, collision gas pressure of 1.0 mTorr, and a scan rate of 0.25 sec. The m/z transitions monitored were: 356 to 339 and 212; 360 to 343 and 216.

Method 2 was developed to analyze all iodothyronines and iodothyronamines in a single injection, and was based generally upon a previously published method (34). A Thermo Surveyor auto-sampler and HPLC pump with a Thermo TSQ Quantum Discovery triple quadrupole mass spectrometer was operated in the positive mode using ESI. Samples were injected (5 µL) onto a Poroshell120 SB C_{18}, 2.1 x 100 mm, 2.7 µm column (Agilent Technologies, Santa Clara, CA). The mobile phase consistent of Solvent A (water + 0.5% acetic acid) and Solvent B (acetonitrile + 0.5% acetic acid) and one of the following gradients: 10%-50% B from 0-8 min, 50% B from 8-10 min, 50%-95% B from 10-11 min, 95% B from 11-13 min, 95%-10% from 13-14 min, 10% B from 14-16 min; or 10%-45% B from 0-14 min, 45%-95% B from 14-15 min, 95% B from 15-17 min, 95%-10% from 17-18 min, 10% B from 18-21 min. Remaining instrument settings were as follows: skimmer offset, 24; spray voltage, 2300 V; sheath gas pressure, 65 psi; aux gas pressure, 20 psi; and capillary temperature, 270 °C. Tube lens and collision energy values for all transitions are provided in Table 5-5. For all samples, collision gas pressure was 1.0 mTorr and scan rate was 0.2 sec.

Table 5-5: Instrument parameters for Method 2.

Compound	Q1 (*m/z*)	Q3 (*m/z*)	Tube Lens (V)	CE (V)
T_0AM	230.05	213.1	178	12
T_1AM	355.95	339	205	12
		212	205	12
d_4-T_1AM	360.0	343.0	205	12
		216.0	205	12
3,5-T_2AM 3,3'-T_2AM	481.9	464.9	237	14
T_3AM rT_3AM	607.75	590.8	224	19
T_4AM	733.5	716.65	208	19
T_0	274.05	228.1	219	9
T_1	399.92	353.95	235	19
3,5-T_2 3,3'-T_2	525.9	480.0	155	20
T_3 rT_3	651.8	605.75	210	23
T_4	777.5	731.5	130	30

Method 3 analyzed all iodothyronines and iodothyronamines using a Shimadzu Prominence HPLC system (Canby, OR) coupled to an AB Sciex Qtrap 5500 triple quadrupole mass spectrometer (Foster City, CA) operated in the positive mode with ESI. Samples were injected (10 µL) onto a Poroshell120 SB C_{18}, 2.1 x 100 mm, 2.7 µm column. The mobile phase consisted of Solvent A (water + 0.05% acetic acid) and Solvent B (water + 0.05% acetic acid), a flow rate of 0.3 mL/min, and the following gradient conditions: 10%-45% B from 0-14 min, 45%-95% B from 14-15 min, 95% B from 15-18 min, 95%-10% B from 18-19 min, 10% B from 19-22 min. The autosampler was kept at 4 °C, and the column at 35 °C. The mass spectrometer instrument settings were as follows: CUR, 50 psi; IS, 5000 V; temperature, 400 °C; GS1, 50 psi; GS2, 50 psi; CAD, high; EP 10 V. The *m/z* transitions monitored and the corresponding DP, CE and CXP values are given in Table 5-6, and dwell time was 20 msec for each *m/z* transition.

Table 5-6: Instrument parameters for Method 3.

Compound	Q1 (*m/z*)	Q3 (*m/z*)	DP (V)	CE (V)	CXP (V)
T_0AM	230.07	213.1	97	17	8
		109.0	97	35	14
		81.0	97	51	10
d_4-T_0AM	234.10	217.0	116	19	6
		113.1	116	35	10
		85.1	116	55	8
T_1AM	355.68	338.8	100	17	12
		212.0	100	27	6
d_4-T_1AM	359.99	343.0	156	19	12
		216.0	156	31	4
		198.1	156	35	12
$3,5$-T_2AM	481.85	464.9	111	23	6
		337.9	111	29	12
		165.1	111	69	12
$3,3'$-T_2AM	481.83	464.9	136	21	6
		337.9	136	31	12
		211.1	136	43	8
T_3AM	607.71	590.7	126	27	8
		463.9	126	31	6
		210.1	126	51	6
rT_3AM	607.70	590.7	134	25	8
		463.8	134	33	16
		152.0	134	129	14
d_4-rT_3AM	611.78	594.8	141	25	8
		467.9	141	37	6
		340.9	141	47	10
T_4AM	733.57	716.6	141	31	4
		335.9	141	57	12
		152.0	141	129	22
d_4-T_4AM	737.62	720.7	151	31	4
		339.9	151	57	12
		185.1	151	87	6
T_0	274.04	257.1	126	17	8
		215.1	126	27	14
		118.9	126	39	18
T_1	399.94	354.0	161	23	16
		340.9	161	33	46
		227.1	161	37	20
$3,5$-T_2	525.85	479.9	160	27	8
		353.0	160	43	6
		324.9	160	55	12
$3,3'$-T_2	525.86	479.9	166	29	6
		381.9	166	29	14
		353.0	166	47	12
T_3	651.62	605.8	170	31	8
		478.9	170	49	8
		128.9	170	67	18
rT_3	651.75	605.8	157	35	8
		507.9	157	33	4
		478.8	157	53	8
T_4	777.15	731.4	146	37	12
		350.8	146	61	12

5.3 Results

5.3.1 Solid Phase Extractions

The existing Scanlan Lab protocol for extraction of endogenous T_1AM was based on a urea denaturation of serum proteins, followed by acetone precipitation and concentration of T_1AM using SPE cation exchange cartridges. This protocol appeared to reliably extract T_1AM from serum samples (Figure 5-1).

Figure 5-1: T_1AM from human serum.
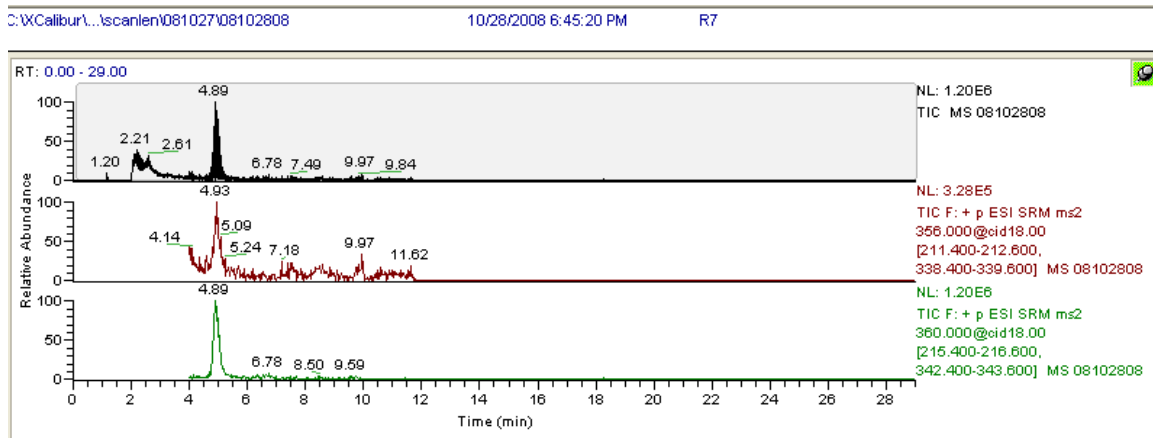
Endogenous T_1AM from a human serum sample, analyzed by LC-MS/MS Method 1; *m/z* transitions: T_1AM, 356 to 339.1 and 212.1; d_4-T_1AM, 360 to 343.1 and 216.1.

However, later discovery of T_1AM contamination in blank samples processed in parallel with serum samples (Figure 5-2) raised doubts about the validity of previous results as well as the reliability of this method.

Figure 5-2: T$_1$AM in serum blank.
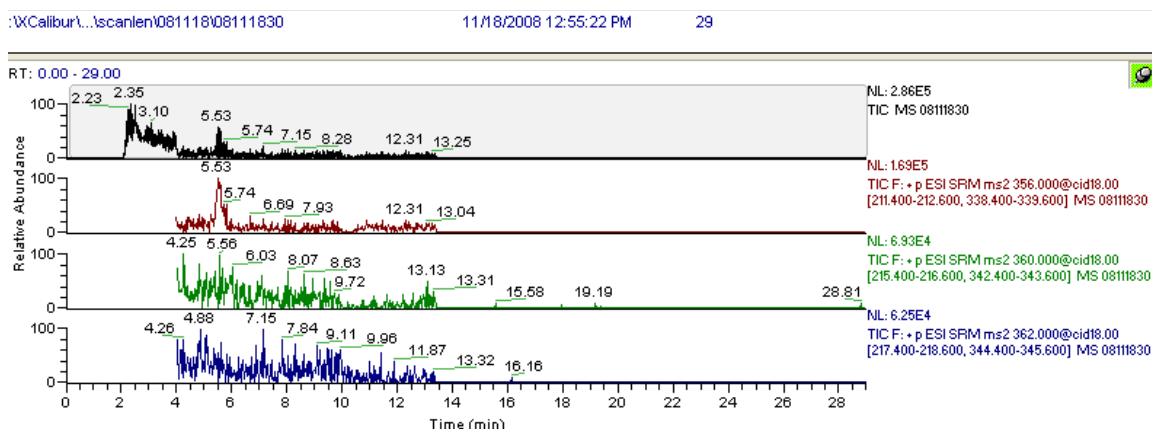
Unlabeled T$_1$AM present in a blank sample processed in parallel with human serum samples, RT = 5.53 minutes; *m/z* transitions: T$_1$AM, 356 to 339.1 and 212.1; d$_4$-T$_1$AM, 360 to 343.1 and 216.1; ^{13}C$_6$-T$_1$AM, 362 to 345.1 and 218.1.

A clean blank sample lacking T$_1$AM contamination was achieved only by moving the extraction procedures to a physically separate lab space from the Scanlan Lab, where no synthesis or use of synthetic T$_1$AM took place. At this same time, the extraction protocol was modified to resemble a previous version used in the Scanlan Lab, which used Proteinase K to denature proteins prior to SPE. This version of the protocol was used to analyze Sample Set I-A, which included human serum and tissues. Under these conditions, T$_1$AM was not detectable in either blank sample or in any serum or tissue sample (Appendix B).

5.3.2 [^{125}I]-T$_1$AM Extractions

The goal of the [^{125}I]-T$_1$AM extractions was to establish conditions that reliably extracted [^{125}I]-T$_1$AM from serum. A crude [^{125}I]-T$_1$AM assay was developed in order to quickly and cheaply identify the efficiency of extraction conditions that could be used in a future LC-

MS/MS based assay. Briefly, [^{125}I]-T$_1$AM was incubated with serum, serum was treated

to extract T$_1$AM, and the presence of [^{125}I]-T$_1$AM in an extract was determined by

counting the radioactivity present, with the desired outcome being extraction of [^{125}I]-

T$_1$AM into the organic or supernatant fraction.

As an initial investigation into the efficiency of [^{125}I]-T$_1$AM extraction from serum, Sample

Set II-A treatments (Table 5-1) were based on previous Scanlan Lab T$_1$AM extraction

protocols or published protocols for the extraction of related compounds, either

iodothyronines (144) or amphetamine (142, 143). Prior to treatment, human serum was

incubated with [^{125}I]-T$_1$AM overnight at 37 °C to allow for equilibration with serum binding

proteins. Sample treatment A8, 2:1 0.03% HCl in acetone, recovered the most

radioactivity in the organic phase (Figure 5-3). The effect of acidity on the recovery of

radioactivity following organic precipitation was optimized in the next set of experiments.

Figure 5-3: Recovery of [^{125}I]-T$_1$AM in Sample Set II-A.
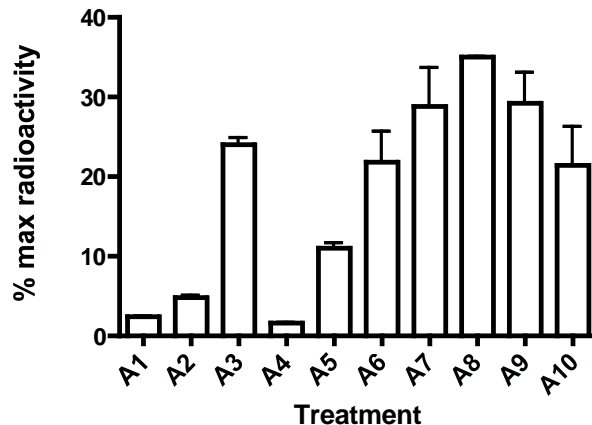
Percent of added radioactivity recovered following incubation of [^{125}I]-T$_1$AM with serum and the following sample treatments: A1, Buffer 1 (1.5 mL 10 M KOH in 8.5 mL saturated NaHCO$_3$) and toluene; A2, Buffer 1 (1.5 mL 10 M KOH in 8.5 mL saturated NaHCO$_3$) and DCM; A3, Buffer 1 (1.5 mL 10 M KOH in 8.5 mL saturated NaHCO$_3$) and EtOAc; A4, 5 M KOH and anhydrous sodium sulfate; A5, 0.1 M NaOH and DCM; A6, 1 M HCl, 40% KOH, CHES buffer (pH 9) and EtOAc; A7, CHES buffer (pH 9), 40% KOH, EtOAc; A8, 0.03% HCl in acetone; A9, EtOAc; A10, Proteinase K and 0.03% HCl in acetone; data are expressed as percentage of total radioactivity added to samples, n = 2.

In Sample Set II-B, a dose response was conducted to determine the optimal acid concentration to use during organic precipitation of serum proteins. Acetonitrile was used in addition to acetone to compare the efficiency of two organic solvents. Human serum was incubated with [^{125}I]-T$_1$AM overnight at 37 °C to allow for equilibration with serum binding proteins. As shown in Figure 5-4, there is no significant difference in the recovery of radioactivity with differing acid concentrations or organic solvent.

Figure 5-4: Recovery of [^{125}I]-T$_1$AM in Sample Set II-B.
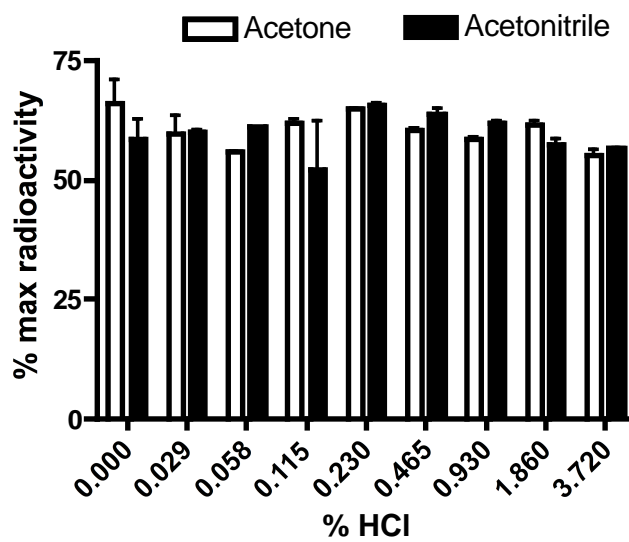
Percent of added radioactivity recovered following incubation of [^{125}I]-T$_1$AM with serum and treating with 2:1 acidified organic solvent; data are expressed as percentage of total radioactivity added to samples, n = 2.

Sample Set II-C repeated the acid dose response in acetone and acetonitrile with human serum and also rat serum, to determine if there are species differences in extraction efficiencies. For Sample Set II-C, [^{125}I]-T$_1$AM was incubated with human or rat serum for 24 or 72 hours, to ensure that equilibration with serum binding proteins is achieved. In addition to acidified acetone or acetonitrile, rat serum samples were brought to a final concentration of 2 N NaOH or 2 N HCl to precipitate proteins in the absence of organic solvent. Radioactivity was counted in the supernatant and the protein pellet in order to determine if 100% of added radioactivity could be accounted for. As shown in Figure 5-5, organic precipitation of human serum resulted in greater than 80% of the added radioactivity being recovered in the supernatant after a 24 hour pre-incubation and this recovery decreased following a 72 hour pre-incubation, but still remained at 70% or greater recovery. These results show greater recovery of radioactivity in the organic

supernatant from human serum than was shown previously with acidified acetone or acetonitrile precipitation (Figure 5-4), and the reason for this is unknown. Recovery of radioactivity from [^{125}I]-T$_1$AM incubated human serum was greater than recovery of radioactivity from [^{125}I]-T$_1$AM incubated rat serum, with the radioactivity recovered never increasing above 75%. In rat serum, there was no difference in recovered radioactivity between organic precipitation or pH dependent precipitation (acidic or basic). Interestingly, a greater percentage of added radioactivity was consistently recovered from human serum vs rat serum, suggesting species differences in protein binding may exist and may require species-specific extraction protocols. Since the primary goal of developing this assay was for use in rodent experiments, rat serum was used for all subsequent method development.

Figure 5-5: Recovery of [^{125}I]-T$_1$AM in Sample Set II-C.
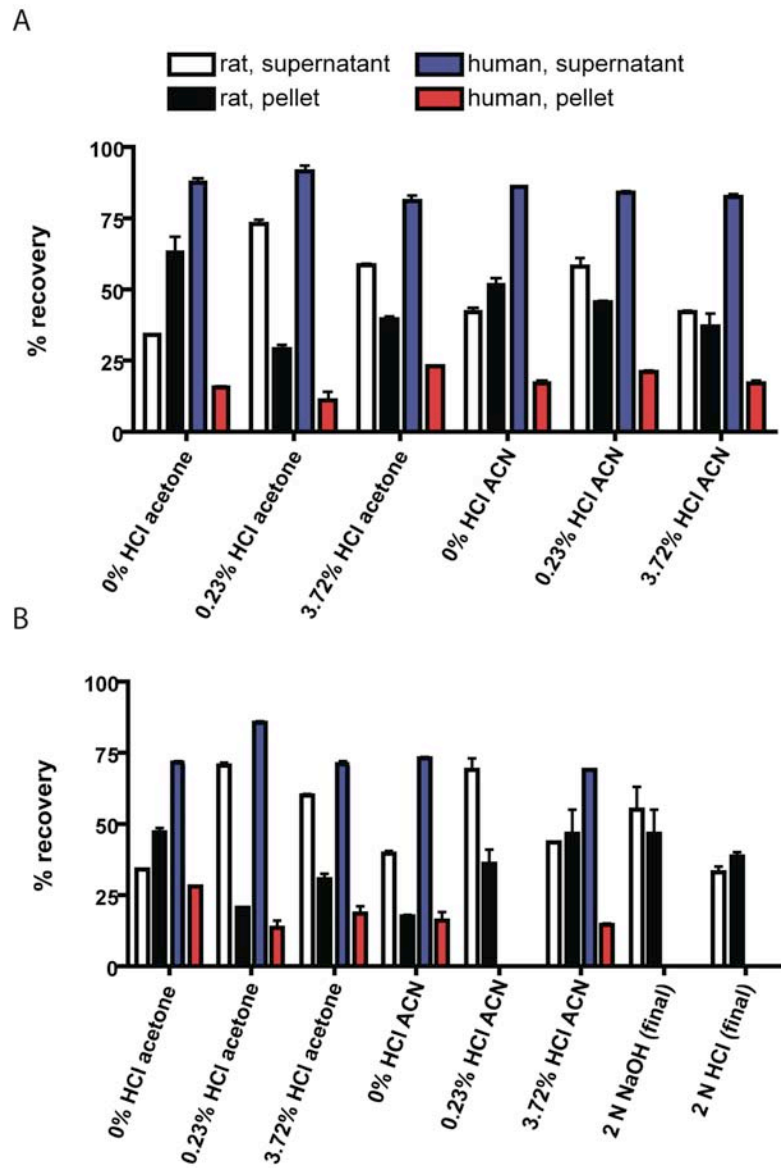
Percent of radioactivity recovered from serum incubated with [^{125}I]-T$_1$AM at 37 °C for 24 hours (A) or 72 hours (B); data are expressed as percentage of total radioactivity added to samples, n = 2.

Concurrent work in the Scanlan Lab identified Apolipoprotein B-100 (ApoB-100) as the primary T$_1$AM binding protein in human serum (130). Based on this work, Sample Set II-D (Table 5-2) utilized treatment conditions modified from literature protocols for the

101

delipidation and isolation of ApoB (145, 146). As shown in Figure 5-6, the ApoB

extraction protocols were unable to recover more than 40% of the added radioactivity in

the organic supernatant, with the majority of the radioactivity remained in the aqueous

fraction or protein pellets.

Figure 5-6: Recovery of [^{125}I]-T$_1$AM in Sample Set II-D.
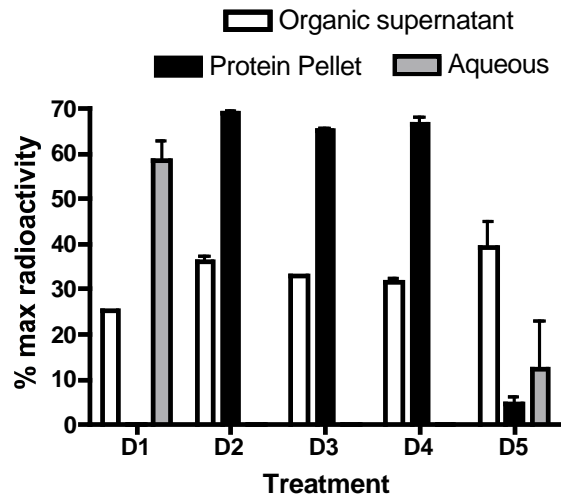
Percent of radioactivity recovered following [^{125}I]-T$_1$AM incubation with rat serum and the following sample treatments: D1, EtOAc:Ether (3:1); D2, EtOAc:Ether (3:1), acetone; D3, isopropanol, overnight; D4, isopropanol, vortex for 1 min; D5, HCl, CHCl$_3$, 40% NaOH, CHCl$_3$; data are expressed as percentage of total radioactivity added to samples, n = 2.

Sample Set II-D conditions (Table 5-2), based on the delipidation and isolation of ApoB,

were inefficient at recovering radioactivity in the organic fraction. This led to the

hypothesis that further disruption of lipoprotein particles may be necessary prior to

extraction of T$_1$AM. Sample Set II-E utilized detergents (non-ionic and zwitterionic) to

disrupt protein structure and facilitate isolation of lipoproteins in order to increase

extraction efficiency of [^{125}I]-T$_1$AM. In addition to detergent treatments, serum was

processed with the commercially available TRIZOL kit (Invitrogen) designed to

sequentially isolate RNA, DNA and protein. As shown in Figure 5-7A, treatment with

detergents resulted in recovery of less than 5% of the added radioactivity. Treatment of

$[^{125}I]$-T_1AM incubated serum with the TRIZOL kit was unable to extract more than 50% of

the added radioactivity into the organic phase, although differences in radioactivity

distribution between either the DNA or protein pellets were observed depending upon

the starting pH of serum (Figure 5-7B).

Figure 5-7: Recovery of $[^{125}I]$-T_1AM in Sample Set II-E.
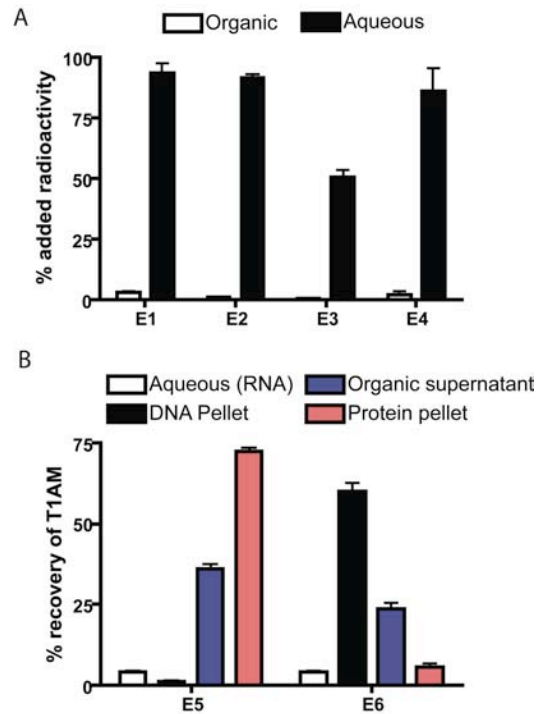
Percent recovery of radioactivity following incubation of serum with $[^{125}I]$-T_1AM and extraction with either detergents (A) or TRIZOL reagent (B). Extraction conditions are as follows: E1, Triton X-100, 40% NaOH, $CHCl_3$; E2, CHAPS, 40% NaOH, $CHCl_3$; E3, Tween20, 40% NaOH, $CHCl_3$; E4, 40% NaOH, $CHCl_3$; E5, TRIZOL reagent protocol; E6, 40% NaOH, TRIZOL reagent protocol; data are expressed as percentage of total radioactivity added to samples, n = 2.

For Sample Set II-F (Table 5-4), detergent-based extractions were repeated with the addition of a pH adjustment to the serum. For Samples F1-F5, the serum was adjusted to pH 2 prior to incubation with detergents, and for Sample F6 the serum was incubated with detergents and adjusted to pH 2 prior to extraction with chloroform. As shown in Figure 5-8, all treatment conditions resulted <5% of the added radioactivity being recovered in the organic (chloroform) phase. In Sample F6, the acetone supernatant, following a previous chloroform extraction, recovered ~18% of the added radioactivity, but more than 50% of the radioactivity remained in the precipitated protein pellet.

Figure 5-8: Recovery of $[^{125}I]$-T_1AM in Sample Set II-F.
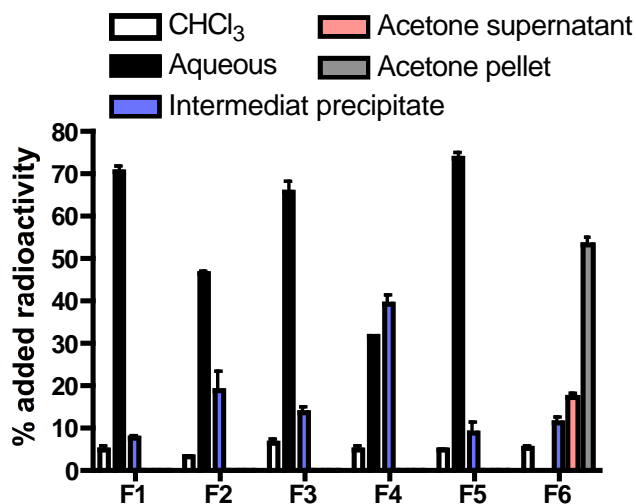
Percent recovery of radioactivity following incubation of serum with $[^{125}I]$-T_1AM and the following extraction conditions: F1, HCl, $CHCl_3$; F2, HCl, Triton X-100, $CHCl_3$; F3, HCl, CHAPS, $CHCl_3$; F4, HCl, Tween 20, $CHCl_3$; F5, HCl, Triton X-100, CHAPS, $CHCl_3$; F6, Triton X-100, CHAPS, HCl, $CHCl_3$, acetone; samples were extracted twice with $CHCl_3$ and combined in the graph above; n = 2.

In incubating serum with $[^{125}I]$-T_1AM, it is possible that T_1AM is present in excess of serum binding sites. In this case, there would be two pools of $[^{125}I]$-T_1AM; the first would

be a protein bound pool, which is the desired target of this extraction development procedure, and the second would be an unbound pool that occurs in excess to protein binding sites, and would theoretically be easier to extract than a protein bound pool. In order to determine the extent of protein bound $[^{125}I]$-T_1AM following incubation with serum, $[^{125}I]$-T_1AM-incubated serum was passed through 0.22 µm centrifugal filters, with the idea being that any $[^{125}I]$-T_1AM bound to protein would be unable to pass through the filter and therefore remain bound to the filter, while free or unbound $[^{125}I]$-T_1AM would be able to pass through and be detectable in the flow-through fraction. Both the centrifugal filter insert and the flow-through were counted. As an added control, $[^{125}I]$-T_1AM was spiked into water and filtered through the 0.22 µm filters as well. Figure 5-9 illustrates that following incubation with serum, ~70% of the added radioactivity is detected in the flow-through, suggesting that incubation results in serum binding of ~30% of the added $[^{125}I]$-T_1AM. However, in the presence of water alone, which lacks binding proteins for T_1AM, ~60% of the added radioactivity is detectable in the flow-through and ~40% remains associated with the filter membrane, suggesting there is a high degree of non-specific adsorption of $[^{125}I]$-T_1AM to the filter membranes. These results indicate that 0.22 µm centrifugal filters are not appropriate for determining the extent of $[^{125}I]$-T_1AM bound to serum proteins after incubation.

Figure 5-9: Recovery of [^{125}I]-T$_1$AM following filtration with 0.22 μm filters.
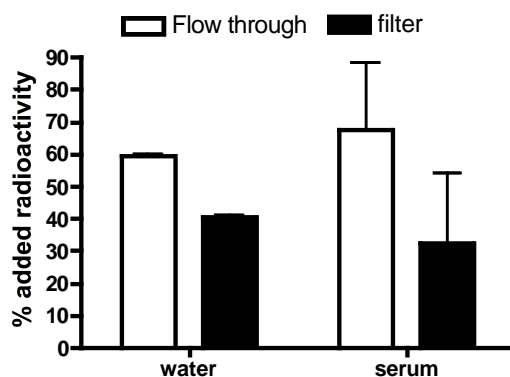
Percent of radioactivity recovered in the flow-through or on the filter membrane following centrifugal filtration of water or serum incubated with [^{125}I]-T$_1$AM; n = 2.

Due to the difficulty in distinguishing between bound and free pools of [^{125}I]-T$_1$AM in serum, it remains unknown how efficient any extraction procedure is at extracting bound [^{125}I]-T$_1$AM. It is possible that in the greatest extraction efficiencies observed (acidic acetone or acetonitrile precipitation of serum proteins, Figure 5-4), the majority of the recovered radioactivity is unbound in the starting sample. In addition, since it is merely the presence of radioactivity that is used as a surrogate measure for the presence of T$_1$AM, extraction efficiencies could also be confounded by possible deiodination of T$_1$AM. In this case, the presence of [^{125}I] is followed without any further accountability of the thyronamine core structure. For these reasons, it was decided to return to LC-MS/MS based detection for further method development studies.

5.3.3 Charcoal Based Extraction

The goal of the charcoal based assay was to non-specifically remove T$_1$AM and iodothyronines from serum using dextran-coated charcoal and then extract the

compounds of interest from the charcoal. It has been reported that commercially

available T_4/T_3 deficient human serum (Sigma-Aldrich) has no detectable T_1AM when

analyzed by an immunoassay (78). The protocol used by Sigma-Aldrich to prepare this

serum includes sequential incubation with dextran-coated charcoal followed by fumed

silica. We therefore reasoned that T_1AM is removed from serum either during the

charcoal incubation or the silica incubation. Charcoal is commonly used to strip

hormones from serum (147), yet ongoing work in the Scanlan Lab was identifying ApoB-

100, a component of lipoprotein particles, as the main T_1AM binding protein in human

serum (130), suggesting that silica mediated delipidation of serum could be the

important step for T_1AM extraction. To determine whether charcoal or silica was more

important for extraction of T_1AM from serum, standards (thyronine and thyronamine mix)

were added to serum samples prior to incubations in order to determine when T_1AM is

removed. Since standards were not pre-incubated with serum, equilibration with serum

binding proteins was likely minimal, facilitating ease of re-extraction and also increasing

the concentration to facilitate detection by LC-MS/MS.

Sample Set III-A was the first attempt at a charcoal and silica based extraction. Serum

samples were incubated with or without endogenously added standards, with or without

an adjustment to ~pH 11. Charcoal pellets were extracted with one of two combinations

of organic solvents, either 1:1 EtOAc:DCM or 1:1 ether:DCM, and all silica pellets were

extracted with 1:1 MeOH:DCM. Extracts from both the charcoal and silica pellets were

analyzed by LC-MS/MS to determine which fraction contained hormones. Of the

conditions tested, no recovery of endogenous hormones was seen, but the greatest

recovery of added standards occurred in the charcoal pellet of serum that was not pH

adjusted, extracted with 1:1 EtOAc:DCM (Figure 5-10).

Figure 5-10: Recovery of standards in Sample Set III-A.
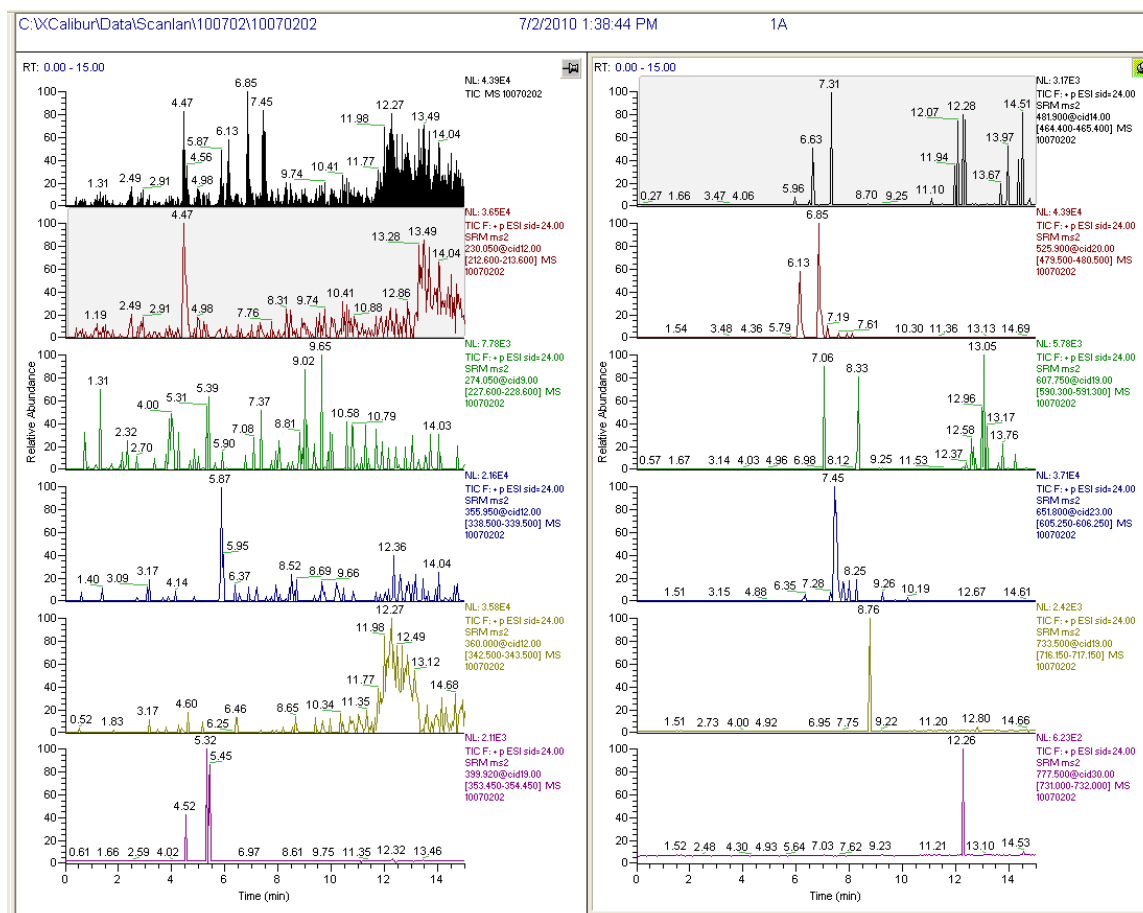
Recovery of exogenously added iodothyronines and iodothyronamines from mouse serum following charcoal incubation and extraction of charcoal with 1:1 EtOAc:DCM. LC-MS/MS Method 2; *m/z* transitions: T_0AM, 230 to 213; T_0, 274 to 228; T_1AM, 356 to 339; d_4-T_1AM, 360 to 343; T_1, 400 to 354; T_2AM, 482 to 465; T_2, 526 to 480; T_3AM, 608 to 591; T_3, 652 to 606; T_4AM, 733.5 to 716.6; T_4, 777.5 to 731.5.

The compounds that appear to be extracted from charcoal include T_0AM, T_1AM, 3,5-T_2, 3,3'-T_2 and T_3. While there are peaks corresponding to the correct retention times of 3,5-T_2AM and 3,3'-T_2AM, the low peak intensity (3.17E3) suggests they are likely not real peaks. It is interesting to note that d_4-T_1AM was added to the sample (10 pmol total) and was not recovered while added T_1AM was recovered. The total T_1AM added to the

sample was 30 pmol, suggesting a potential limit of detection for T_1AM. D_4-T_1AM was not recovered from any sample from Sample Set III-A (Appendix B).

In Sample Set III-B, serum samples were incubated again with both charcoal and silica to determine the distribution of re-extracted compounds between the two fractions. Based on the results from Sample Set III-A, the amount of d_4-T_1AM added to each sample was increased to 30 pmol, and ether/DCM was no longer used to extract charcoal pellets. Charcoal pellets were extracted with either EtoAc/DCM or MeOH/DCM, with or without 1% HCl. Silica pellets were extracted with MeOH:DCM:NH_4OH (50:50:1), and ammonium hydroxide (NH_4OH) was added to the solvents since it was previously used with MeOH to elute T_1AM from SPE cation exchange cartridges (81). Based on a literature report using high heat and high pressure (>100 °C and >1500 psi) to extract compounds from activated charcoal (148), heat was added during the charcoal extraction step. Charcoal pellets were extracted by incubating the pellet with organic solvents at 60 °C for 1 hr. A mixture of endogenous standards was added to some samples to facilitate ease of extraction and detection. In Sample Set III-B, extracting the charcoal pellet with 1:1 MeOH:DCM with 1% HCl recovered all of the endogenously added standards (Figure 5-11).

Figure 5-11: Recovery of standards in Sample Set III-B.
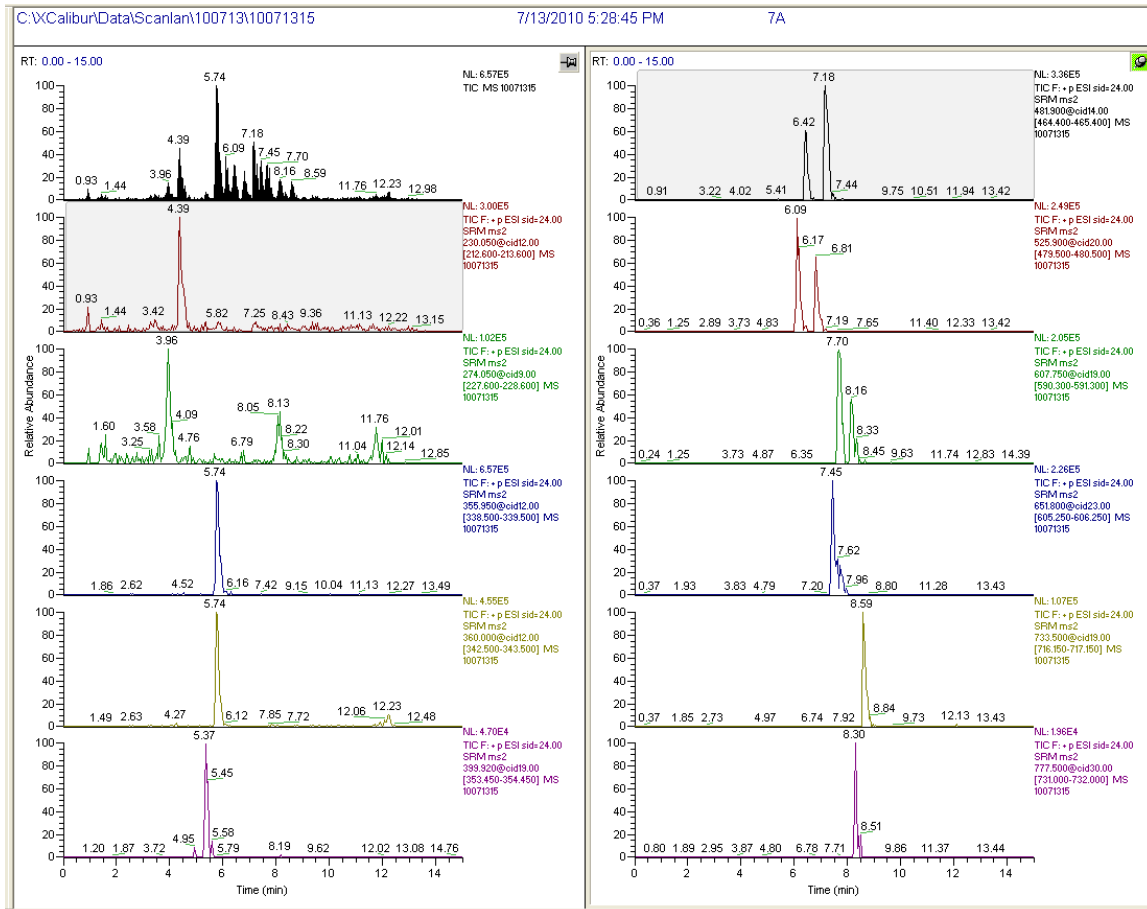
Recovery of exogenously added iodothyronines and iodothyronamines from mouse serum following charcoal incubation and extraction of charcoal with 1:1 MeOH:DCM + 1% HCl, for 1 hr at 60 °C. LC-MS/MS Method 2; m/z transitions: T_0AM, 230 to 213; T_0, 274 to 228; T_1AM, 356 to 339; d_4-T_1AM, 360 to 343; T_1, 400 to 354; T_2AM, 482 to 465; T_2, 526 to 480; T_3AM, 608 to 591; T_3, 652 to 606; T_4AM, 733.5 to 716.6; T_4, 777.5 to 731.5.

While these extraction conditions were able to recover exogenously added hormones,

they were not effective at recovery endogenous hormones, with the exception of T_4

(Figure 5-12). This indicates that some pre-treatment of serum to disrupt protein binding

of endogenous hormones is necessary prior to incubation with charcoal.

Chromatograms for remaining treatment conditions in Sample Set III-B are in Appendix

B.

Figure 5-12: Recovery of endogenous T$_4$ from Sample Set III-B.
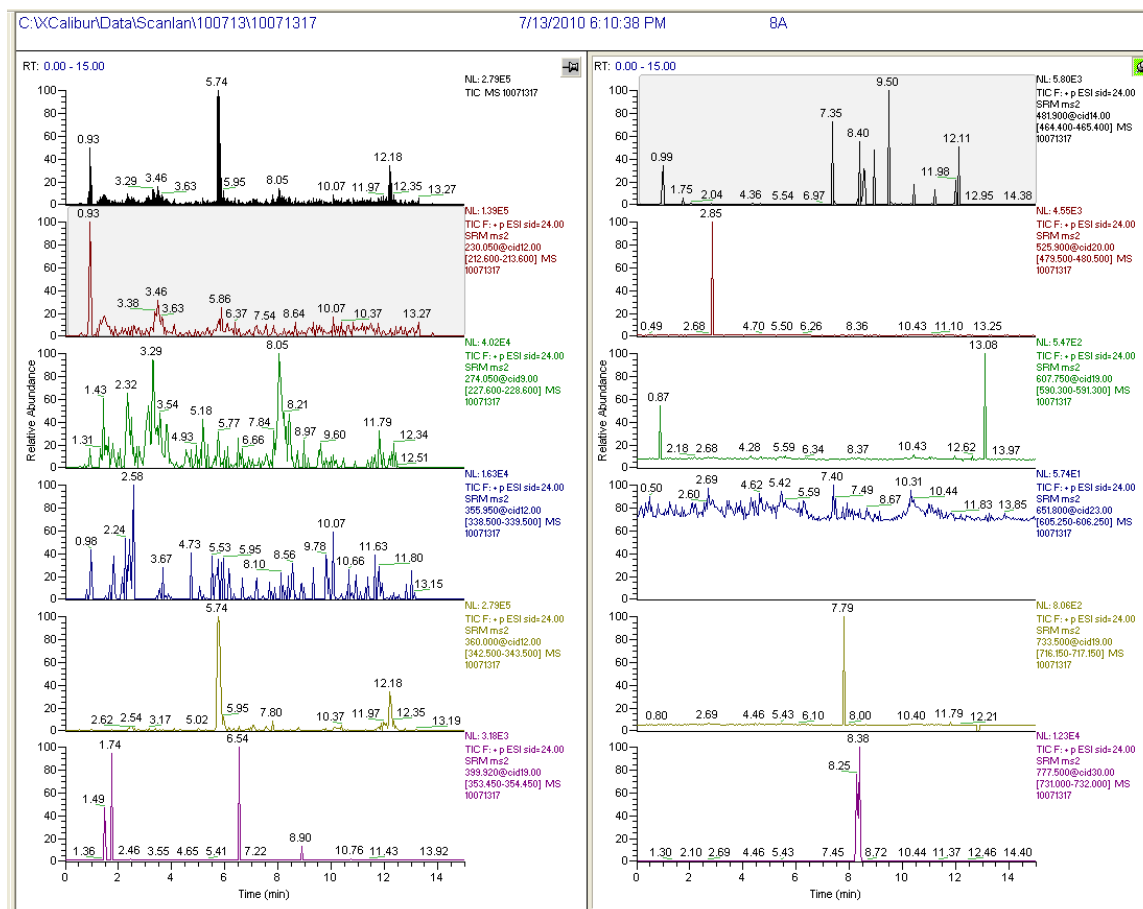
Recovery of endogenous T$_4$ from mouse serum following charcoal incubation and extraction of charcoal with 1:1 MeOH:DCM + 1% HCl, for 1 hr at 60 °C. LC-MS/MS Method 2; *m/z* transitions: T$_0$AM, 230 to 213; T$_0$, 274 to 228; T$_1$AM, 356 to 339; d$_4$-T$_1$AM, 360 to 343; T$_1$, 400 to 354; T$_2$AM, 482 to 465; T$_2$, 526 to 480; T$_3$AM, 608 to 591; T$_3$, 652 to 606; T$_4$AM, 733.5 to 716.6; T$_4$, 777.5 to 731.5.

In order to extract T$_1$AM and other endogenous thyronamines and thyronines, Sample

Set III-C involved pre-treating serum samples to dissociate proteins prior to incubating

with charcoal. Treatments used in Sample Set III-C included Proteinase K, Lipoprotein

lipase, urea and acid induced denaturation. Samples were incubated again with both

111

charcoal and serum to determine if there is a difference between exogenous standards and endogenous hormones in which fraction they are recovered. In these treatments, no compounds were ever recovered from the silica pellet (Appendix B). Treatment with urea resulted in a small peak for T_1AM and T_4 (Figure 5-13). Interestingly, any sample that included Proteinase K in the sample treatment did not recover d_4-T_1AM, although standards that were spiked into water and treated with urea, proteinase K and lipoprotein lipase did recover all standards, including d_4-T_1AM (Appendix B).

Figure 5-13: Recovery of endogenous T_1AM and T_4 in Sample Set III-C.
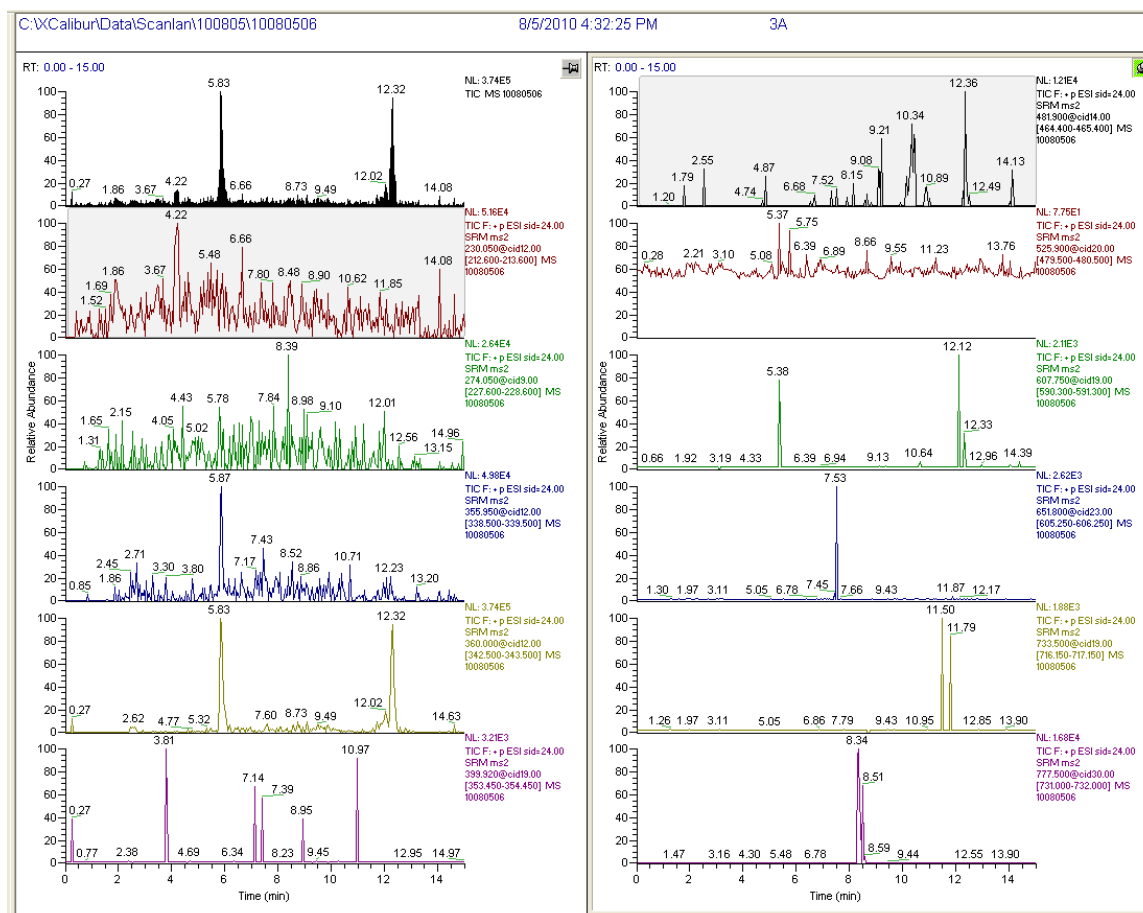
Recovery of endogenous T_1AM and T_4 from mouse serum following incubation with 2:1 10M urea, charcoal, and extraction of charcoal with 1:1 MeOH:DCM + 1% HCl, for 1 hr at 60 °C. LC-MS/MS Method 2; *m/z* transitions: T_0AM, 230 to 213; T_0, 274 to 228; T_1AM, 356 to 339; d_4-T_1AM, 360 to 343; T_1, 400 to 354; T_2AM, 482 to 465; T_2, 526 to 480; T_3AM, 608 to 591; T_3, 652 to 606; T_4AM, 733.5 to 716.6; T_4, 777.5 to 731.5.

Since urea treatment seemed the most promising treatment from Sample Set III-C,

Sample Set III-D included urea and guanidinium-HCl treatments (149), as well as

Protection Solution, which was previously used in the extraction of thyronines (92), and a

sodium-chloride incubation, which was used in the extraction of T_1AM published by

collaborators (77). For urea and guanidinium-HCl, samples were either treated without

adjusting pH, or the pH was adjusted to 4-5 with HCl following urea or guanidinium-HCl incubations. Treatment with guanidinium-HCl, with or without a serum pH adjustment did not recover any compounds, with the exception of d_4-T_1AM and perhaps T_0AM. Treatment with NaCl did not recover any compounds. Protection solution resulted in recovery of T_1AM, but no other compounds. Urea with a serum pH adjustment recovered T_4 (Appendix B) while urea without a serum pH adjustment recovered T_1AM, T_1, 3,5-T_2, 3,3'-T_2, T_3 and T_4 (Figure 5-14). All remaining LC-MS/MS chromatographs are shown in Appendix B.

Figure 5-14: Recovery of endogenous compounds in Sample Set III-D following urea treatment.
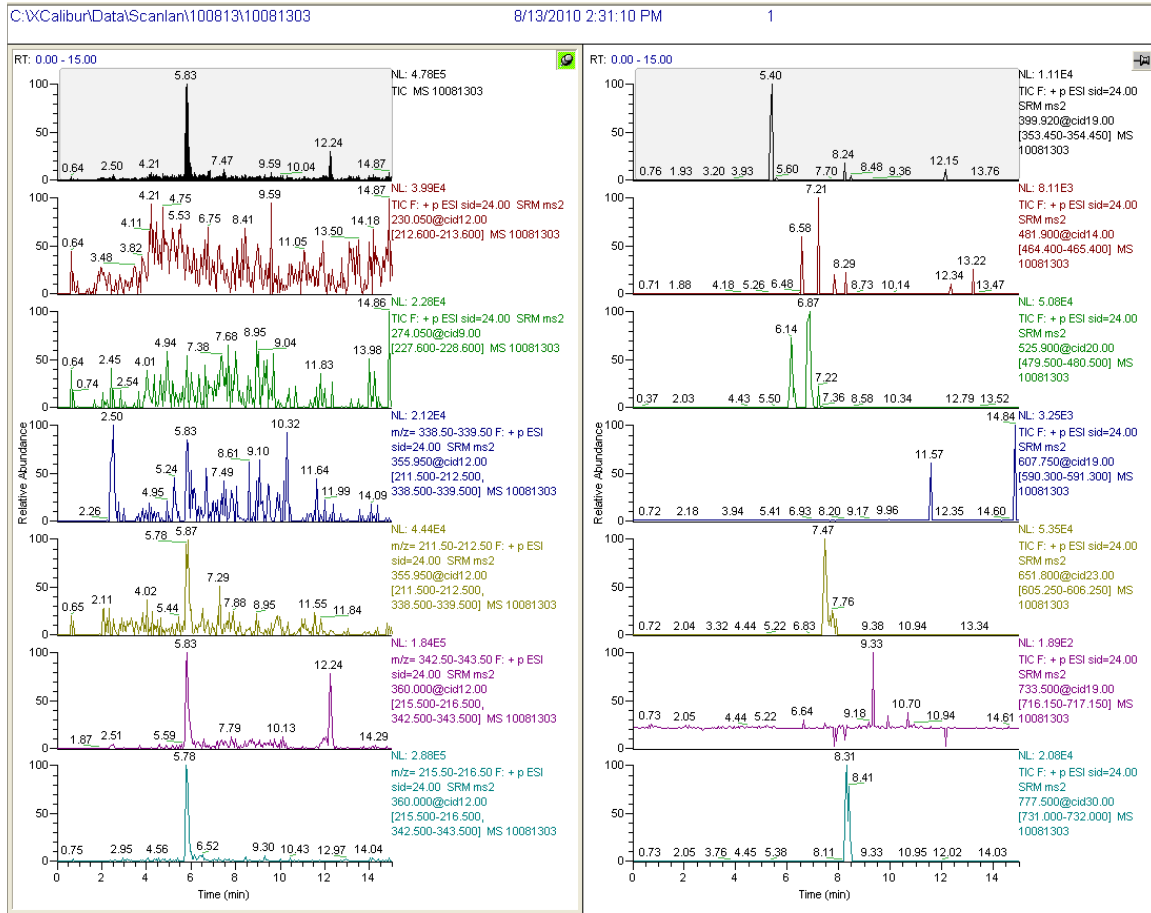
Recovery of endogenous T_1AM, T_1, $3,5-T_2$, $3,3'-T_2$, T_3 and T_4 from mouse serum following incubation with 2:1 10M urea, charcoal, and extraction of charcoal with 1:1 MeOH:DCM + 1% HCl, for 1 hr at 60 °C. LC-MS/MS Method 2; m/z transitions: T_0AM, 230 to 213; T_0, 274 to 228; T_1AM, 356 to 339 and 356 to 212; d_4-T_1AM, 360 to 343 and 360 to 216; T_1, 400 to 354; T_2AM, 482 to 465; T_2, 526 to 480; T_3AM, 608 to 591; T_3, 652 to 606; T_4AM, 733.5 to 716.6; T_4, 777.5 to 731.5.

Sample Set III-E focused on repeating the best treatments from Sample Set III-D, mainly

urea and Protection Solution treatments. Samples were treated with urea, Protection

Solution, Protection Solution and urea, or Protection Solution with acetone and urea.

Treatment with urea resulted in recovery of T_0AM, T_1AM, T_1, $3,5-T_2$, $3,3'-T_2$, T_3AM,

rT_3AM, T_3, rT_3, T_4AM and T_4 (FIGURE 5-15). Treatment with Protection Solution and urea or Protection Solution with acetone and urea both recovered T_1AM and T_4 but no other compounds (Appendix B).

Figure 5-15: Recovery of endogenous compounds in Sample Set III-E.

Extraction of endogenous T_0AM, T_0, T_1AM, T_1, 3,5-T_2, 3,3'-T_2, T_3AM, rT_3AM, T_3, rT_3, T_4AM and T_4 from mouse serum following incubation with 2:1 10M urea, charcoal, and extraction of charcoal with 1:1 MeOH:DCM + 1% HCl, for 1 hr at 60 °C. LC-MS/MS Method 2; *m/z* transitions: T_0AM, 230 to 213; T_0, 274 to 228; T_1AM, 356 to 339 and 356 to 212; d_4-T_1AM, 360 to 343 and 360 to 216; T_1, 400 to 354; T_2AM, 482 to 465; T_2, 526 to 480; T_3AM, 608 to 591; T_3, 652 to 606; T_4AM, 733.5 to 716.6; T_4, 777.5 to 731.5.

While this extraction protocol initially appeared successful at simultaneously extracting

endogenous thyronamines and thyronines, it proved to be irreproducible in the future,

and ultimately the charcoal based extraction approach was abandoned.

5.3.4 Zucchi Lab Protocol

Collaborators in Riccardo Zucchi's lab at the University of Pisa published a protocol to

extract T_1AM from rat tissues (77). This protocol was successfully used to extract T_1AM

from mouse liver (see Chapter 3). Due to this success, an effort was made to establish

this protocol as a functional and reproducible assay for mouse T_1AM in our lab in

Portland. Using the Zucchi protocol to extract a control mouse liver, d_4-T_0AM, d_4-T_1AM

and d_4-T_4AM internal standards were recovered and traces of T_3 and T_4 may be

detectable when analyzed by LC-MS/MS Method 3 (Figure 5-16). Standards analyzed

by Method 3 are in Appendix B.

Figure 5-16: Analysis of iodothyronines and iodothyronamines in mouse liver.
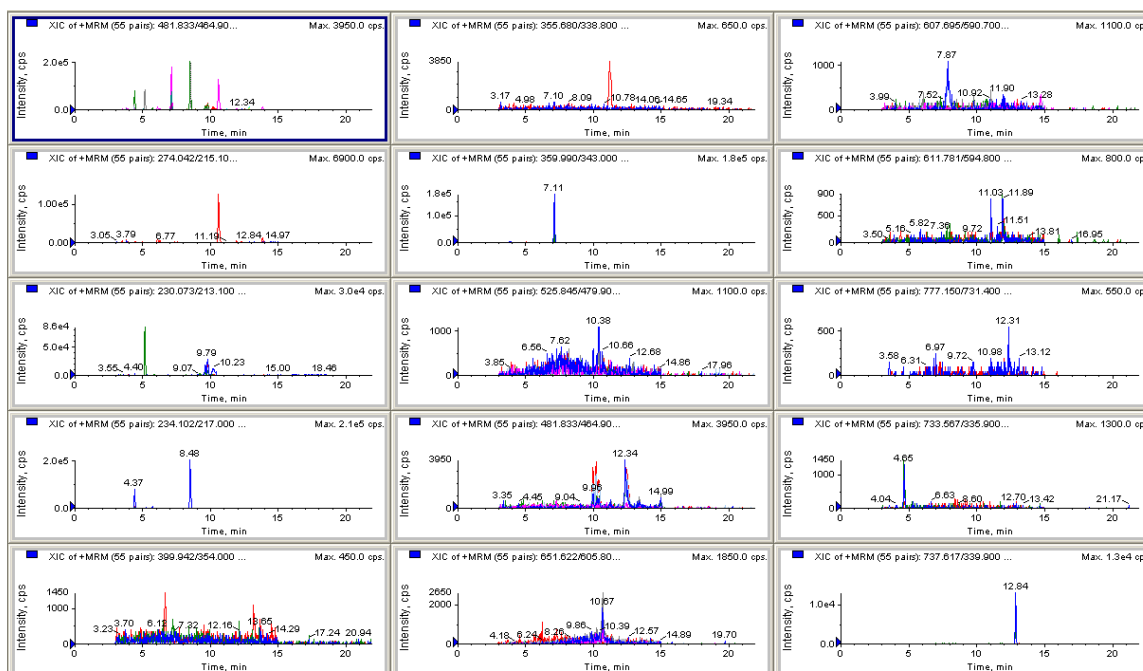
Extraction of endogenous T_0AM, T_0, T_1AM, T_1, 3,5-T_2, 3,3'-T_2, T_3AM, rT_3AM, T_3, rT_3, T_4AM and T_4 from mouse liver following extraction with the Zucchi protocol. LC-MS/MS Method 3; XIC of each above panel as follows: upper left is TIC; 274.0, T_0; 230.1, T_0AM; 234, d_4-T_0AM; T_1, 400.2; 356.2, T_1AM; 360.3, d_4-T_1AM; 526.0, 3,5-T_2 and 3,3'-T_2; 481.8, 3,5-T_2AM and 3,3'-T_2AM; 651.9, T_3 and rT_3; 607.9, T_3AM and rT_3AM; 611.8, d_4-rT_3AM; 777.7, T_4; 733.7, T_4AM; 738.0, d_4-T_4AM.

In some samples analyzed by LC-MS/MS Method 3, there appeared to be a small amount of T_1AM contamination in blank samples (Appendix B). It was determined, however, that injection of a corresponding concentration of unextracted d_4-T_1AM standard (1 pmol on column) also showed a peak for T_1AM (Figure 5-17). Integration of the peak areas (1.04e6 for d_4-T_1AM and 6.43e3 for T_1AM) indicates two interesting things. First, the quantity of T_1AM in d_4-T_1AM corresponds to 0.15% non-deuterated. Second, the quantity of T_1AM detected corresponds to <2 fmol on column, which indicates that Method 3 has adequate sensitivity to detect endogenous T_1AM at the levels previously reported (77).

118

Figure 5-17: T_1AM in d_4-T_1AM standard.
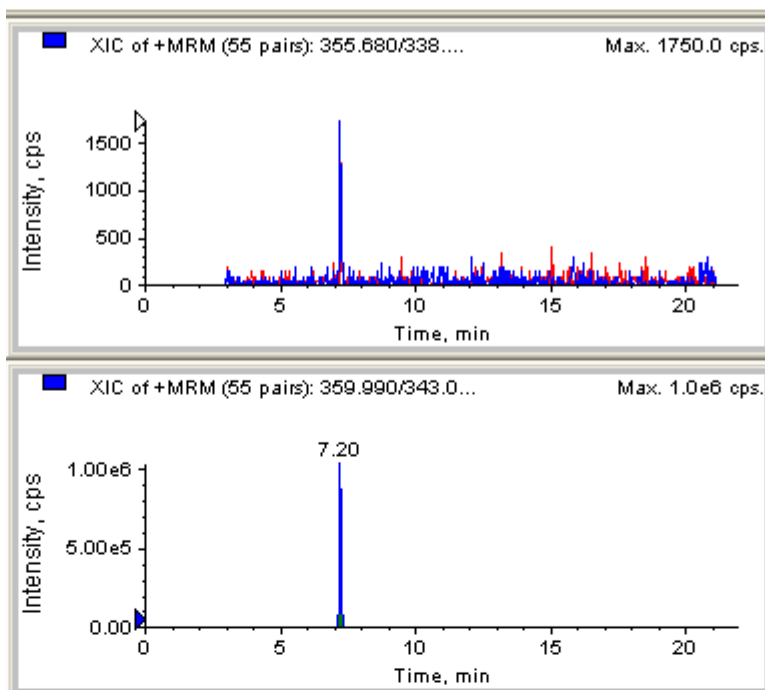
A T_1AM peak is present in an injection of d_4-T_1AM standard, LC-MS/MS Method 3; *m/z*: T_1AM, 355 to 338; d_4-T_1AM, 359 to 343.

Since this extraction protocol has successfully extracted endogenous T_1AM from mouse liver (Chapter 3), the impact on extraction of a number of potential variables between the Scanlan Lab and the Zucchi Lab was investigated. First, it is unclear whether the Zucchi Lab uses silanized or non-silanized vial inserts in their LC-MS/MS sample vials, so both insert types were analyzed. Second, ionization efficiencies when redissolving the final dried residue in H_2O:MeOH:acetic acid (90:10:1) (86) and MeOH:0.1 M HCl (1:1) (77) were compared. Finally, the Zucchi Lab does not filter their samples prior to LC-MS/MS analysis while the Scanlan Lab filters all samples through 0.22 µm filters, so the impact of filtering samples was investigated. Four control mouse livers were processed in

parallel until the final step. Two liver samples were redissolved in H_2O:MeOH:acetic acid

(90:10:1) and placed into a silanized or non-silanized sample vial insert. Two liver

samples were redissolved in MeOH:0.1 M HCl (1:1) and placed into a silanized or non-

silanized sample vial insert. Samples were analyzed by LC-MS/MS, filtered through

0.22 µm filters, and re-injected. Peak areas were integrated to compare the effect of

silanized inserts, acid composition and filtering (Figure 5-18). No difference was

observed between filtered and non-filtered samples, except that T_4 was undetectable in

the H_2O:MeOH:acetic acid samples in both silanized and non-silanized inserts after

filtering. Endogenous T_4, T_3 and internal standard d_4-T_1AM all had increased peak areas

when the samples were redissolved with 1:1 MeOH:0.1 M HCl, and the peak area for T_3

was increased when using the silanized sample vial inserts. These sample conditions

did not impact the ability to detect endogenous compounds that were not previously

detected (Appendix B).

Figure 5-18: Optimization of d_4-T_1AM, T_4 and T_3 peak areas.
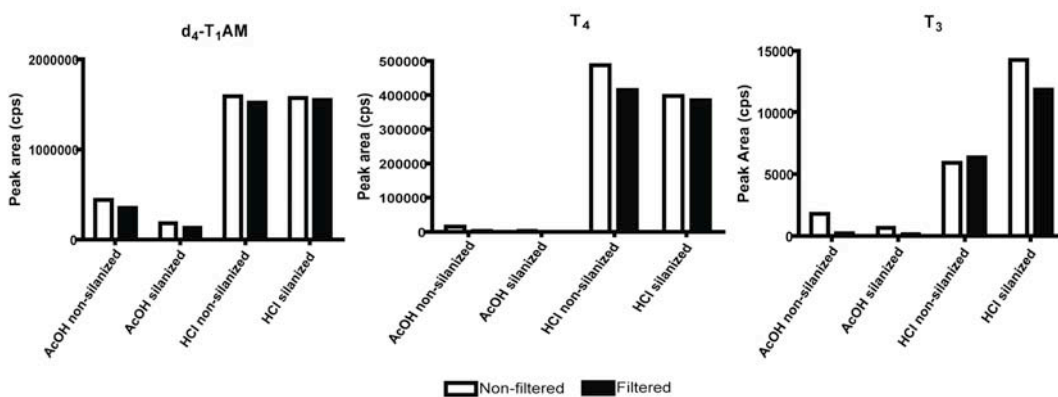
Peak areas of d_4-T_1AM, T_4 and T_3 when dissolved in H_2O/MeOH/acetic acid or MeOH/0.1M HCl,
in non-silanized or silanized vial inserts, with or without filtering through 0.22 µm filters; analyzed
by LC-MS/MS Method 3.

The next aspect to be assessed was the recovery of d_4-T_1AM internal standard. Integrating the peak areas for d_4-T_1AM in the unextracted internal standards and processed liver samples from above, redissolved in 1:1 MeOH:0.1 M HCl, (Appendix B), the recovery of d_4-T_1AM in the processed samples averages 36%. This indicates that a considerable portion of the internal standard is not being recovered, and a similar or greater extent of sample loss for endogenous T_1AM could be contributing to the lack of detection. For comparison, the Zucchi Lab typically observes recovery of d_4-T_1AM between 55-90% (Alessandro Saba, personal communication).

5.4 Discussion

Extracting endogenous T_1AM for analysis by LC-MS/MS has proven to be a challenging task. While a successful protocol is not reported here, a number of approaches were investigated. Based on the work presented here, the following discussion focuses on some aspects of method development that could be addressed in the future.

From a technical standpoint, the low recovery of d_4-T_1AM (35%) is a major concern that needs to be addressed. This suggests that material is being lost at some point in the extraction. The Zucchi protocol uses Bond-Elut Certify SPE, as did all other SPE based methods discussed here, and could represent a potential source for loss of sample recovery. This could occur either through inefficient adsorption of sample onto the column or inefficient elution of sample from the column. While no other SPE brands have been used during this method development, many other brands are available commercially. A report in the literature investigated the recovery of 4'-hydroxymethamphetamine using different brands of SPE and found the recovery of their

compound of interest to be lowest when using Bond-Elut Certify (150). For this reason, if SPE continues to be used in future T_1AM extraction methods, it is necessary to compare recovery efficiencies of different SPE brands to maximize T_1AM recovery.

Another step to systematically optimize would be evaporation of samples. Methods presented here evaporated samples both in a speedvac and under nitrogen gas, but a comparison of sample recovery or loss was never made between the two methods. Also, it would be worth assessing the impact of heating during evaporation, since this is a possibility with both evaporation methods. A difference between the Zucchi Lab and Scanlan Lab in evaporating samples is that the Zucchi Lab evaporates all samples in eppendorf tubes while the Scanlan Lab evaporates samples in borosilicate tubes. Determining the recovery of sample from each tube type may also be critical for minimizing sample loss and maximizing recovery of d_4-T_1AM.

The charcoal based extraction may be worth revisiting in the future. Charcoal is known to extract iodothyronines from serum (147) and apparently removes T_1AM from serum as well (78). These reports suggest that a failure to detect T_1AM is likely the result of an inability to re-extract compounds, including T_1AM, from charcoal, rather than a lack of extraction from serum during the charcoal incubation. Further work to optimize conditions to re-extract compounds from charcoal may be beneficial in establishing a reliable assay. It should also be noted that while T_0AM is the only other thyronamine that has been reported to be endogenous (75), it is unclear if anyone has looked for endogenous high-iodinated thryonamines. A general extraction approach such as the charcoal assay combined with LC-MS/MS Method 3, which monitors for all iodothyronamines, may help address this question.

122

One additional observation was made between the two instances when extraction methods appeared to be successful. Both the existing solid phase extraction that was inherited and the charcoal based extraction appeared to reliably extract T_1AM from serum during the summer months. Both methods were unable to successfully extract T_1AM from serum in the fall. This was an interesting seasonal correlation that was noted between the two methods, but the significance of this observation, if any, remains unknown.

Finally, the possibility exists that the difficulty in measuring endogenous T_1AM is related to covalently modifications of the compound. This hypothesis originated with conflicting reports of endogenous concentrations of T_1AM when measured by LC-MS/MS (77) or immunoassay (78). Subsequent work has identified covalently modified T_1AM in mouse serum and tissues following injection of T_1AM (Chapter 4). If endogenous T_1AM exists in a modified form, this would interfere with detection by LC-MS/MS by shifting the *m/z* transitions that would need to be modified. In some cases, optimizing extraction conditions to extract for the conjugate may be necessary, such as a sulfonate, which will likely exist in a deprotonated state. In other cases, conditions to reliably cleave a modification may result in an increased pool of unmodified T_1AM that could be measured, such as a glucuronide (Chapter 4). In all cases, *m/z* transitions for any modified T_1AM should be added to LC-MS/MS methods in order to monitor both conjugated and unconjugated forms. However, the presence of covalently modified T_1AM endogenously needs to be established before further work is pursued in this area.

Chapter 6: Summary and Future Directions

6.1 Summary

Since its discovery as an endogenous compound in 2004, 3-iodothyronamine (T_1AM) has been hypothesized, if not just assumed, to be a decarboxylated and deiodinated metabolite of thyroxine (T_4) (75). The work presented in this dissertation directly tests this hypothesis and further investigates the status of T_1AM within the context of thyroid hormone (TH) metabolism.

To test the hypothesis that T_1AM is an extrathyroidal metabolite of T_4, a hypothyroid mouse was used for TH metabolism using a stable isotope labeled T_4 (Chapter 2). The stable isotopes allow for distinction between endogenous compounds and those arising through metabolism of the labeled precursor. We found that endogenous liver T_1AM levels depend upon thyroid gland function, but are independent of extrathyroidal metabolism of T_4 (Chapter 3). This suggests that T_1AM or a T_1AM biosynthetic precursor is secreted directly from the thyroid gland, a result that was not anticipated at the outset of this research.

Based primarily on *in vitro* studies showing similar metabolism between T_1AM and TH, we hypothesized that *in vivo* metabolism may play an important role in regulating availability of endogenous T_1AM. *In vitro* studies showed T_1AM was a substrate for both deiodination and sulfation (86, 87). Only one *in vivo* studied investigated the metabolism of T_1AM, and observed the oxidatively deaminated 3-iodothyroacetic acid (TA_1) as a metabolite in rat following injection of T_1AM (88). No prior *in vivo* studies looked for the presence of covalently modified T_1AM, and no prior study investigated T_1AM metabolism in mice. Using information dependent acquisition (IDA) methods and liquid

chromatography-tandem mass spectrometry (LC-MS/MS), we performed an unbiased screen for T_1AM metabolite in mouse serum following a single IP injection. Consistent with the prior studies, T_1AM was sulfated and oxidatively deaminated in mouse serum (Chapter 4). Using this approach, two novel compounds were identified in mouse serum: N-acetyl-T_1AM (Ac-T_1AM) and T_1AM-glucuronide. In contrast to the *in vitro* study, deiodination of T_1AM did not appear to be a major pathway of metabolism. Unexpectedly, the iodine-free metabolites thyronamine (T_0AM) and thyroacetic acid (TA_0), were not major metabolites present in serum. One possibility for the low serum concentrations of the non-iodinated compounds in serum is that deiodination results in rapid elimination. This would be consistent with previous reports of thyronine (T_0) and TA_0 being detected in urine (29, 30). These metabolites are also differentially distributed to tissues, suggesting metabolism may be critical for regulating tissue availability and biological activity of endogenous T_1AM.

6.2 Future directions

The most pressing issue in future research on biosynthetic and metabolic pathways of T_1AM is to establish a reliable and reproducible assay for extraction and analysis of T_1AM by LC-MS/MS. A great deal of effort in the Scanlan Lab was made to establish such an assay, with no success (Chapter 5). One important future direction in this area is to determine the conjugation states of endogenous T_1AM. Both T_1AM-glucuronide and O-sulfonate-T_1AM (S-T_1AM) are present in serum at greater concentrations that unmodified T_1AM following a single IP injection of T_1AM (Chapter 4). If a considerable portion of endogenous T_1AM is present as either the glucuronide or sulfate conjugates, they would not be detected with the current LC-MS/MS methods monitoring specifically

for unmodified T_1AM. Moreover, extraction methods targeting T_1AM are not likely to optimally extract these modified forms of T_1AM. Quantifying tissue distribution of metabolites will also provide insights into tissue specific actions of T_1AM.

Once a reliable assay for T_1AM is developed, additional experiments can be conducted to further elucidate the biosynthetic origins of T_1AM. While the data presented here indicate that T_1AM biosynthesis is dependent upon the thyroid gland (Chapter 3), there are many questions remaining. The first question is whether T_1AM is a direct product of the thyroid gland or if it arises through extrathyroidal metabolism of a gland product other than T_4. A potential candidate for an alternate thyroid gland precursor is 3,5-diiodothyronine (3,5-T_2). There is no direct evidence to indicate that 3,5-T_2 is a metabolite of T_3 (25, 31, 34, 38), which suggests that it arises solely through direct gland secretion. To answer this question, an experiment could be conducted similar to the one described for T_1AM, in which stable isotope labeled T_4 is used to hormone replace hypothyroid mice, and serum or tissues are analyzed for labeled 3,5-T_2. This would necessitate extraction conditions to reliably extract 3,5-T_2 from mouse serum or tissues, which was not apart of the extraction and analysis in the labeled T_4 to T_1AM experiment.

In terms of possibly being a direct product of the thyroid gland, several questions remain unanswered. First, cleavage of thyroglobulin to produce an ethylamine side chain rather than an amino acid side chain would necessitate the existence of an alternate and currently unknown mechanism. Decarboxylation within the gland could be possible, but the likely candidate for iodothyronine decarboxylation, aromatic l-amino acid decarboxylase, does not catalyze this reaction *in vitro*, and the existence of thyroid specific decarboxylases remains unknown. Finally, T_4 is secreted from the thyroid gland

in response to thyroid stimulating hormone (TSH). There is one report that measures T_1AM and TSH levels, and finds no correlation between the two values (78). If T_1AM is a direct product of the thyroid gland, it would be necessary to determine if it is secreted in response to TSH or in response to an alternate stimulus.

Another important question to be addressed is the endogenous status of other iodothyronamines. To date, only T_1AM and T_0AM have been reported as endogenous (75), but it remains unclear if di-, tri- or tetraiodothyronamines are present as well. Answering this question may influence future experiments on determining the biosynthetic origins of T_1AM. For instance, if T_4AM or T_3AM were endogenous, this would likely eliminate the possibility of $3,5-T_2$ as a precursor for T_1AM, or suggest that multiple pathways generate iodothyronamines from iodothyronines. Understanding the complete profile of iodothyronamines is critical to furthering our understanding of THs and the function of the thyroid gland.

Chapter 7: References

1. **Yen PM** 2001 Physiological and molecular basis of thyroid hormone action. Physiol Rev 81:1097-1142

2. **Braverman LE, Utiger RD** 2005 Introduction to Hypothyroidism. In: Braverman LE, Utiger RD eds. Werner & Ingbar's The Thyroid. 9th ed. Philadelphia: Lippincott Williams & Wilkins

3. **Braverman LE, Utiger RD** 2005 Introduction to Thyrotoxicosis. In: Braverman LE, Utiger RD eds. Werner & Ingbar's The Thyroid. 9th ed. Philadelphia: Lippincott Wiliams & Wilkins

4. **Railton TC** 1894 Sporadic Cretinism Treated by Administration of the Thyroid Gland. Br Med J 1:1180-1181

5. **Smith T** 1894 Case of Sporadic Cretinism Treated with Thyroid Gland. Br Med J 1:1178-1180

6. **Hutchison R** 1896 Preliminary Note on the Active Substance in the Thyroid. Br Med J 1:722-723

7. **Kendall EC** 1915 A method for the decomposition of the proteins of the thyroid, with a description of certain constituents. J Biol Chem 20:501-509

8. **Kendall EC** 1919 Isolation of the iodine compound which occurs in the thyroid: First paper. J Biol Chem 39:125-147

9. **Kendall EC, Osterberg AE** 1919 The chemical identification of thyroxine: Second paper. J Biol Chem 40:265-334

10. **Gross J, Pitt-Rivers R** 1951 Unidentified iodine compounds in human plasma in addition to thyroxine and iodide. Lancet 2:766-767

11. **Gross J, Pitt-Rivers R** 1952 The identification of 3:5:3'-L-triiodothyronine in human plasma. Lancet 1:439-441

12. **Pitt-Rivers R, Stanbury JB, Rapp B** 1955 Conversion of thyroxine to 3-5-3'-triiodothyronine in vivo. J Clin Endocrinol Metab 15:616-620

13. **Braverman LE, Ingbar SH, Sterling K** 1970 Conversion of thyroxine (T4) to triiodothyronine (T3) in athyreotic human subjects. J Clin Invest 49:855-864

14. **Gentile F, Di Lauro R, Salvatore G** 1995 Biosynthesis and Secretion of Thyroid Hormones. In: Degroot LJ ed. Endocrinology. 3rd ed. Philadelphia: W.B. Saunders Co.; 517-542

15. **Dunn JT** 2001 Biosynthesis and Secretion of Thyroid Hormones. In: Degroot LJ, Jameson JL eds. Endocrinology. 4th ed. Philadelphia: W.B. Saunders Co.; 1290-1300

16. **Weiss SJ, Philp NJ, Grollman EF** 1984 Iodide transport in a continuous line of cultured cells from rat thyroid. Endocrinology 114:1090-1098

17. **Taurog A, Dorris ML, Doerge DR** 1996 Mechanism of simultaneous iodination and coupling catalyzed by thyroid peroxidase. Arch Biochem Biophys 330:24-32

18. **Kunisue T, Fisher JW, Kannan K** 2011 Determination of six thyroid hormones in the brain and thyroid gland using isotope-dilution liquid chromatography/tandem mass spectrometry. Anal Chem 83:417-424

19. **St Germain DL, Galton VA, Hernandez A** 2009 Minireview: Defining the roles of the iodothyronine deiodinases: current concepts and challenges. Endocrinology 150:1097-1107

20. **Kohrle J** 2000 The deiodinase family: selenoenzymes regulating thyroid hormone availability and action. Cell Mol Life Sci 57:1853-1863

21. **Kohrle J** 2000 The selenoenzyme family of deiodinase isozymes controls local thyroid hormone availability. Rev Endocr Metab Disord 1:49-58

22. **Galton VA, Schneider MJ, Clark AS, St Germain DL** 2009 Life without thyroxine to 3,5,3'-triiodothyronine conversion: studies in mice devoid of the 5'-deiodinases. Endocrinology 150:2957-2963

23. **Refetoff S, Nicoloff JT** 1995 Thyroid Hormone Transport and Metabolism. In: Degroot LJ ed. Endocrinology. 3rd ed. Philadelphia: WB Saunders Co; 560-582

24. **Kohrle J** 1999 Local activation and inactivation of thyroid hormones: the deiodinase family. Mol Cell Endocrinol 151:103-119

25. **Pinna G, Brodel O, Visser T, Jeitner A, Grau H, Eravci M, Meinhold H, Baumgartner A** 2002 Concentrations of seven iodothyronine metabolites in brain regions and the liver of the adult rat. Endocrinology 143:1789-1800

26. **Nishikawa M, Inada M, Naito K, Ishii H, Tanaka K, Mashio Y, Imura H** 1981 Age-related changes of serum 3,3'-diiodothyronine, 3',5'-diiodothyronine, and 3,5-diiodothyronine concentrations in man. J Clin Endocrinol Metab 52:517-522

27. **Corcoran JM, Eastman CJ** 1983 Radioimmunoassay of 3-L-monoiodothyronine: application in normal human physiology and thyroid disease. J Clin Endocrinol Metab 57:66-70

28. **Smallridge RC, Wartofsky L, Green BJ, Miller FC, Burman KD** 1979 3'-L-Monoiodothyronine: development of a radioimmunoassay and demonstration of in vivo conversion from 3',5'-diiodothyronine. J Clin Endocrinol Metab 48:32-36

29. **Pittman CS, Buck MW, Chambers JB, Jr.** 1972 Urinary metabolites of 14 C-labeled thyroxine in man. J Clin Invest 51:1759-1766

30. **Chopra IJ, Boado RJ, Geffner DL, Solomon DH** 1988 A radioimmunoassay for measurement of thyronine and its acetic acid analog in urine. J Clin Endocrinol Metab 67:480-487

31. **Leonard JL, Mellen SA, Larsen PR** 1983 Thyroxine 5'-deiodinase activity in brown adipose tissue. Endocrinology 112:1153-1155

32. **Sakurada T, Rudolph M, Fang SL, Vagenakis AG, Braverman LE, Ingbar SH** 1978 Evidence that triiodothyronine and reverse triiodothyronine are sequentially deiodinated in man. J Clin Endocrinol Metab 46:916-922

33. **Smallridge RC, Whorton NE** 1984 3'-Monoiodothyronine degradation in rat liver homogenate: enzyme characteristics and documentation of deiodination by high-pressure liquid chromatography. Metabolism 33:1034-1038

34. **Piehl S, Heberer T, Balizs G, Scanlan TS, Kohrle J** 2008 Development of a validated liquid chromatography/tandem mass spectrometry method for the distinction of thyronine and thyronamine constitutional isomers and for the identification of new deiodinase substrates. Rapid Commun Mass Spectrom 22:3286-3296

35. **Chopra IJ, Chua Teco GN** 1982 Characteristics of inner ring (3 or 5) monodeiodination of 3,5-diiodothyronine in rat liver: evidence suggesting marked similarities of inner and outer ring deiodinases for iodothyronines. Endocrinology 110:89-97

36. **Pangaro L, Burman KD, Wartofsky L, Cahnmann HJ, Smallridge RC, O'Brian JT, Wright FD, Latham K** 1980 Radioimmunoassay for 3,5-diiodothyronine and evidence for dependence on conversion from 3,5,3'-triiodothyronine. J Clin Endocrinol Metab 50:1075-1081

37. **Maciel RM, Chopra IJ, Ozawa Y, Geola F, Solomon DH** 1979 A radioimmunoassay for measurement of 3,5-diiodothyronine. J Clin Endocrinol Metab 49:399-405

38. **van der Heide SM, Visser TJ, Everts ME, Klaren PH** 2002 Metabolism of thyroid hormones in cultured cardiac fibroblasts of neonatal rats. J Endocrinol 174:111-119

39. **Moreno M, de Lange P, Lombardi A, Silvestri E, Lanni A, Goglia F** 2008 Metabolic effects of thyroid hormone derivatives. Thyroid 18:239-253

40. **Yoder Graber AL, Ramirez J, Innocenti F, Ratain MJ** 2007 UGT1A1*28 genotype affects the in-vitro glucuronidation of thyroxine in human livers. Pharmacogenet Genomics 17:619-627

41. **Hillier AP** 1972 Transport of thyroxine glucuronide into bile. J Physiol 227:195-200

42. **de Herder WW, Bonthuis F, Rutgers M, Otten MH, Hazenberg MP, Visser TJ** 1988 Effects of inhibition of type I iodothyronine deiodinase and phenol sulfotransferase on the biliary clearance of triiodothyronine in rats. Endocrinology 122:153-157

43. **Rooda SJ, Otten MH, van Loon MA, Kaptein E, Visser TJ** 1989 Metabolism of triiodothyronine in rat hepatocytes. Endocrinology 125:2187-2197

44. **Hays MT, Cavalieri RR** 1992 Deiodination and deconjugation of the glucuronide conjugates of the thyroid hormones by rat liver and brain microsomes. Metabolism 41:494-497

45. **Faber J, Busch-Sorensen M, Rogowski P, Kirkegaard C, Siersbaek-Nielsen K, Friis T** 1981 Urinary excretion of free and conjugated 3',5'-diiodothyronine and 3,3'-diiodothyronine. J Clin Endocrinol Metab 53:587-593

46. **van der Heide SM, Joosten BJ, Everts ME, Klaren PH** 2004 Activities of UDP-glucuronyltransferase, beta-glucuronidase and deiodinase types I and II in hyper- and hypothyroid rats. J Endocrinol 181:393-400

47. **Rutgers M, Heusdens FA, Bonthuis F, de Herder WW, Hazenberg MP, Visser TJ** 1989 Enterohepatic circulation of triiodothyronine (T3) in rats: importance of the microflora for the liberation and reabsorption of T3 from biliary T3 conjugates. Endocrinology 125:2822-2830

48. **van der Heide SM, Joosten BJ, Dragt BS, Everts ME, Klaren PH** 2007 A physiological role for glucuronidated thyroid hormones: preferential uptake by H9c2(2-1) myotubes. Mol Cell Endocrinol 264:109-117

49. **Kester MH, Kaptein E, Roest TJ, van Dijk CH, Tibboel D, Meinl W, Glatt H, Coughtrie MW, Visser TJ** 1999 Characterization of human iodothyronine sulfotransferases. J Clin Endocrinol Metab 84:1357-1364

50. **Kester MH, Kaptein E, Roest TJ, van Dijk CH, Tibboel D, Meinl W, Glatt H, Coughtrie MW, Visser TJ** 2003 Characterization of rat iodothyronine sulfotransferases. Am J Physiol Endocrinol Metab 285:E592-598

51. **Chopra IJ** 2004 A radioimmunoassay for measurement of 3,3'-diiodothyronine sulfate: Studies in thyroidal and nonthyroidal diseases, pregnancy, and fetal/neonatal life. Metabolism 53:538-543

52. **Wu SY, Polk DH, Huang WS, Fisher DA** 1999 Fetal-to-maternal transfer of 3,3',5-triiodothyronine sulfate and its metabolite in sheep. Am J Physiol 277:E915-919

53. **Wu SY, Polk D, Fisher DA, Huang WS, Reviczky AL, Chen WL** 1995 Identification of 3,3'-T2S as a fetal thyroid hormone derivative in maternal urine in sheep. Am J Physiol 268:E33-39

54. **Visser TJ, Mol JA, Otten MH** 1983 Rapid deiodination of triiodothyronine sulfate by rat liver microsomal fraction. Endocrinology 112:1547-1549

55. **Wu SY, Green WL, Huang WS, Hays MT, Chopra IJ** 2005 Alternate pathways of thyroid hormone metabolism. Thyroid 15:943-958

56. **Galton VA, Pitt-Rivers R** 1959 The identification of the acetic acid analogues of thyroxine and tri-iodothyronine in mammalian tissues. Biochem J 72:319-321

57. **Albright EC, Lardy HA, Larson FC, Tomita K** 1956 Enzymatic conversion of thyroxine and triiodothyronine to the corresponding acetic acid analogues. Endocrinology 59:252-254

58. **Albright EC, Lardy HA, Larson FC, Tomita K** 1957 Enzymatic conversion of thyroxine to tetraiodothyroacetic acid and of triiodothyronine to triiodothyroacetic acid. J Biol Chem 224:387-397

59. **Albright EC, Tomita K, Larson FC** 1959 In vitro metabolism of triiodothyronine. Endocrinology 64:208-214

60. **Jouan P, Michel R, Roche J, Wolf W** 1956 The recovery of 3:5:3' -triiodothyroacetic acid and 3:3' -diiodothyronine from rat kidney after injection of 3:5:3' triiodothyronine. Endocrinology 59:425-432

61. **Pittman CS, Chambers JB, Jr., Read VH** 1971 The extrathyroidal conversion rate of thyroxine to triiodothyronine in normal man. J Clin Invest 50:1187-1196

62. **Rutgers M, Heusdens FA, Bonthuis F, Visser TJ** 1989 Metabolism of triiodothyroacetic acid (TA3) in rat liver. II. Deiodination and conjugation of TA3 by rat hepatocytes and in rats in vivo. Endocrinology 125:433-443

63. **Plaskett LG** 1961 Studies on the degradation of thyroid hormones in vitro with compounds labelled in either ring. Biochem J 78:652-657

64. **Wynn J, Gibbs R** 1962 Thyroxine degradation. II. Products of thyroxine degradation by rat liver microsomes. J Biol Chem 237:3499-3505

65. **Pittman CS, Chambers JB, Jr.** 1969 The carbon structure of thyroxine metabolites in urine. Endocrinology 84:705-710

66. **Pittman CS, Read VH, Chambers JB, Jr., Nakafuji H** 1970 The integrity of the ether linkage during thyroxine metabolism in man. J Clin Invest 49:373-380

67. **Meinhold H, Beckert A, Wenzel KW** 1981 Circulating diiodotyrosine: studies of its serum concentration, source, and turnover using radioimmunoassay after immunoextraction. J Clin Endocrinol Metab 53:1171-1178

68. **Davis PJ, Leonard JL, Davis FB** 2008 Mechanisms of nongenomic actions of thyroid hormone. Front Neuroendocrinol 29:211-218

69. **Lin HY, Davis FB, Gordinier JK, Martino LJ, Davis PJ** 1999 Thyroid hormone induces activation of mitogen-activated protein kinase in cultured cells. Am J Physiol 276:C1014-1024

70. **Gaddum JH** 1927 Quantitative observations on thyroxine and allied substances: I. The use of tadpoles. J Physiol 64:246-254

71. **Ashley JN, Harington CR** 1928 Some derivatives of thyroxine. Biochem J 22:1436-1445

72. **Tomita K, Lardy HA** 1960 Enzymic conversion of iodinated thyronines to iodinated thyroacetic acids. J Biol Chem 235:3292-3297

73. **Tomita K, Lardy HA** 1956 Synthesis and biological activity of some triiodinated analogues of thyroxine. J Biol Chem 219:595-604

74. **Pittman CS** 1979 Hormone Metabolism. In: Degroot LJ ed. Endocrinology. New York: Grune & Stratton; 365-372

75. **Scanlan TS, Suchland KL, Hart ME, Chiellini G, Huang Y, Kruzich PJ, Frascarelli S, Crossley DA, Bunzow JR, Ronca-Testoni S, Lin ET, Hatton D, Zucchi R, Grandy DK** 2004 3-Iodothyronamine is an endogenous and rapid-acting derivative of thyroid hormone. Nat Med 10:638-642

76. **Braulke LJ, Klingenspor M, DeBarber A, Tobias SC, Grandy DK, Scanlan TS, Heldmaier G** 2008 3-Iodothyronamine: a novel hormone controlling the balance between glucose and lipid utilisation. J Comp Physiol [B] 178:167-177

77. **Saba A, Chiellini G, Frascarelli S, Marchini M, Ghelardoni S, Raffaelli A, Tonacchera M, Vitti P, Scanlan TS, Zucchi R** 2010 Tissue Distribution and Cardiac Metabolism of 3-Iodothyronamine. Endocrinology 151:5063-5073

78. **Hoefig CS, Kohrle J, Brabant G, Dixit K, Yap B, Strasburger CJ, Wu Z** 2011 Evidence for extrathyroidal formation of 3-iodothyronamine in humans as provided by a novel monoclonal antibody-based chemiluminescent serum immunoassay. J Clin Endocrinol Metab 96:1864-1872

79. **Galli E, Marchini M, Saba A, Berti S, Tonacchera M, Vitti P, Scanlan TS, Iervasi G, Zucchi R** 2012 Detection of 3-iodothyronamine in human patients: a preliminary study. J Clin Endocrinol Metab 97:E69-74

80. **Chiellini G, Frascarelli S, Ghelardoni S, Carnicelli V, Tobias SC, DeBarber A, Brogioni S, Ronca-Testoni S, Cerbai E, Grandy DK, Scanlan TS, Zucchi R** 2007 Cardiac effects of 3-iodothyronamine: a new aminergic system modulating cardiac function. Faseb J 21:1597-1608

81. **DeBarber AE, Geraci T, Colasurdo VP, Hackenmueller SA, Scanlan TS** 2008 Validation of a liquid chromatography-tandem mass spectrometry method to enable quantification of 3-iodothyronamine from serum. J Chromatogr A 1210:55-59

82. **Regard JB, Kataoka H, Cano DA, Camerer E, Yin L, Zheng YW, Scanlan TS, Hebrok M, Coughlin SR** 2007 Probing cell type-specific functions of Gi in vivo identifies GPCR regulators of insulin secretion. J Clin Invest 117:4034-4043

83. **Ianculescu AG, Giacomini KM, Scanlan TS** 2008 Identification and characterization of 3-iodothyronamine (T1AM) intracellular transport. Endocrinology

84. **Panas HN, Lynch LJ, Vallender EJ, Xie Z, Chen GL, Lynn SK, Scanlan TS, Miller GM** 2010 Normal thermoregulatory responses to 3-iodothyronamine, trace amines and amphetamine-like psychostimulants in trace amine associated receptor 1 knockout mice. J Neurosci Res 88:1962-1969

85. **Snead AN, Santos MS, Seal RP, Miyakawa M, Edwards RH, Scanlan TS** 2007 Thyronamines inhibit plasma membrane and vesicular monoamine transport. ACS Chem Biol 2:390-398

86. **Piehl S, Heberer T, Balizs G, Scanlan TS, Smits R, Koksch B, Kohrle J** 2008 Thyronamines are isozyme-specific substrates of deiodinases. Endocrinology 149:3037-3045

87. **Pietsch CA, Scanlan TS, Anderson RJ** 2007 Thyronamines are substrates for human liver sulfotransferases. Endocrinology 148:1921-1927

88. **Wood WJ, Geraci T, Nilsen A, Debarber AE, Scanlan TS** 2008 Iodothyronamines are Oxidatively Deaminated to Iodothyroacetic Acids in vivo. Chembiochem

89. **Gu J, Soldin OP, Soldin SJ** 2007 Simultaneous quantification of free triiodothyronine and free thyroxine by isotope dilution tandem mass spectrometry. Clin Biochem 40:1386-1391

90. **Kahric-Janicic N, Soldin SJ, Soldin OP, West T, Gu J, Jonklaas J** 2007 Tandem mass spectrometry improves the accuracy of free thyroxine measurements during pregnancy. Thyroid 17:303-311

91. **Jonklaas J, Kahric-Janicic N, Soldin OP, Soldin SJ** 2009 Correlations of free thyroid hormones measured by tandem mass spectrometry and immunoassay with thyroid-stimulating hormone across 4 patient populations. Clin Chem 55:1380-1388

92. **Wang D, Stapleton HM** 2010 Analysis of thyroid hormones in serum by liquid chromatography-tandem mass spectrometry. Anal Bioanal Chem 397:1831-1839

93. **Chopra IJ** 1972 A radioimmunoassay for measurement of thyroxine in unextracted serum. J Clin Endocrinol Metab 34:938-947

94. **Soldin SJ, Soukhova N, Janicic N, Jonklaas J, Soldin OP** 2005 The measurement of free thyroxine by isotope dilution tandem mass spectrometry. Clin Chim Acta 358:113-118

95. **Chalmers J, Dickson G, Elks J, Hems B** 1949 The Synthesis of Thyroxine and Related Substances. Part V: A Synthesis of L-Thyroxine from L-Tyrosine. Journal of the Chemical Society:3424-2433

96. **Borrows ET, Clayton JC, Hems BA** 1949 Thyroxine and Related Substances. Part I. The Preparation of Tyrosine and Some of its Derivatives, and a New Route to Thyroxine. J Chem Soc:S185-S190

97. **Gennari C, Longari C, Ressel S, Salom B, Mielgo A** 1998 Synthesis of Chiral Vinylogous Sulfonamidopeptides (vs-Peptides). Eur J Org Chem:945-959

98. **Hart ME, Suchland KL, Miyakawa M, Bunzow JR, Grandy DK, Scanlan TS** 2006 Trace amine-associated receptor agonists: synthesis and evaluation of thyronamines and related analogues. J Med Chem 49:1101-1112

99. **Yamada Y, Akiba A, Arima S, Okada C, Yoshida K, Itou F, Kai T, Satou T, Takeda K, Harigaya Y** 2005 Synthesis of Linear Tripeptides for Right-Hand Segments of Complestatin. Chemical & Pharmaceutical Bulletin 53:1277-1290

100. **Barluenga J, Garcia-Martin MA, Gonzalez JM, Clapes P, Valencia G** 1996 Iodination of aromatic residues in peptides by reaction with IPy2BF4. Chemical Communications 13:1505-1506

101. **Bovonsombat P, Khanthapura P, Krause MM, Leykajarakul J** 2008 Facile syntheses of 3-halo and mixed 3,5-dihalo analogues of N-acetyl-L-tyrosine via sulfonic acid-catalysed regioselective monohalogenation. Tetrahedron Lett 49:7008-7011

102. **Evans DA, Katz JL, West TR** 1998 Synthesis of diaryl ethers through the copper-promoted arylation of phenols with arylboronic acids. An expedient synthesis of thyroxine. Tetrahedron Lett 39:2937-2940

103. **Corey EJ, Szekely I, Shiner CS** 1977 Synthesis of 6,9alpha-oxido-11alpha, 15alpha-dihydroxyprosta-(E)5,(E)13-dienoic acid, an isomer of PGI2 (Vane's PGX). Tetrahedron Lett 40:3529-3532

104. **Sterling K, Lashof JC, Man EB** 1954 Disappearance from serum of I131-labeled l-thyroxine and l-triiodothyronine in euthyroid subjects. J Clin Invest 33:1031-1035

105. **McConnon J, Row VV, Volpe** 1971 Simultaneous comparative studies of thyroxine and tri-iodothyronine distribution and disposal rates. J Endocrinol 51:17-30

106. **Surks MI, Oppenheimer JH** 1971 Metabolism of phenolic- and tyrosyl-ring labeled L-thyroxine in human beings and rats. J Clin Endocrinol Metab 33:612-618

107. **Nicoloff JT, Low JC, Dussault JH, Fisher DA** 1972 Simultaneous measurement of thyroxine and triiodothyronine peripheral turnover kinetics in man. J Clin Invest 51:473-483

108. **Surks MI, Schadlow AR, Stock JM, Oppenheimer JH** 1973 Determination of iodothyronine absorption and conversion of L-thyroxine (T 4) to L-triiodothyronine (T 3) using turnover rate techniques. J Clin Invest 52:805-811

109. **Inada M, Kasagi K, Kurata S, Kazama Y, Takayama H, Torizuka K, Fukase M, Soma T** 1975 Estimation of thyroxine and triiodothyronine distribution and of the conversion rate of thyroxine to triiodothyronine in man. J Clin Invest 55:1337-1348

110. **Demeneix BA, Henderson NE** 1978 Thyroxine metabolism in active and torpid ground squirrels, Spermophilus richardsoni. Gen Comp Endocrinol 35:86-92

111. **DiStefano JJ, 3rd, Feng D** 1988 Comparative aspects of the distribution, metabolism, and excretion of six iodothyronines in the rat. Endocrinology 123:2514-2525

112. **Salamonczyk GM, Oza VB, Sih CJ** 1997 A concise synthesis of thyroxine (T-4) and 3,5,3'-triiodo-L-thyronine (T-3). Tetrahedron Lett 38:6965-6968

113. **De meyer M, Guerit N, Hantson AL** 2004 Synthesis of Thyroid Hormones Labelled with Carbon-13. In: Dean DC, Filer CN, McCarthy KE eds. Synthesis and Application of Isotopically Labelled Compounds

114. **Nagao H, Imazu T, Hayashi H, Takahashi K, Minato K** 2011 Influence of thyroidectomy on thyroxine metabolism and turnover rate in rats. J Endocrinol 210:117-123

115. **Sorimachi K, Cahnmann HJ** 1977 A simple synthesis of [3,5-125I]Diiodo-L-thyroxine of high specific activity. Endocrinology 101:1276-1280

116. **Ocasio CA, Scanlan TS** 2008 Characterization of thyroid hormone receptor alpha (TRalpha)-specific analogs with varying inner- and outer-ring substituents. Bioorg Med Chem 16:762-770

117. **Cheng SY, Leonard JL, Davis PJ** 2010 Molecular aspects of thyroid hormone actions. Endocr Rev 31:139-170

118. **Sun ZQ, Ojamaa K, Coetzee WA, Artman M, Klein I** 2000 Effects of thyroid hormone on action potential and repolarizing currents in rat ventricular myocytes. Am J Physiol Endocrinol Metab 278:E302-307

119. **Bergh JJ, Lin HY, Lansing L, Mohamed SN, Davis FB, Mousa S, Davis PJ** 2005 Integrin alphaVbeta3 contains a cell surface receptor site for thyroid hormone that is linked to activation of mitogen-activated protein kinase and induction of angiogenesis. Endocrinology 146:2864-2871

120. **Burman KD, Strum D, Dimond RC, Djuh YY, Wright FD, Earll JM, Wartofsky L** 1977 A radioimmunoassay for 3,3'-L-diiodothyronine (3,3'T2). J Clin Endocrinol Metab 45:339-352

121. **Medina-Gomez G, Calvo RM, Obregon MJ** 2008 Thermogenic effect of triiodothyroacetic acid at low doses in rat adipose tissue without adverse side effects in the thyroid axis. Am J Physiol Endocrinol Metab 294:E688-697

122. **Hernandez A, Martinez ME, Liao XH, Van Sande J, Refetoff S, Galton VA, St Germain DL** 2007 Type 3 deiodinase deficiency results in functional abnormalities at multiple levels of the thyroid axis. Endocrinology 148:5680-5687

123. **Christ S, Biebel UW, Hoidis S, Friedrichsen S, Bauer K, Smolders JW** 2004 Hearing loss in athyroid pax8 knockout mice and effects of thyroxine substitution. Audiol Neurootol 9:88-106

124. **Trajkovic M, Visser TJ, Mittag J, Horn S, Lukas J, Darras VM, Raivich G, Bauer K, Heuer H** 2007 Abnormal thyroid hormone metabolism in mice lacking the monocarboxylate transporter 8. J Clin Invest 117:627-635

125. **Ueta CB, Olivares EL, Bianco AC** 2011 Responsiveness to thyroid hormone and to ambient temperature underlies differences between brown adipose tissue and skeletal muscle thermogenesis in a mouse model of diet-induced obesity. Endocrinology 152:3571-3581

126. **van Buul-Offers S, Hackeng WH, Schopman W** 1983 Thyroxine and triiodothyronine levels in Snell mice. Acta Endocrinol (Copenh) 102:396-409

127. **Trajkovic-Arsic M, Muller J, Darras VM, Groba C, Lee S, Weih D, Bauer K, Visser TJ, Heuer H** 2010 Impact of monocarboxylate transporter-8 deficiency on the hypothalamus-pituitary-thyroid axis in mice. Endocrinology 151:5053-5062

128. **Theodossiou C, Skrepnik N, Robert EG, Prasad C, Axelrad TW, Schapira DV, Hunt JD** 1999 Propylthiouracil-induced hypothyroidism reduces xenograft tumor growth in athymic nude mice. Cancer 86:1596-1601

129. **Henderson JD, Esham RH** 2001 Generic substitution: issues for problematic drugs. South Med J 94:16-21

130. **Roy G, Placzek E, Scanlan TS** 2012 ApoB-100-containing lipoproteins are major carriers of 3-iodothyronamine in circulation. J Biol Chem 287:1790-1800

131. **Hoefig CS, Renko K, Piehl S, Scanlan TS, Bertoldi M, Opladen T, Hoffmann GF, Klein J, Blankenstein O, Schweizer U, Kohrle J** 2012 Does the aromatic L-amino acid decarboxylase contribute to thyronamine biosynthesis? Mol Cell Endocrinol 349:195-201

132. **Ackermans MT, Klieverik LP, Ringeling P, Endert E, Kalsbeek A, Fliers E** 2010 An online solid-phase extraction-liquid chromatography-tandem mass

spectrometry method to study the presence of thyronamines in plasma and tissue and their putative conversion from 13C6-thyroxine. J Endocrinol 206:327-334

133. **Cooper DS** 1984 Antithyroid drugs. N Engl J Med 311:1353-1362

134. **Van Sande J, Massart C, Beauwens R, Schoutens A, Costagliola S, Dumont JE, Wolff J** 2003 Anion selectivity by the sodium iodide symporter. Endocrinology 144:247-252

135. **de la Vieja A, Calero M, Santisteban P, Lamas L** 1997 Identification and quantitation of iodotyrosines and iodothyronines in proteins using high-performance liquid chromatography by photodiode-array ultraviolet-visible detection. J Chromatogr B Biomed Sci Appl 688:143-149

136. **Miyakawa M, Scanlan TS** 2006 Synthesis of [125I]-, [2H]-, and [3H]-Labeled 3-Iodothyronamine (T1AM). Synthetic Communications 36:891-902

137. **Hood A, Klaassen CD** 2000 Differential effects of microsomal enzyme inducers on in vitro thyroxine (T(4)) and triiodothyronine (T(3)) glucuronidation. Toxicol Sci 55:78-84

138. **Shah VP, Midha KK, Findlay JW, Hill HM, Hulse JD, McGilveray IJ, McKay G, Miller KJ, Patnaik RN, Powell ML, Tonelli A, Viswanathan CT, Yacobi A** 2000 Bioanalytical method validation--a revisit with a decade of progress. Pharm Res 17:1551-1557

139. **Buitendijk M, Galton VA** 2012 Is the kidney a major storage site for thyroxine as thyroxine glucuronide? Thyroid 22:187-191

140. **Tai SS, Bunk DM, White Et, Welch MJ** 2004 Development and evaluation of a reference measurement procedure for the determination of total 3,3',5-

145

triiodothyronine in human serum using isotope-dilution liquid chromatography-tandem mass spectrometry. Anal Chem 76:5092-5096

141. **Hilz H, Wiegers U, Adamietz P** 1975 Stimulation of proteinase K action by denaturing agents: application to the isolation of nucleic acids and the degradation of 'masked' proteins. Eur J Biochem 56:103-108

142. **Kankaanpaa A, Gunnar T, Ariniemi K, Lillsunde P, Mykkanen S, Seppala T** 2004 Single-step procedure for gas chromatography-mass spectrometry screening and quantitative determination of amphetamine-type stimulants and related drugs in blood, serum, oral fluid and urine samples. J Chromatogr B Analyt Technol Biomed Life Sci 810:57-68

143. **Hidvegi E, Fabian P, Hideg Z, Somogyi G** 2006 GC-MS determination of amphetamines in serum using on-line trifluoroacetylation. Forensic Sci Int 161:119-123

144. **Brown S, Eales JG** 1977 Measurement of L-thyroxine and 3,5,3'-triiodo-L-thyronine levels in fish plasma by radioimmunoassay. Can J Zool 55:293-299

145. **Huang G, Lee DM, Singh S** 1988 Identification of the thiol ester linked lipids in apolipoprotein B. Biochemistry 27:1395-1400

146. **Egusa G, Brady DW, Grundy SM, Howard BV** 1983 Isopropanol precipitation method for the determination of apolipoprotein B specific activity and plasma concentrations during metabolic studies of very low density lipoprotein and low density lipoprotein apolipoprotein B. J Lipid Res 24:1261-1267

147. **Cao Z, West C, Norton-Wenzel CS, Rej R, Davis FB, Davis PJ** 2009 Effects of resin or charcoal treatment on fetal bovine serum and bovine calf serum. Endocr Res 34:101-108

148. **Campos-Candel A, Llobat-Estelles M, Mauri-Aucejo AR** 2007 Desorption of BTEX from activated charcoal using accelerated solvent extraction: evaluation of occupational exposures. Anal Bioanal Chem 387:1517-1523

149. **Monera OD, Kay CM, Hodges RS** 1994 Protein denaturation with guanidine hydrochloride or urea provides a different estimate of stability depending on the contributions of electrostatic interactions. Protein Sci 3:1984-1991

150. **Romhild W, Krause D, Bartels H, Ghanem A, Schoning R, Wittig H** 2003 LC-MS/MS analysis of pholedrine in a fatal intoxication case. Forensic Sci Int 133:101-106

Appendix A: ^{1}H and ^{13}C NMR and MS/MS Fragmentation Spectra

Boc-L-Tyrosine-OMe
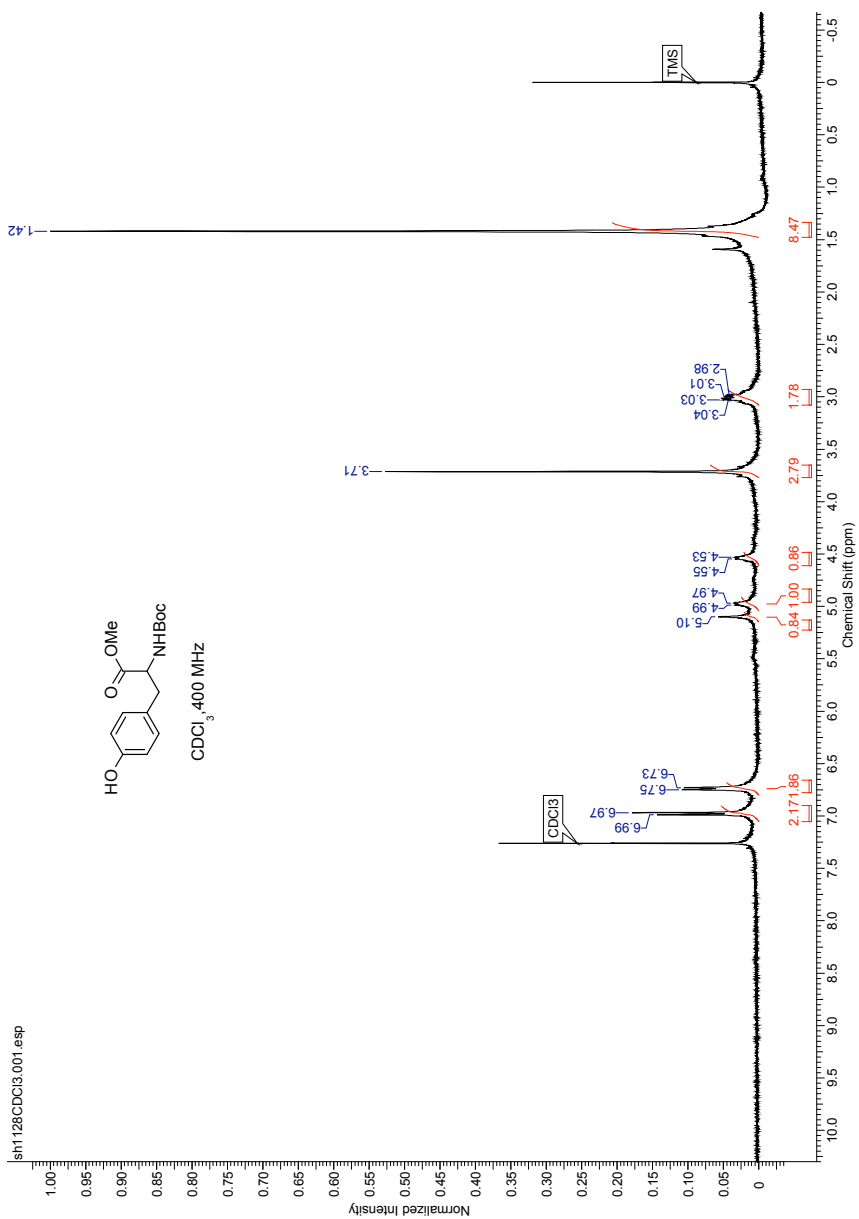
Boc-OMe-$^{13}C_9$-^{15}N-L-tyrosine (2); collision energy (CE) = 10V.

Boc-3,5-diiodo-L-Tyrosine-OMe

CDCl$_3$, 400 MHz

sh1129UCDCl3.001.esp

151
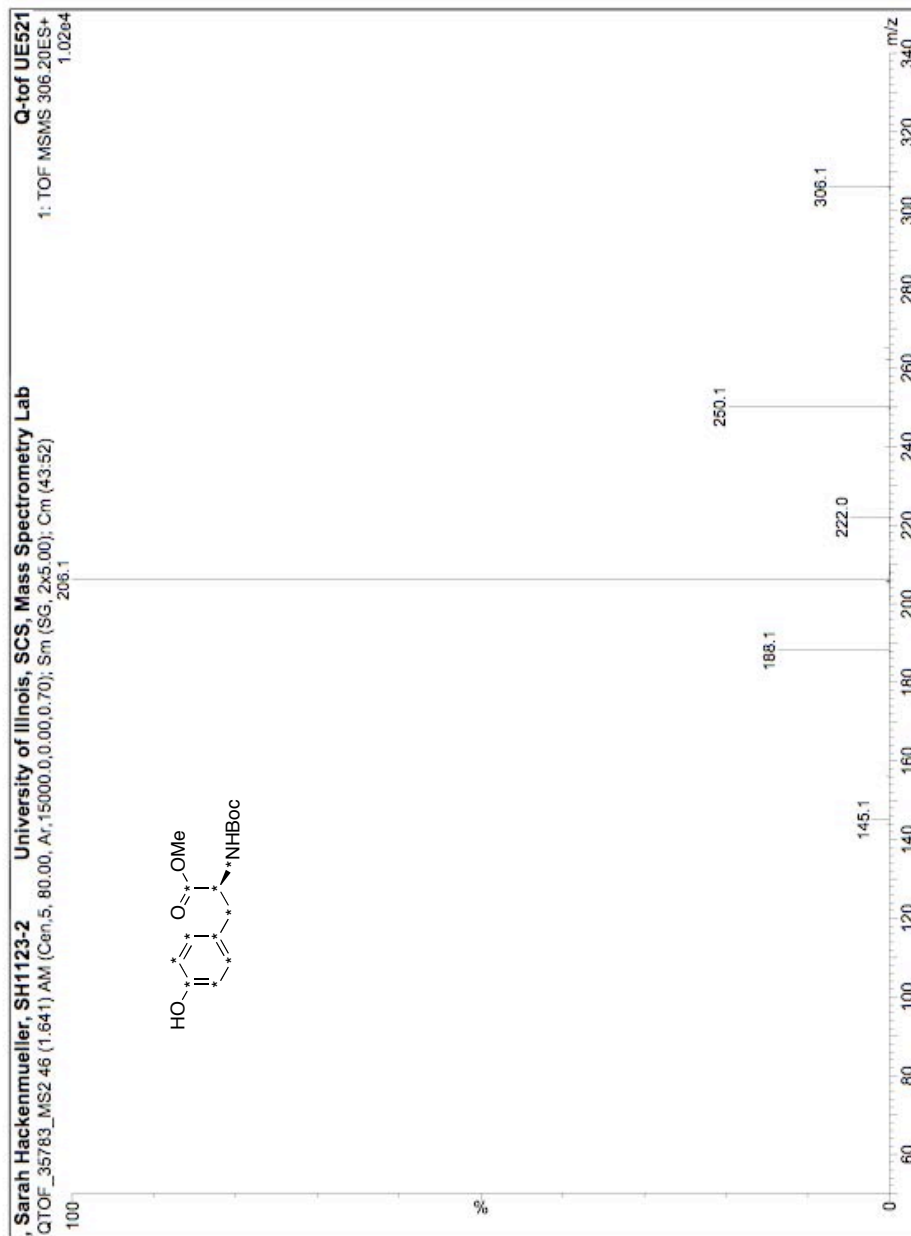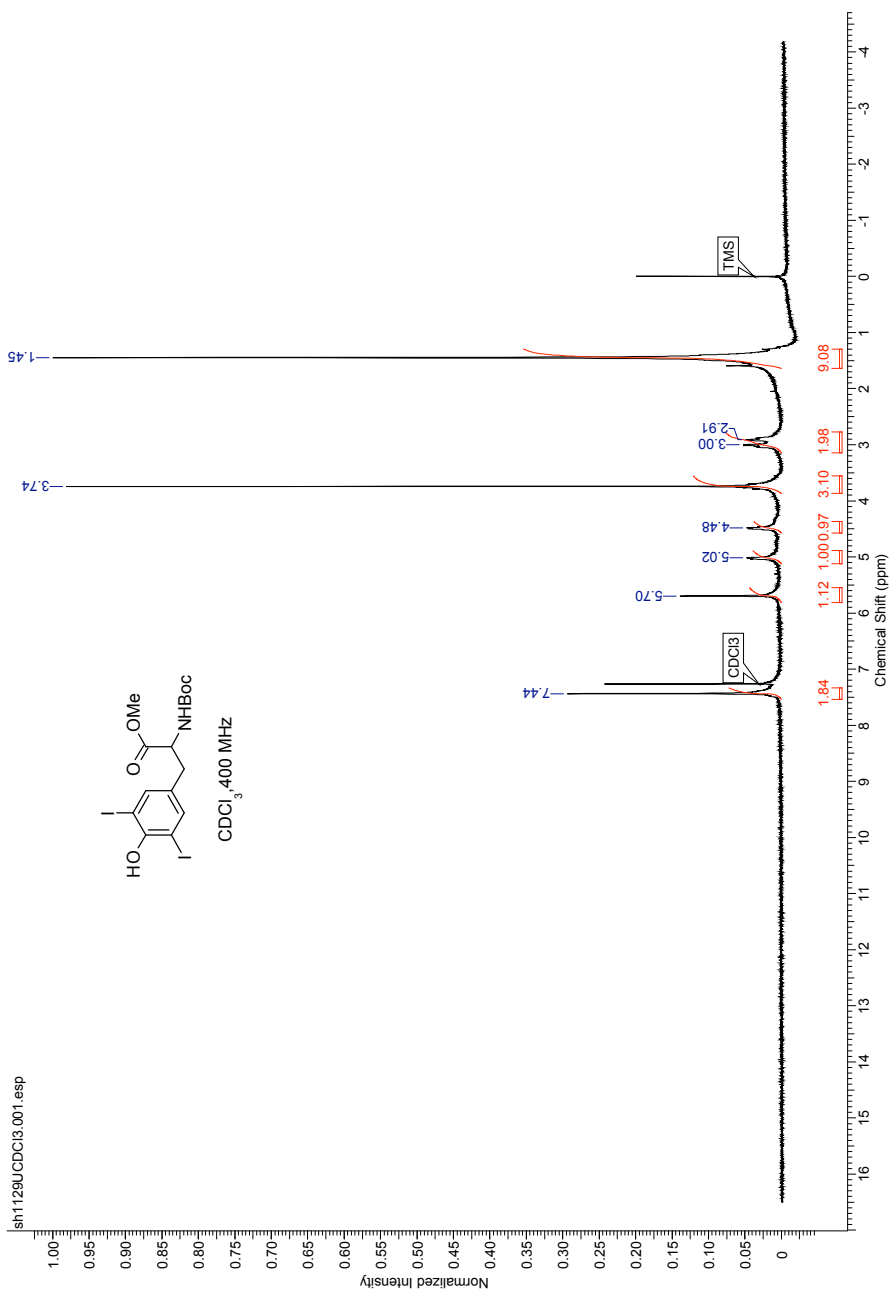
MS/MS spectrum of 3,5-Diiodo-Boc-OMe-¹³C₉-¹⁵N-L-Tyrosine (3); CE = 20V.

Boc-3,5-diiodo-L-Thyronine-OMe

SH1132LCDCl3.001.esp

TMS

EtOAc

EtOAc

1.45

9.07

2.88
2.89
2.92
2.94
3.07
3.08
3.09
3.11

2.30

3.76

3.00

EtOAc

4.54

4.68

1.71
1.50

5.10
5.12

0.83

6.63
6.66
6.75
6.77
6.79
6.85
6.88

4.88

CDCl3

7.63

1.81

Chemical Shift (ppm)

Normalized Intensity

CDCl₃, 400 MHz

153
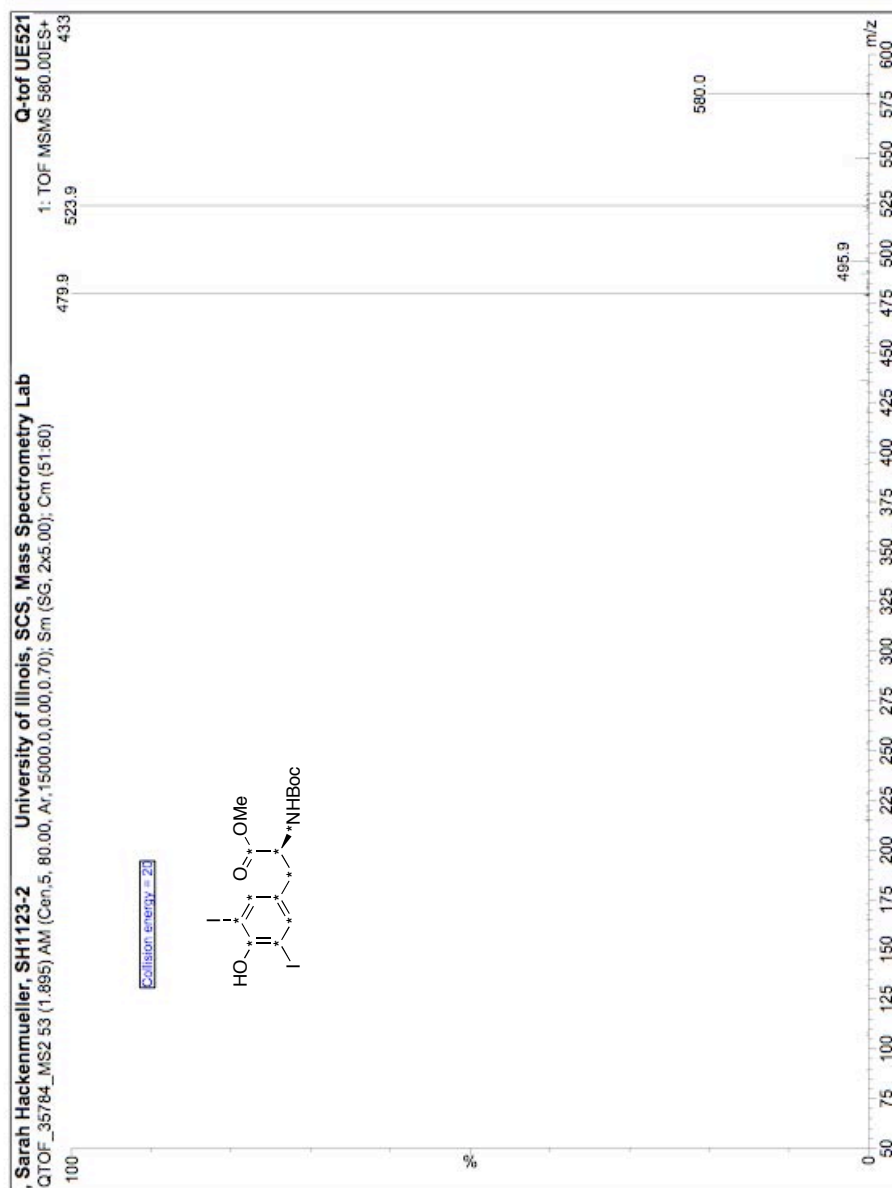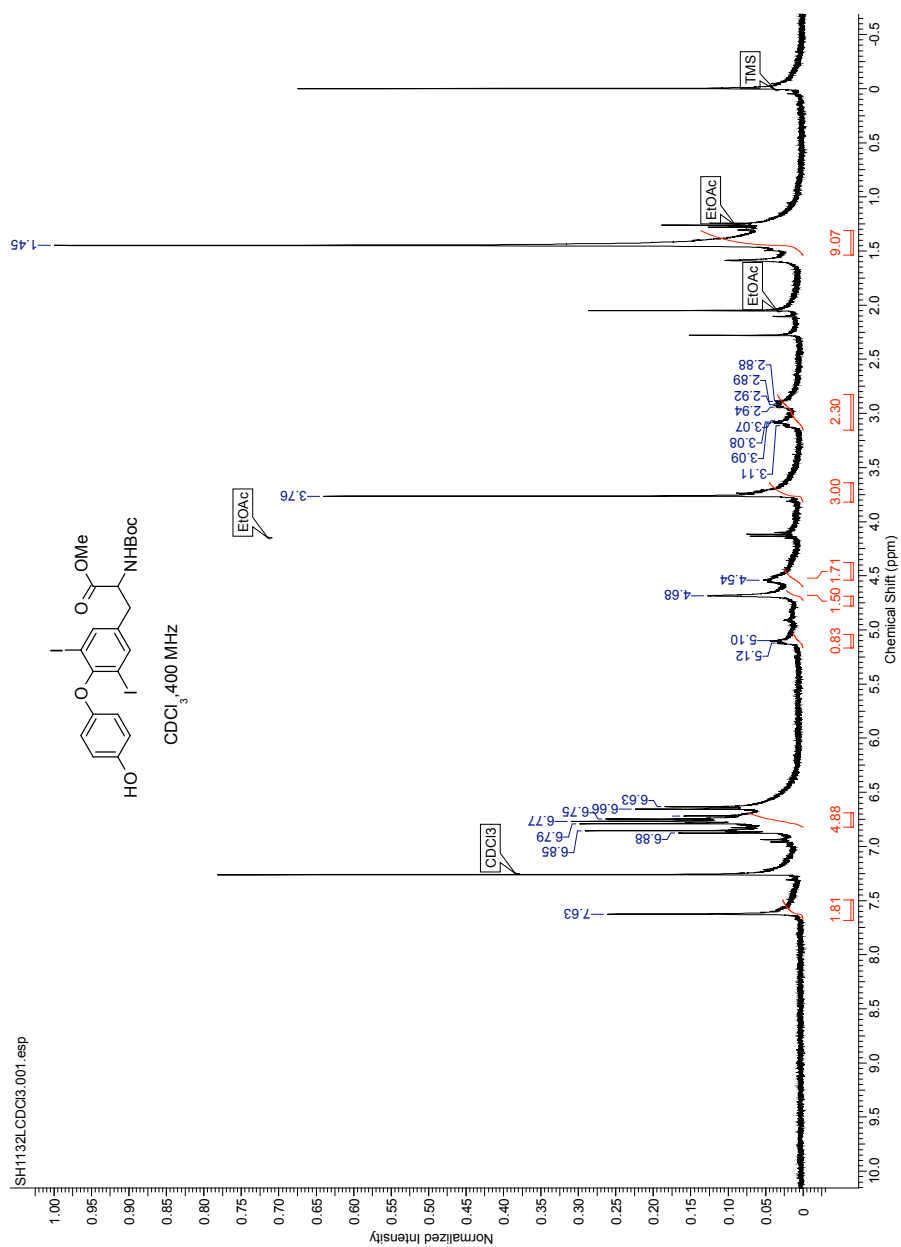
MS/MS spectrum of 3,5-Diiodo-Boc-OMe-$^{13}C_9$-^{15}N-L-Thyronine (4); CE = 9V.
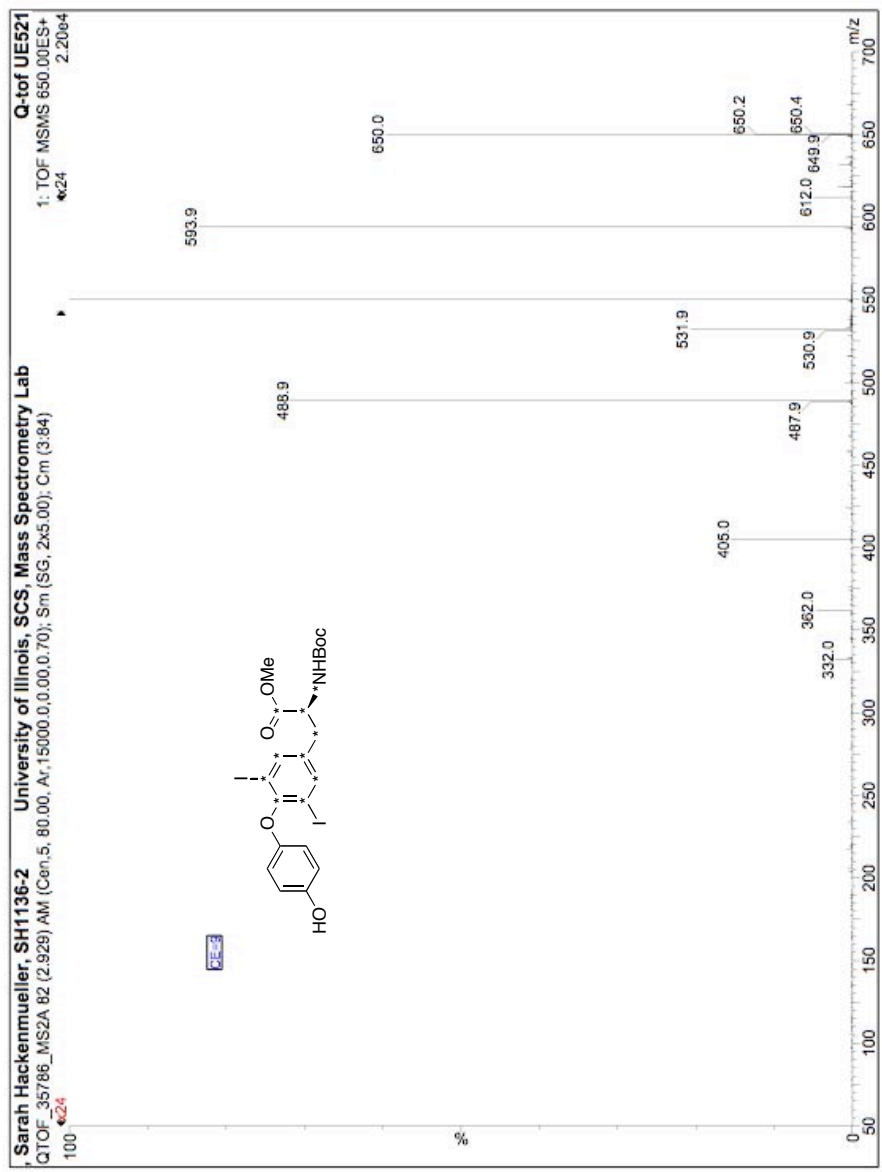
3,5-Diiodo-Boc-OMe-$^{13}C_9$-^{15}N-L-Thyronine (4) ^{1}H NMR (middle), ^{13}C-decoupled ^{1}H NMR (bottom) and difference spectrum (top).
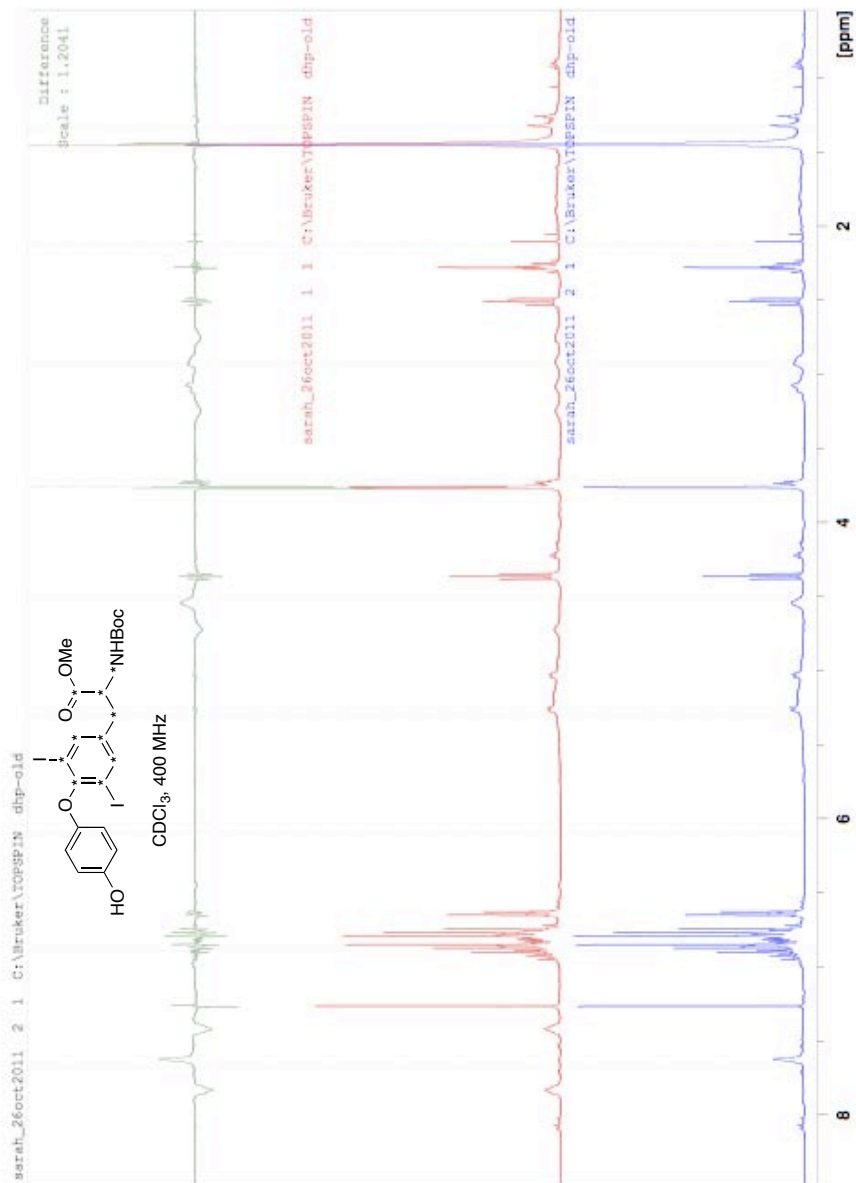
3,5-Diiodo-Boc-OMe-$^{13}C_9$-^{15}N-L-Thyronine (4) ^{13}C NMR.
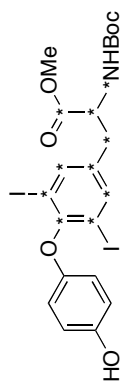
3,5-Diiodo-Boc-OMe-[13]C$_9$-^{15}N-L-Thyronine (4) HSQC.
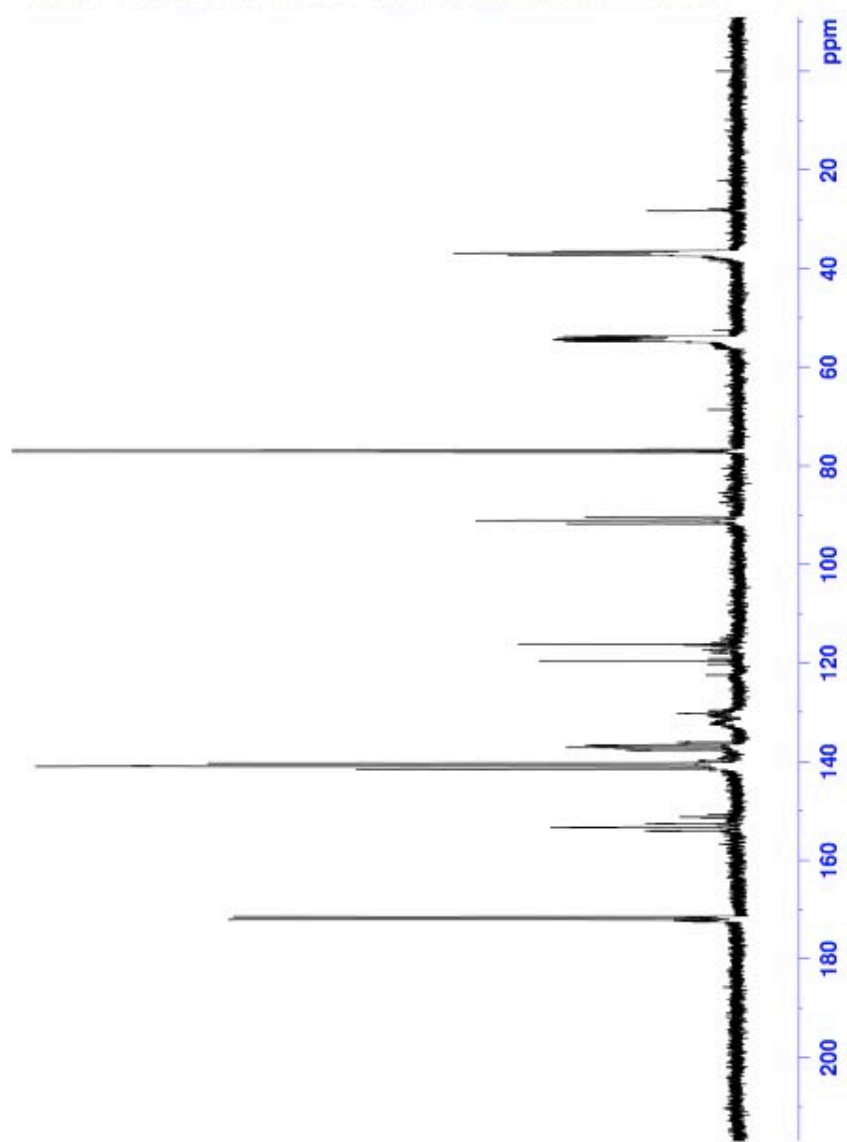
3,5-Diiodo-Boc-OMe-$^{13}C_9$-^{15}N-L-Thyronine (4) HMBC.
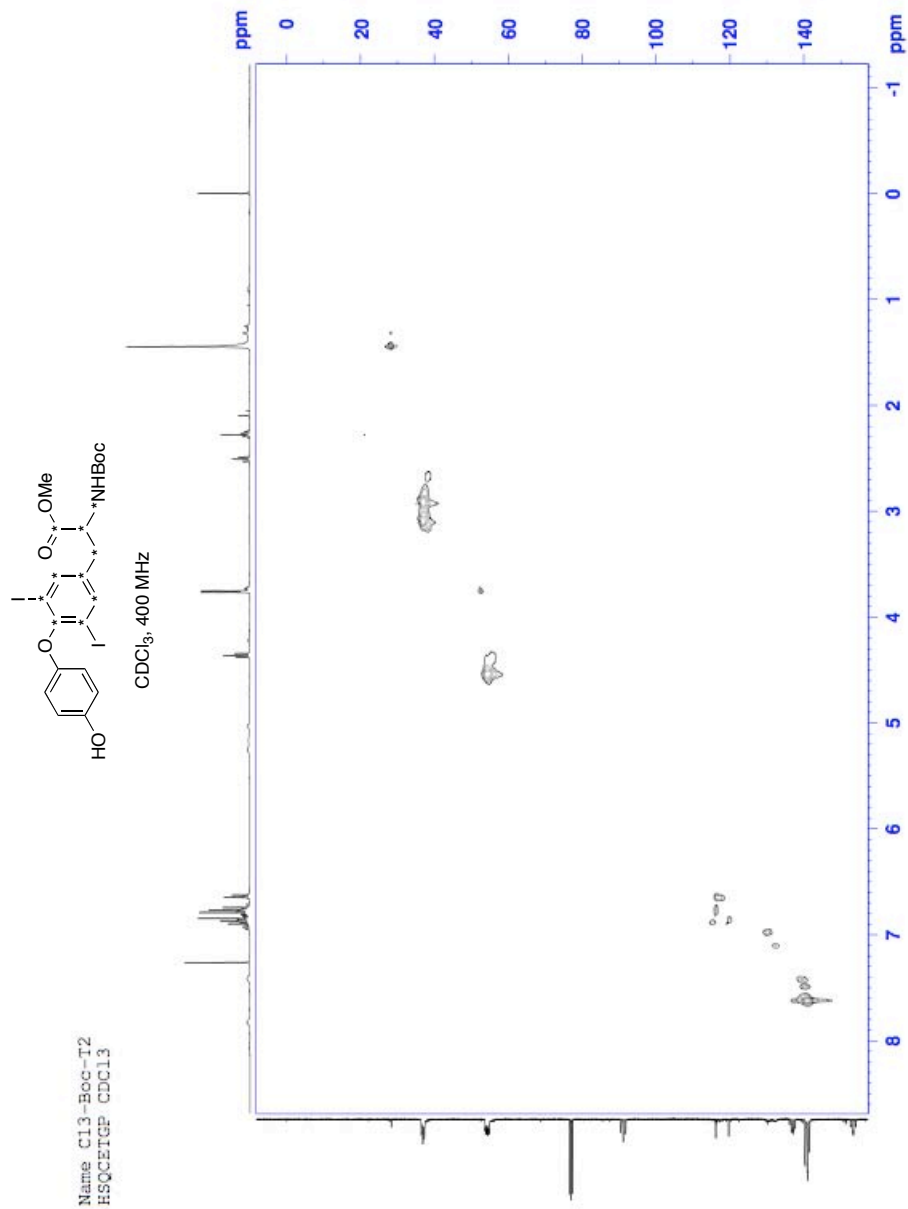
MS/MS of 3,5-Diiodo-$^{13}C_9$-^{15}N-L-Thyronine ($^{13}C_9$-^{15}N-T$_2$) (5); CE = 10 and 30V.

159

Boc-3,3',5,5'-tetraiodo-L-thyronine-OMe

160
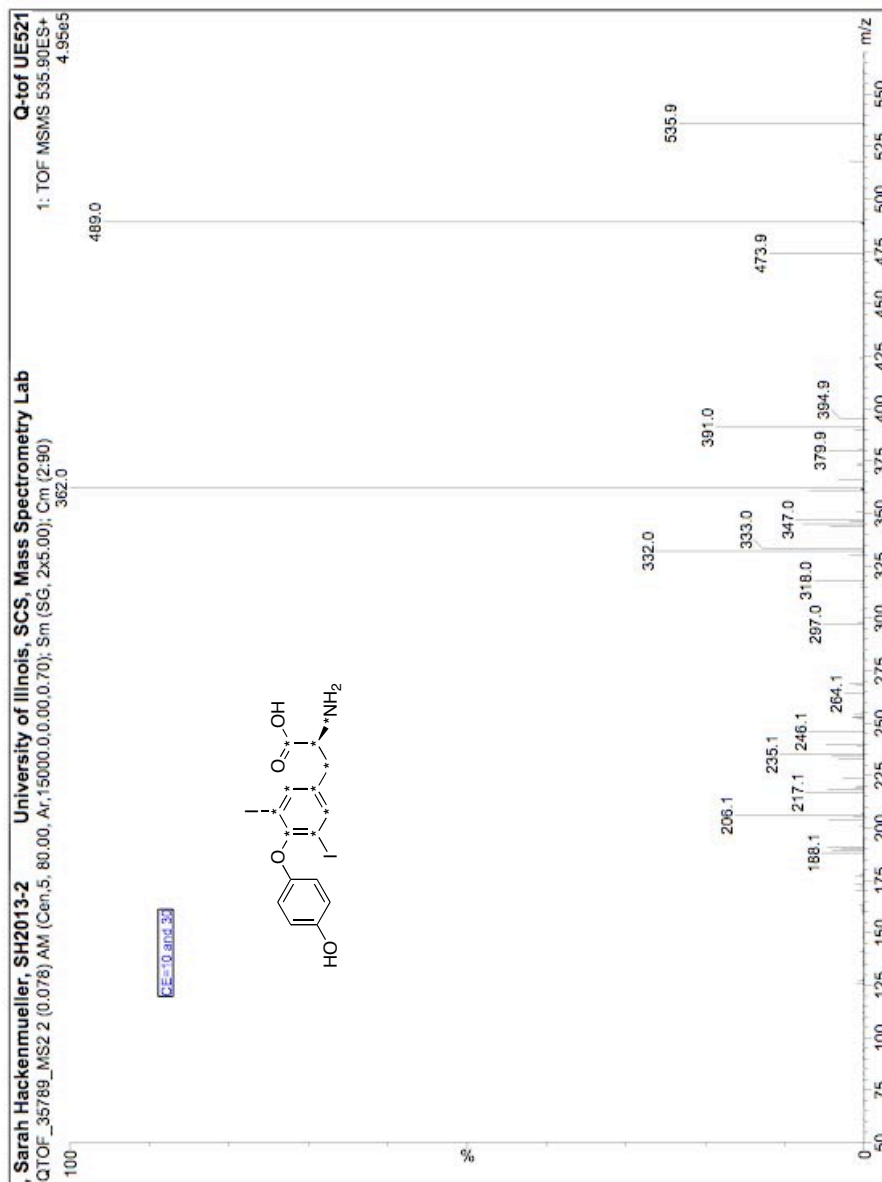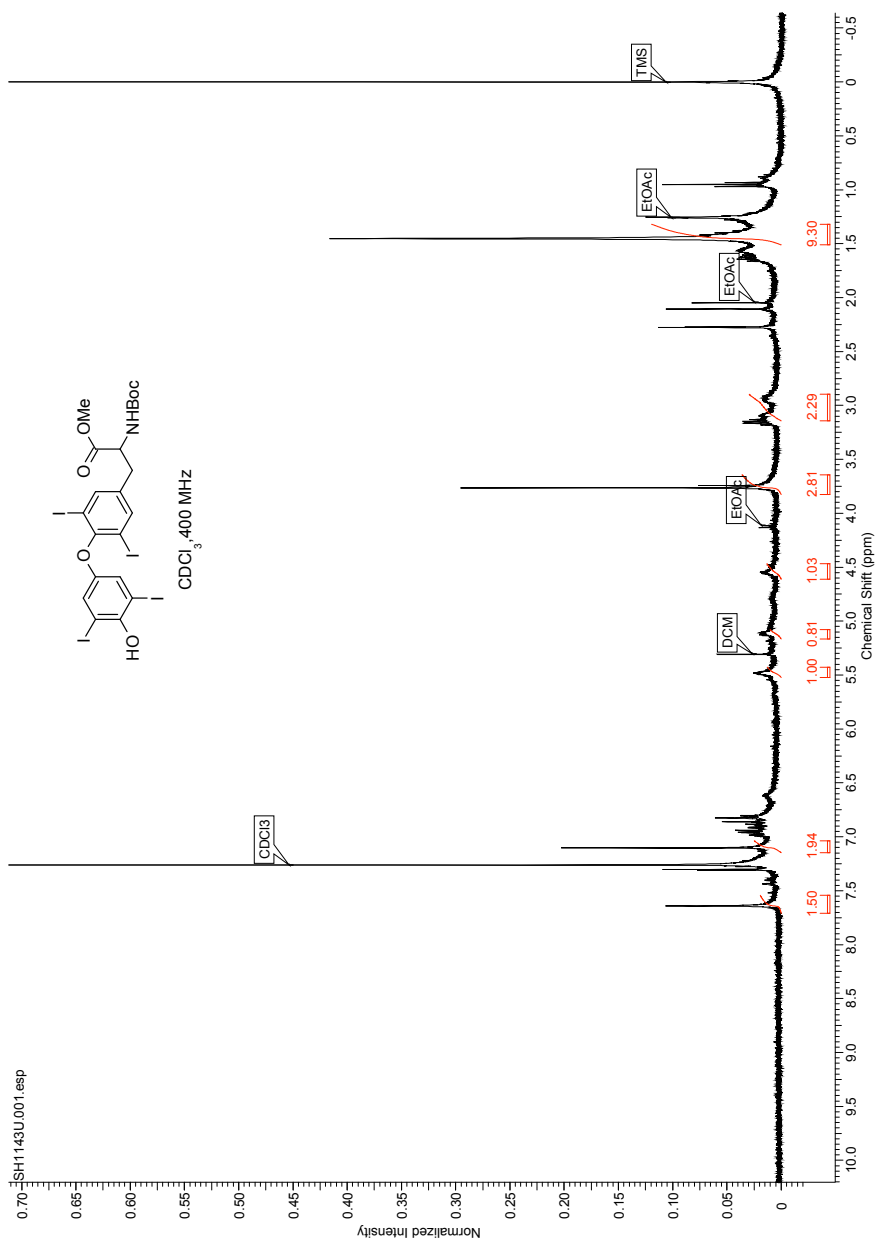
MS/MS spectrum of 3,3',5,5'-tetraiodo-N-Boc-OMe-$^{13}C_9$-^{15}N-L-thyronine (6); CE = 10V.
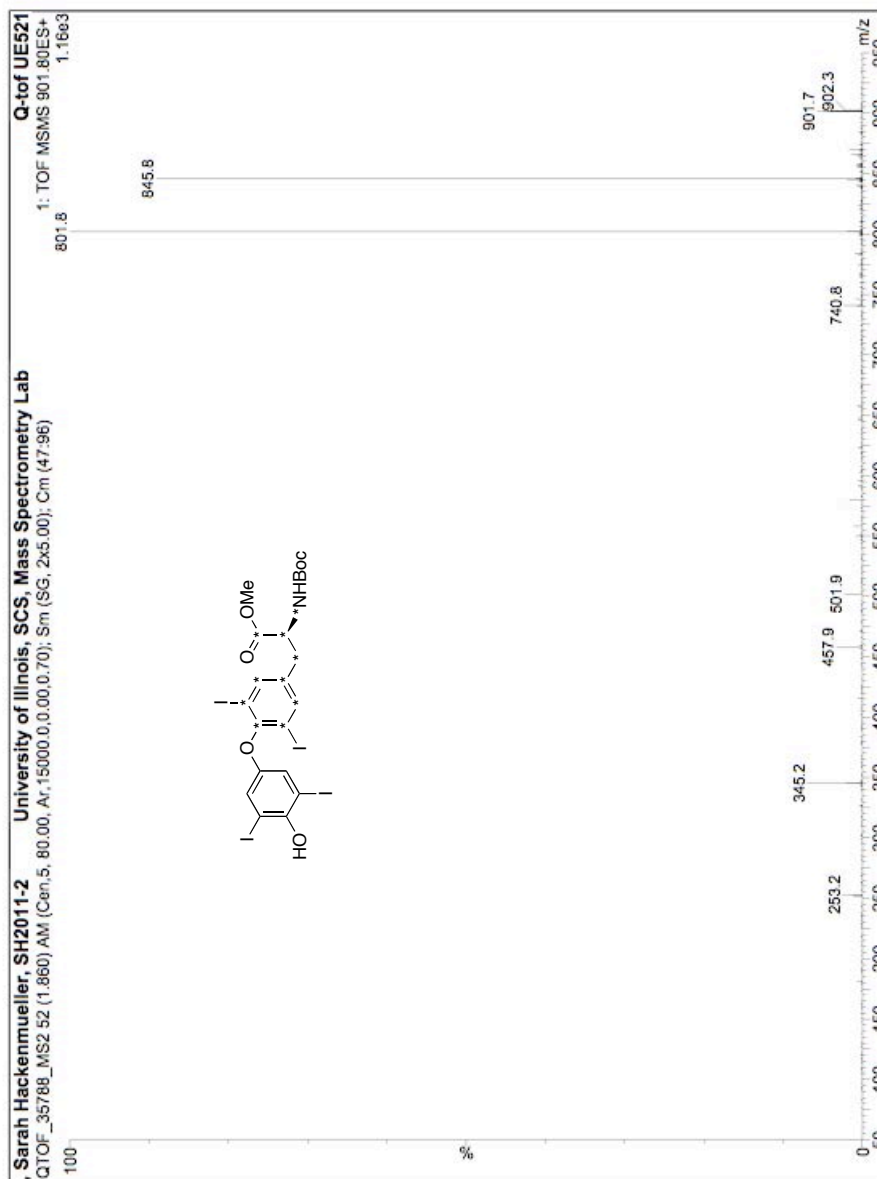
MS/MS of 3,3',5,5'-Tetraiodo-$^{13}C_9$-^{15}N-L-Thyronine ($^{13}C_9$-^{15}N-T$_4$) (7); CE = 30V.
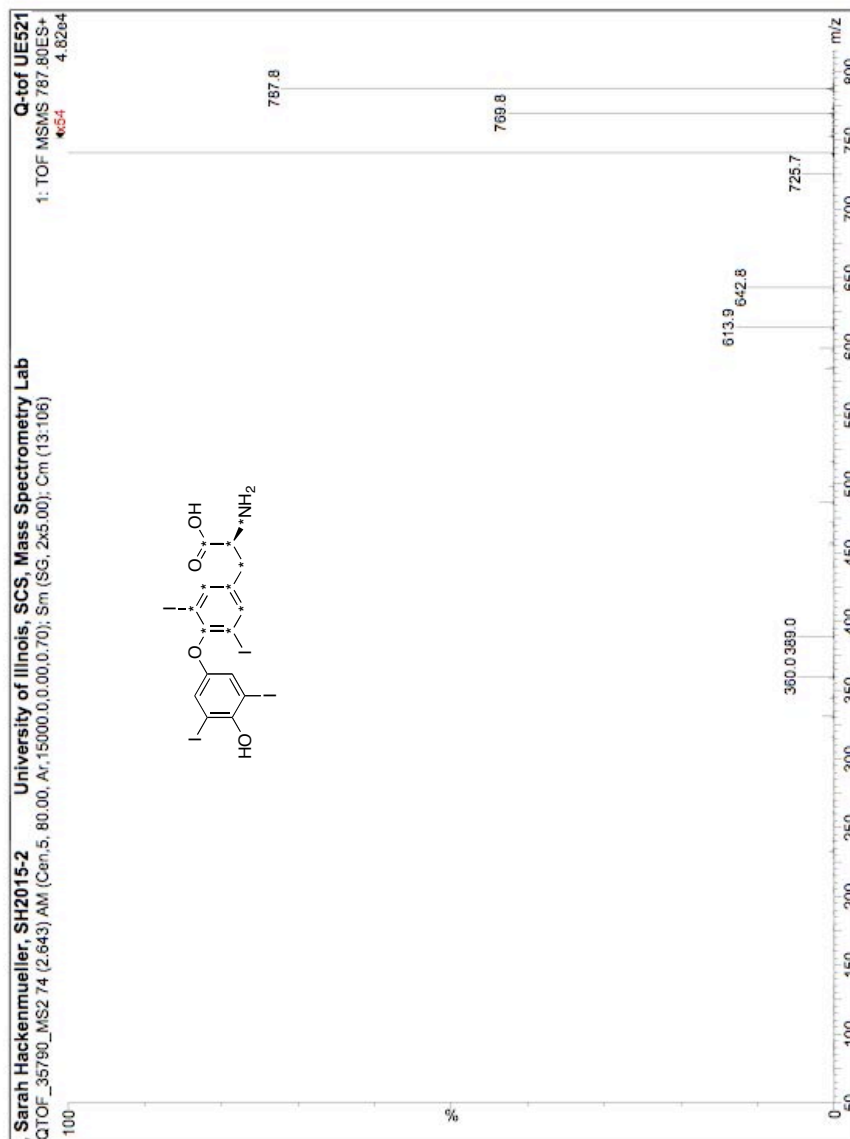
N-acetyl-3-iodothyronamine

400MHz, d_6-DMSO

Ac-T1AM.001.esp

DMSO

H2O

Chemical Shift (ppm)

Normalized Intensity

163
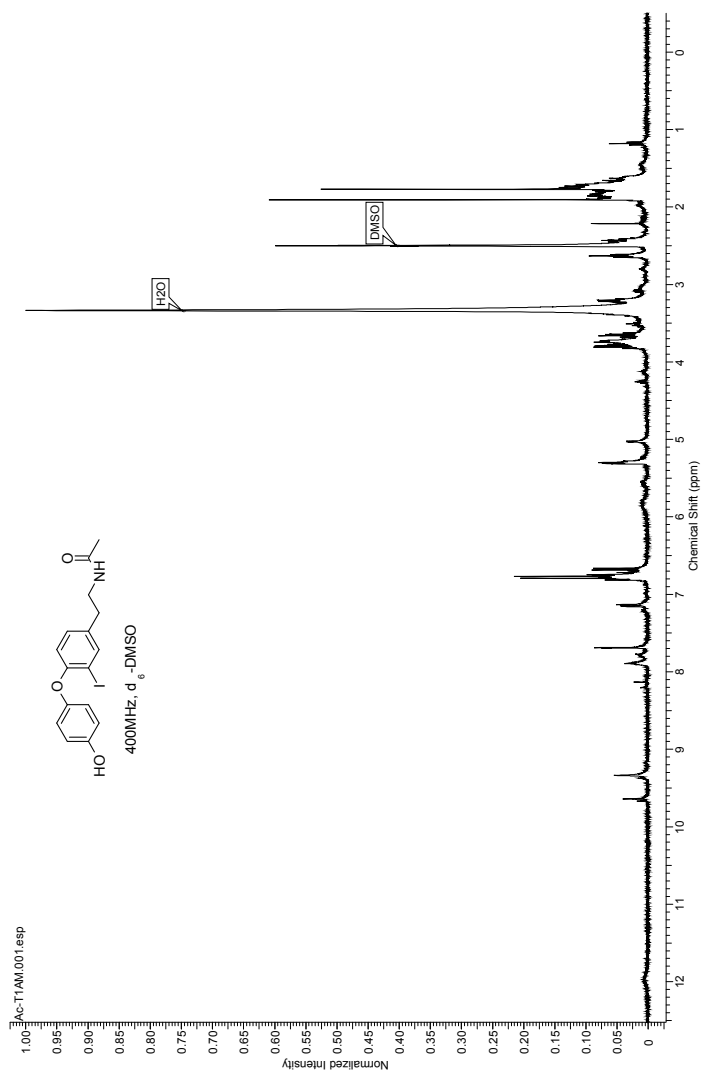
Appendix B: LC-MS/MS Chromatograms

Sample Set I-A: Serum blank
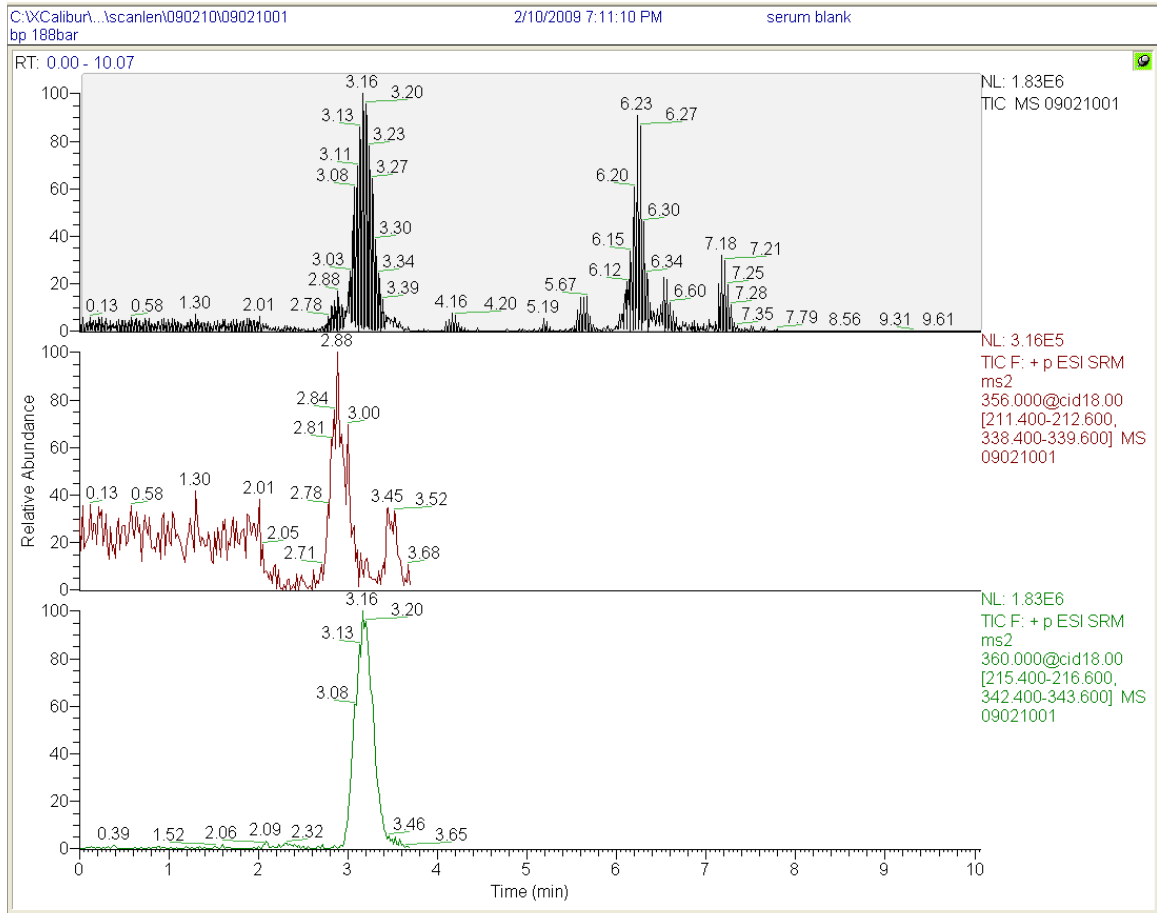
Sample Set I-A: Tissue Blank
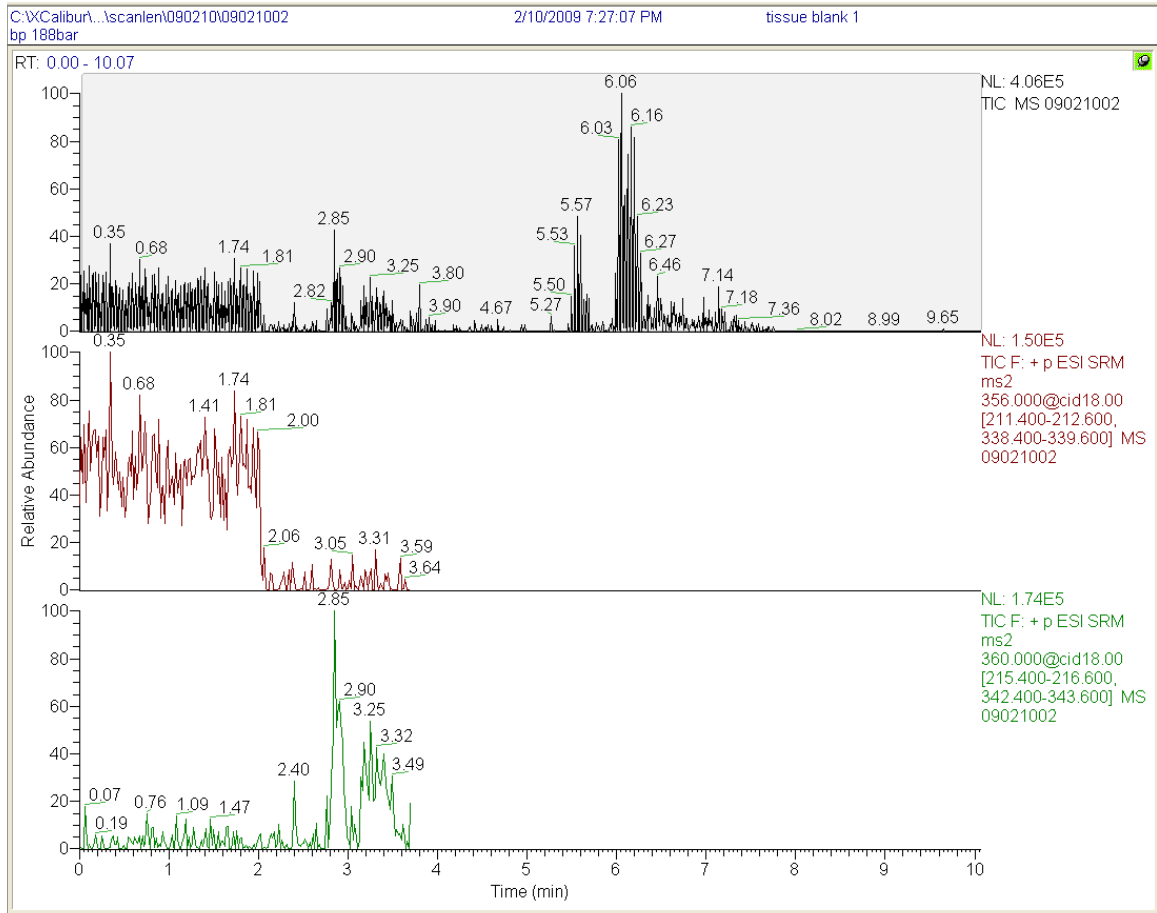
Sample Set I-A: Serum Sample 1
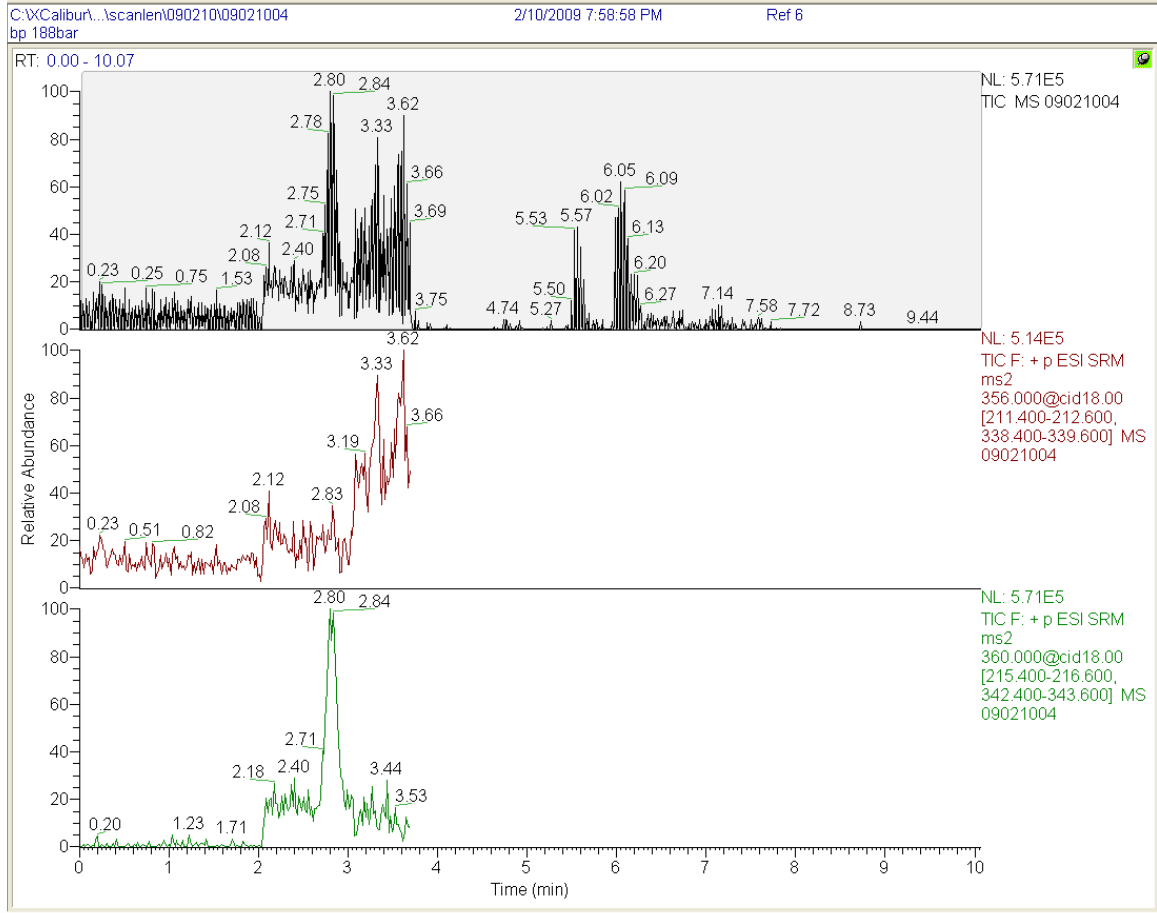
Sample Set I-A: Serum Sample 2
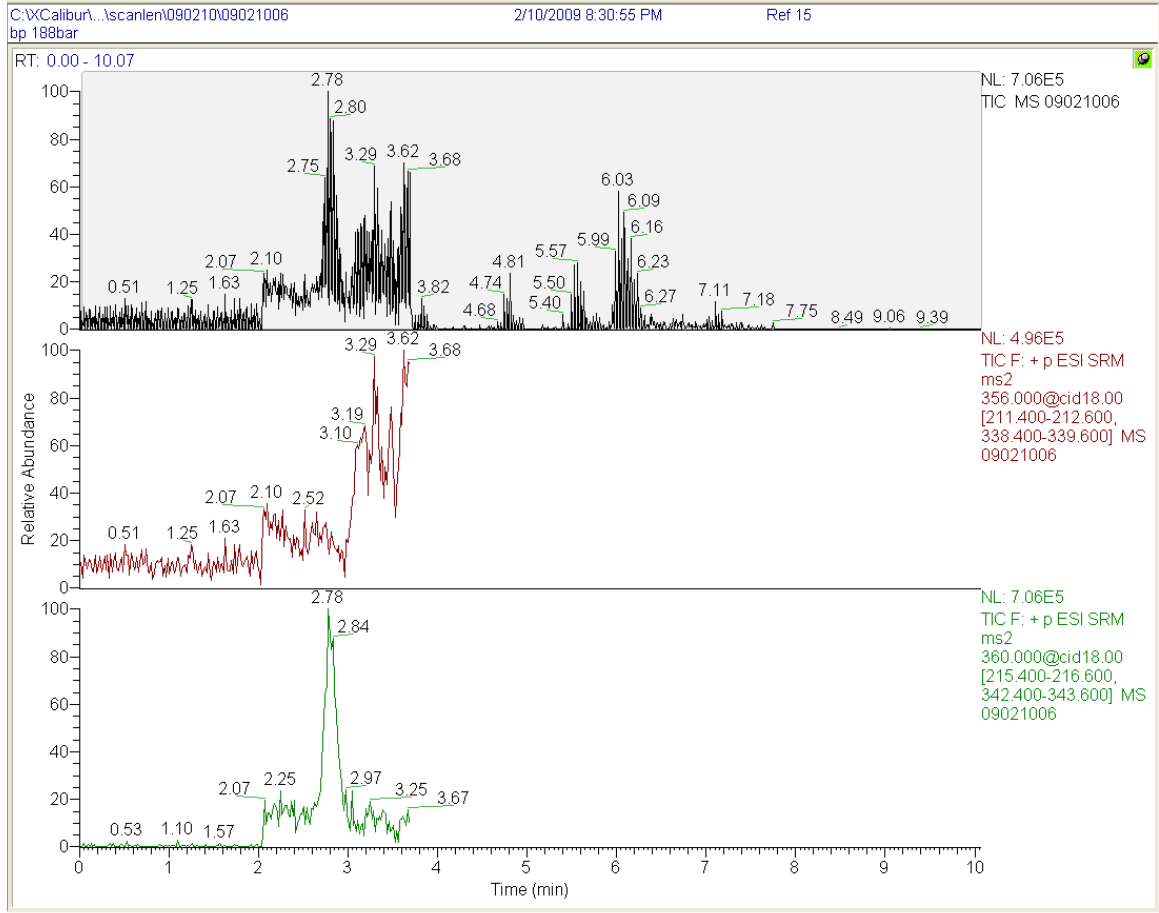
Sample Set I-A: Thyroid

Sample Set I-A: Fat

170
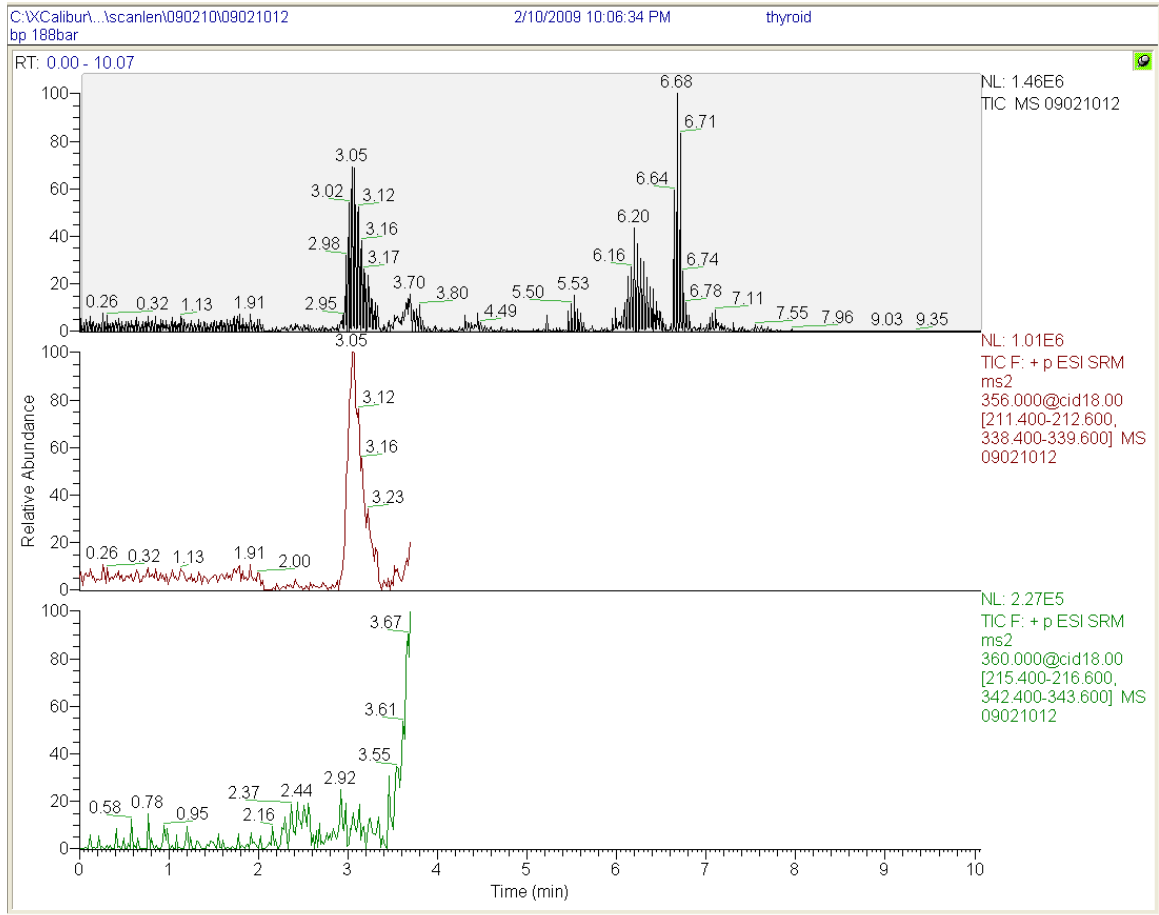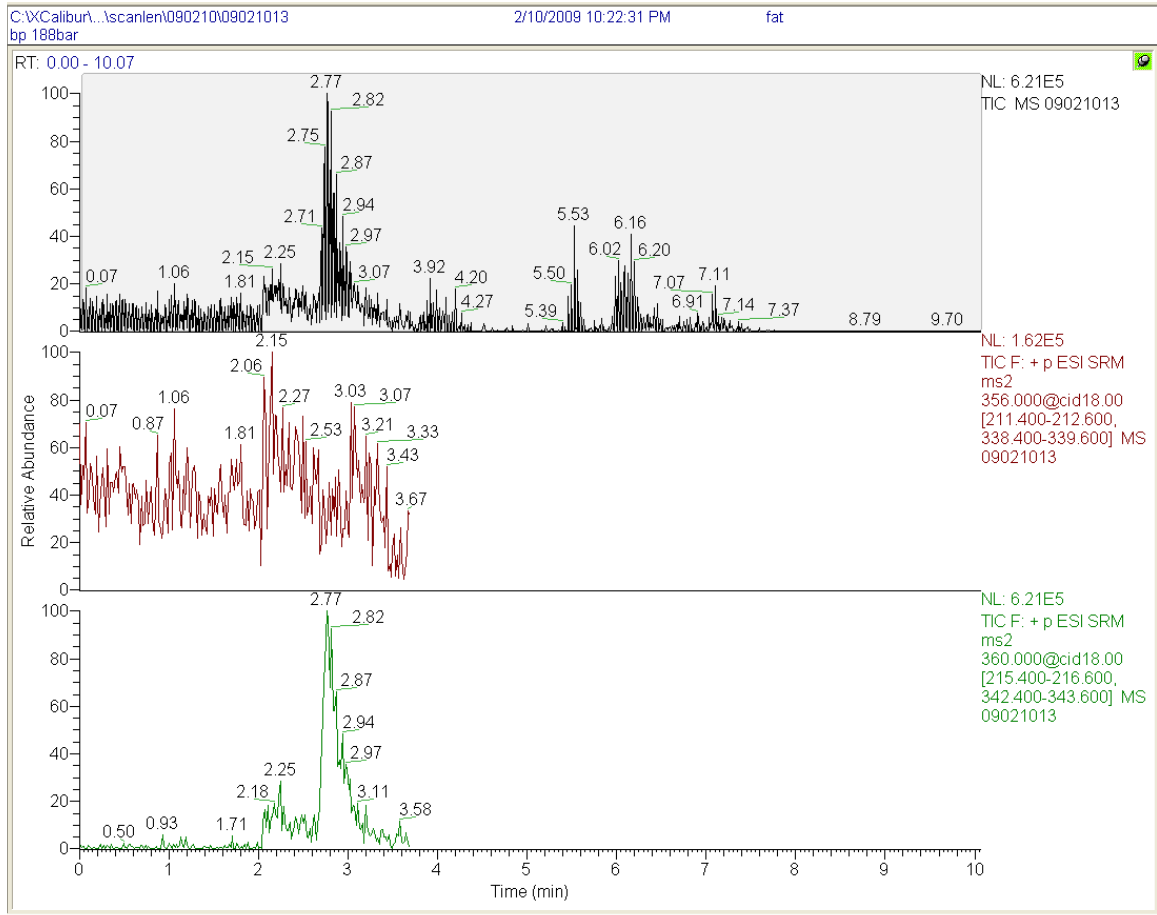
Sample Set III-A: Standards
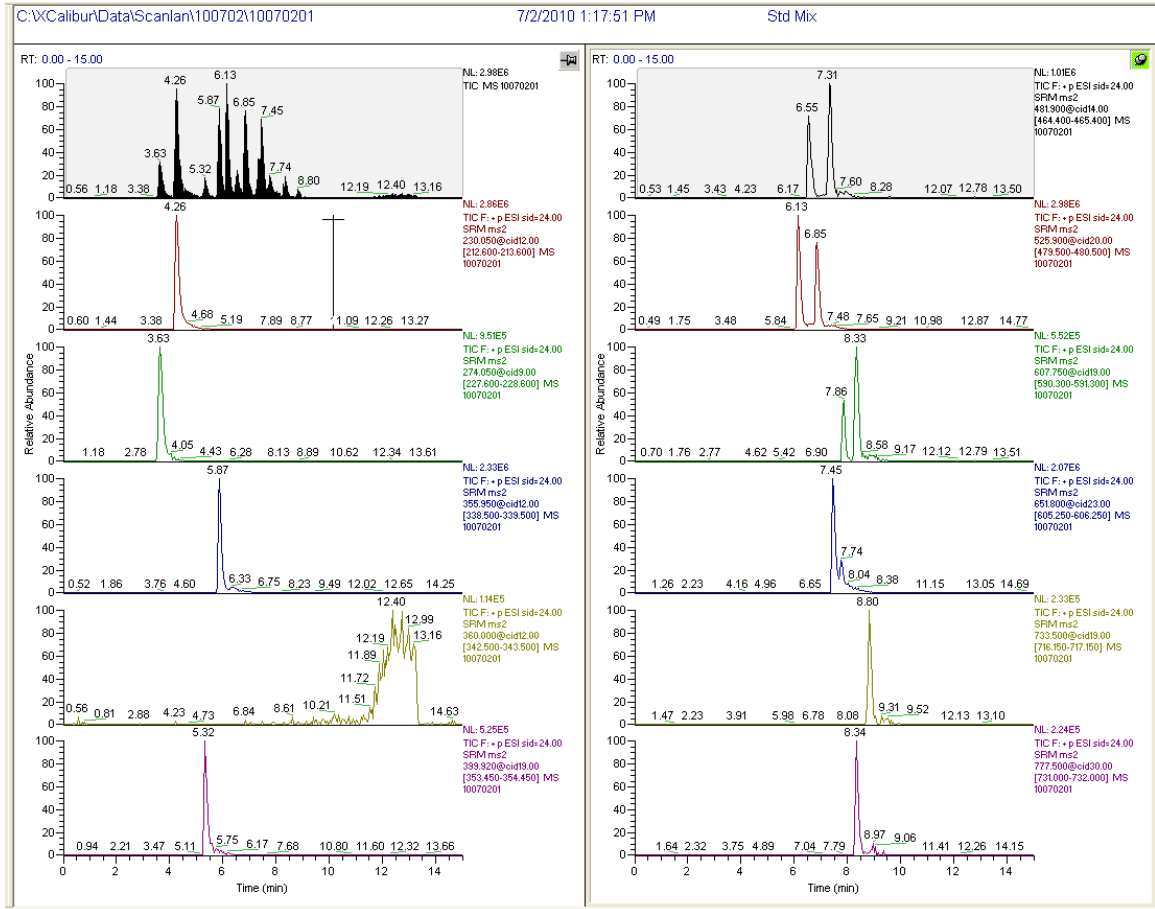
Sample Set III-A: Silica, MeOH/DCM, with standards

C:\XCalibur\Data\Scanlan\100702\10070203   7/2/2010 1:59:36 PM   1B
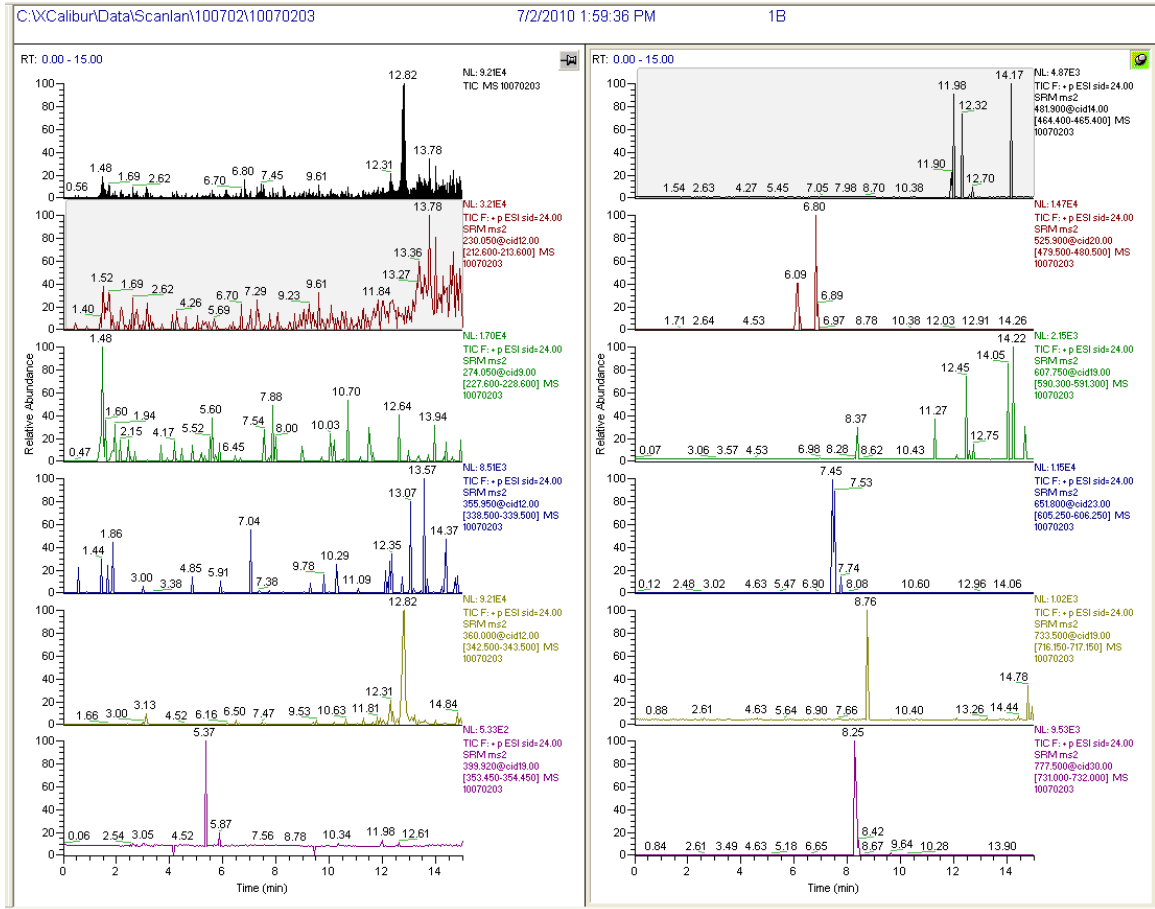
Sample Set III-A: Charcoal, EtOAc/DCM, without standards
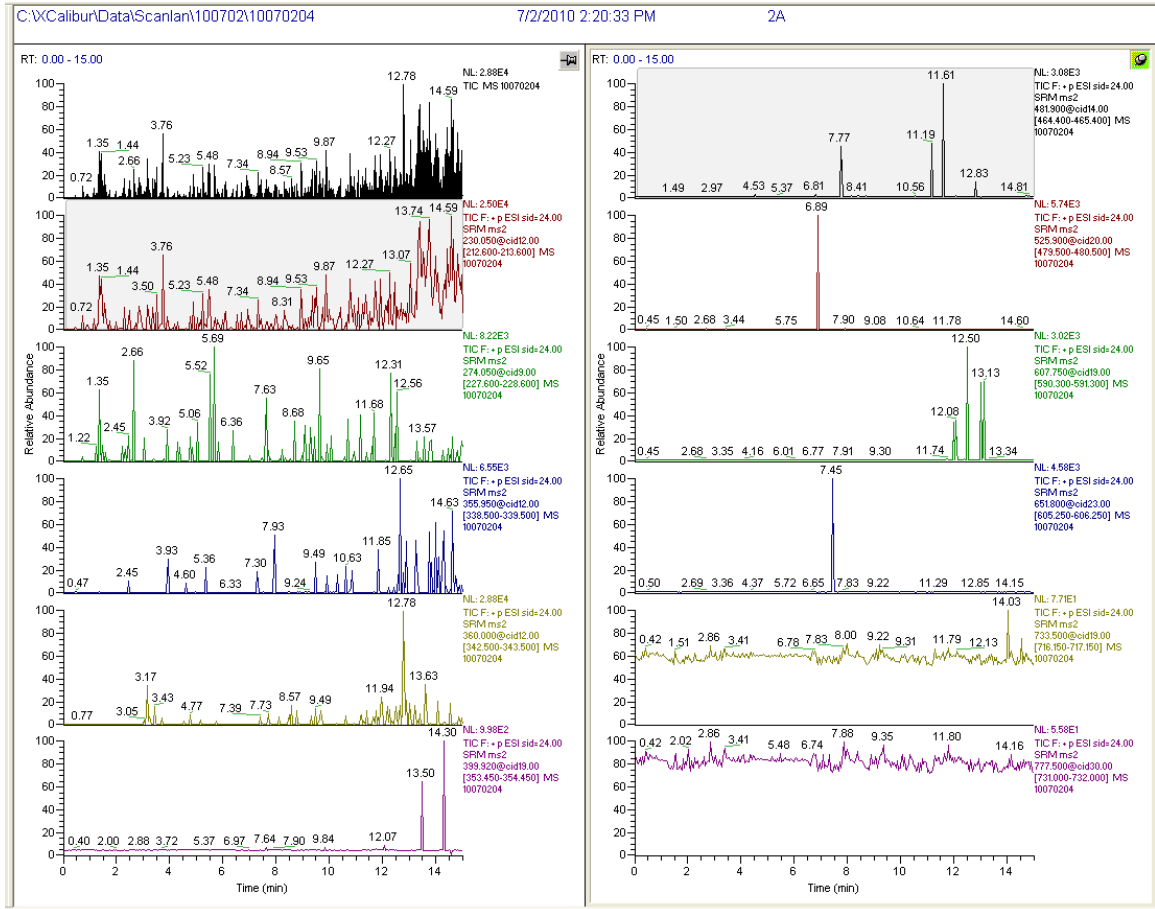
Sample Set III-A: Silica, MeOH/DCM, without standards
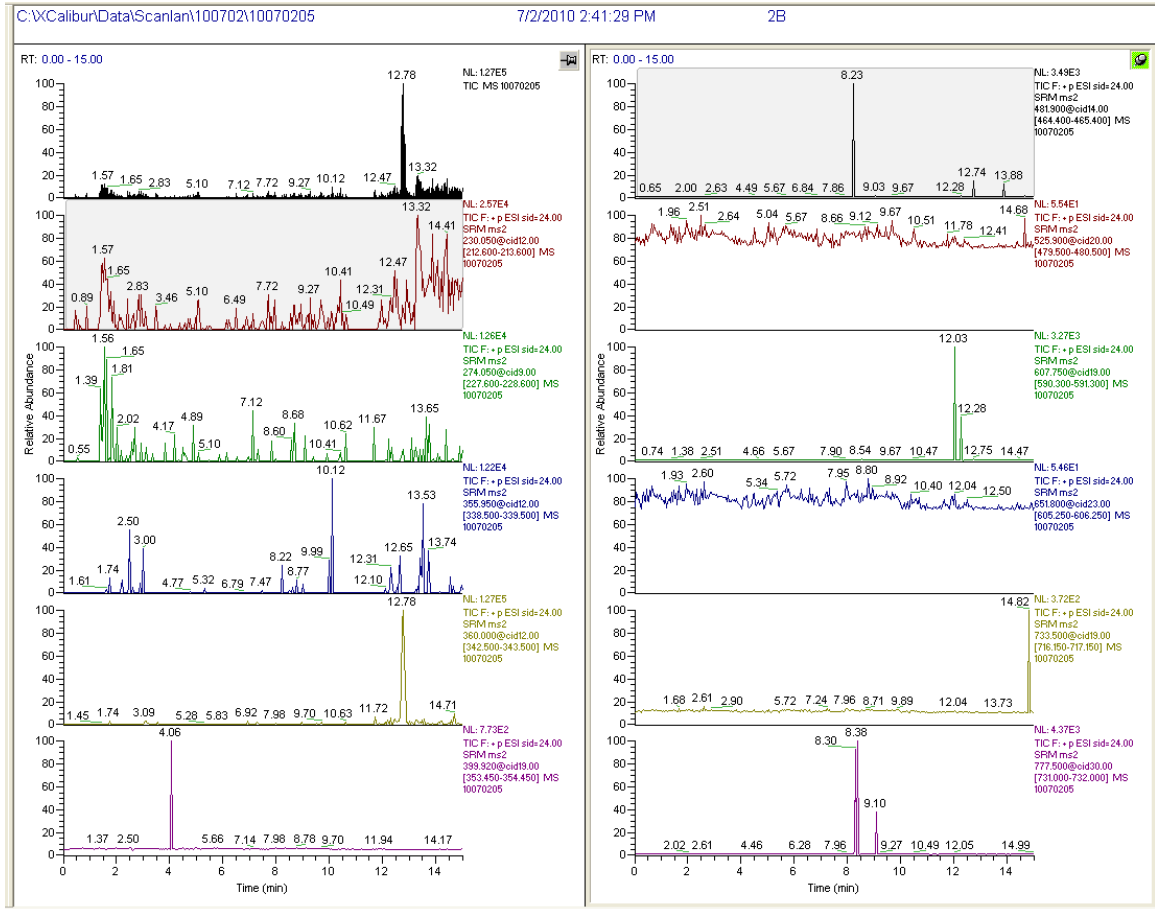
Sample Set III-A: Charcoal, Ether/DCM, with standards
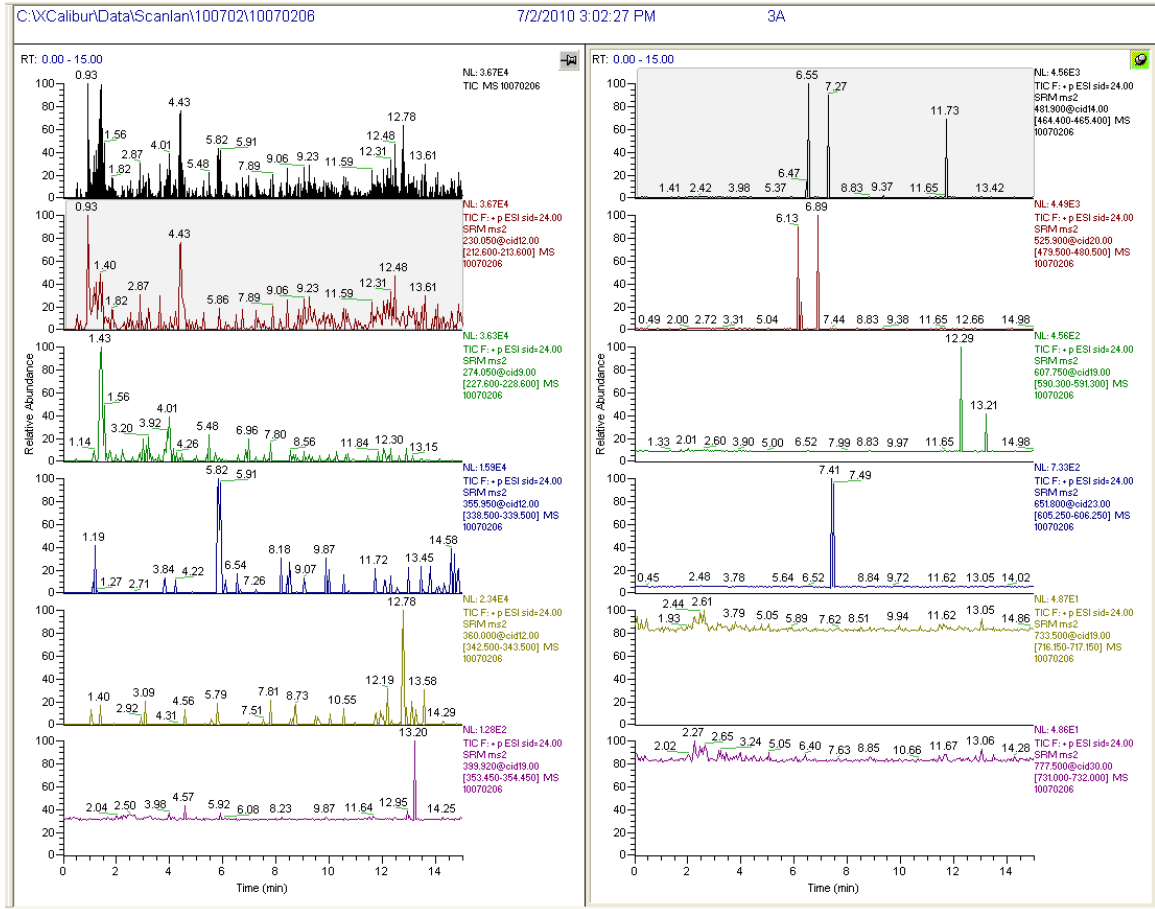
Sample Set III-A: Charcoal, Ether/DCM, without standards
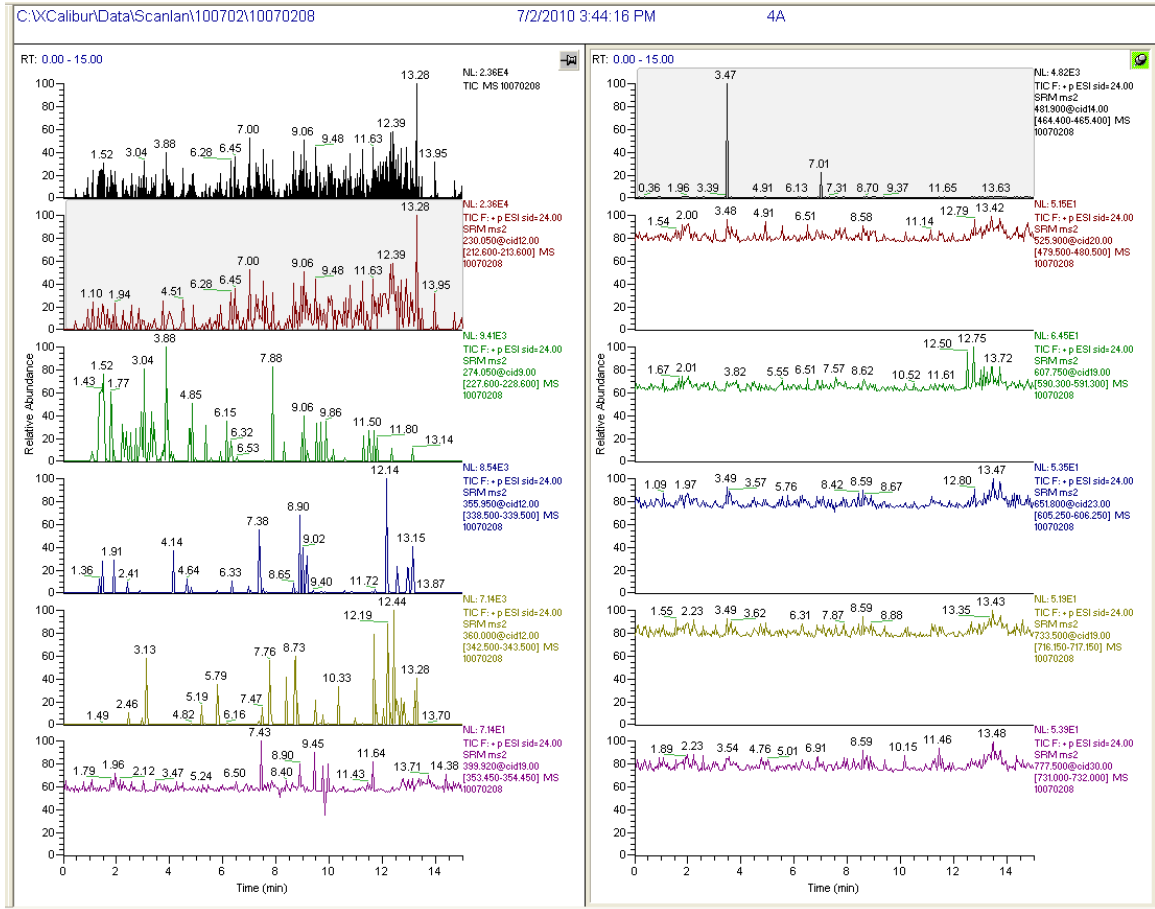
Sample Set III-A: Charcoal, EtOAc/DCM, pH 11, with standards
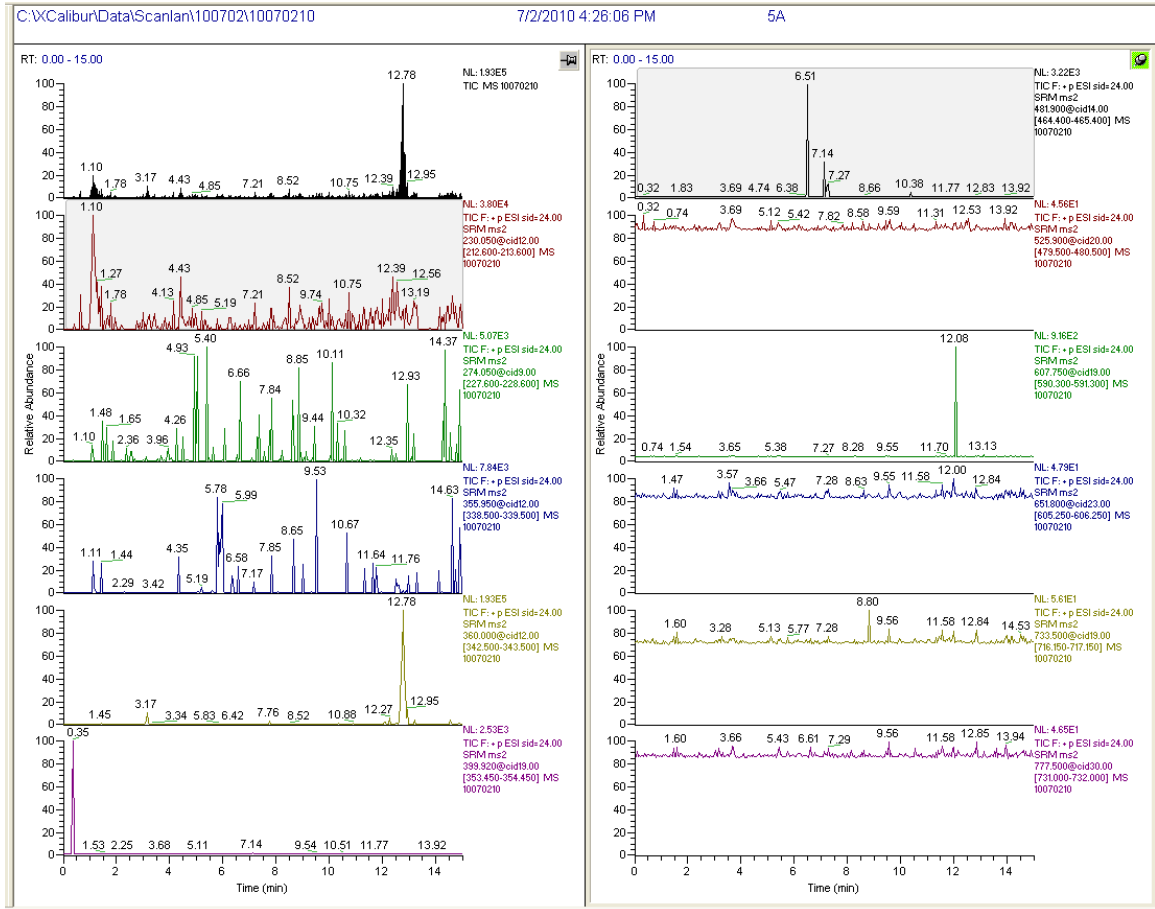
Sample Set III-A: Silica, MeOH/DCM, pH 11, with standards
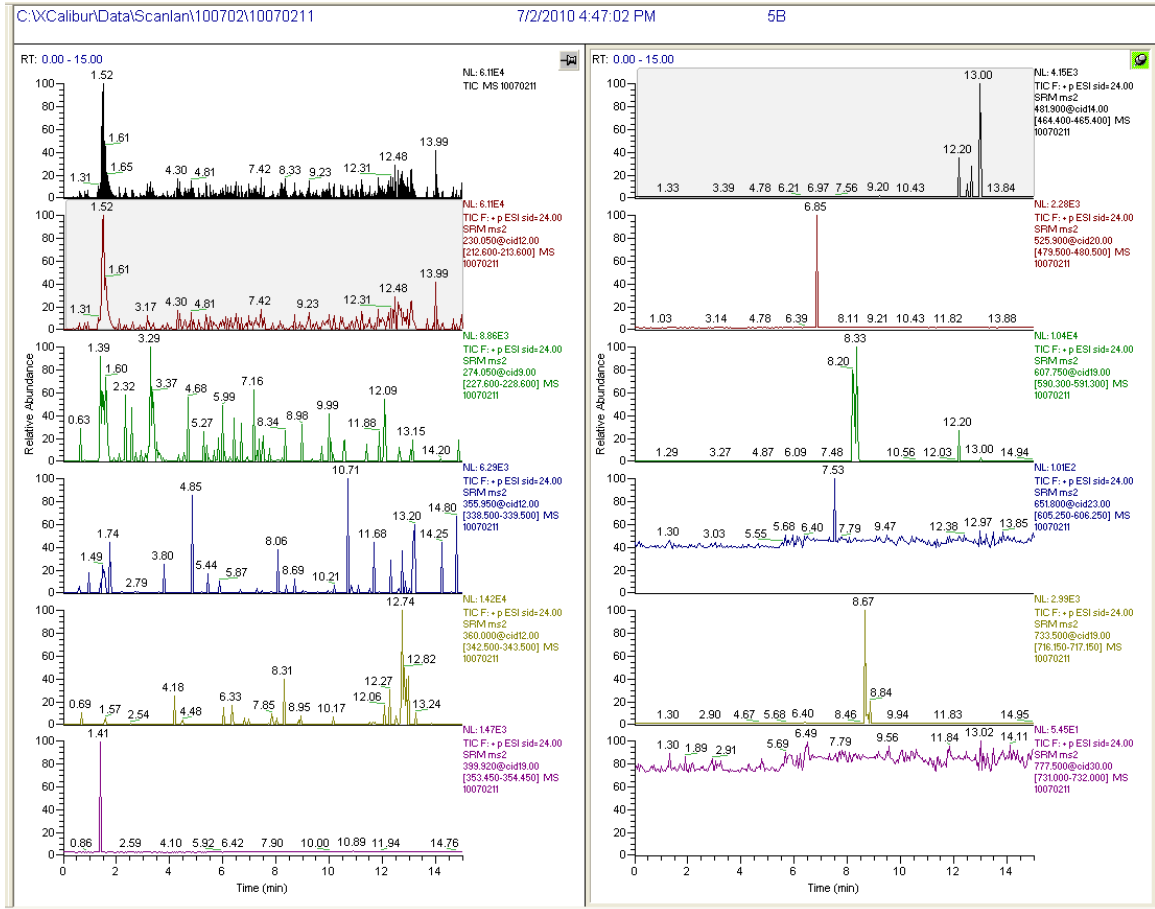
Sample Set III-A: Charcoal, EtOAc/DCM, pH 11, without standards
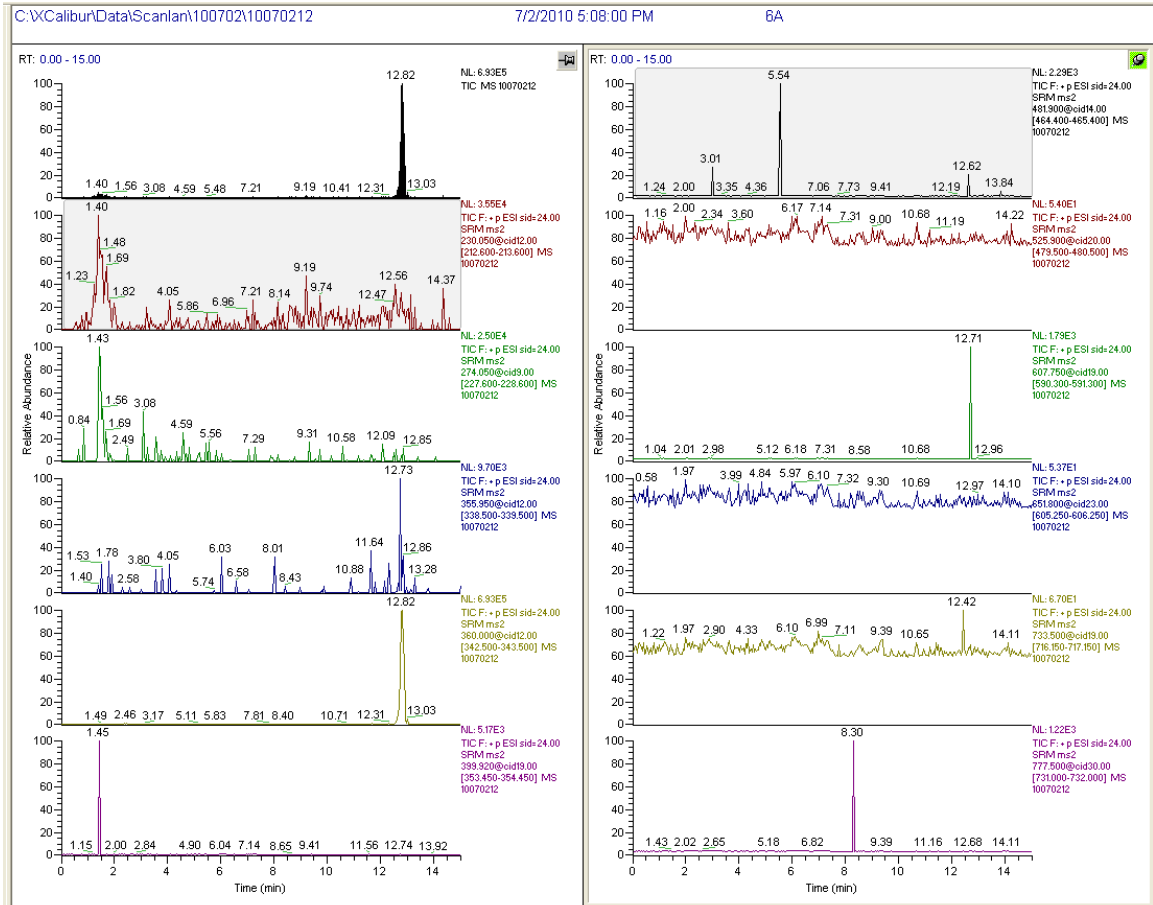
Sample Set III-A: Silica, MeOH/DCM, pH 11, without standards
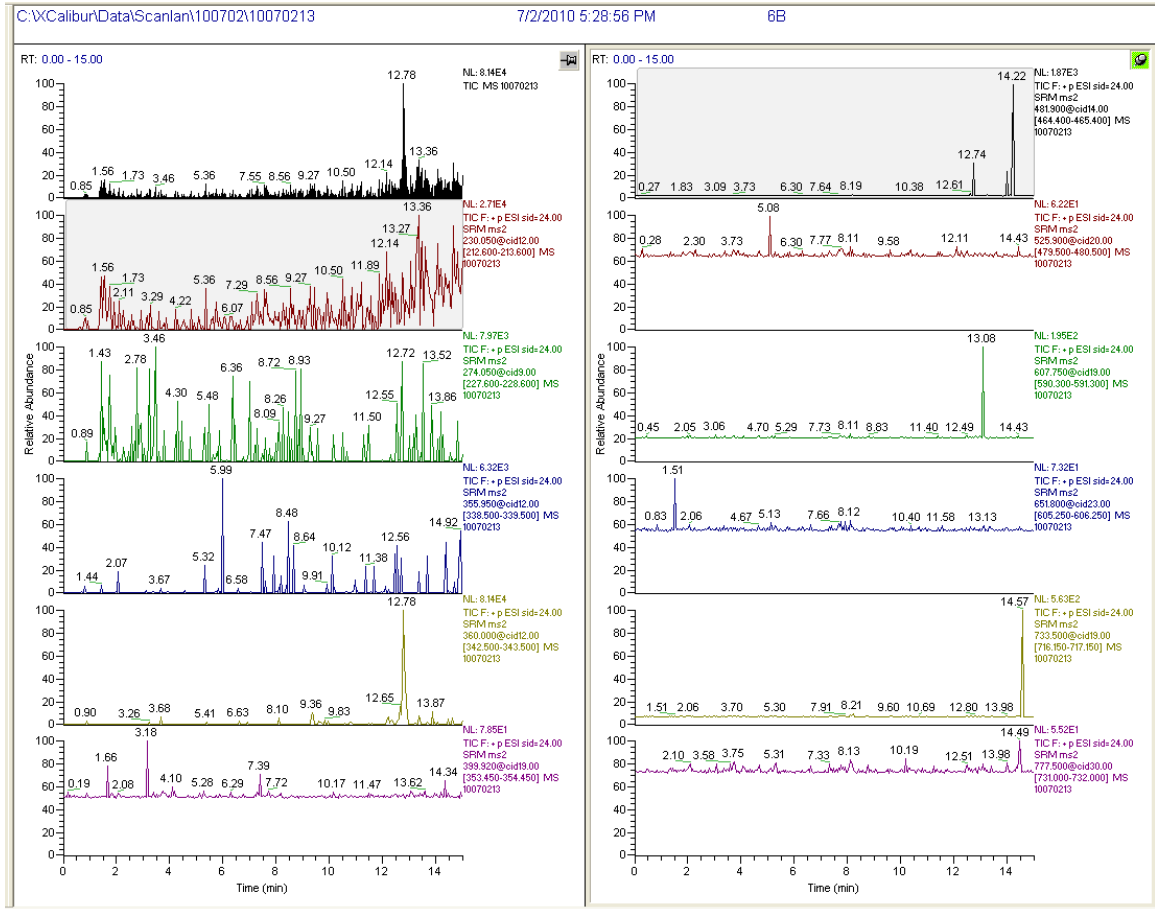
Sample Set III-A: Charcoal, Ether/DCM, pH 11, with standards
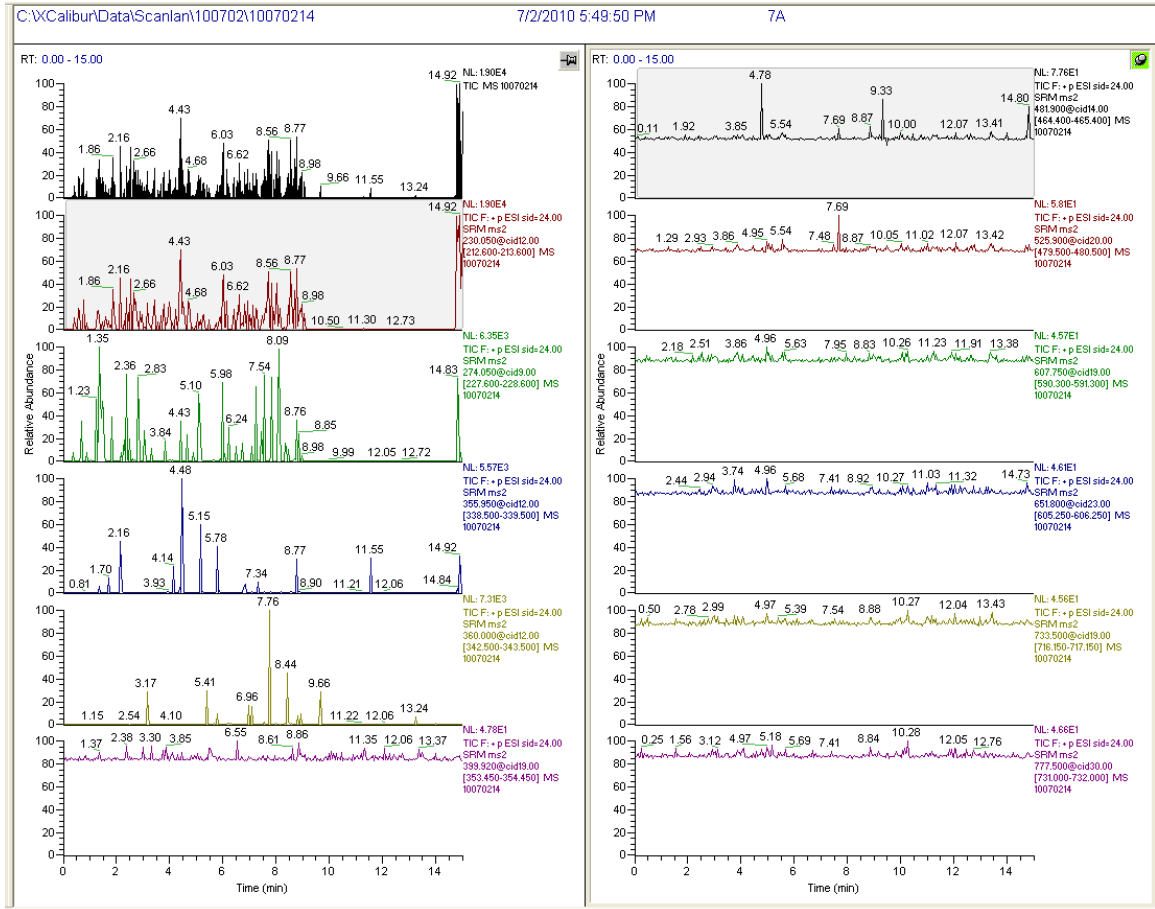
Sample Set III-A: Charcoal, Ether/DCM, pH 11, without standards

C:\XCalibur\Data\Scanlan\100702\10070216   7/2/2010 6:31:37 PM   8A
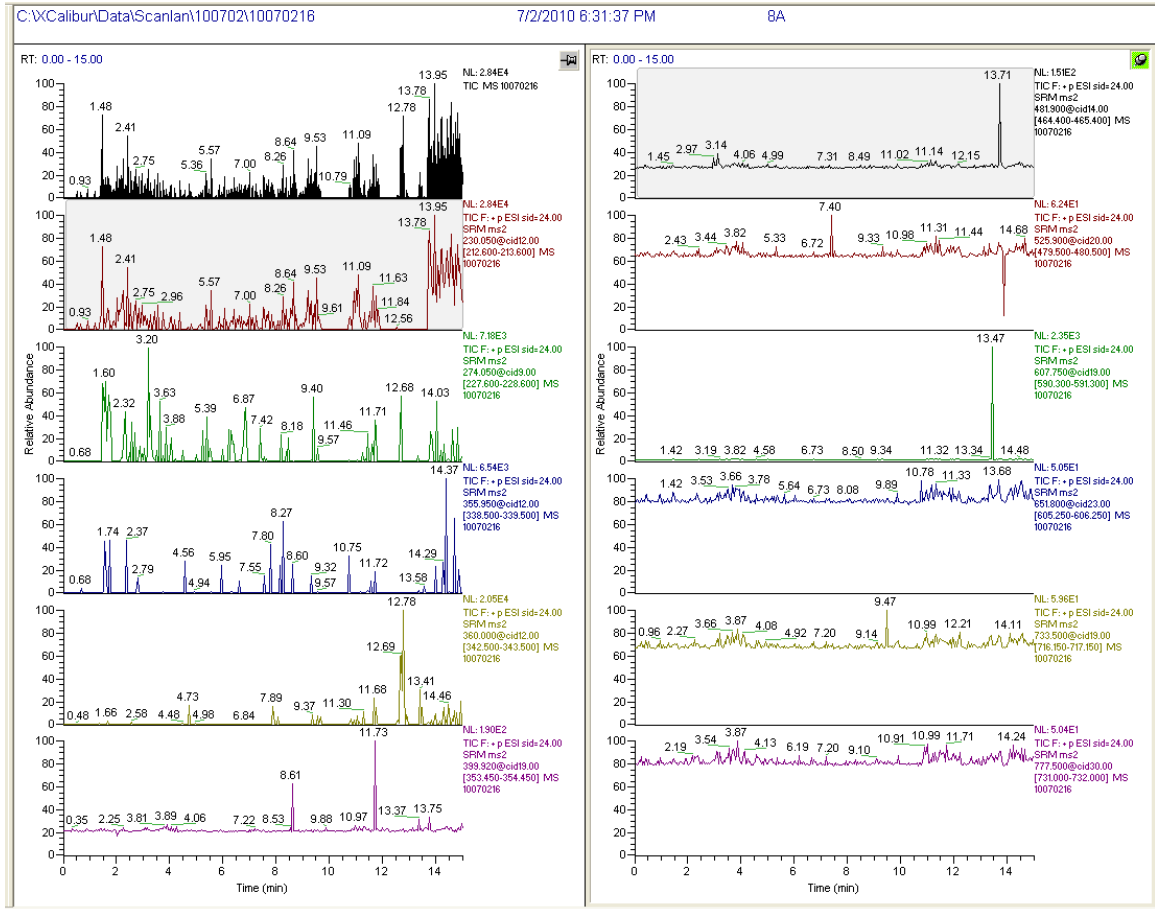
Sample Set III-B: Charcoal, EtOAc/DCM, 60 °C, with standards
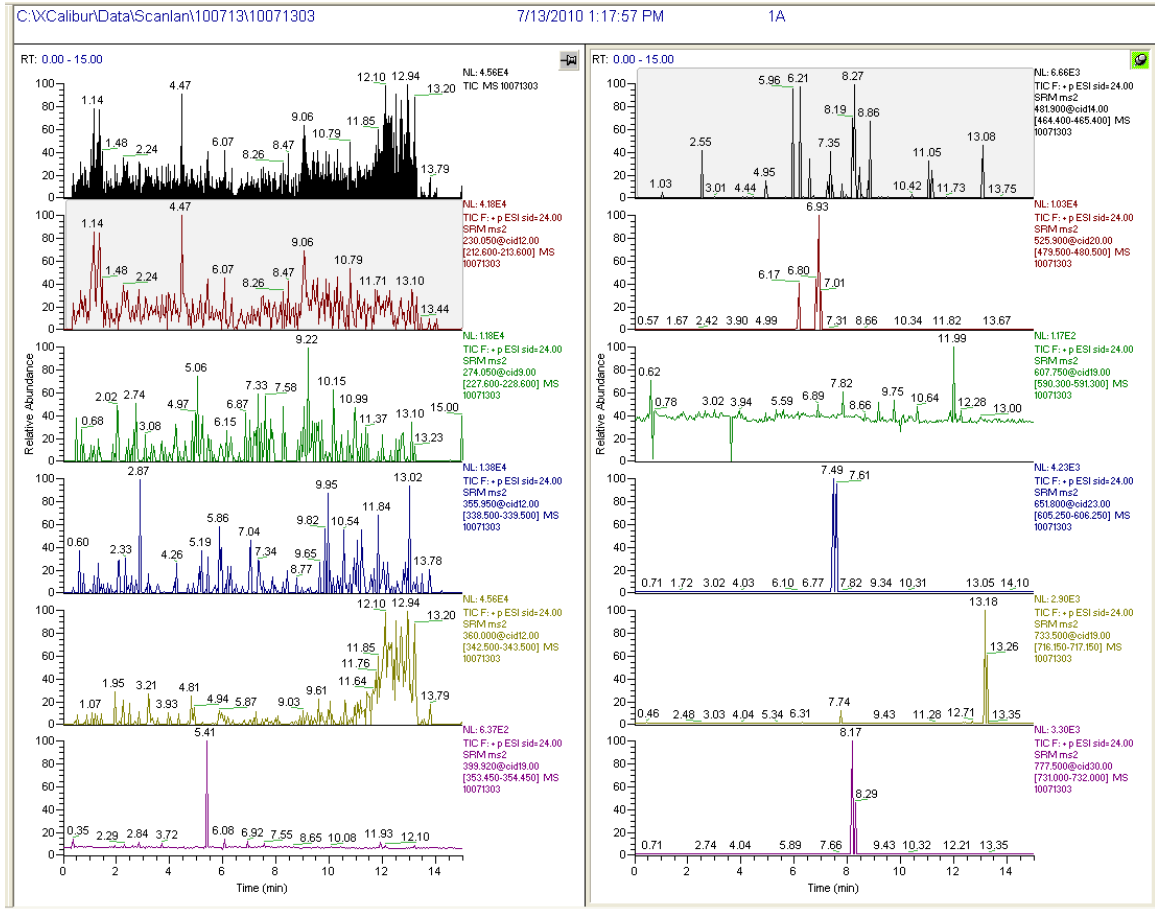
Sample Set III-B: Silica, MeOH/DCM/NH₄OH, with standards
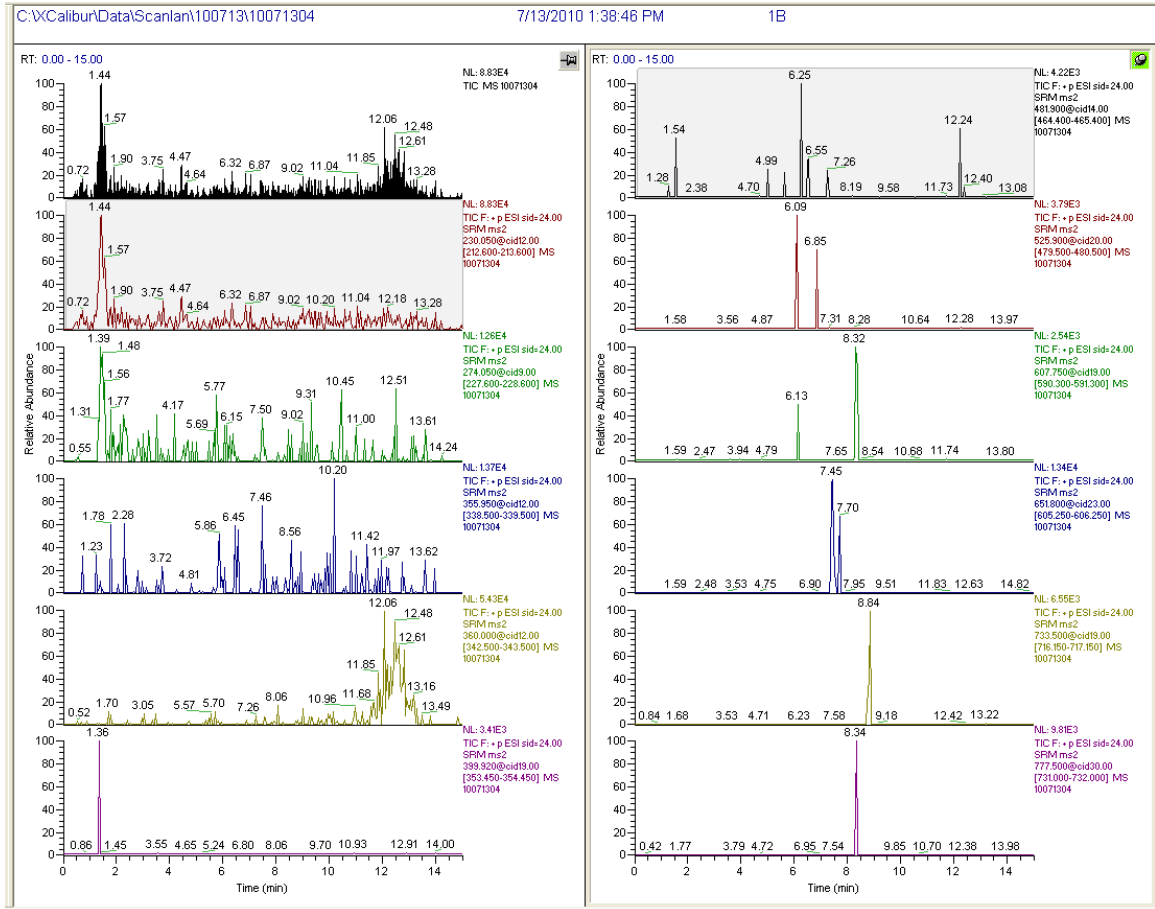
Sample Set III-B: Charcoal, EtOAc/DCM, 60 °C, without standards
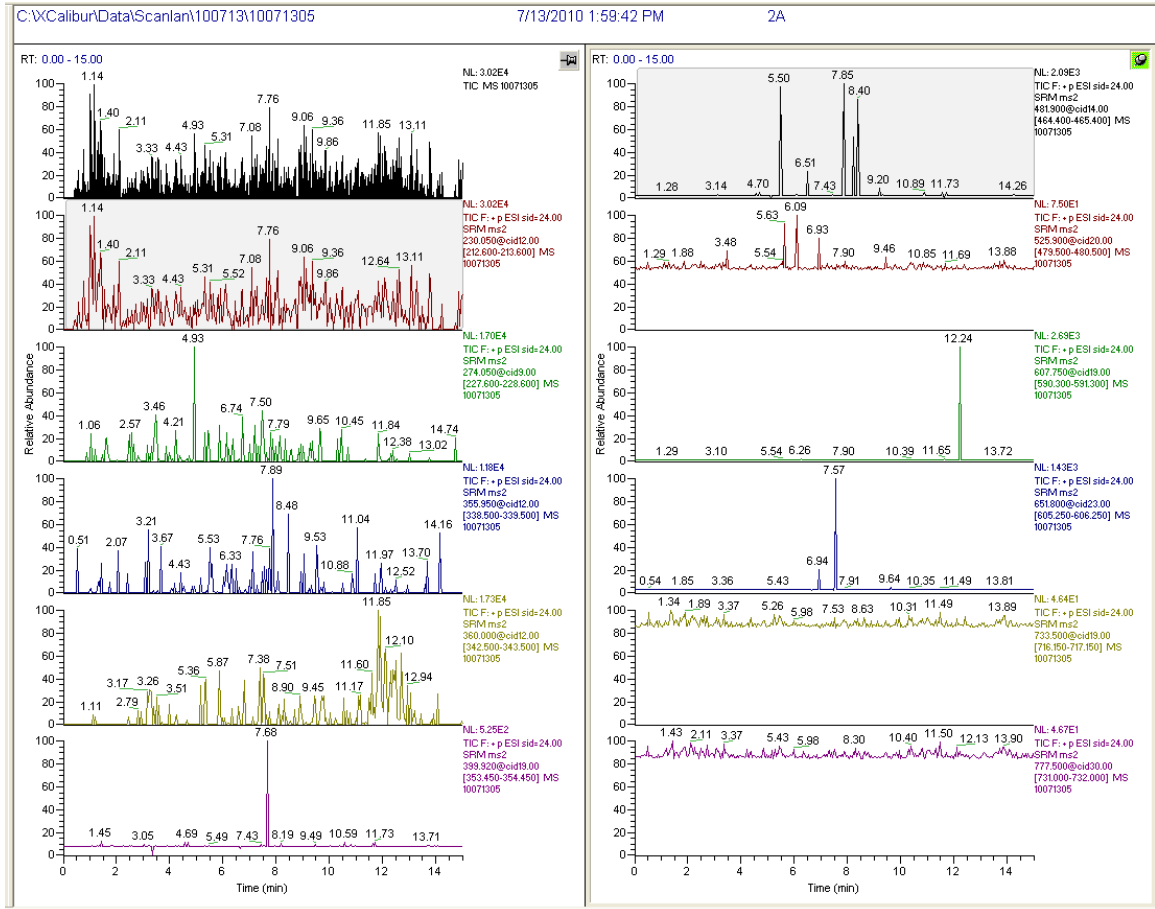
Sample Set III-B: Silica, MeOH/DCM/NH₄OH, without standards
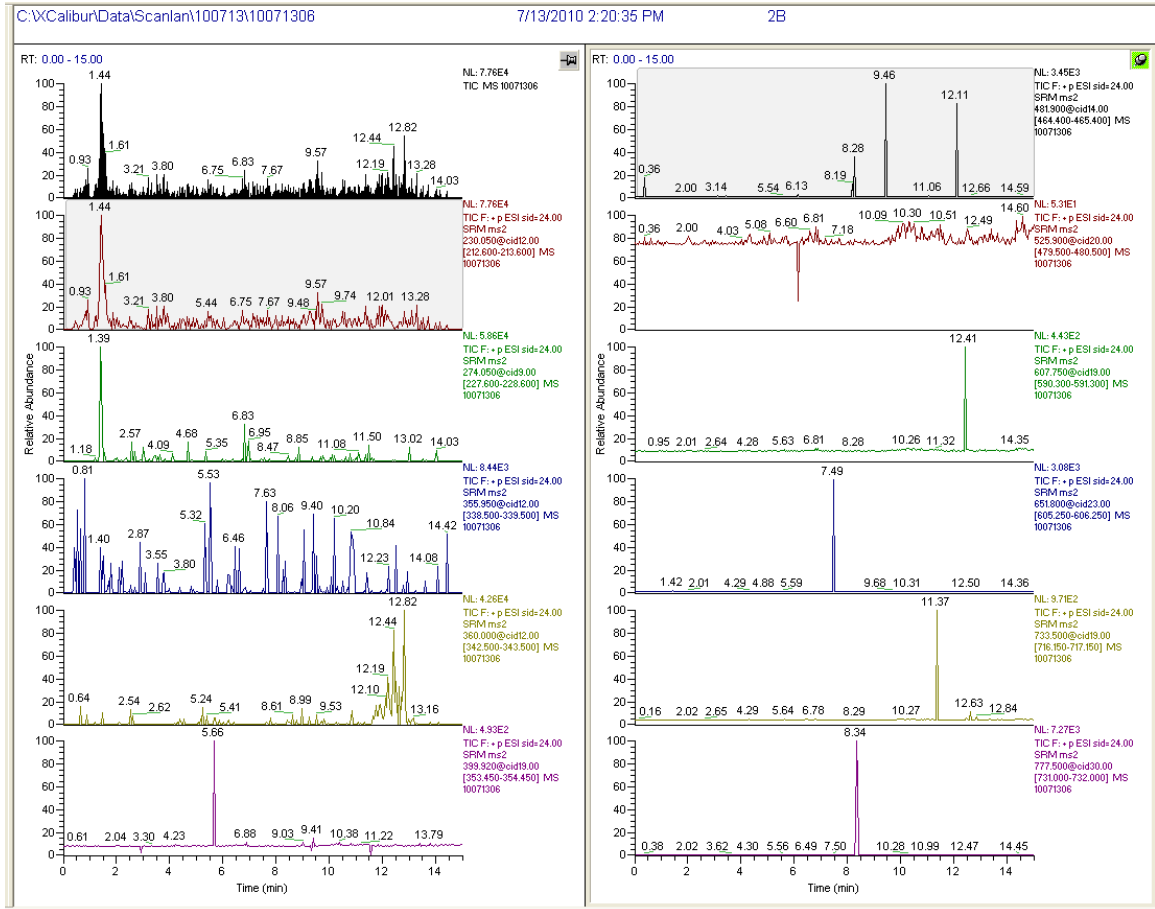
Sample Set III-B: Charcoal, MeOH/DCM, 60 °C, with standards
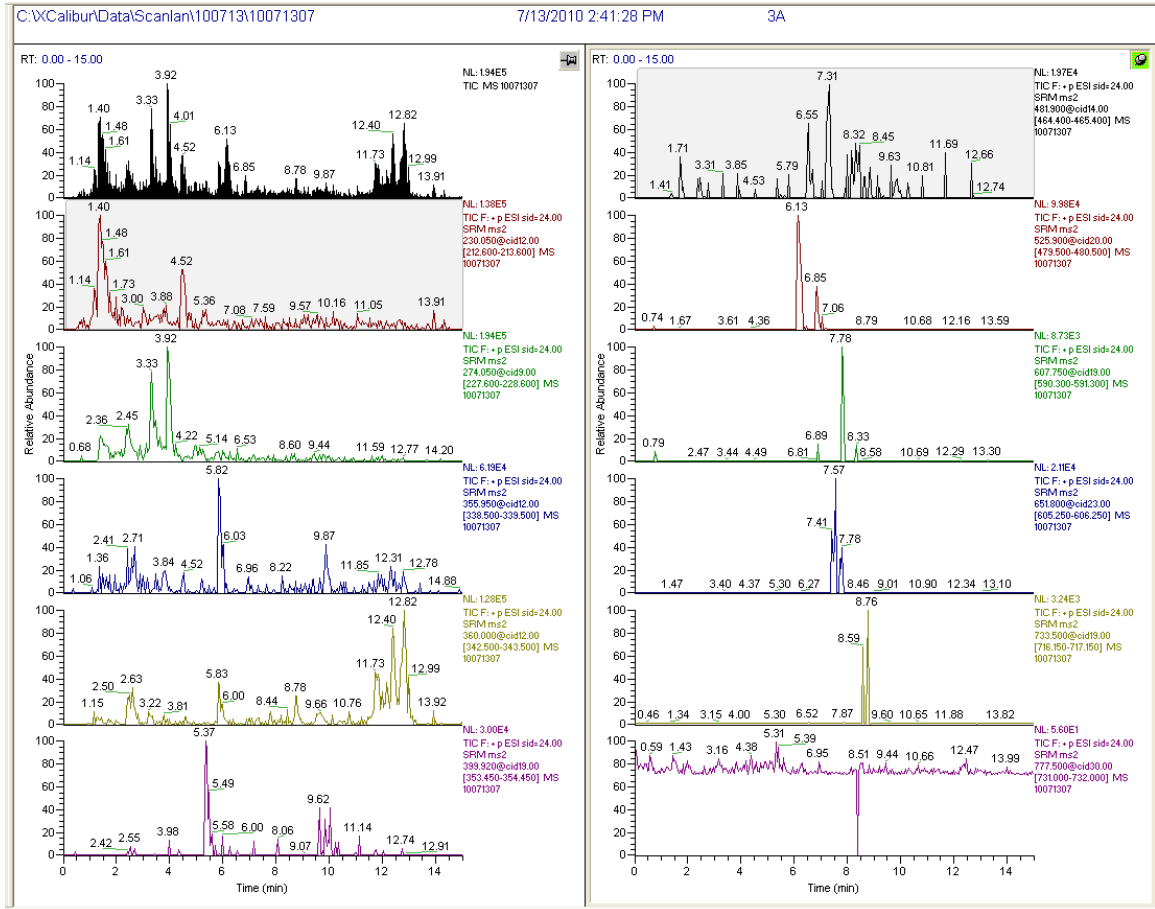
Sample Set III-B: Charcoal, MeOH/DCM, 60 °C, without standards
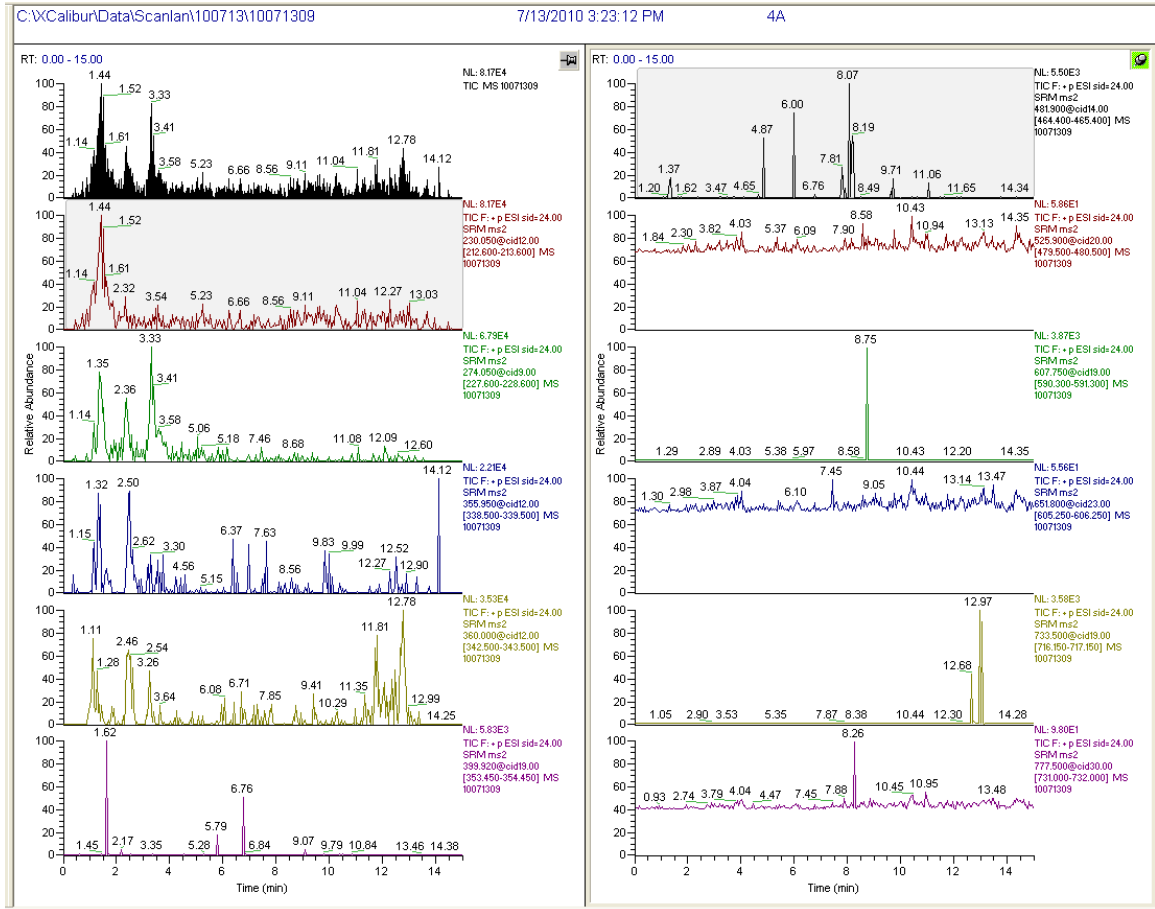
Sample Set III-B: Charcoal, EtOAc/DCM/HCl, 60 °C, with standards

189
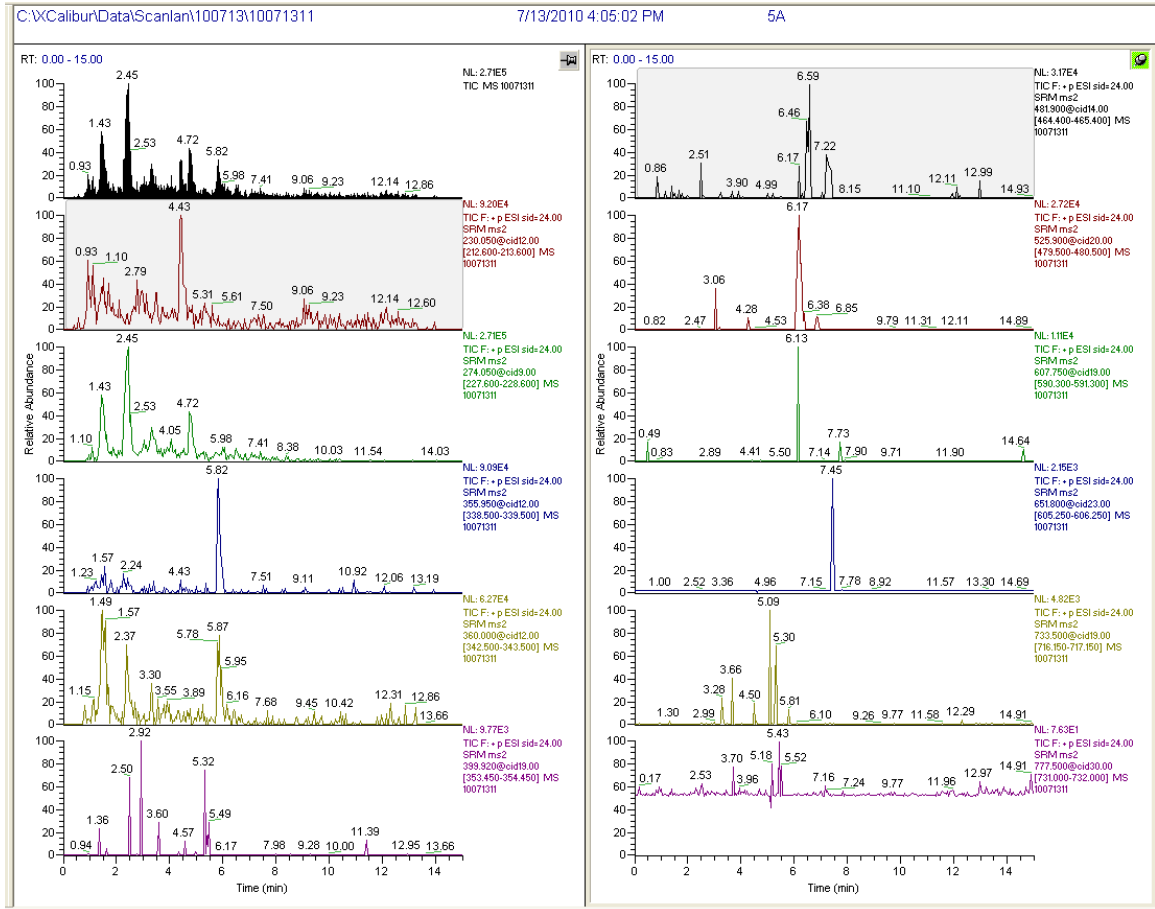
Sample Set III-B: Charcoal, EtOAc/DCM/HCl, 60 °C, without standards
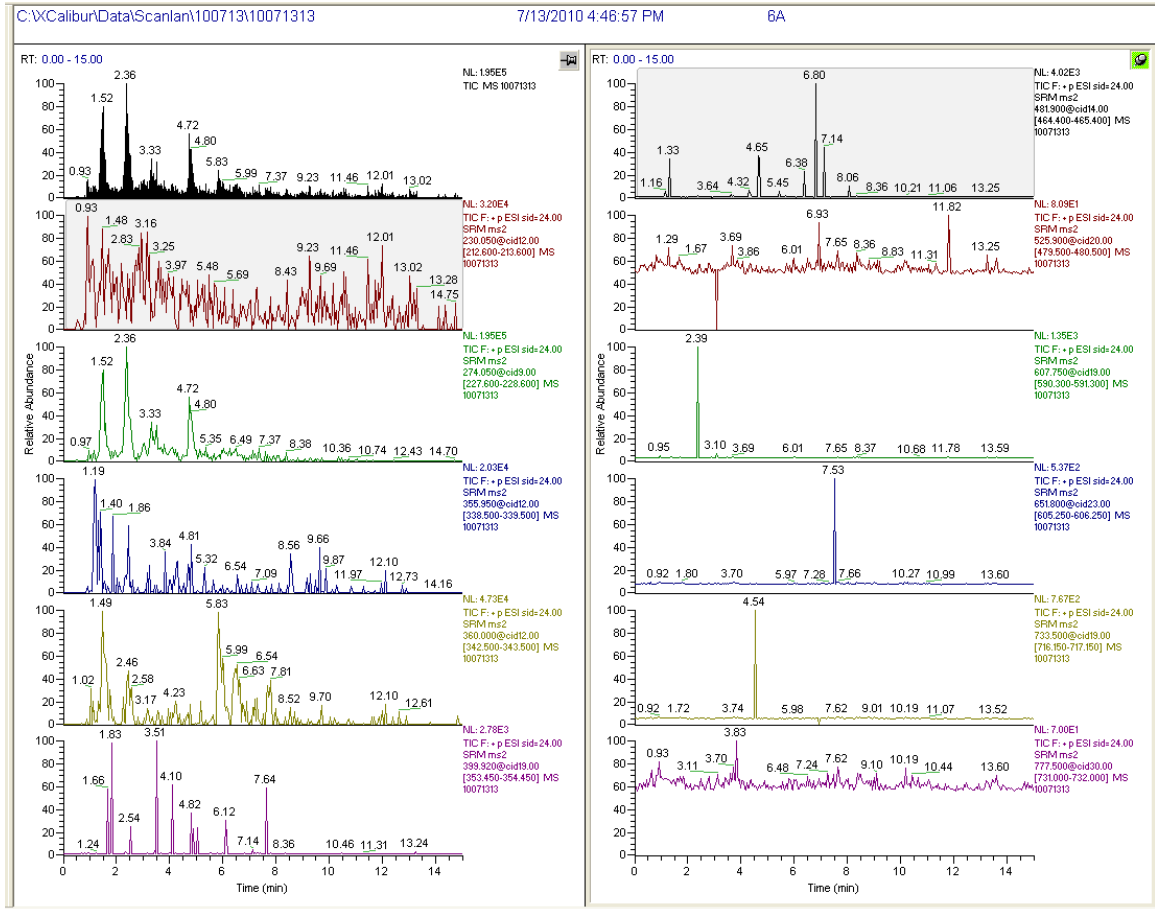
Sample Set III-B: Charcoal, MeOH/DCM, RT, with standards
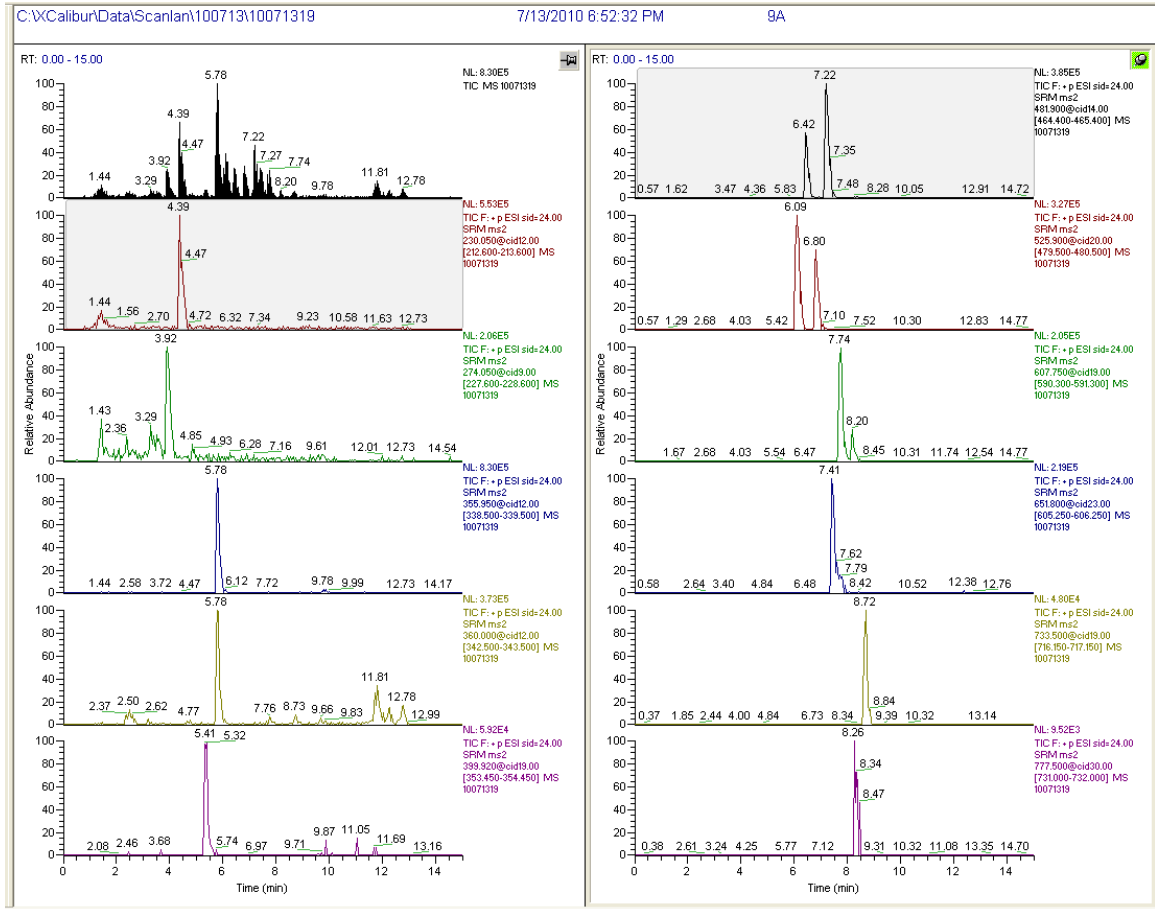
Sample Set III-B: Charcoal, MeOH/DCM, RT, without standards
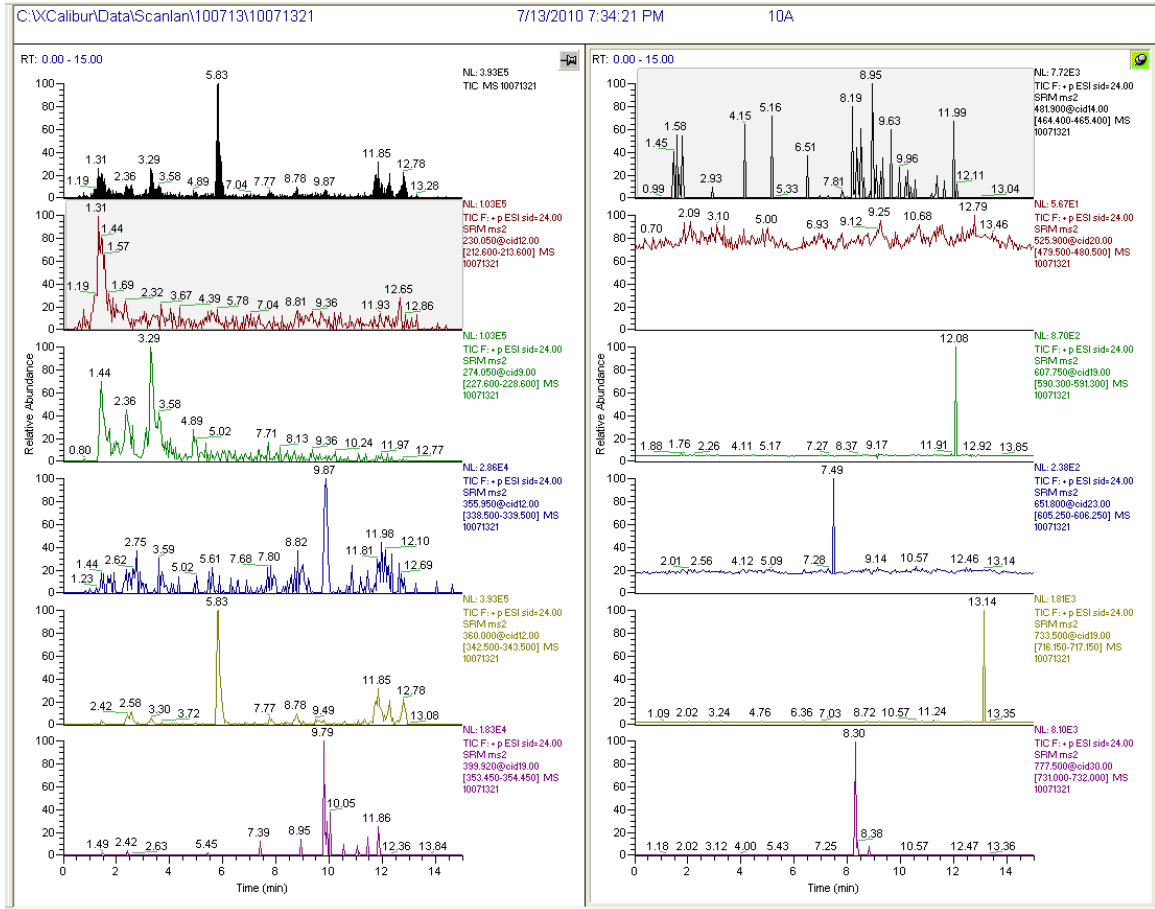
Sample Set III-C: Proteinase K, charcoal
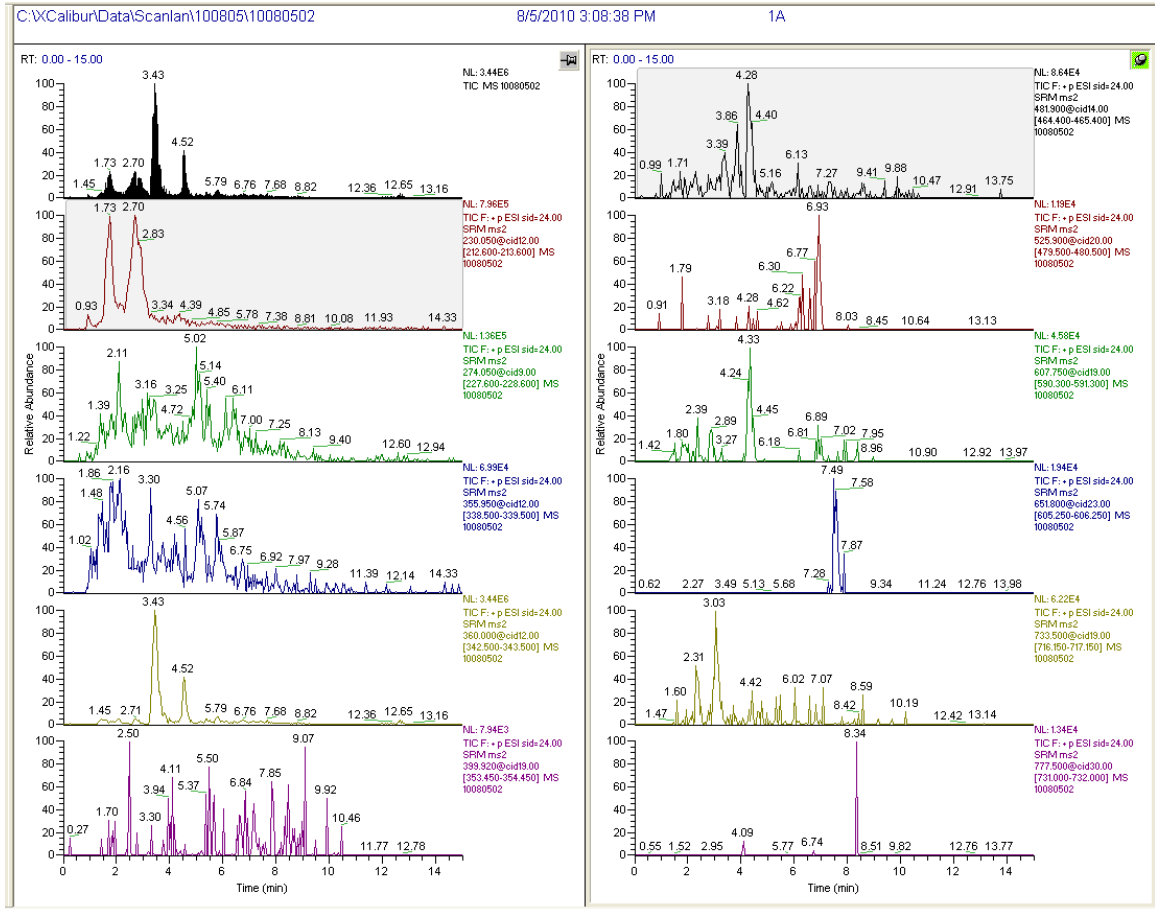
Sample Set III-C: Proteinase K, silica
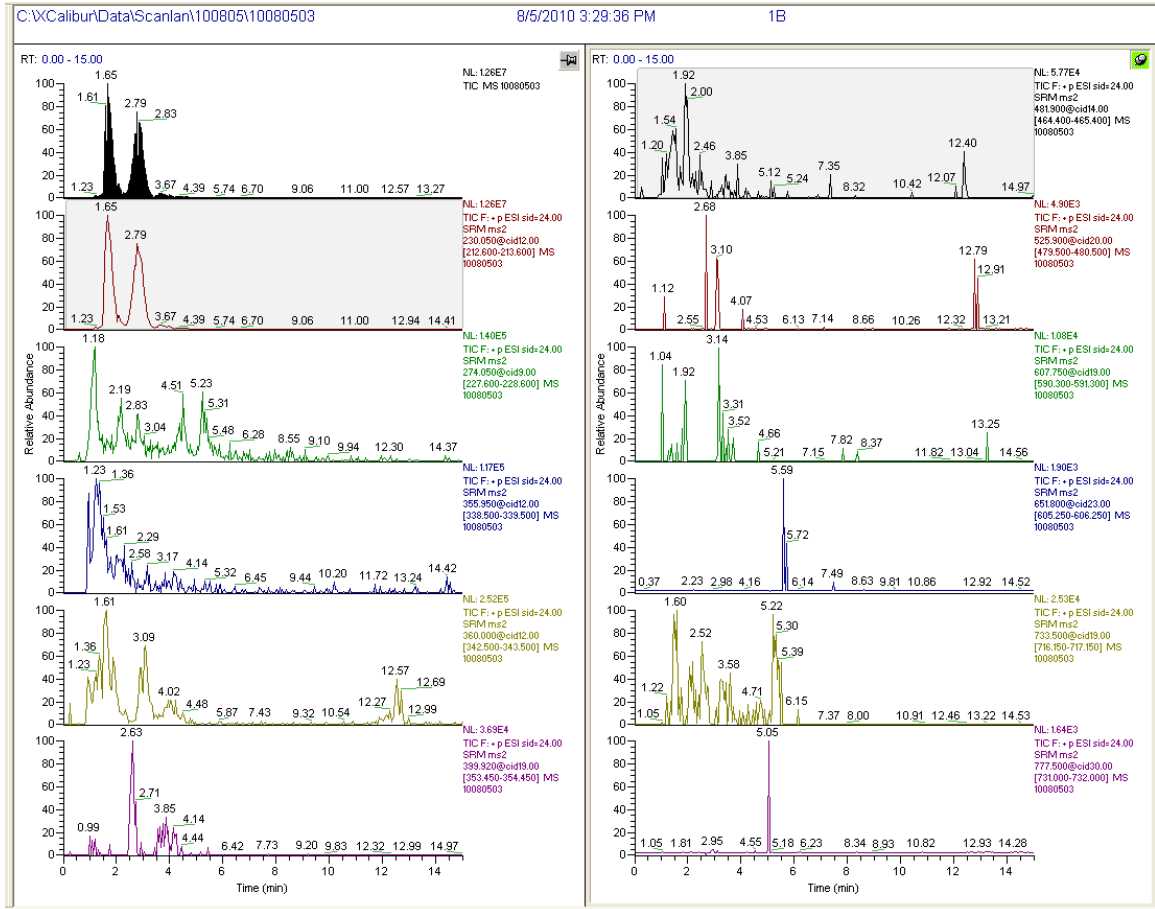
Sample Set III-C: Lipoprotein lipase, charcoal
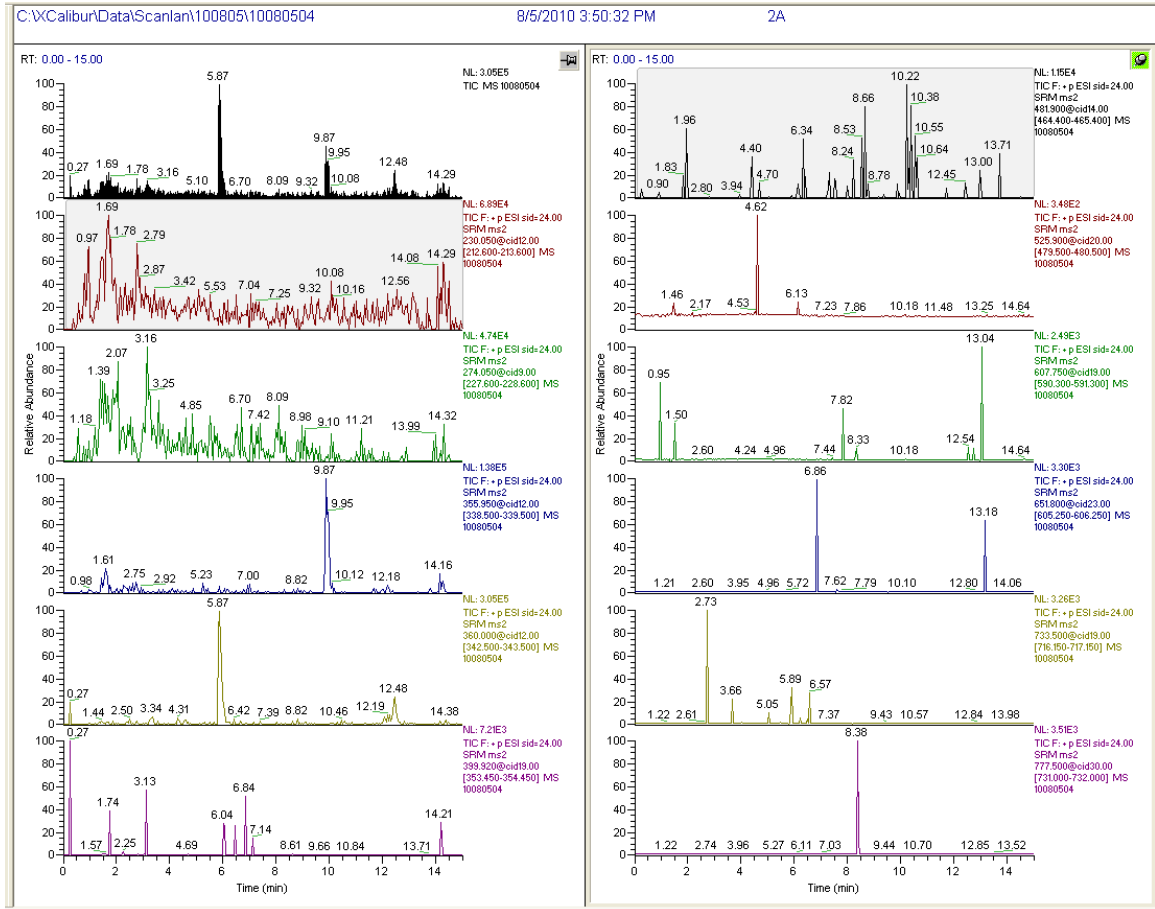
Sample Set III-C: Lipoprotein lipase, silica
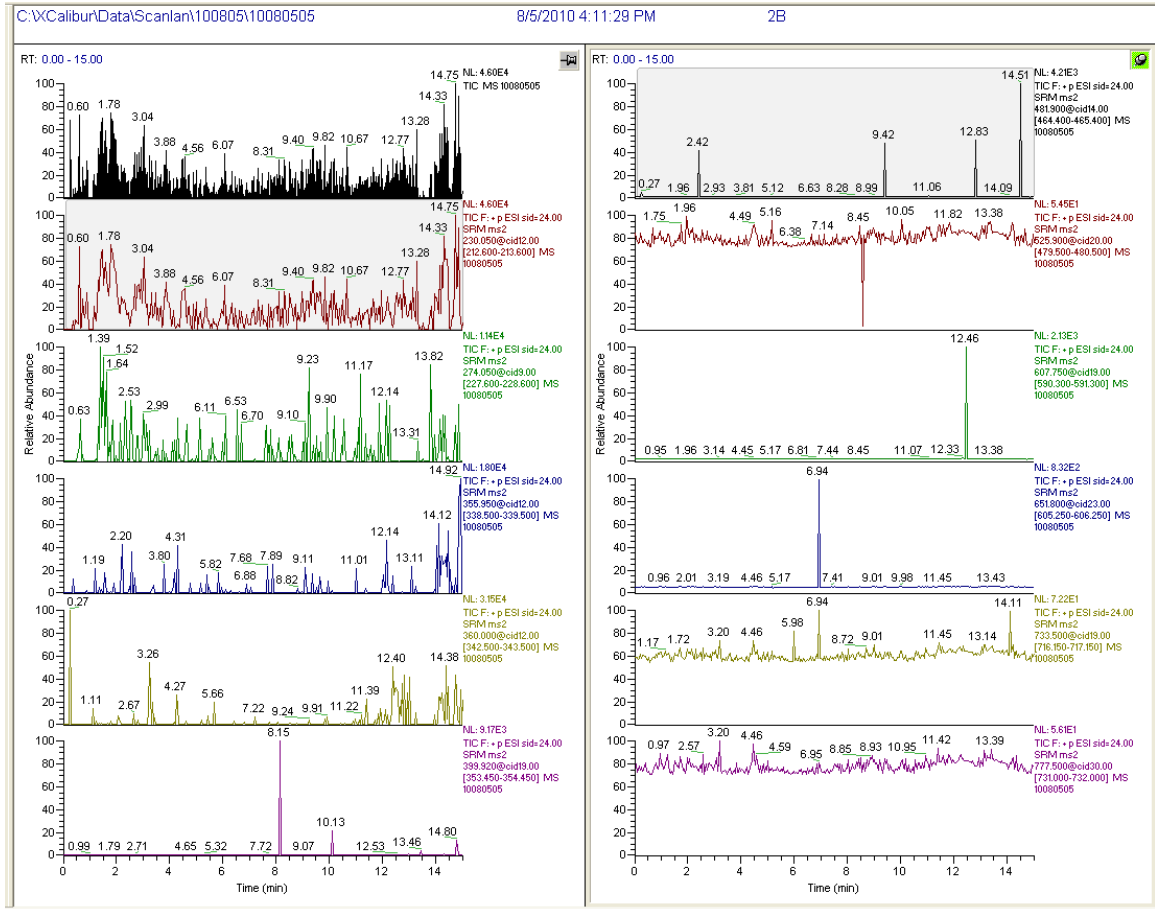
Sample Set III-C: Urea, silica
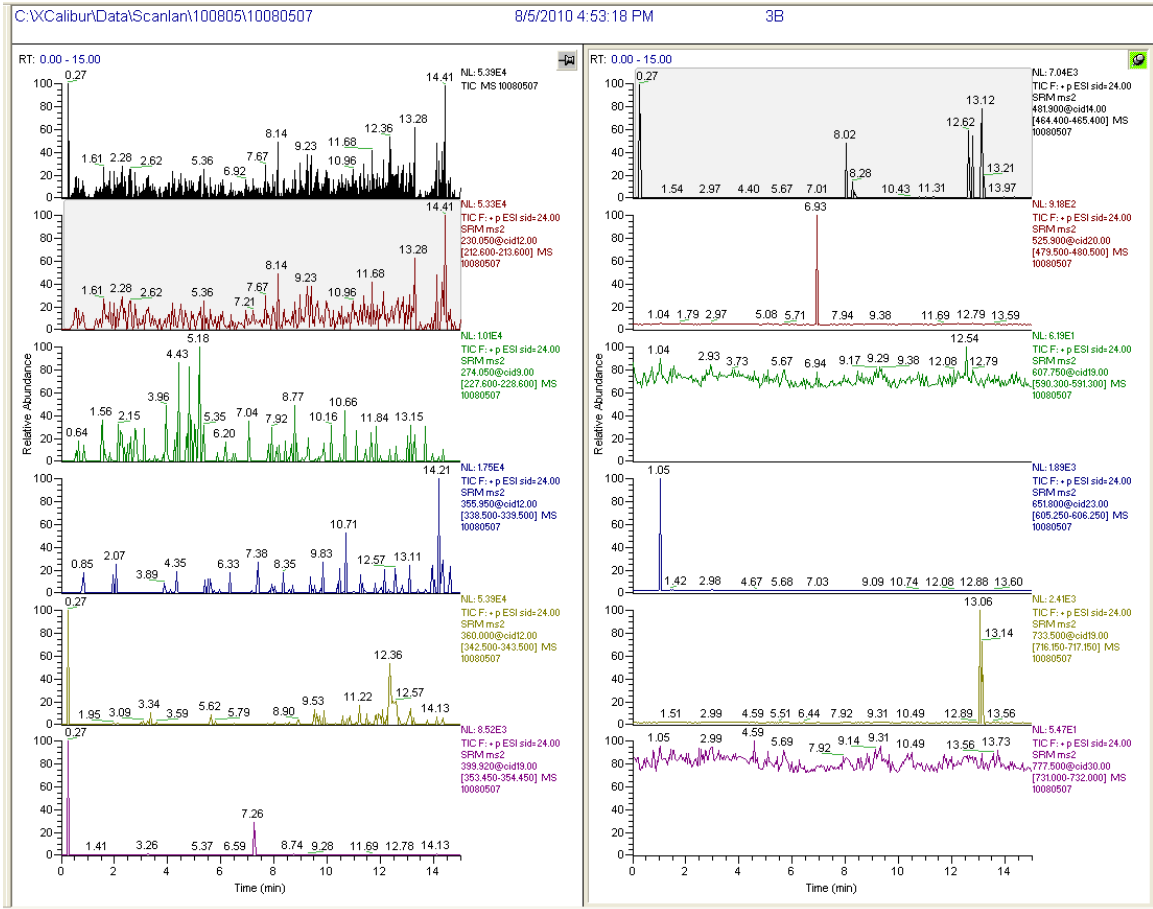
Sample Set III-C: HCl, charcoal
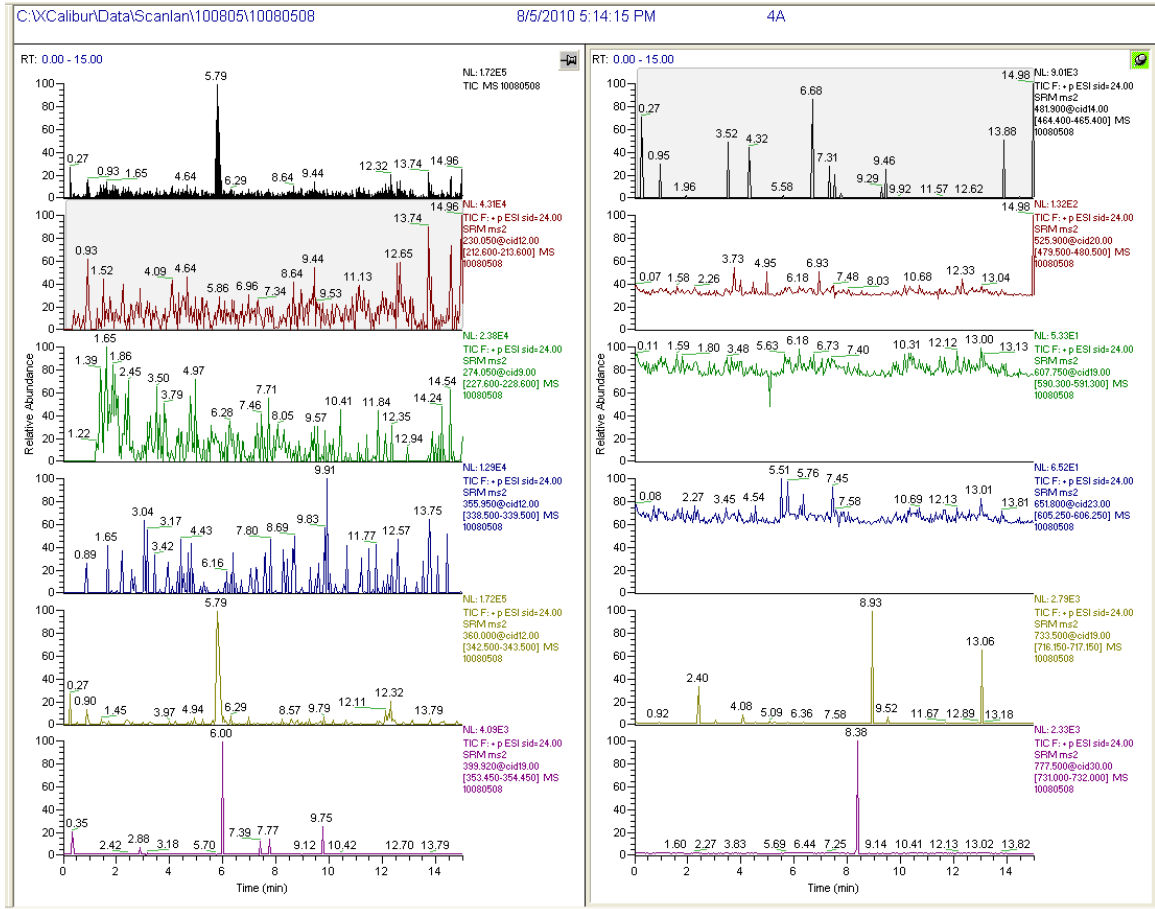
Sample Set III-C: Urea and Proteinase K, charcoal
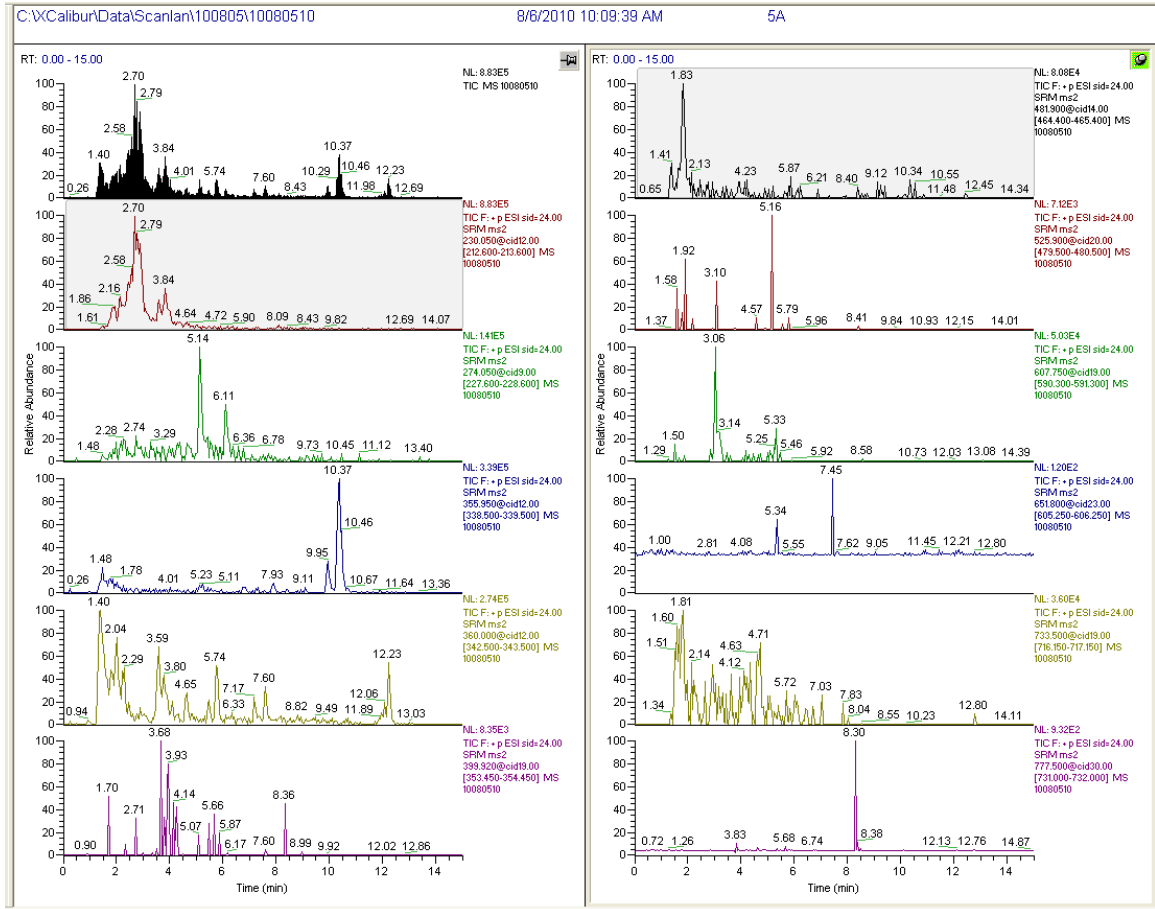
Sample Set III-C: Urea and Proteinase K, silica
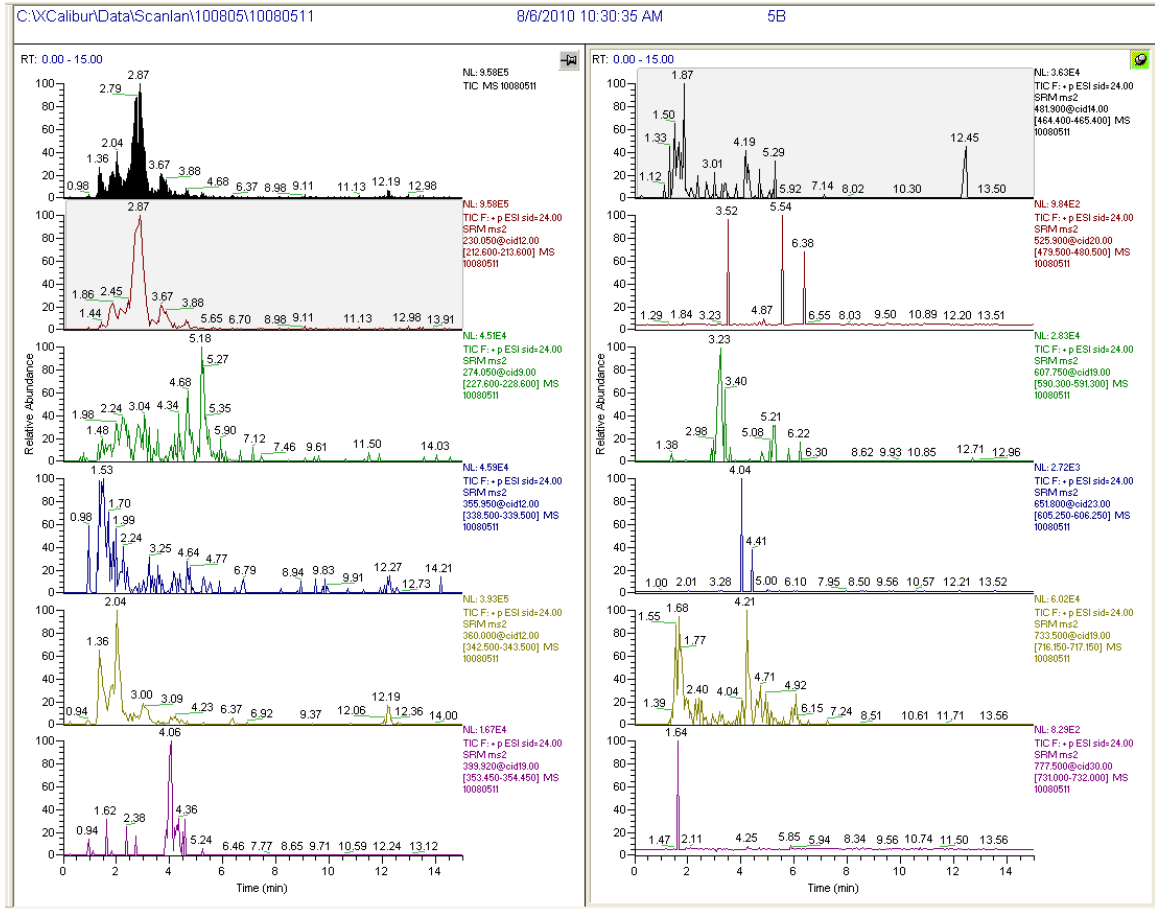
Sample Set III-C: Proteinase K and Lipoprotein lipase, charcoal
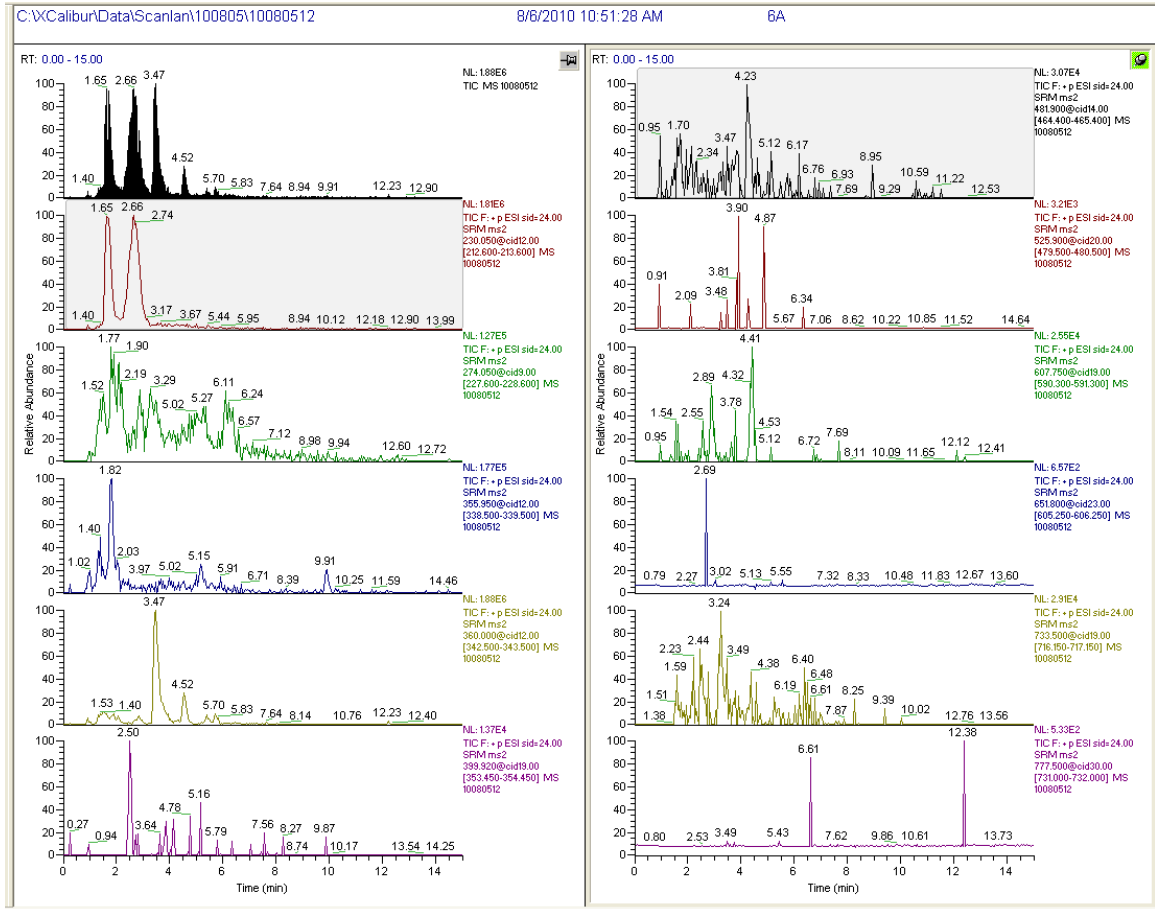
Sample Set III-C: Proteinase K and Lipoprotein lipase, silica
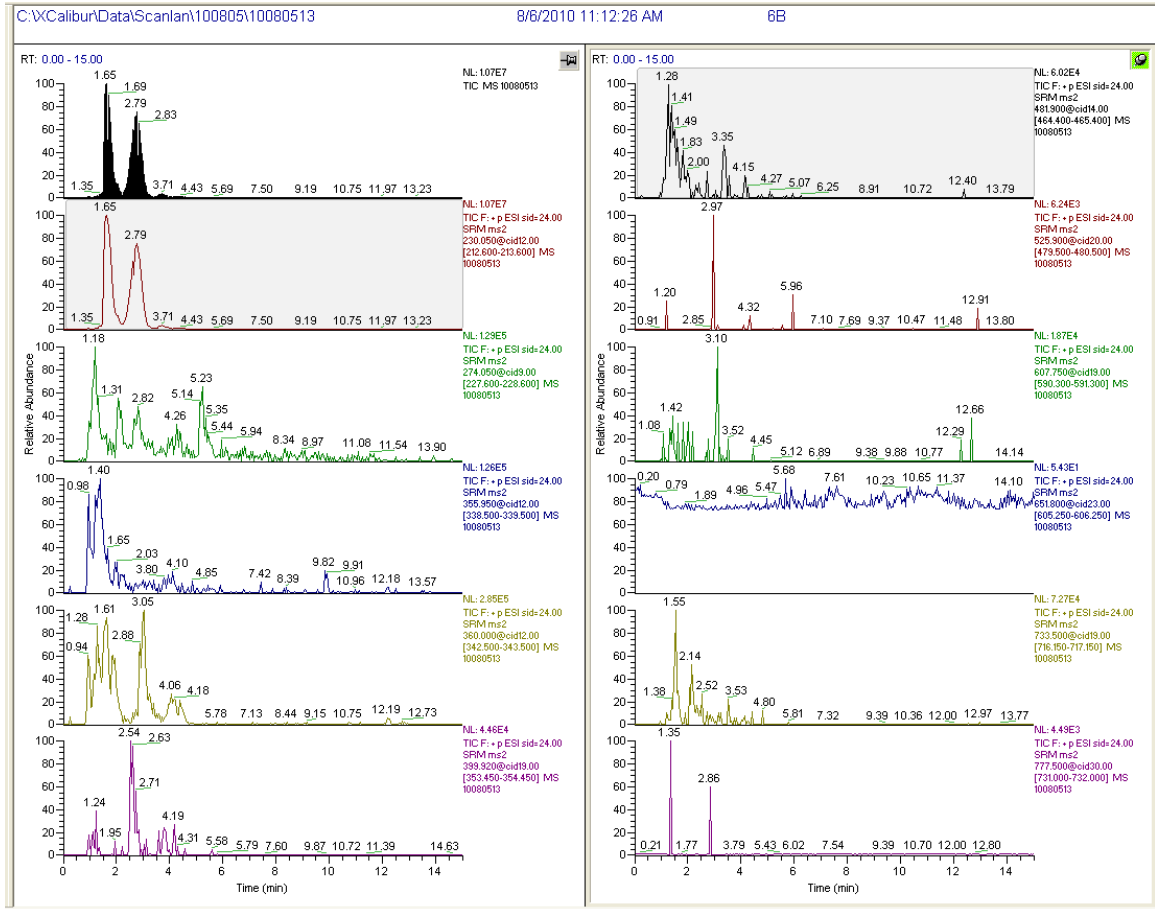
Sample Set III-C: Urea, Proteinase K and Lipoprotein lipase, charcoal
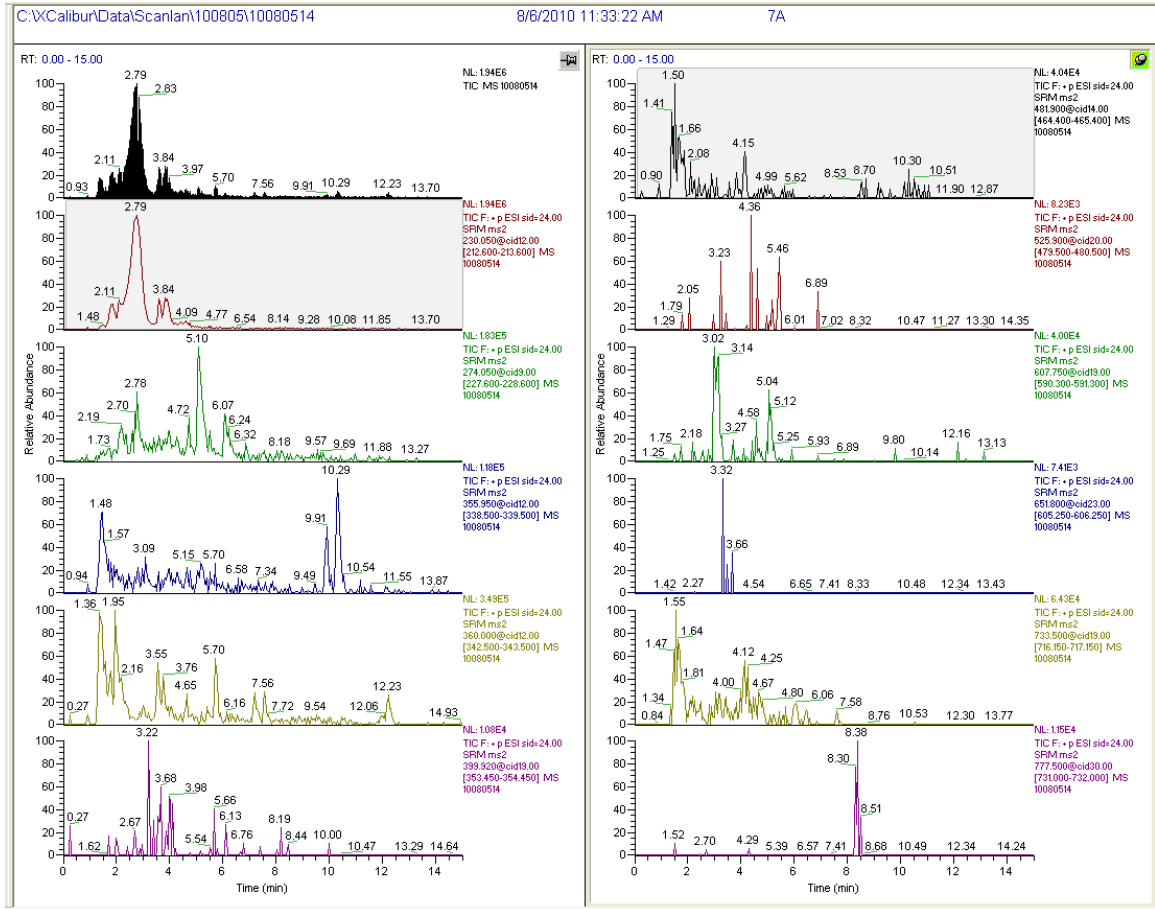
Sample Set III-C: Urea, Proteinase K and Lipoprotein lipase, silica
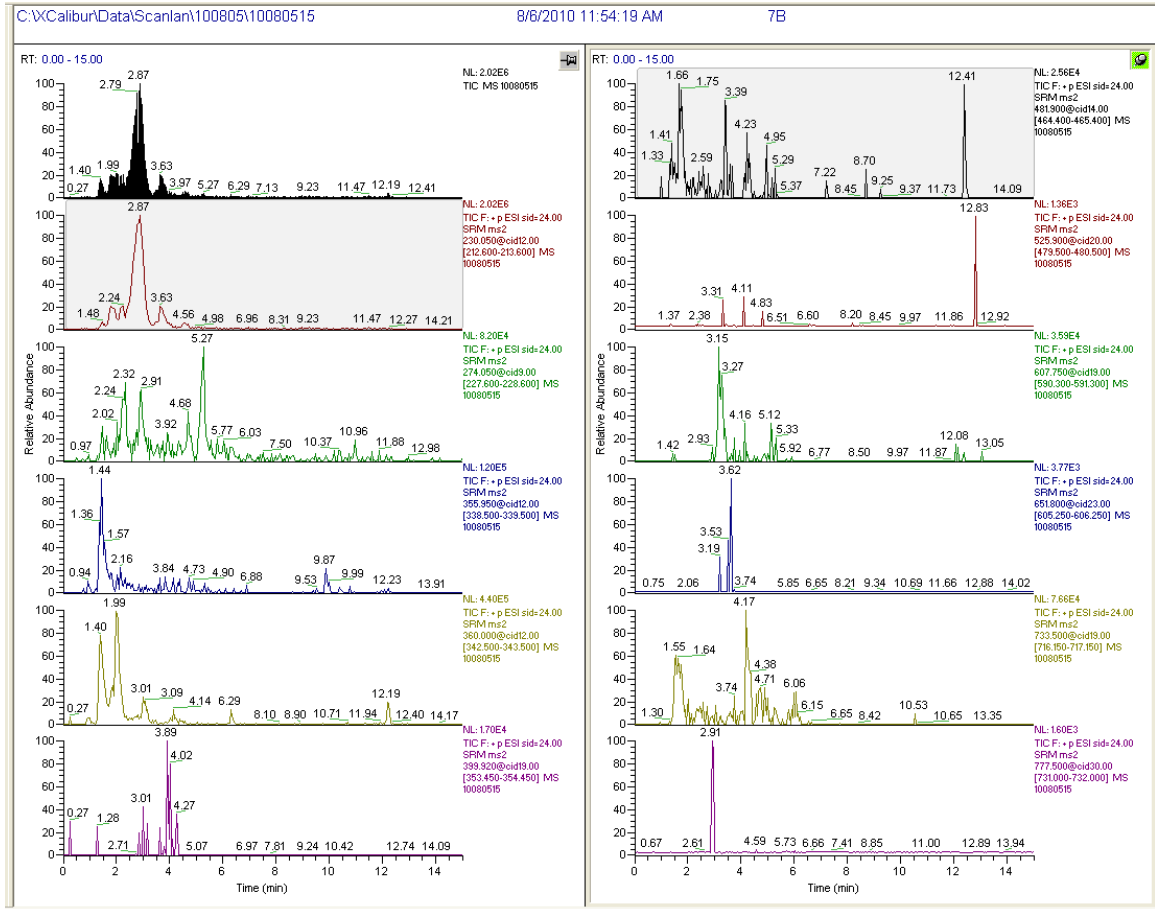
Sample Set III-C: Standards in urea, Proteinase K and Lipoprotein lipase, charcoal
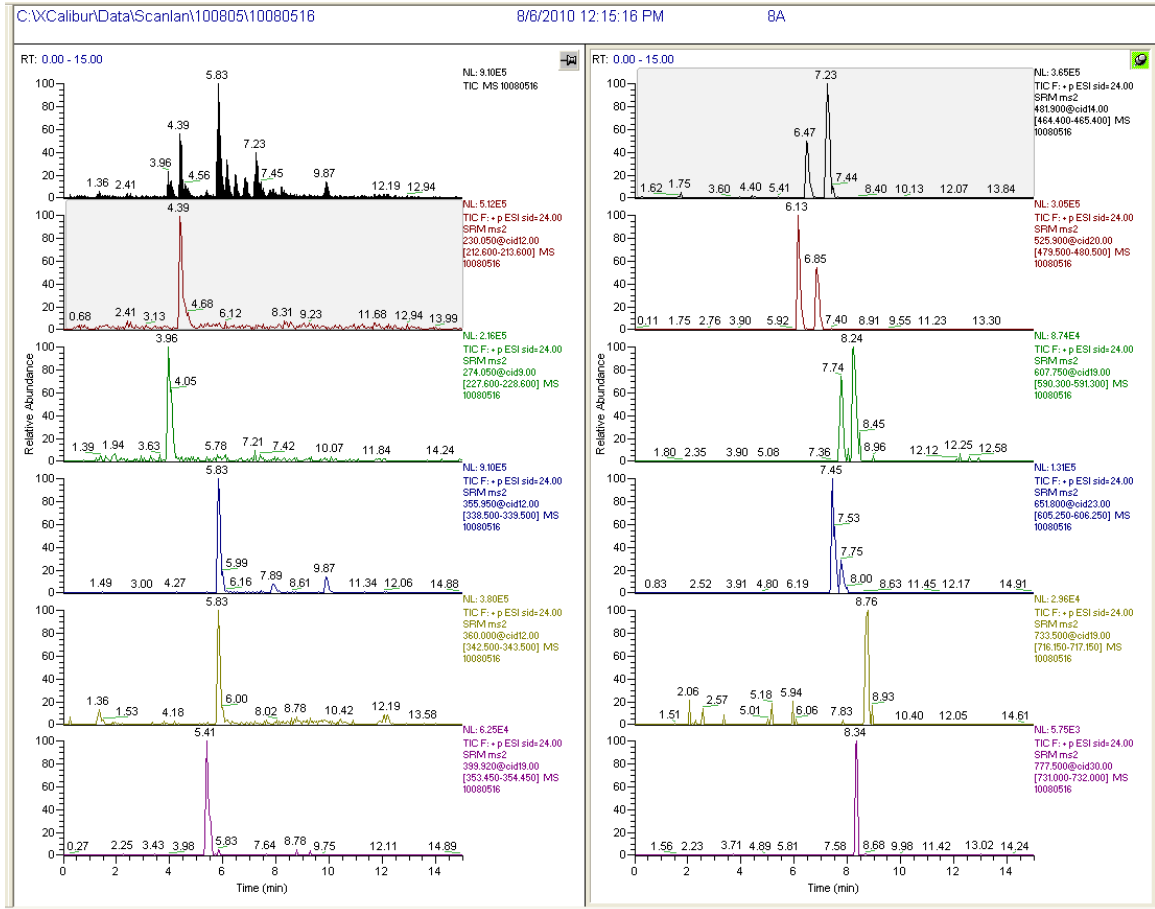
Sample Set III-D: Urea, pH 5, charcoal
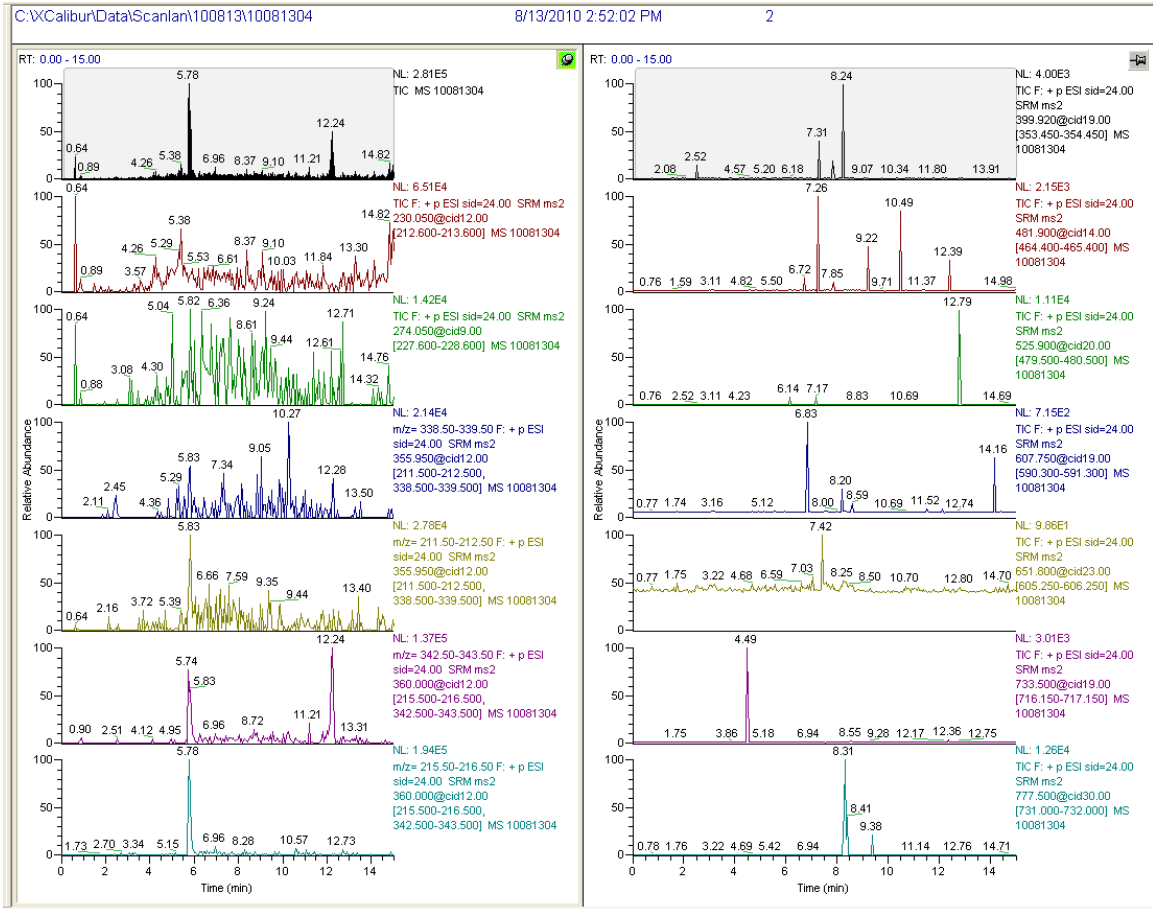
Sample Set III-D: Protection solution, charcoal
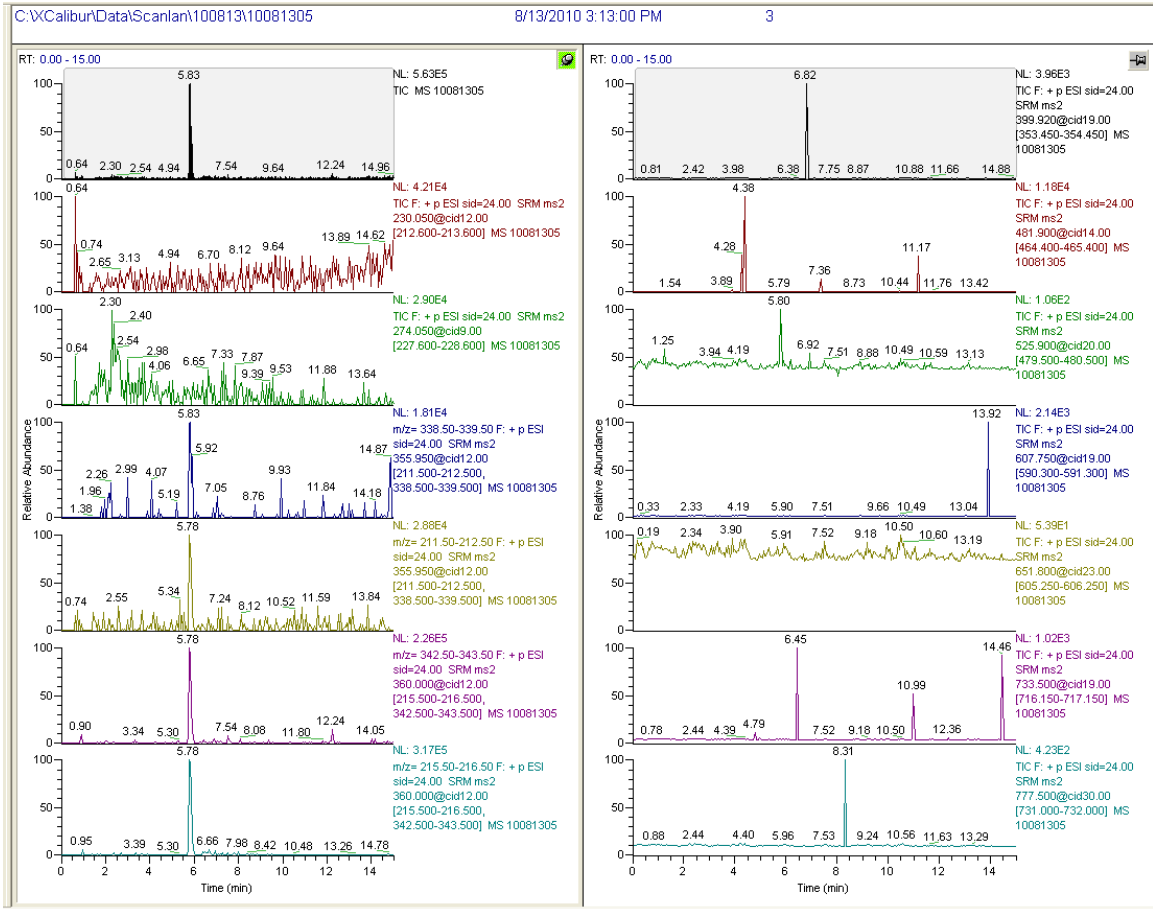
Sample Set III-D: NaCl and acetone, charcoal
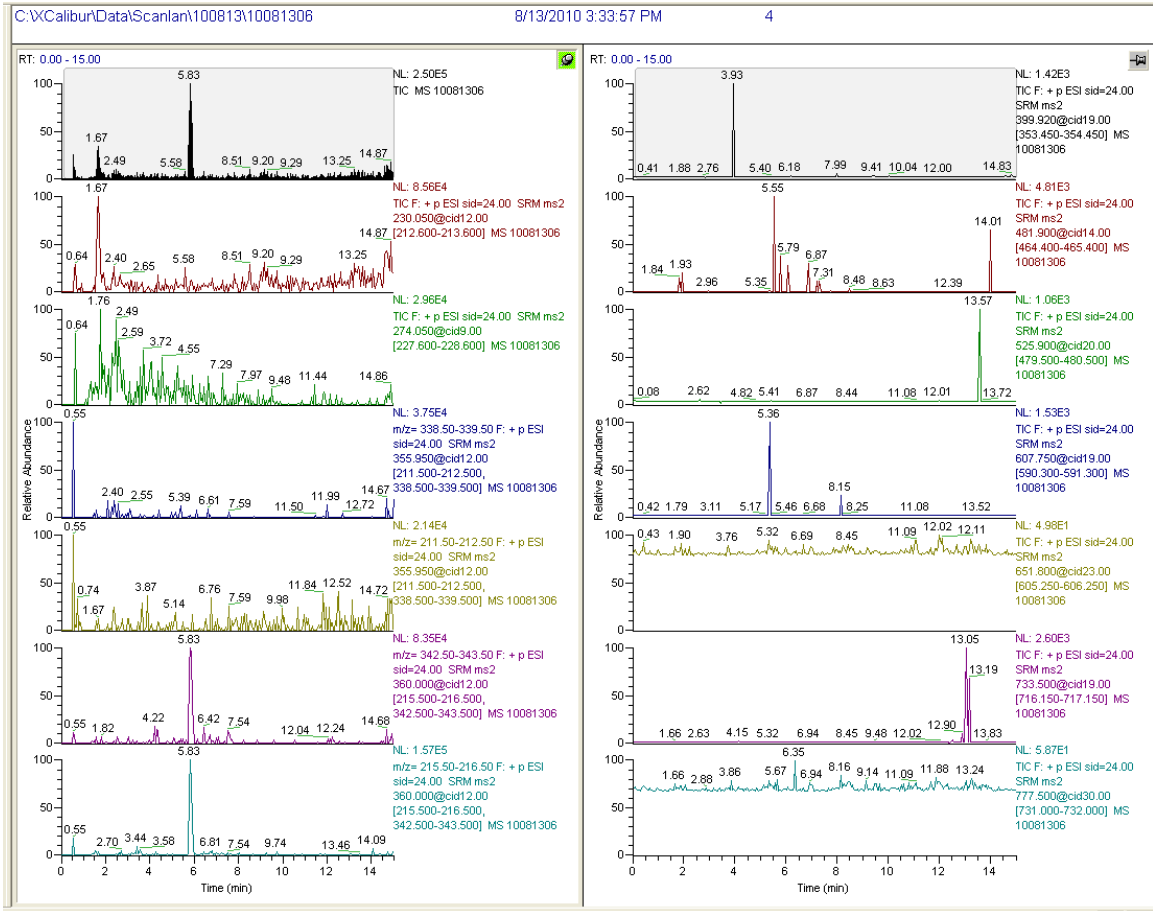
Sample Set III-D: Guanidinium-HCl, charcoal
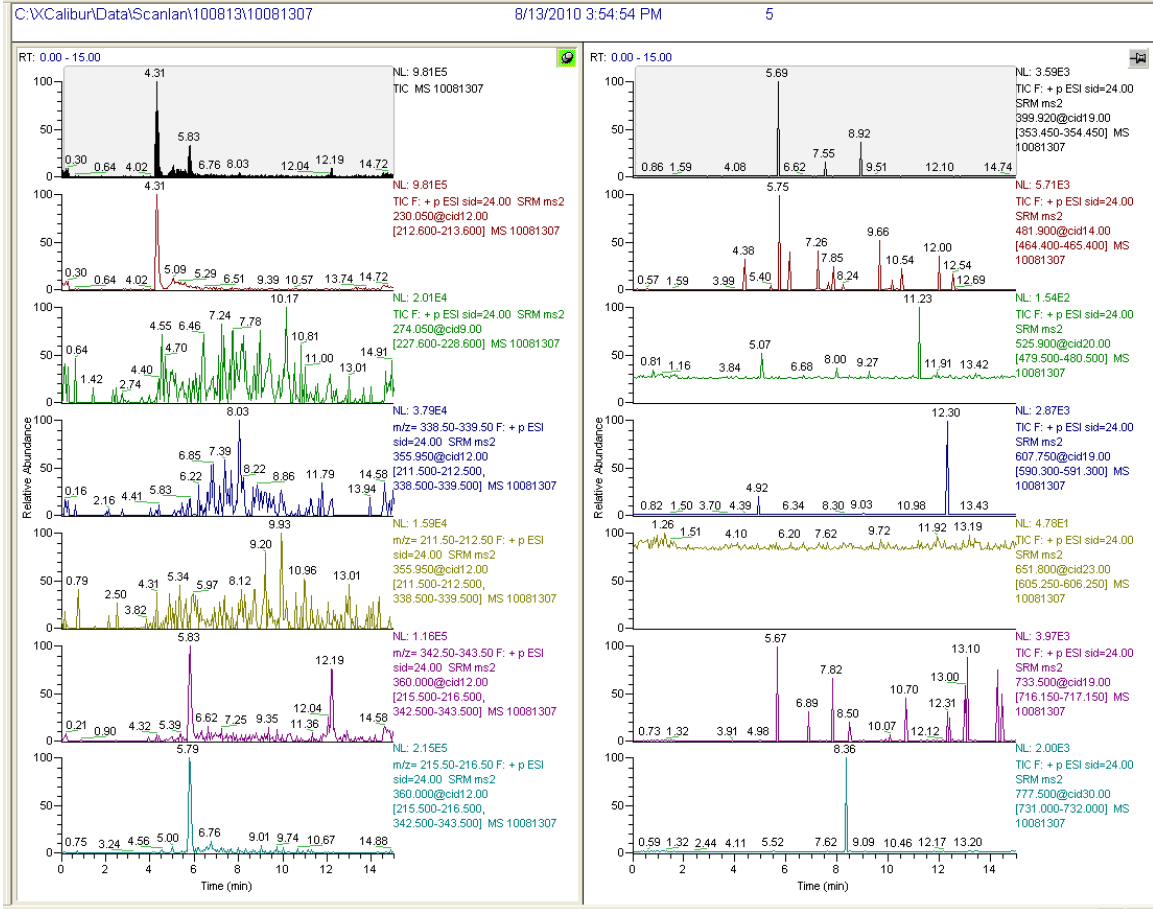
C:\XCalibur\Data\Scanlan\100813\10081307   8/13/2010 3:54:54 PM   5

209

Sample Set III-D: Guanidinium-HCl, pH 4, charcoal

Sample Set III-E: Protection solution, charcoal
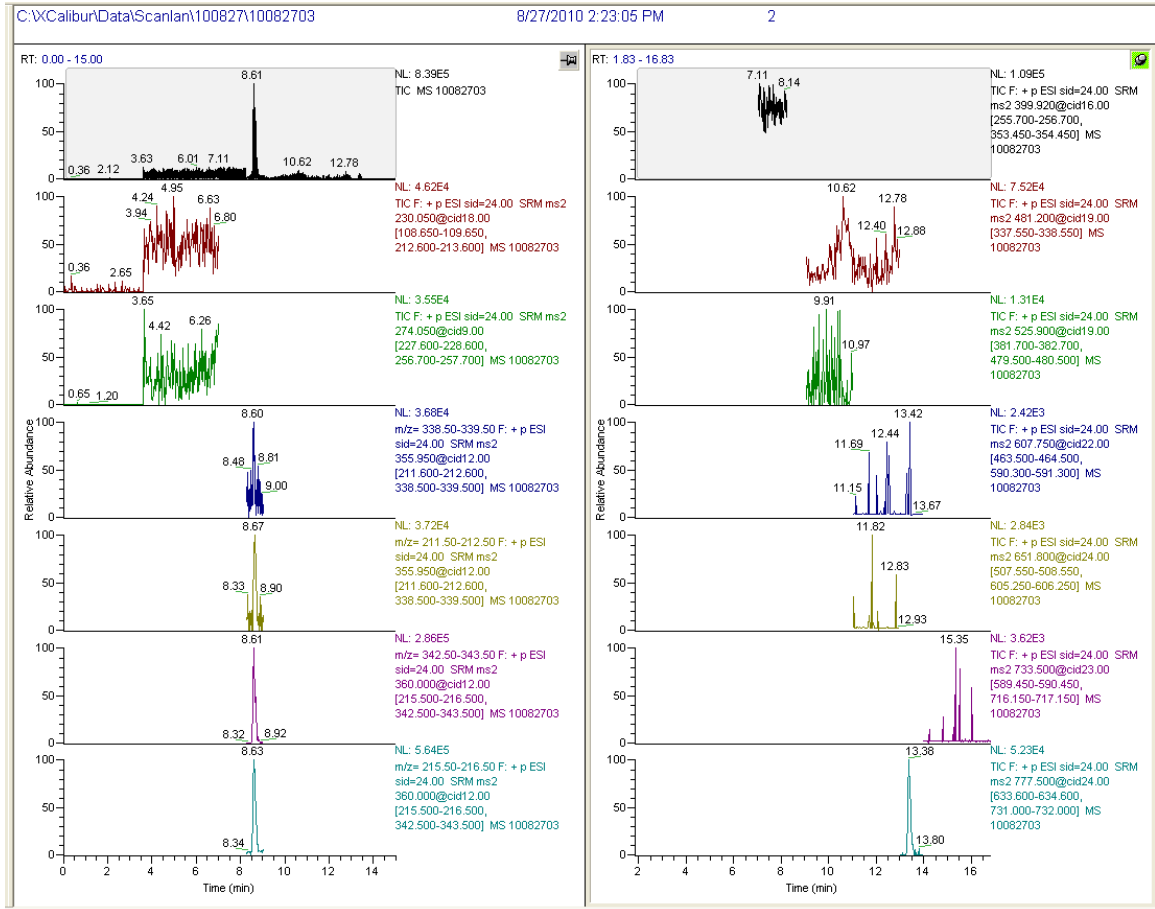
Sample Set III-E: Protection solution and urea, charcoal
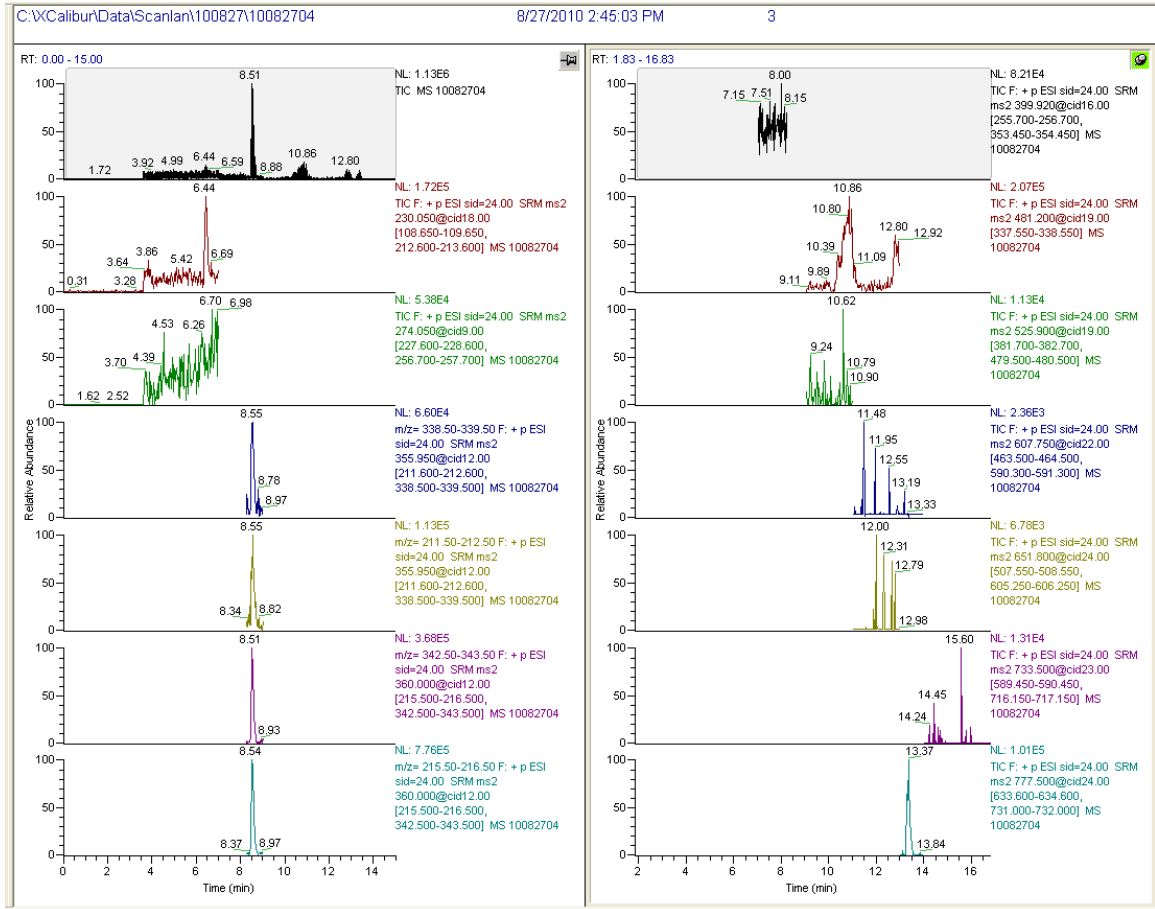
Sample Set III-E: Protection solution, acetone and urea, charcoal
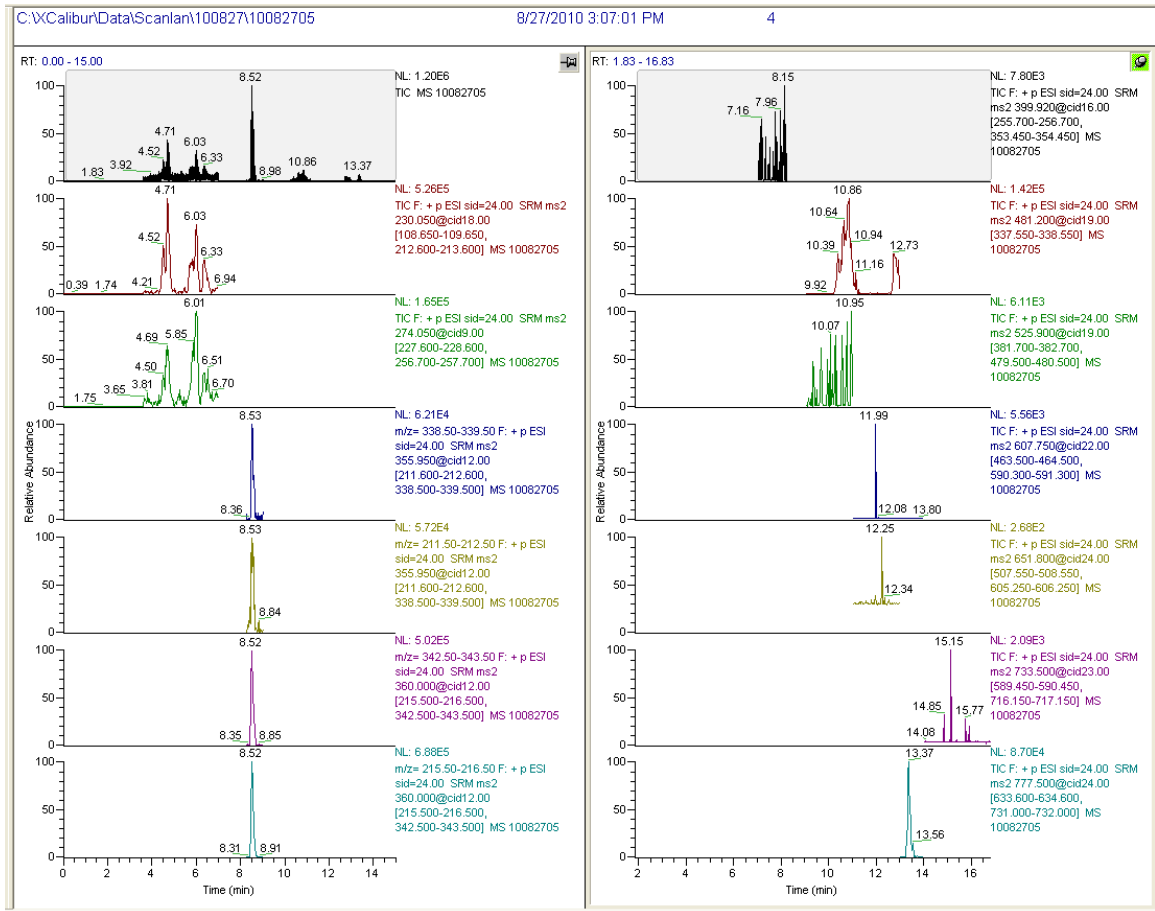
Zucchi Protocol: Standards, LC-MS/MS Method 3
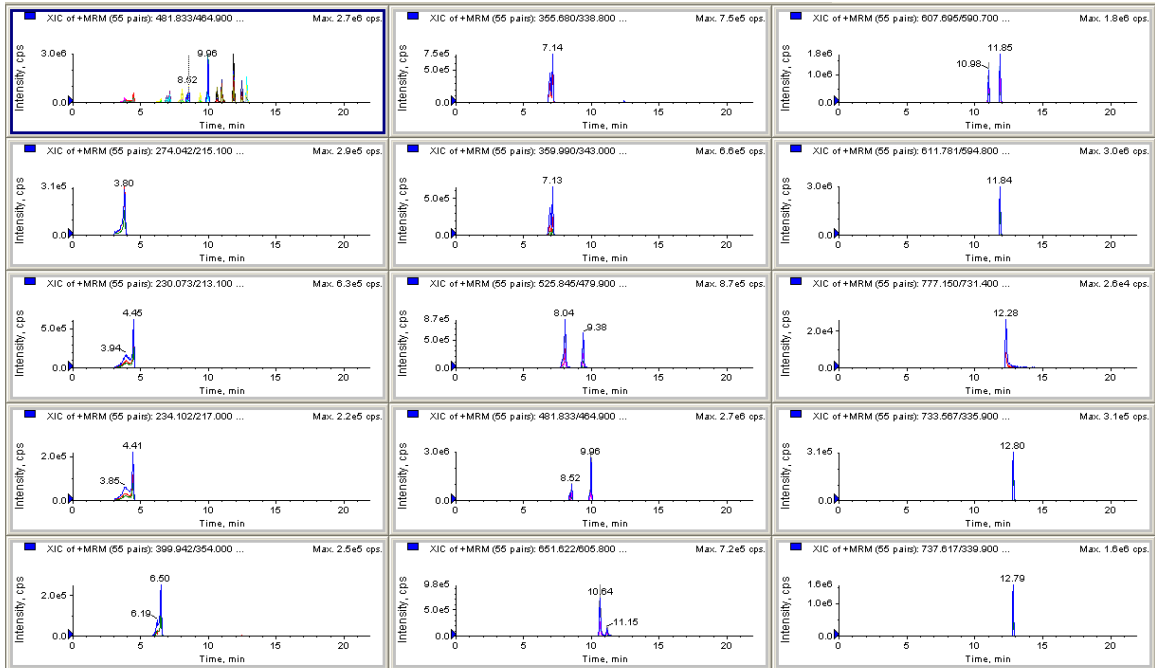
Zucchi Protocol: Blank sample, T$_1$AM and d$_4$-T$_1$AM
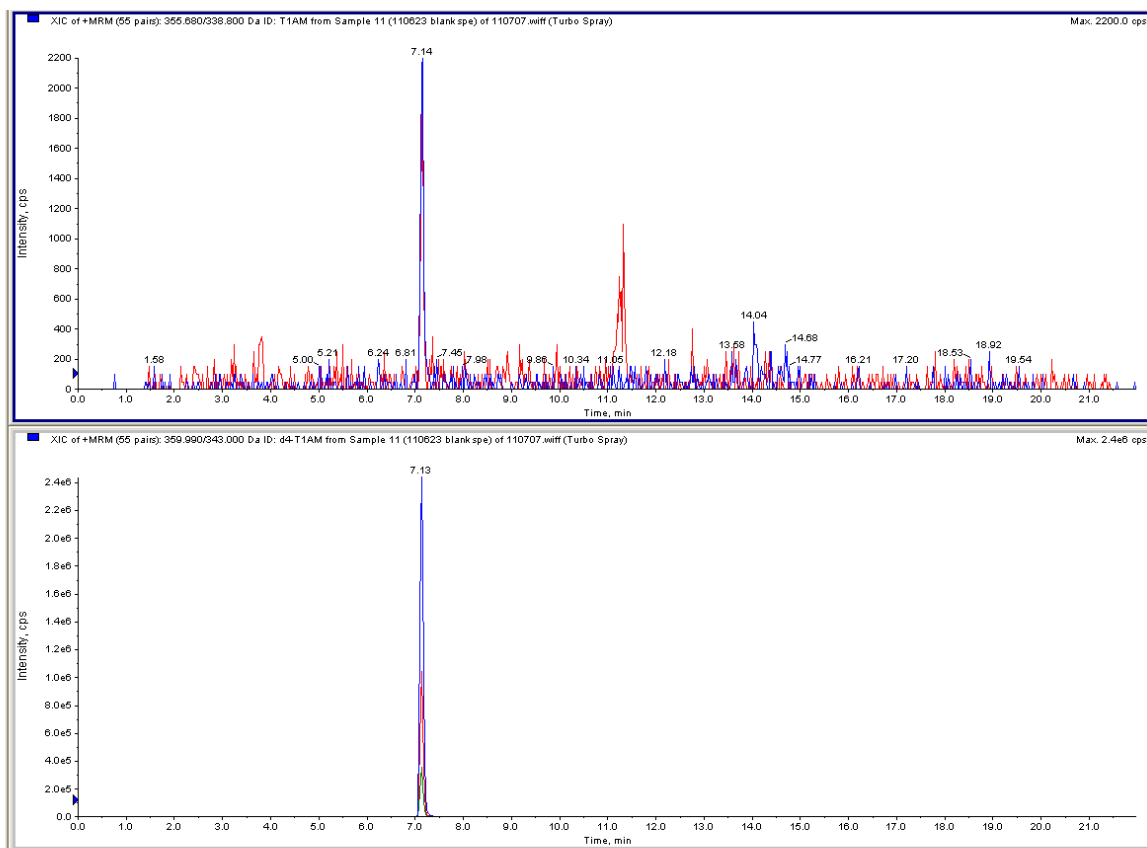
Zucchi Protocol: Liver, H₂O/MeOH/acetic acid, non-silanized, non-filtered
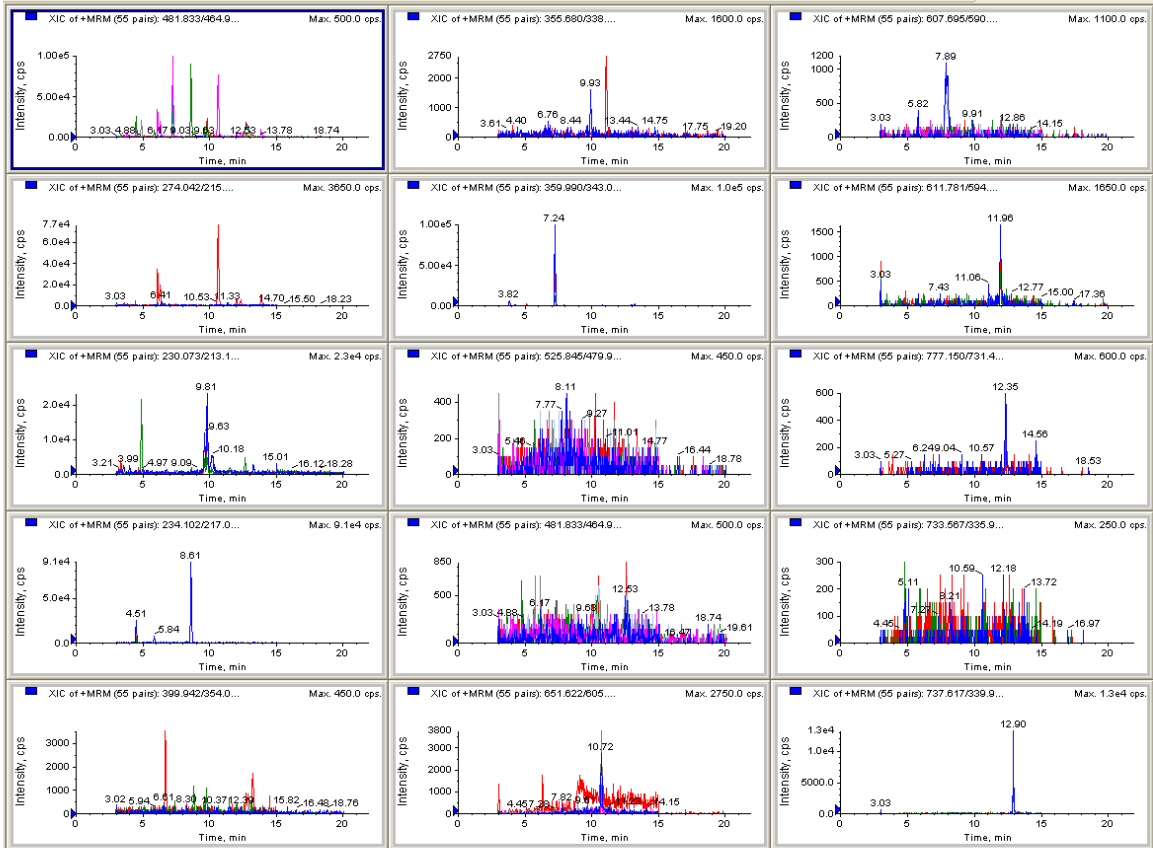
Zucchi Protocol: Liver, H₂O/MeOH/acetic acid, silanized, non-filtered

217
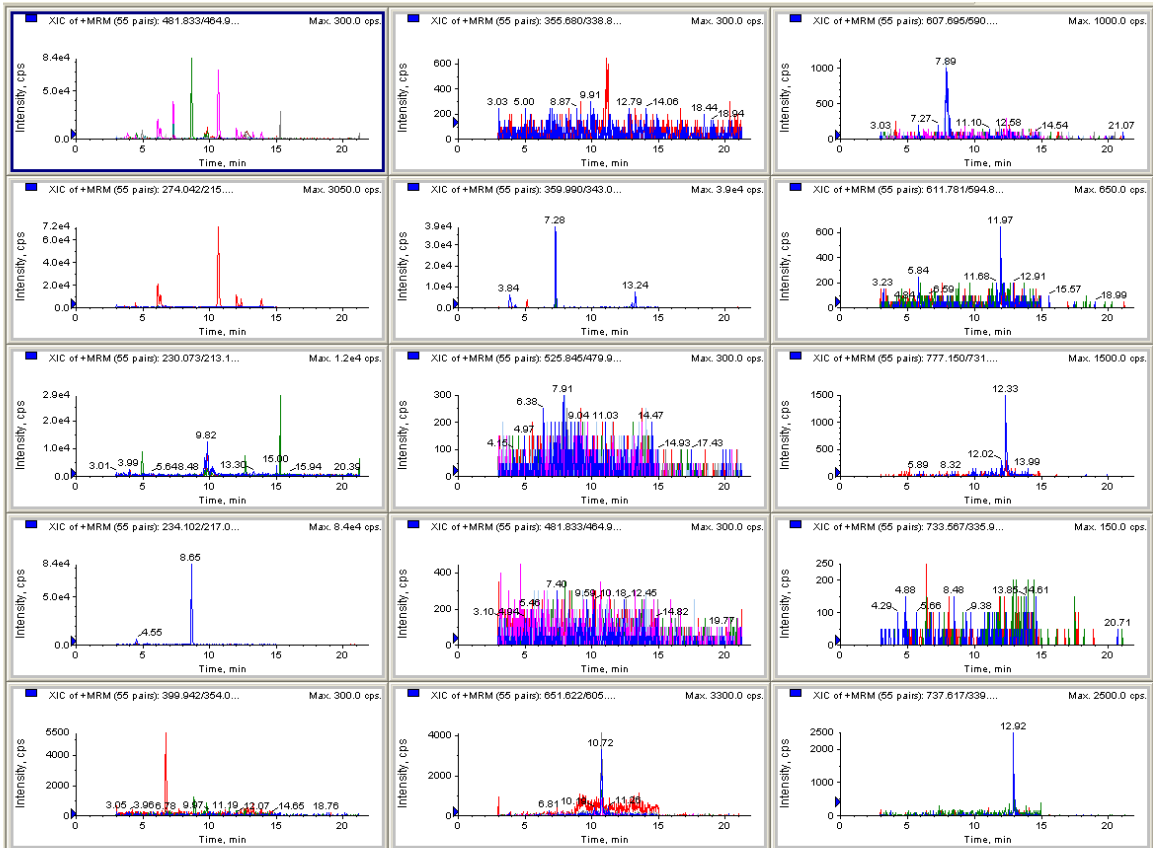
Zucchi Protocol: Liver, MeOH/0.1M HCl, non-silanized, non-filtered
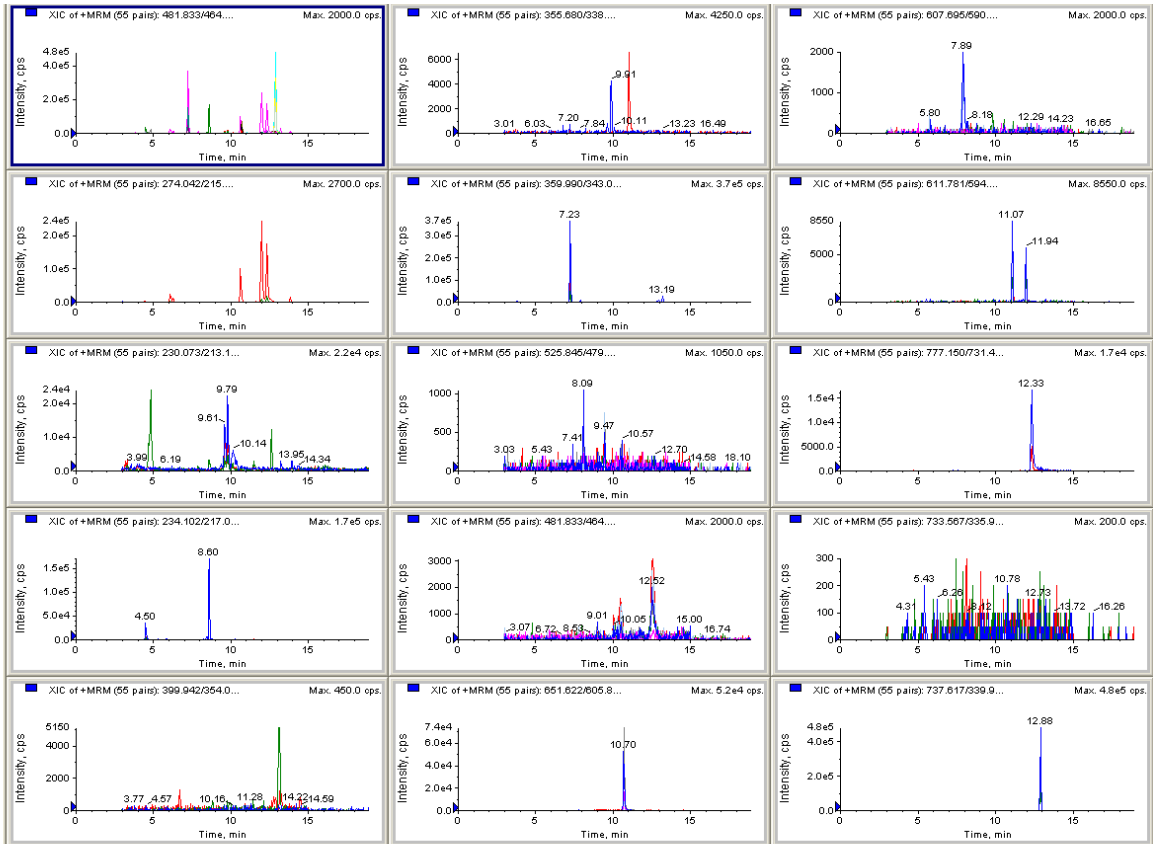
Zucchi Protocol: Liver, MeOH/0.1M HCl, silanized, non-filtered
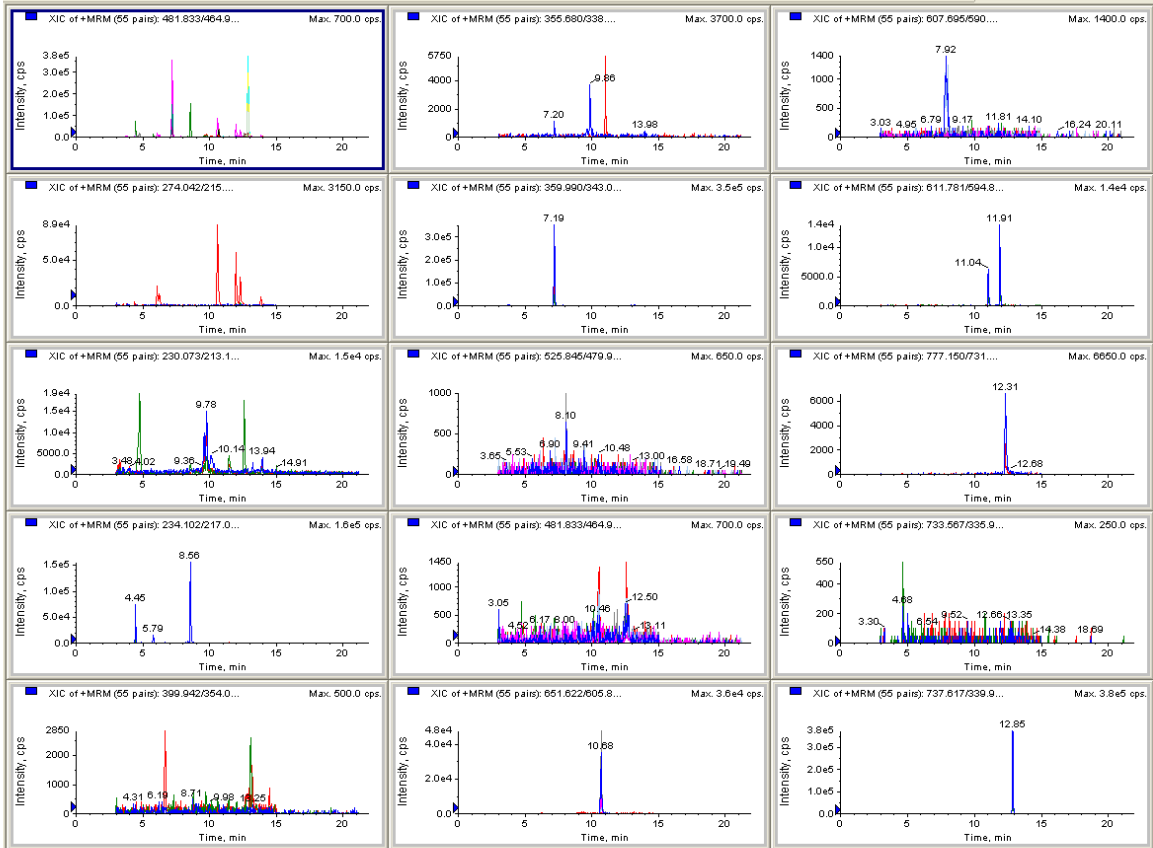
Zucchi Protocol: Liver, H₂O/MeOH/acetic acid, non-silanized, filtered
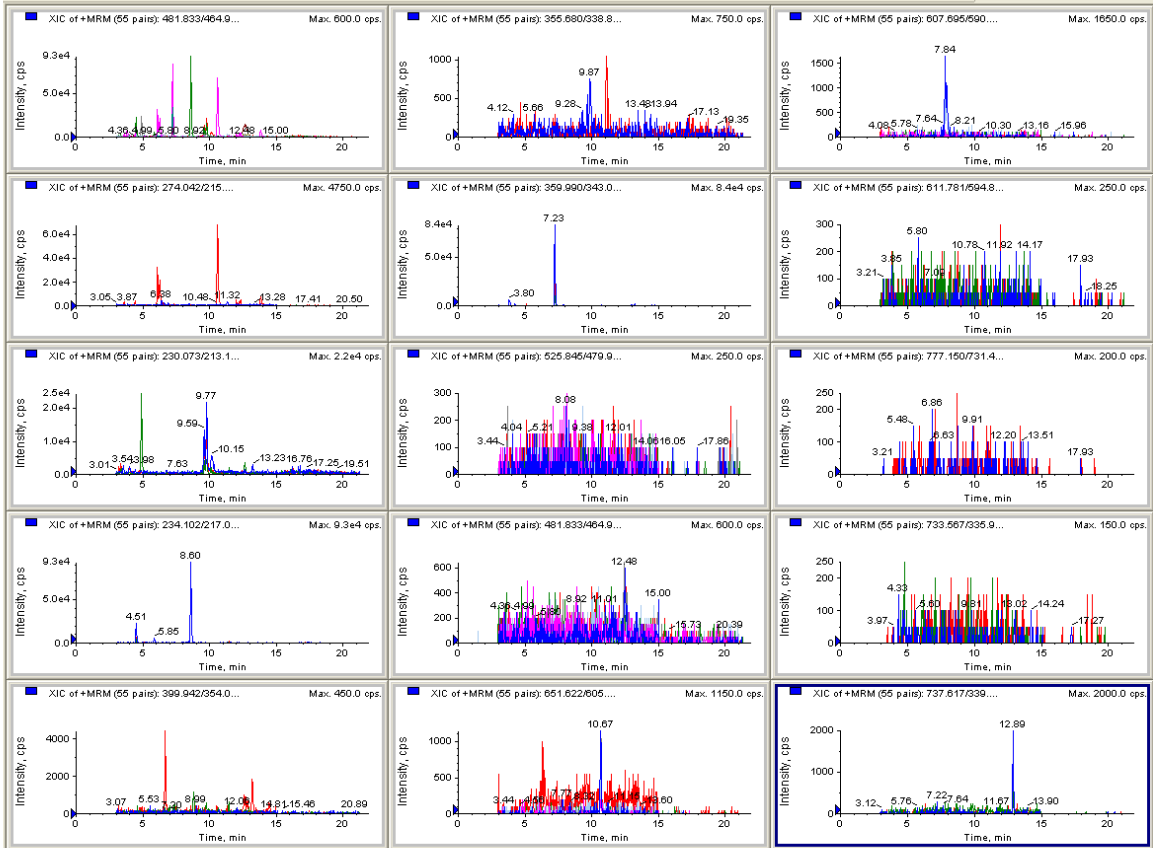
Zucchi Protocol: Liver, H₂O/MeOH/acetic acid, silanized, filtered
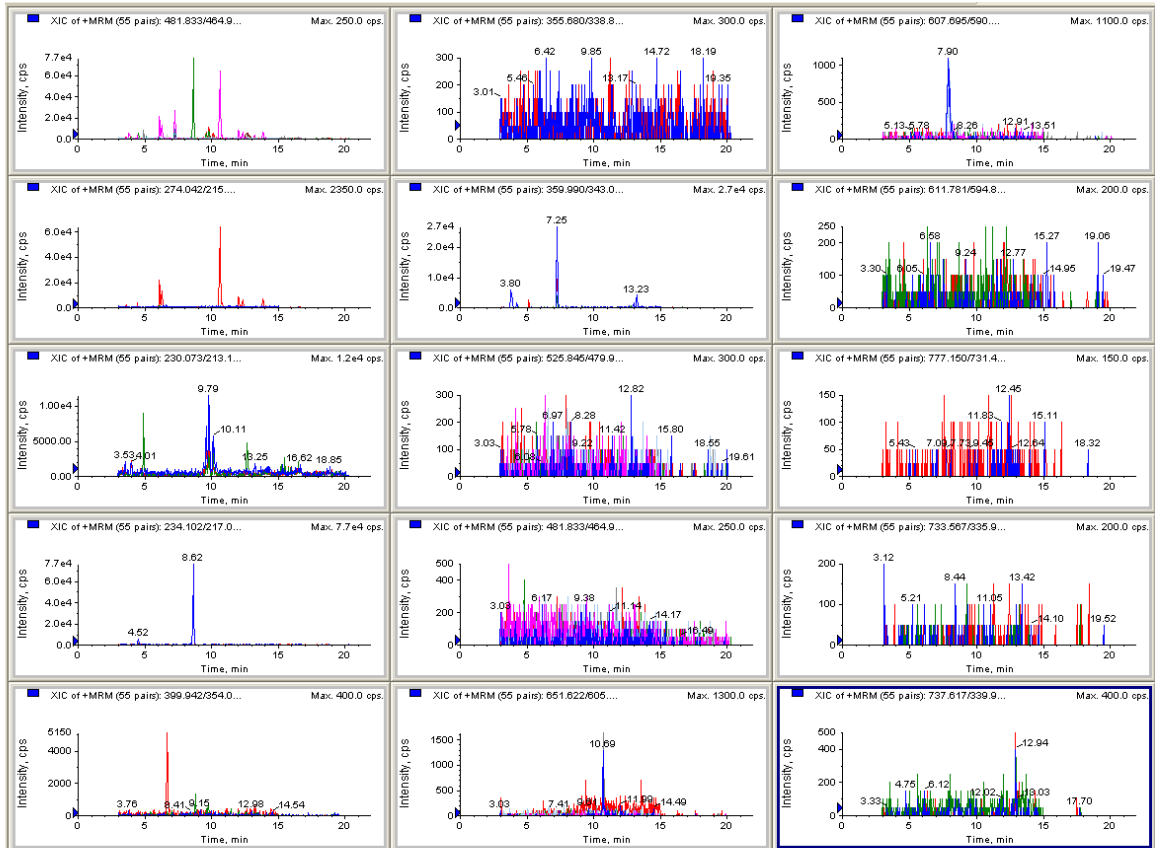
Zucchi Protocol: Liver, MeOH/0.1M HCl, non-silanized, filtered
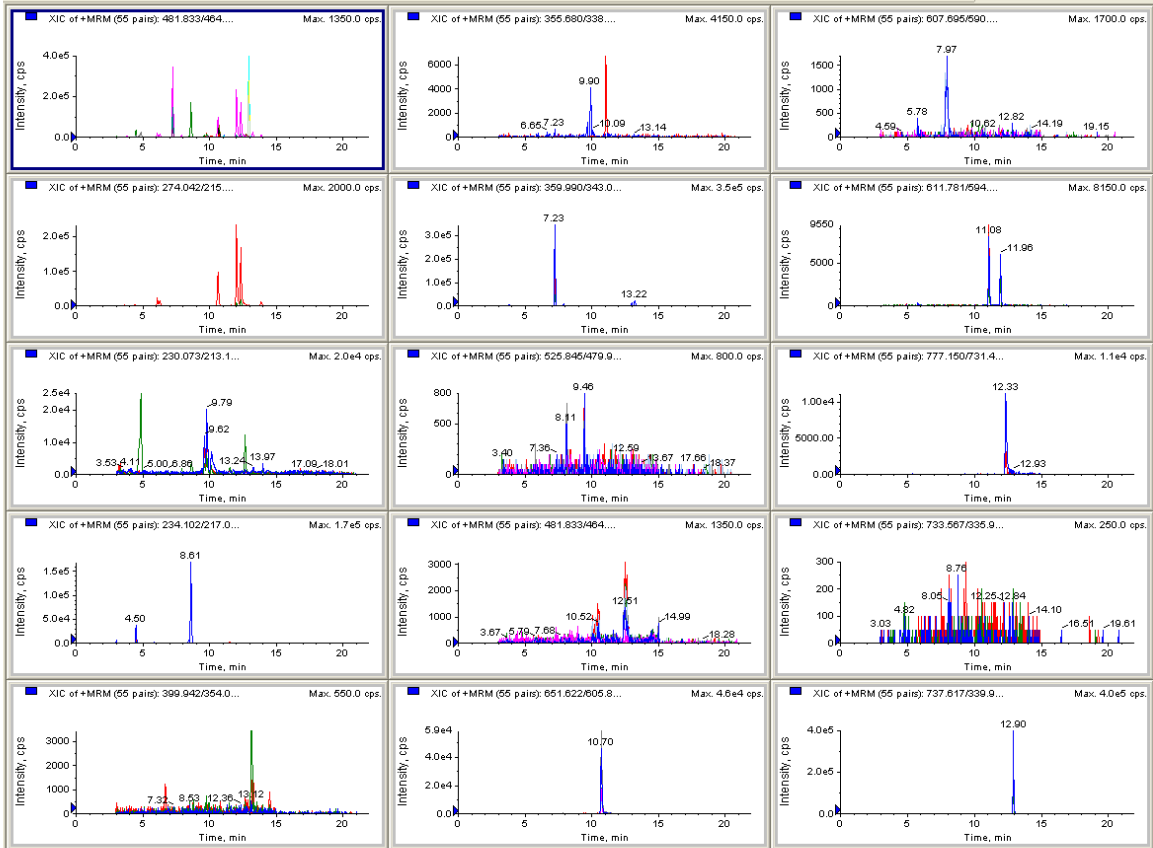
Zucchi Protocol: Liver, MeOH/0.1M HCl, silanized, filtered